Design, Development and Fabrication of Thiophene and Benzothiadiazole Based Conjugated Polymers for Photovoltaics

A thesis submitted by

Radhakrishna Ratha
Roll No. 11615303

to

Indian Institute of Technology Guwahati

For the award of the degree of

Doctor of Philosophy

Center for Nanotechnology
Indian Institute of Technology Guwahati
Guwahati - 781039
India

February, 2018

INDIAN INSTITUTE OF TECHNOLOGY GUWAHATI
Guwahati, Assam-781039, India
Centre for Nanotechnology

STATEMENT

I do hereby declare that the work contained in the thesis entitled **'Design Development and Fabrication of Thiophene and Benzothiadiazole Based Conjugated Polymers for Photovoltaics'** is the result of investigations carried out by me in the Center for Nanotechnology, Indian Institute of Technology Guwahati, Guwahati, Assam India under the supervision of Dr. Parameswar Krishnan Iyer, Professor, Department of Chemistry, Indian Institute of Technology Guwahati, Guwahati, Assam, India. This work has not been submitted elsewhere for the award of any degree.

Radhakrishna Ratha
Center for Nanotechnology
Indian Institute of Technology Guwahati
Guwahati-781039, Assam, India

February 2018

TH-1906_11615303

INDIAN INSTITUTE OF TECHNOLOGY GUWAHATI
Guwahati, Assam-781039, India
Centre for Nanotechnology

CERTIFICATE

This is to certify that the work contained in the thesis entitled **'Design Development and Fabrication of Thiophene and Benzothiadiazole Based Conjugated Polymers for Photovoltaics** by Radhakrishna Ratha, a Ph.D. student of Center for Nanotechnology, Indian Institute of Technology Guwahati, for the award of degree of Doctor of Philosophy has been carried out under my supervision and this work has not been submitted elsewhere for any degree.

Prof. Parameswar Krishnan Iyer
Thesis Supervisor
Department of Chemistry, Centre for Nanotechnology,
Indian Institute of Technology Guwahati,
Guwahati -781039, Assam, India

February, 2018

TH-1906_11615303

ACKNOWLEDGEMENTS

At this stage of ending truly memorable and overwhelming journey towards my intellectual destination, it is really hard to list all the people who sincerely helped me and I would like to thank all of them who have made this thesis possible.

First of all, I would like to express my sincere gratitude to my thesis supervisor professor Parameswar Krishnan Iyer for his kind support, advice, encouragement and introducing me to an interdisciplinary area of research. I earnestly thank him for his astute guidance, freedom to work, encouragement, inspiration and creative and scientific ideas, which helped me to enhance my knowledge.

I sincerely thank and would like to acknowledge my sincere gratitude to my doctoral committee members, Professor Aditya Narayan Panda, Professor Mohd. Qureshi and Dr. Tapas Kumar Mandal for their insightful advices and suggestions and crucial comments which certainly helped me a lot in betterment of my thesis.

I am thankful to all faculty members in the Centre for Nanotechnology and Department of Chemistry IIT Guwahati for their help and encouragement and also the non-teaching staff of the Centre for Nanotechnology and Department for their technical support. I am thankful to the Central Instruments Facility (CIF), IIT Guwahati for different characterization facilities.

I like to thank few of my friends and colleagues, Anargha, Biswa, Manu, Bikash, Banaja, Mona, Smita, Nandita, Moumita, Mili, Saumya bhai, Rosalin didi, Himanshu bhai, Santosh bhai, Deepankar bhaiya, who were there with me at those demanding times of highs and lows. With my friends, seniors and juniors my Ph.D. period became cherishably wonderful and will be echoing forever in corridors my mind. Definitely I am going to treasure the fantastic moments shared. I am very lucky to have extremely cooperative and friendly seniors–Gunin bhaiya, Prasanta bhaiya, Atul bhaiya, Muthuraj, Subarao and Meenakshi. My lab juniors Bhim, Suresh, Sameer, Anamika Dey, Anamika Kalita, Debojit, Ashish, Dipjyoti, Arvin, Akhtar, Sayan, Gopi, Raman, Adil, Subrata, Niranjan, Maimur, Debashish, Nehal, Rabindra, Ritesh, Indrani, Rahul, Nystha, Ramesh,

Priyanka, Himani, Ekta, Retwick, Nasima, Viki, Anmesha who made my experiences with them unforgettable with their help and care. Thanks go to all other departmental seniors, batch mates and juniors for making my days memorable with them.

TH-1906_11615303

ACKNOWLEDGEMENTS

I gratefully acknowledge all my teachers at School and specially Rabi sir, Giri sir and Sabat sir at K.S.U.B College, Bhanjanagara, Orissa, India and Dr. Sandhya A. Mishra, Dr. Naveen Ratha, Chakrapani sir, Basudev sir, Bibhu sir, at Khallikote Autonomous College, Berhampur, Orissa, India for their best teaching, constant motivations and precious advices which are of great impact on me.

Finally, my Ph.D. endeavour could not be completed without the endless love, unending support, tolerance and blessings from my family. I would like to express my sincere gratitude to my parents, family members and relatives.

Radhakrishna Ratha

TH-1906_11615303

Contents

Statement I

Certificate II

Acknowledgements III

Synopsis VIII

Chapter 1: Introduction

1.1 Introduction 1

1.2 Objective of the present work and summary 28

1.3 References 30

Chapter 2: Photo stability enhancement of poly(3-hexylthiophene)-PCBM nano-composites by addition of multi walled carbon nanotubes under ambient conditions

Abstract 38

1.1 Introduction 38

1.2 Results and discussion 39

1.3 Conclusion 47

1.4 Experimental 48

1.5 References 49

Chapter 3: Insight into the synthesis and fabrication of 5,6-*alt*-benzothiadiazole based D-π-A CPs for bulk-heterojunction solar cell

Abstract 51

1.1 Introduction 51

1.2 Results and discussion 52

1.3 Conclusion 59

1.4 Experimental 60

TH-1906_11615303

1.5 References 64

Chapter 4: Substituting non-conjugating ester group into side chain of benzothiadiazole improves optical, electrochemical properties, morphology of active layer and solar cell performance of D-A polymer for photovoltaics

Abstract 67

1.1 Introduction 67

1.2 Results and discussion 69

1.3 Conclusion 78

1.4 Experimental 79

1.5 References 85

Chapter 5: 6,7-Di(thiophen-2-yl)naphtho[2,3-c][1,2,5]thiadiazole and 4,6,7,9-tetra(thiophen-2-yl)naphtho[2,3-c][1,2,5]thiadiazole as new acceptor units for D-A type co-polymer towards fabrication of polymer solar cell

Abstract 88

1.1 Introduction 88

1.2 Results and discussion 90

1.3 Conclusion 98

1.4 Experimental 98

1.5 References 102

Appendix A1 105

Appendix A2 108

Appendix A3 109

TH-1906_11615303

Appendix A4 120

Appendix A5 138

Thesis overview 146

Publication and conferences 147

Shockley–Queisser limit 148

Future Prospective 149

भारतीय प्रौद्योगिकी संस्थान गुवाहाटी • Indian Institute of Technology Guwahati •

TH-1906_11615303

TH-1906_11615303

SYNOPSIS

The content of this synopsis report entitled **"Design, development and fabrication of thiophene and benzothiadiazole based conjugated polymers for photovoltaics"** is divided into five chapters. In chapter 1 the respective research area, where design synthesis and fabrication of conjugated polymers, along with the scope and significance of the subsequent chapters are discussed. In chapter 2 photostability enhancement of P3HT-PCBM by using appropriate ratio of MWCNT in ambient conditions have been discussed. Chapter 3 discusses about synthesis of poly(ortho-arylene-vinylene) type of polymer alternating at 5,6-position of BT namely P1 and P2 in the polymer main chain. Chapter 4 demonstrates that on functionalization of methyl acetate group at 5,6-positions of BT red-shift absorbance, lowered the $LUMO^{optical}$, improves phase separation in active layer of PSC and hence improves solar cell performance compared to its methyl counterpart. Chapter 5 results in synthesis of newer napthothiadiazole (NT) based D-A polymer and their BHJ solar cell performance.

Chapter 1: Introduction to polymer solar cell

Polymer solar cells (PSCs) have gained much attention owing to its several advantages such as large area solution processability, fine tuning of band gap on polymer backbone and amorphous nature of polymer that allow fabrication on light weight flexible substrates. These properties make CPs attractive for solar cell researchers and a PCE of ~13% has been achieved recently. These polymer solar cells will be cheaper and flexible in nature compared to present commercialized expensive silicon solar cells. Generally a blend of p-type CP (Figure 2) and an n-type acceptor (Figure 2) are used to sandwich between an anode and a cathode (Device geometry and mechanism of a polymer solar cell has been shown in Figure 1).

TH-1906_11615303

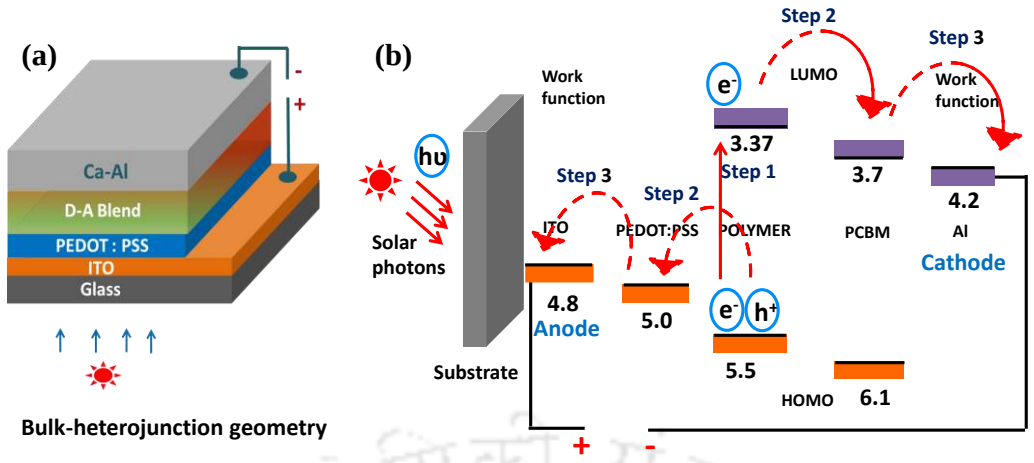

Figure 1 Bulk-heterojunction polymer solar cell (a) device structure (b) mechanism.

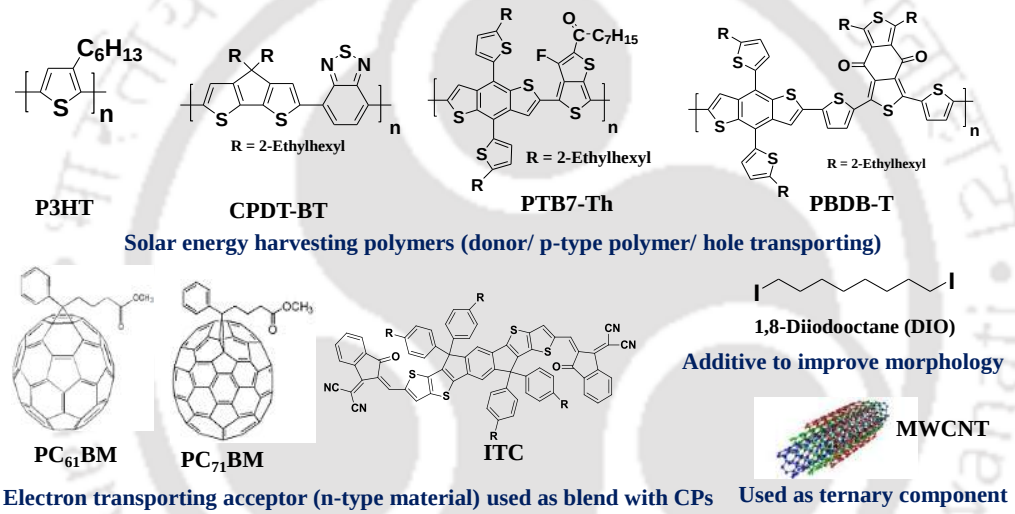

Figure 2 Structure of frequently studied polymers and acceptor units for PSC, along with additive and ternary component.

Generally CPs have been synthesized by the combination of π-electron acceptor, such as [2,1,3-benzothiadiazole (BT), thieno[3,4-b]pyrazine (Tp), quinoxaline (Q)] and π-electron donor, such as [thiophene (Th), cyclopentadithiophene (CPDT), benzo[1,2-b:4,5-b´]dithiophene (BDT), fluorene (FL), carbazole (Cz)] either as D-A, D-A-D or D-π-A (π refers to extended conjugation). D-A combination creates intra molecular charge transfer between donor and acceptor leading to red shift of absorbance, a spectral region where earth receives the most solar photon flux. In the past few years, using these conjugated structures, the desired parameters of molecular structure of a CP for PSCs have been successfully achieved, such as: low dihedral angle along conjugation backbone (a dihedral angle of $< 20^0$ are highly desirable) with high molar extinction coefficient, low

TH-1906_11615303

band gap of less than 1.8 eV with suitably positioned HOMO and LUMO level (as difference between HOMO of donor and LUMO of acceptor directly proportional to V_{OC}), deeper HOMO level for better air stability, hole mobility in the order of 10^{-2} to 10^{-3} $cm^2V^{-1}s^{-1}$, better solubility along with enhanced film forming property in common organic solvents. All of the above characteristics within a CP directly affect solar cell parameters like Jsc, V_{OC}, FF, PCE (definition given in chapter 1) and significant improvement of PSC performance by modifying structure have been witnessed in recent years. But limiting PCE and photodegradation nature on exposure to ultraviolet radiation in presence of oxygen and moisture limit these CPs to be used for commercial application. Hence detail and progressive study about them are highly essential for in depth understanding of structure property relationship.

Chapter 2: Photo stability enhancement of poly(3-hexylthiophene)-PCBM nano-composites by addition of multi walled carbon nanotubes under ambient conditions

Even though widely used poly(3-hexylthiophene):phenyl-C61-butyric acid methyl ester (P3HT-PCBM) composites for optoelectronic devices, especially bulk-heterojunction (BHJ) solar cells could give efficient polymer solar cells with 4-5% PCE, a major problem of photo stability is associated with it and remains unsolved. P3HT-PCBM composite was found to be degrading on irradiation with ultraviolet radiation or a solar simulator providing AM 1.5G illumination (1000 Wm^{-2}, 72 ± 2 °C or 330 Wm^{-2}, 25 °C), in presence of oxygen and moisture. It is important to stabilize the P3HT-PCBM binary mixture which is the most frequently used composite for BHJ solar cells. Herein, a systematic study has been performed on the photo stability of this binary mixture in the presence of MWCNT at various ratios and optimized the conditions that could be utilized for fabricating photovoltaic devices even under ambient conditions. The P3HT-PCBM binary mixture was converted to a ternary composite by sonicating with MWCNT, (Figure 3a and 4a) maintaining the total amount of carbon nanomaterial (PCBM-MWCNT) within 10% (w/w). It was found that P3HT-PCBM (7%)-MWCNT (3%) is a better photo stable composite than P3HT and P3HT-PCBM (10%) even on extended UV exposure under ambient conditions (Figure 3b and 4a). UV-visible (solution and film), fluorescence spectral analysis and transmission electron micrograph (TEM) with selected area electron diffraction (SAED) pattern have been used as a tool to study the photo stability (Figure 4b and 4c).

TH-1906_11615303

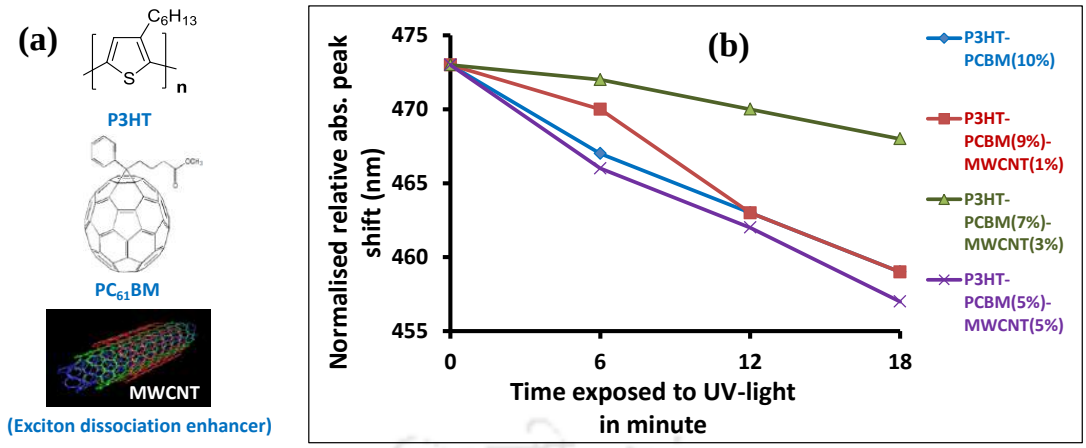

Figure 3 (a) Structures of polymer P3HT, $PC_{61}BM$ and MWCNT used for this study (b) solid state photodegradation comparison of composites of P3HT: PCBM: MWCNT shows high photostability for P3HT-PCBM (7%)-MWCNT (3%).

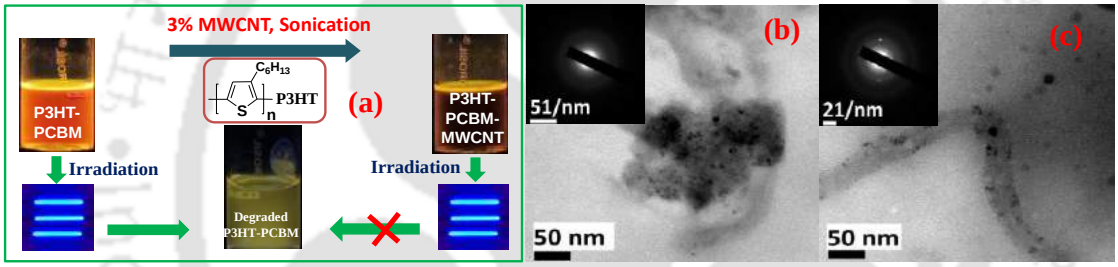

Figure 4 (a) Pictorial representation for photostability enhancement of P3HT-PCBM by MWCNT. TEM image confirming better photostability of composite (b) P3HT-PCBM (7%)-MWCNT (3%) (c) P3HT-PCBM (7%)-MWCNT (3%) degraded up to 20 minutes.

Chapter 3: Insight into the synthesis and fabrication of 5,6-*alt*-benzothiadiazole based D-π-A conjugated copolymers for bulk-heterojunction solar cell

In this approach two poly(o-arylene-vinylene) (POAV) type polymers, where benzothiadiazole (BT) has been attached alternatively to donor via two vinyl-bond (additional π-bond that can extend conjugation and reduce the dihedral angle between donor and acceptor) at 5 and 6 position of BT rather than commonly chosen 4 and 7 have been synthesized. Two extensively used hole transporting donor units: 3-hexylthiophene and 4,4-bis-(2-ethylhexyl)-4H-cyclopenta[2,1-*b*;3,4-*b'*]-dithiophene have been chosen, to obtain 5,6-*alt*-BT based D-π-A type polymers and to give an insight into its potential as a donor in a BHJ solar cell (Figure 5a). POAV polymers show bi-humped UV-visible

TH-1906_11615303

(Figure 5b) spectra as like D-A polymers. POAV CPs have been used as donor to fabricate solar cells, with a device structure ITO/PEDOT:PSS/P1orP2-$PC_{61}BM$ or $PC_{71}BM$ /Al or Ca:Al. Without annealing or use of additives, maximum V_{OC} of 0.68 V, fill factor of 30.2%, quantum efficiency of 22% (Figure 6b) and maximum power conversion efficiency (PCE) of 0.76% have been achieved with P2 (Figure 6a). In similar device configuration with P1 PCE was 0.34% (Figure 6a). This approach makes o-arylene kind of (POAV) polymer useful for optoelectronic application with commonly used fullerene/non-fullerene derivatives as acceptor, where an appropriate phase separation between donor and acceptor is an important factor for charge separation.

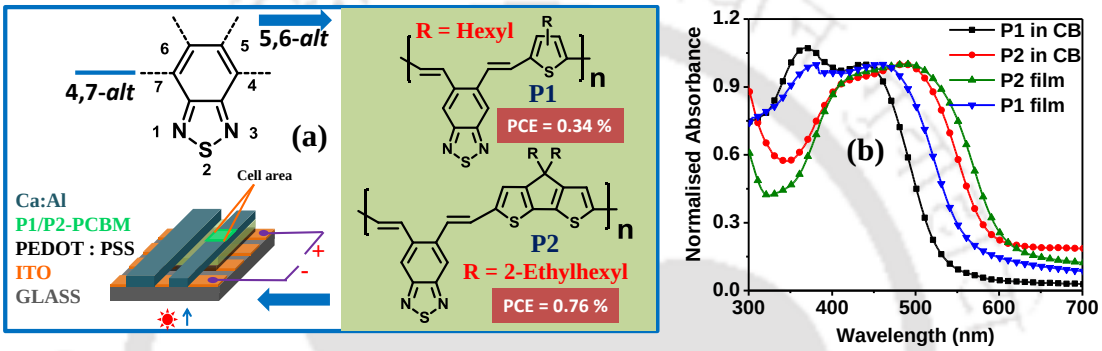

Figure 5 (a) Schematic representation for design, synthesis of 5,6-*alt*-BT-based polymer and its solar cell performance investigation. (b) UV-visible spectra for synthesized POAV type polymer, both in solution and in film state.

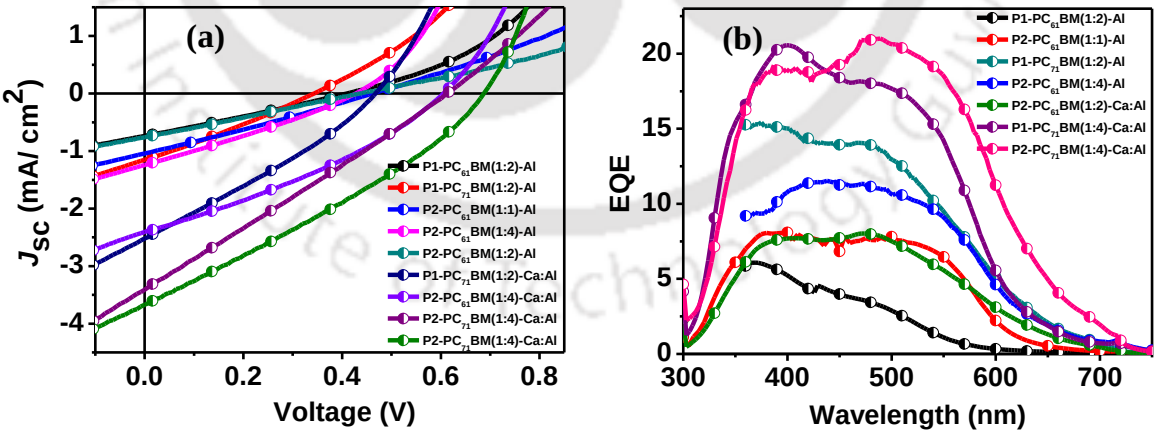

Figure 6 (a) J-V curve (b) external quantum efficiency for POAV type polymer.

TH-1906_11615303

Chapter 4: Substituting non-conjugating ester group into side chain of benzothiadiazole improves optical, electrochemical properties, morphology of active layer and solar cell performance of D-A polymer for photovoltaics

Herein, the effect of non-conjugated ester functionalization at 5,6-position of 2,1,3-benzothiadaizole (BT) in donor (D)-acceptor (A) polymer used for photovoltaic devices has been investigated. Position 5 and 6 of BT have been functionalized with methyl acetate group and its structure property relationship have been compared with BT having methyl group at 5,6-positions using four types of D-A polymers (Figure 7a). Alternate co-polymers of newly synthesized methyl and methyl acetate derivatives of BT and Th-BT-Th with commonly used donors such as dithiophene (DTh) and benzodithiophene (BDT) have been synthesized using Stille coupling reaction, namely P(1,2,3,4)-Me and P(1,2,3,4)-Ac. Synthesized ester functionalized polymers stable up to 250 °C (Figure 9a). It has been studied that side chain ester group lowers the dihedral angle, improves optical (Figure 7b) and electrochemical properties of CPs used for PSC, improves phase separation of active layer (Figure 9b to e) and solar cell performance of fabricated PSC compared to its methyl counterpart, as investigated between P(1,2.3,4)-Me and P(1,2,3,4)-Ac. On fabrication of BHJ solar cell with device configuration **ITO/PEDOT:PSS/P-PC$_{71}$BM/LiF/Al**, polymer having methyl acetate functionalization such as P2-Ac, P3-Ac and P4-Ac results in higher PCE of 1.36%, 1.17 % and 0.35% compared to their methyl counterpart P2-Me, P3-Me and P4-Me with PCE of 0.9%, 0.54% and 0.17% respectively (Figure 8a). With 1,8-diiodooctane (DIO) as additive, a PCE of 1.96% has been achieved with P3-Ac with a EQE of 36% (Figure 8b).

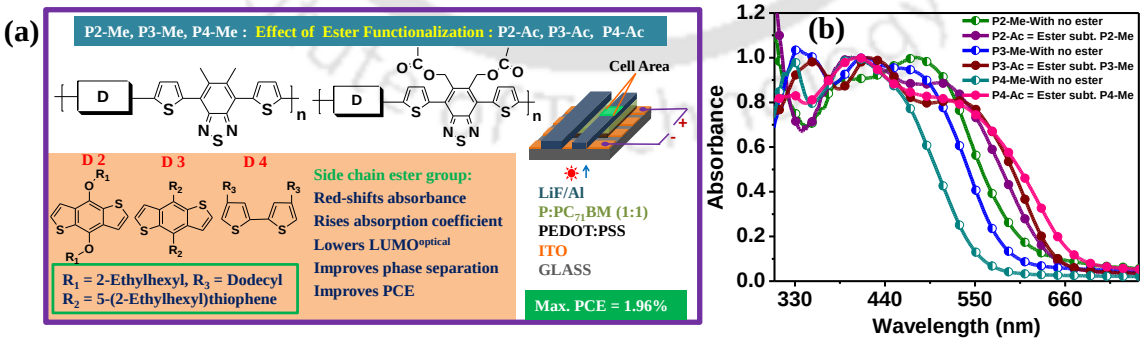

Figure 7 (a) Schematic representation and collective superior performance of ester group at position 5 and 6 of BT as side chain and over methyl (b) thin film UV-visible spectra.

TH-1906_11615303

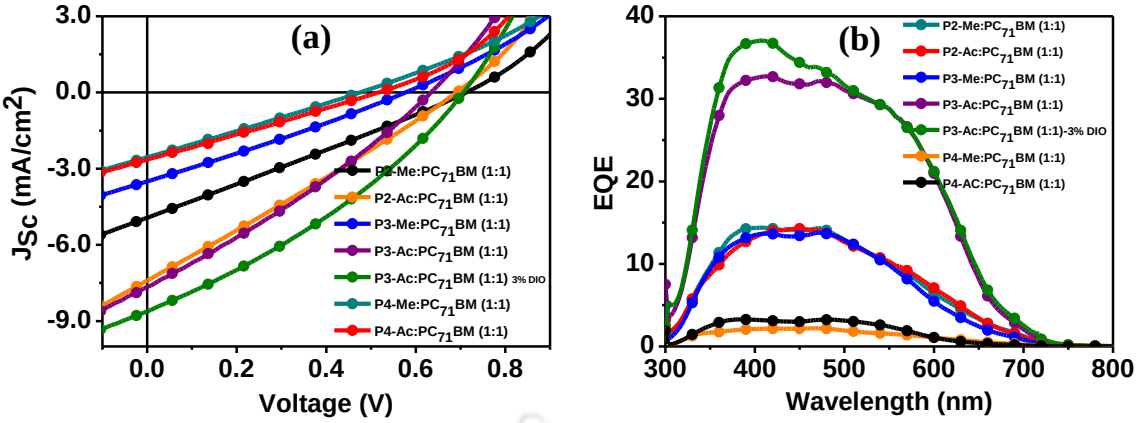

Figure 8 (a) J-V curve for fabricated solar cells (b) external quantum efficiency.

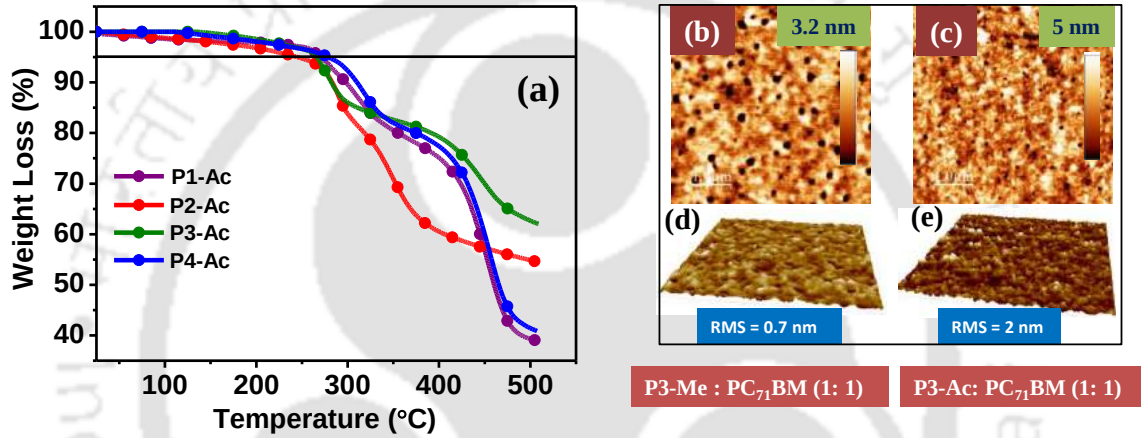

Figure 9 (a) TGA spectra showing thermal stability up to 250 °C for ester substituting polymers. (b to e) improved morphology for methyl acetate substituting polymers compared to their methyl counterpart.

Chapter 5: 6,7-Di(thiophen-2-yl)naphtho[2,3-c][1,2,5]thiadiazole and 4,6,7,9-tetra(thiophen-2-yl)naphtho[2,3-c][1,2,5]thiadiazole as new acceptor units for D-A type co-polymer towards fabrication of polymer solar cell

This work emphasize on the synthesis of two new acceptor units for donor (D)-acceptor (A)-based polymers used in photovoltaic devices, namely 4,9-dibromo-6,7-di(thiophen-2-yl)naphtho[2,3-c][1,2,5]thiadiazole [a derivative of naphtho[2,3-c][1,2,5]thiadiazole (NT), substituted with two thiophene (Th) units on 6 and 7 position of it (NT-Th)] and 4,9-bis(5-bromothiophen-2-yl)-6,7-di(thiophen-2-yl)naphtho[2,3-c][1,2,5]thiadiazole (Th-NT-Th) with two additional Th units substituted at 4,7 position of NT-Th. Both the NT-based acceptors have been designed using 5,6-position of benzothiadiazole (BT) and synthesized by Wittig coupling reaction. Alternate D-A co-polymer of new NT-based

TH-1906_11615303

acceptors with commonly used donor 4,8-bis((2-ethylhexyl)oxy)benzo[1,2-b:4,5-b´]dithiophene (BDT) via Stille coupling results new conjugated polymers (CPs) namely **P(BDT-NTTh)** and **P(BDT-ThNTTh)**. Newly synthesized acceptor units distinguishes itself from existing literature of naphtho[2,3-c][1,2,5]thiadiazole (NT) acceptor in having additional two Th units attached at 6,7 position of NT, imparting into it a 2-dimensional (2D) type of conjugated structure (Figure 10a). Both **P(BDT-NTTh)** and **P(BDT-ThNTTh)** have ICT band in 700 to 800 nm region (Figure 10b) a necessary requirement for a CP for PSC. Photovoltaic performance of both the CPs has been investigated by fabricating BHJ solar cell with configuration **ITO/PEDOT:PSS/Polymer-PC$_{71}$BM/LiF/Al**, which results a PCE of 0.34% and 1.31% with **P(BDT-NTTh)** and **P(BDT-ThNTTh)** respectively (Figure 11a and 11b). Hole-mobility for blend of **P(BDT-NTTh)** and **P(BDT-ThNTTh)** with PC$_{71}$BM have been calculated using space charge limited current (SCLC) method by fabricating hole only devices with configuration **ITO/PEDOT:PSS/Polymer-PC$_{71}$BM/Cu** and results mobility of $2.2*10^{-6}$ and $1.5*10^{-5}$ $cm^2V^{-1}s^{-1}$ respectively.

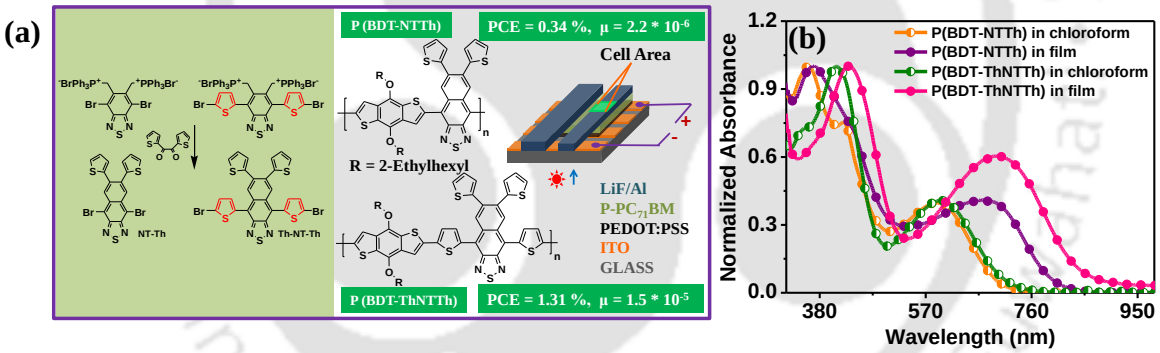

Figure 10 Schematic representations for synthesis of NT-based new acceptors and polymers with PSC performance (a) UV-visible spectra in chloroform and film.

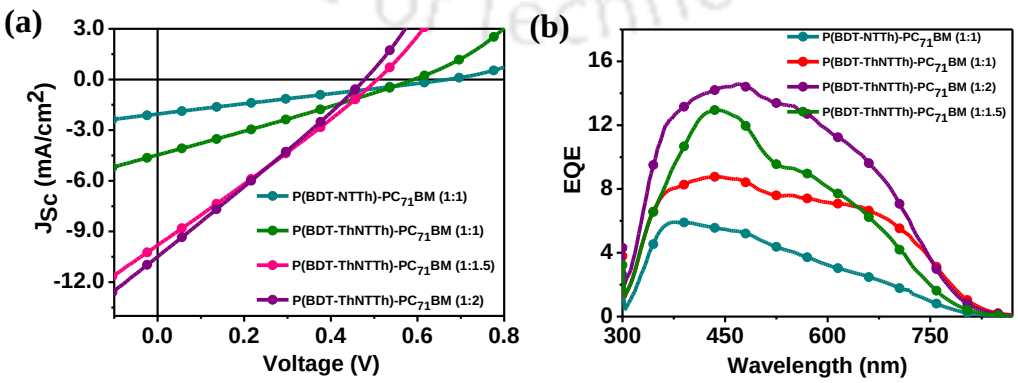

Figure 11 Solar cell performance of NT based polymers (a) J-V curve (b) EQE spectra.

TH-1906_11615303

Conclusion and thesis overview

Here effort has been given to investigate further, on structural change leading to change in optoelectronic property by synthesizing newer acceptor units using with 5,6-position of BT. Synthesized acceptor units for donor (D)-acceptor (A)-based conjugated polymers used in photovoltaic devices are 4,9-dibromo-6,7-di(thiophen-2-yl)naphtho[2,3-c][1,2,5]thiadiazole(NT-Th), 4,9-bis(5-bromothiophen-2-yl)-6,7-di(thiophen-2-yl)naphtho[2,3-c][1,2,5]thiadiazole (Th-NT-Th) and (4,7-bis(5-bromothiophen-2-yl)benzo[c][1,2,5]thiadiazole-5,6-diyl)bis(methylene)diacetate. Further efforts have been given towards durability measures for blend of thiophene containing donor polymer and acceptor used for solar cell fabrication (such as PCBM), by preparing composites with MWCNT. Such systems can be used to bring high performance material with improved photo stability for future optoelectronic application.

TH-1906_11615303

Chapter 1

Introduction: An Overview of Conjugated Polymers and Solar Cell

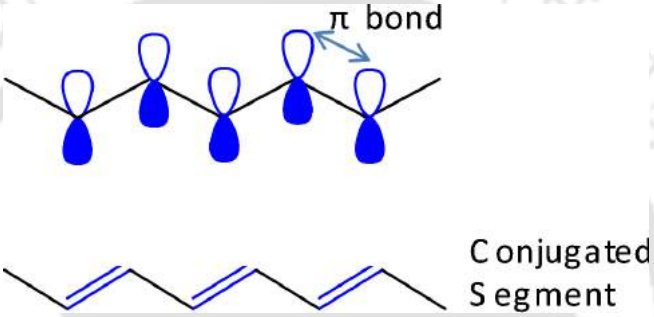

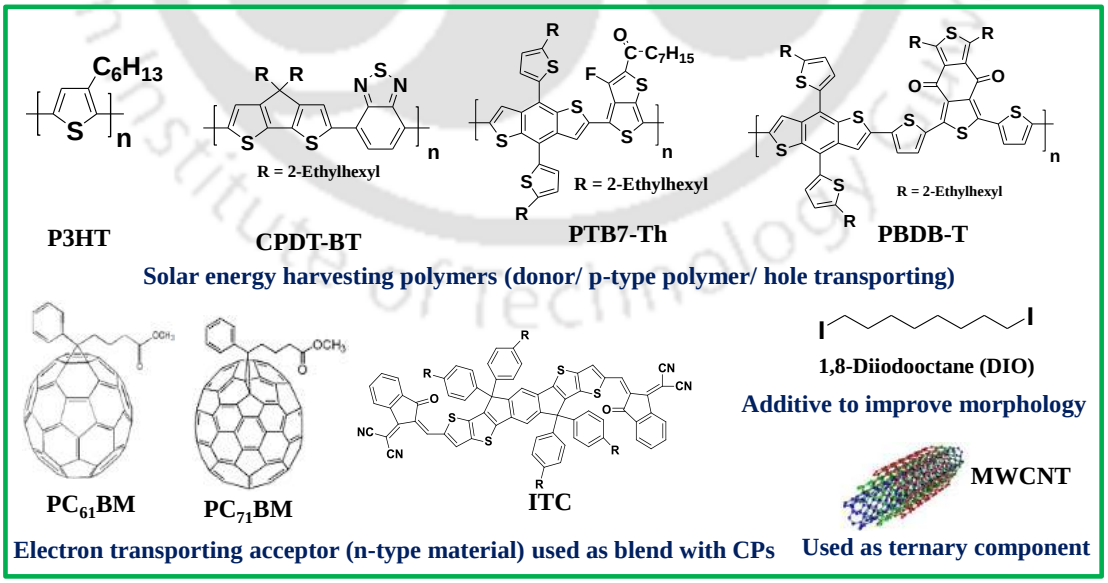

TH-1906_11615303

1.1 Introduction

1.1.1 Discovery of conjugated polymer

Conjugated polymers (CPs) are an important class of materials which are used in a wide variety of applications. In 1977, it was first discovered that chemical doping of polyacetylene causes several order enhancement of electrical conductivity.[1] It was believed that stable charge-transfer π complex was formed during the halogen doping. This great contribution was made by Hideki Shirakawa of the University of Tsukuba in Japan, Alan MacDiarmid of the University of Pennsylvania at Philadelphia and Alan Heeger of the University of California at Santa Barbara and this led them to get Nobel Prize in chemistry in the year 2000. CPs are unsaturated organic macromolecules having alternating saturated and unsaturated bonds along the backbone. All CPs consist of σ-bonds through the overlapping sp^2 hybrid orbitals and the remaining out-of plane p_z orbitals which overlaps with neighboring p_z orbitals and forms π-bonds. Therefore, the electrons that constitute the π-bonds are delocalized over the entire polymer backbone even though the chemical structures of CPs are presented as alternating single and double bonds. These continuous delocalized π-bonds along the backbone was the origin of the absorbance, emissive property and conductive property of CPs. CPs can be obtained with a variety of backbone structures, such as poly(acetylene) (PA),[2] poly(para-phenylenes) (PPP),[3] poly(para-phenylene vinylene) (PPV),[4] poly(para-phenylene ethynylene) (PPE),[5] polythiophene (PT),[6] polypyrrole (PPy),[2] polyaniline (PANI)[7] and polyfluorene (PF)[8] as shown in Figure 1.1. Because of the significant photophysical and electrochemical properties, CPs have been synthesized and investigated extensively as an active material in light emitting diodes (LEDs),[9] light-emitting electrochemical cells,[10] plastic lasers,[11] sensors,[12] field effect transistors,[13] and solar cells.[14]

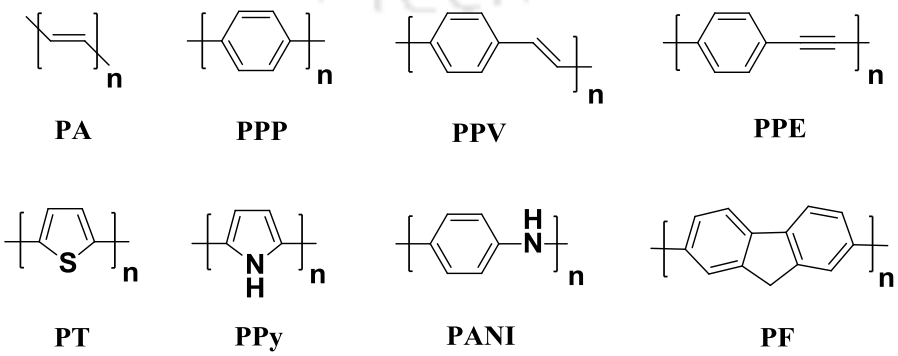

Figure 1.1 Molecular structure of some commonly used CPs.

TH-1906_11615303

1.1.2 Solar cell

Energy crisis is one of the major issues the world is facing due to high production cost and deficit of raw materials like coal, water, gasoline and fossil fuel. Even though the present source of energy is dependent on above listed sources the day is not far that our entire source of raw material (used to produce electricity) available on earth's crust will cease to exist one day. In the present situation solar cell which converts directly solar light to electricity, has evolved as an alternate renewable technology for production of electricity with no cost of raw material. Solar cell operates as per the photovoltaic effect (discovered in 1839 by Edmund Becquerel a French experimental physicist, who experimented with an electrolytic cell made up of two metal electrodes): certain materials produced small amounts of electric current when exposed to light. In 1905, Einstein explained the photoelectric effect (when photons in the UV range are illuminated on a metal surface, free electrons escape from the metal surface due to excitation energy from the incident light) (Figure 1.2a), which established the foundation for a theoretical understanding of the photovoltaic effect. In most cases, when absorbed photons in a material pump ground state electrons to the excited state, the excited electrons promptly relax to the ground state. However, in photovoltaic devices, the excited electrons and the produced hole in the ground state should be collected separately to produce electricity (Figure 1.2b).

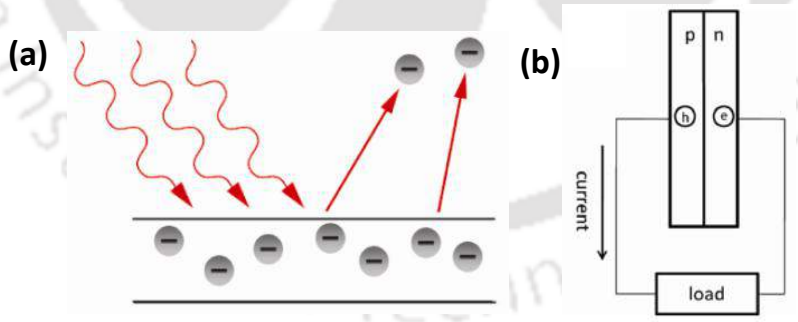

Figure 1.2 (a) Photoelectric effect (b) photovoltaic effect (figures taken from e-source).

1.1.2.1 Characterizations and parameters of solar cell

1.1.2.1.1 Current-Voltage characteristics (I-V curve)

Solar cell device is basically a diode, where in-between two electrodes (cathode and anode) a material having distinct band gap that matches with solar photo flux received by

TH-1906_11615303

earth has been sandwiched. I-V curve of solar cell follows a diode curve in dark (no solar radiation falls on it), with voltage V and current I_{Dark} (Figure 1.3). When solar photons shine on it, the I-V curve shrinks down to fourth quadrant and power can be extracted from the cell. As power generate, hence the convention is negative. With intense solar radiation the I-V curve shifts more to the fourth quadrant (more power can be generated).

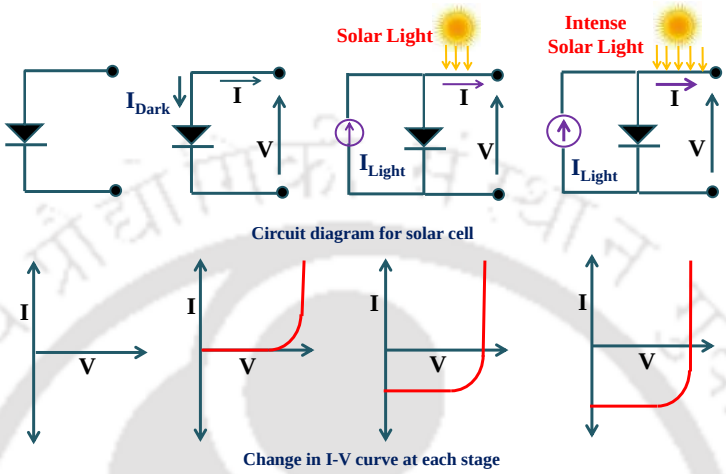

Figure 1.3 Current-Voltage **(**I-V) curve of solar cell.

1.1.2.1.2 Current (I_{sc}) and Voltage (V_{oc}) from a solar cell

I_{sc} is the current through the solar cell when the voltage across the solar cell is zero and when the solar cell is short circuited, hence it is called short circuit current. It is the maximum possible current that can be drawn from the cell. It depends upon many factors like: (i) the area of the solar cell; it has been seen with small area of the cell that the short-circuit current is high, to remove the dependence solar cell performance on active layer area, it is generally represented as short-circuit current density (J_{sc}) (unit, mA/cm^2) rather than the short-circuit current (mA); (ii) I_{sc} from a solar cell is directly dependent on the light intensity (which related to number of photons and power of incident light); and (iii) absorption and reflection of the solar cell. Moreover, the open-circuit voltage (V_{oc}) is the maximum voltage available from a solar cell, at zero current.

1.1.2.1.3 Fill factor (FF)

FF is defined as the ratio of the maximum power from the solar cell to the product of V_{oc} and I_{sc} (maximum power possible theoretically). Graphically, the FF is a measure of the squareness of the I-V curve (Figure 1.4a and 1.4b) of solar cell and is also the area of the largest rectangle which will fit in the I-V curve.

TH-1906_11615303

% of FF = (Maximum power (P_m)/Theoretical power (P_T))*100

= [(I_{max} X V_{max})/(I_{sc} X V_{oc})]*100

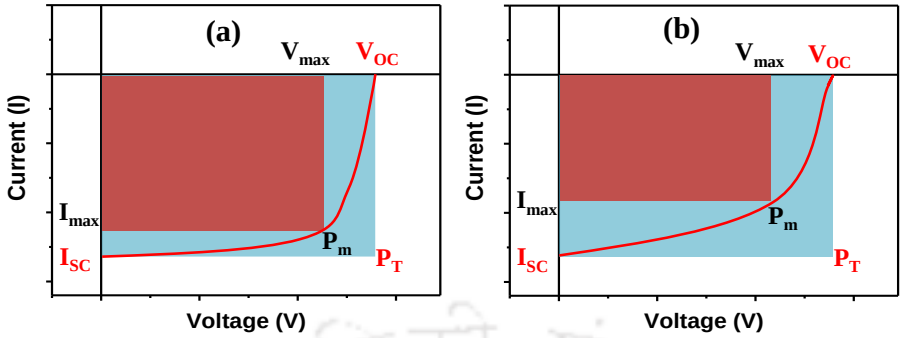

Figure 1.4 Fill factor of solar cell (a) I-V curve with high FF (b) I-V curve with low FF.

1.1.2.1.4 External quantum efficiency (EQE)

EQE is the ratio of the number of carriers collected by the solar cell to the number of photons of a given energy incident on the solar cell (graphically described in Figure 1.5).

EQE = [(collected electrons per second)/(incident photons per second)]*100

= [(current generated/energy of one electron)/(total power of photons/energy of one photon)]*100

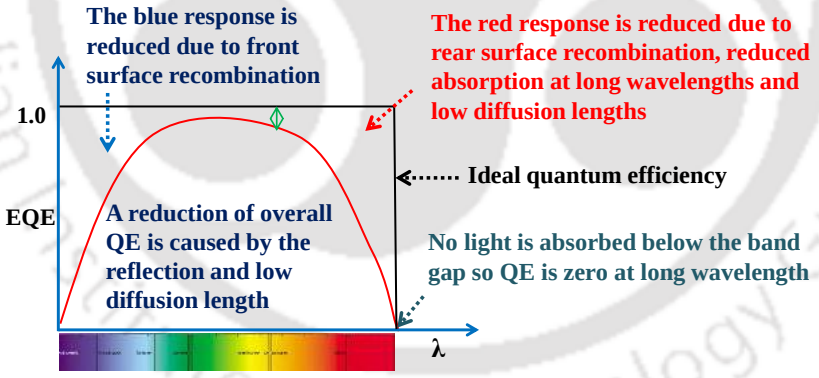

Figure 1.5 External quantum efficiency of solar cell.

1.1.2.1.5 Efficiency of a solar cell (power conversion efficiency, PCE)

Efficiency of solar cell is defined as the ratio of energy output (P_{out}) from the solar cell to input energy from the sun (P_{in}), generally represented in percentage.

$$PCE = [P_{out}/P_{in}]*100 = [(I_{max}*V_{max})/P_{in}]*100 = [(FF*V_{oc}*I_{sc})/P_{in}]*100$$

1.1.2.1.6 Shockley–Queisser (SQ) limit

TH-1906_11615303

Shockley–Queisser limit has been discussed at the end of the thesis in page no 149.

1.1.2.2 Types of solar cell

Various solar cells have been categorized into three main generations of solar cells: (1) **first generation solar cell,** mainly refers to silicon/germanium semiconductor-based solar cell[15] and is being used for household purpose, street lights (mainly comprising of crystalline silicon); **second generation solar cell,** mostly having CdS/CdTe, CdS/Cu (In, Ga)S_2 and hydrogenated amorphous silicon (Si: H)[16] as a semiconducting material (here the cost of material was reduced as compared to crystalline-silicon based solar cell); **third generation solar cell,** mainly classified into (i) polymer solar cell,[17] (ii) dye-sensitized solar cell,[18] (iii) perovskite solar cell,[19] (iv) quantum dot solar cell[20] and (v) hybrid solar cells (comprising two or many components as semiconducting material).[21,22] Third generation solar cells are widely studied in recent time with large number of research articles published in last decade, because of their advantage of low cost, ease of fabrication technique, light weight, flexibility and comparable efficiency to silicon solar cell. To have a broad understanding about solar cell devices, here discussion on four major types of solar cell devices has been briefed.

1.1.2.2.1 p-n Junction semiconductor solar cell

The photovoltaic effect was experimentally demonstrated first by French physicist Edmond Becquerel and in 1839 he built the world's first photovoltaic cell. Later, In 1883 Charles Fritts built the first solid state photovoltaic cell by coating the semiconductor selenium with a thin layer of gold to form the junctions; the device was only around 1% efficient. Practical application of photovoltaic cell was publicly demonstrated on 25 April 1954 at Bell Laboratories by Daryl Chapin, Calvin Souther Fuller and Gerald Pearson and finally solar cells gained prominence after incorporation onto the 1958 Vanguard I satellite by United States of America. The conventional solar cell is silicon (Si) semiconductor-based (silicon doped phosphorous (n-type) in junction with silicon doped boron (p-type) solar cell, although other types of semiconductor junctions have been experimented. Later, it has been developed by various groups and this mostly used solar cell with practical PCE of 14% and has been applied in many house hold purpose (Figure 1.6c). Gallium-Arsenide (Ga-As) semiconductor based solar cell used mostly for space applications (satellite) is another important form of semiconductor solar cell which

TH-1906_11615303

attracts attention with practical PCE of 19%. But the high cost of Ga and Si based solar cell are due to molecular beam epitaxy (MBE) used for thin film deposition of crystalline silicon/gallium; and limits frequent use of such solar cell. Mechanistically a silicon solar cell operates like a p-n junction. The solar harvesting layer is a combination of p-type semiconductor, called base (silicon doped phosphorous) and a n-type semiconductor, called emitter (silicon doped with boron). The active layer is sandwiched with an anode (generally ITO) and a cathode (generally Al). The exciton formed gets separated by the depletion layer caused by the p-n junction (as shown in Figure 1.6a and 1.6b), with electron moved to anode and hole to cathode (http://www.pveducation.org/pvcdrom).

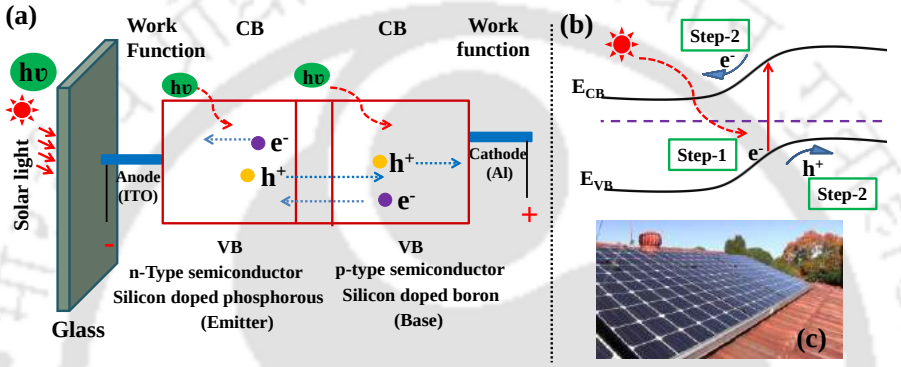

Figure 1.6 Mechanism of silicon solar cell (a) transport of generated hole and electrons to respective electrode (b) excitation of electron from ground state by solar photons to generate exciton (c) a silicon solar cell mounted on roof top.

1.1.2.2.2 Polymer solar cell (PSC)

Polymer solar cells (PSCs) with solution processable polymer-fullerene blend as active layer to harvest solar energy has gained momentum[23,24] in last 10 to 15 years to replace silicon solar cell. The concept[25] of aromatic heterocyclic based semiconducting polymers to be used as solar harvesting material was first implemented in 1995 by Gang Yu from China along with Alan J. Heeger by using MEH-PPV/$PC_{61}BM$ as active layer to harvest solar photons, which showed a PCE of 0.95%[26] and established semiconducting organic polymers as alternative promising candidate for solar cell. Later, in 2003 P3HT-$PC_{61}BM$ based solar cell[27] has been fabricated by F. Padinger and co-workers from Austria, who achieved a PCE of 3.5%. Further use of P(CPDT-BT)-PCBM as active layer[28] material by Jin Y. Kim and Alan J. Heeger in 2007, along with P3HT-PCBM in tandem configuration of device structure with PCE of 6.5%, proved polymer solar cell a promising alternate cost effective approach. To date a PCE of 13% has been achieved[29] and day by day it is

TH-1906_11615303

improving to reach to a stage of >15%, to be able to fabricate in industry.[30] Mechanistically when solar light strikes on PSC, exciton generates within polymer layer (called donor, p-type polymer, which largely harvest solar photons) and subsequently due to the available low energy level by the fullerene derivative (acceptor, n-type material), the donor transfers its excited electron to acceptor, hence exciton gets separated and collected at respective electrode (Figure 1.7 shows stepwise mechanism of PSC).[31]

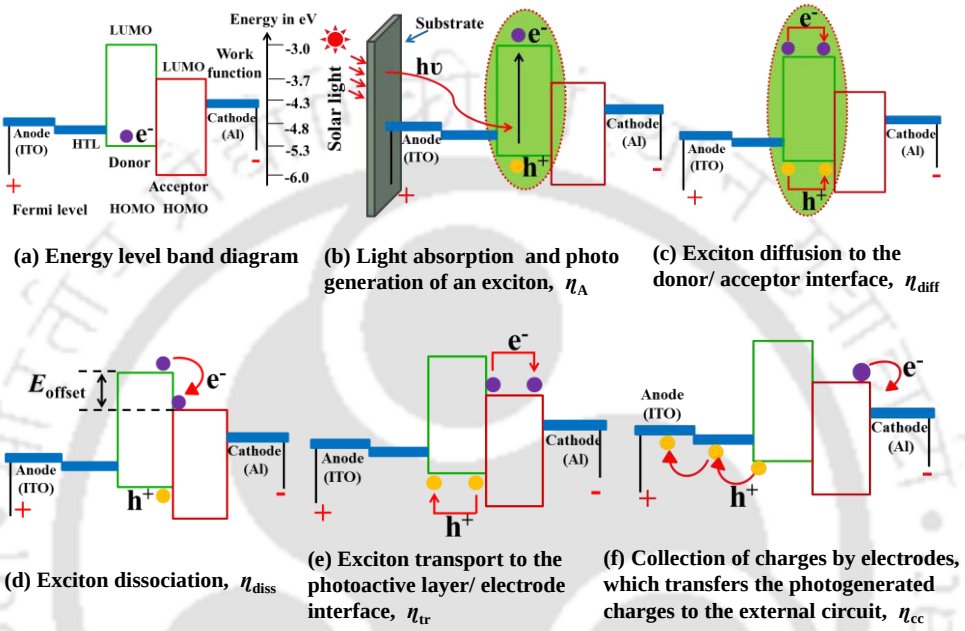

Figure 1.7 General device geometry and mechanism of PSC (η refers to efficiency).

1.1.2.2.3 Dye-sensitized solar cell (DSSC)

Few drawbacks of polymer solar cell are low PCE and low work function metal used as cathode are unstable in ambient conditions, which makes necessity use of expensive inert atmosphere glove box. To reduce cost of solar cell to lowest possible number and improve the PCE, DSSC have been engineered. First DSSC was reported in 1991 by various researchers from Swiss Federal Institute of Technology[32] and later, in 2006 first solid state dye sensitized solar cell was reported by Rossier Iten from Switzerland with use of hole transporting layer (HTL). Though DSSC produce a high PCE than polymer solar cell, but the use of I_2/LiI electrolyte reduces its life time half the number (~4 years) than polymer solar cell (~7 years) and use of high temperature calcination for deposition of TiO_2 layer makes it unsuitable to fabricate on flexible substrate. Mechanistically (Figure 1.8) the dye layer absorbs solar photons and transfers the formed exciton to TiO_2 layer, followed by transporting to anode. The generated hole on dye HOMO gets filled by

TH-1906_11615303

the electrolyte I_2/LiI oxidation which further gets reduced by H_2PtCl_4. (https://www.gamry.com/assets/Uploads/Dye-Solar-Cells-05-19-2015-Part-1-App-Note.pdf).

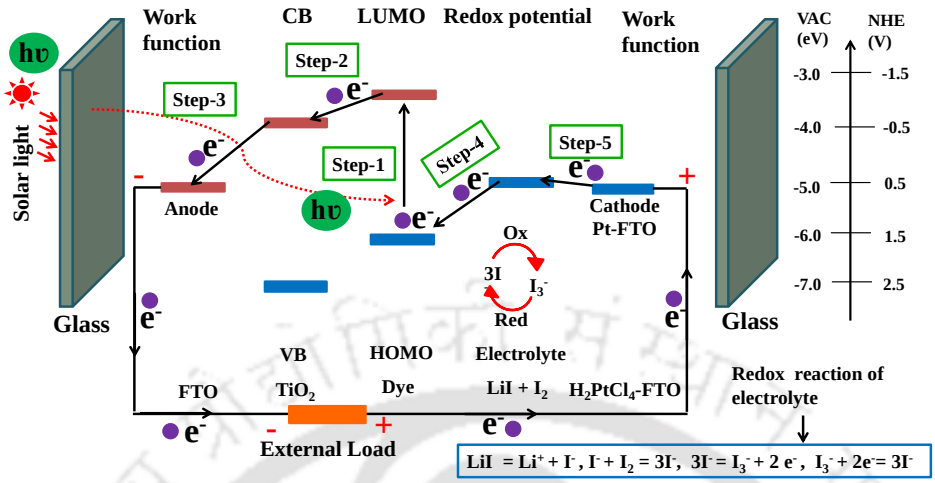

Figure 1.8 Device geometry and mechanism of dye-sensitized solar cell.

1.1.2.2.4 Perovskite solar cell

The first use of perovskite into solar cell[33] was reported by Miyasaka et al. in 2009 with PCE of 3.8%. Breakthrough result came in 2016 with PCE of ~20%.[19] In the present day PCE of perovskite solar cell are in the range to replace traditional silicon solar cell. But the instability (life time about 1 year[34]) of perovskites limits its use for practical purpose.[35] Mechanistically, a perovskite solar cell operates as shown in Figure 1.9.

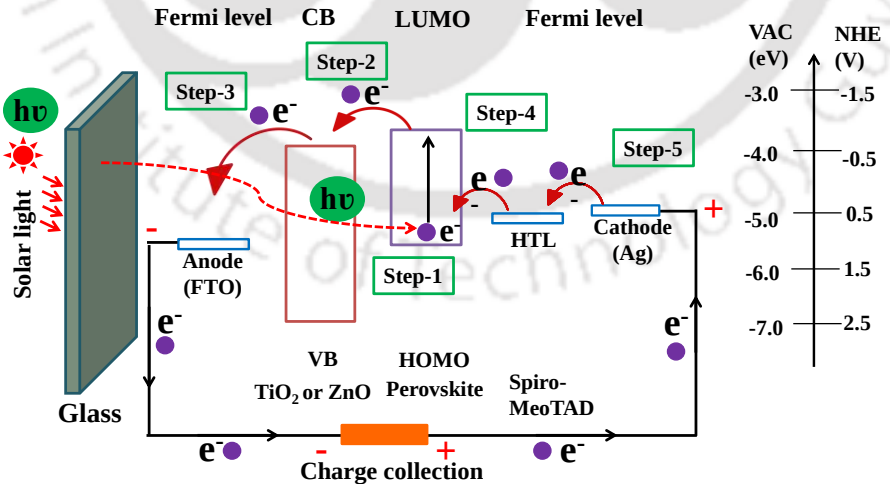

Figure 1.9 A Conventional device geometry and mechanism of perovskite solar cell.

TH-1906_11615303

1.1.3 Designing conjugated polymers for solar cell

In research articles appearing recently, PSCs have gained much attention owing to its several advantages such as large area solution processability,[36] band gap tuning on polymer backbone,[37-39] morphological tunability that leads to improved device performance[40] and amorphous nature of polymer that allow fabrication on light weight flexible substrates.[41] PSC harvest solar photons with no cost using a CP with defined band gap and converts it to electrical energy in a mechanically fabricated device. Design and synthesis of new CPs and detailed progressive study about them are most crucial to have an in-depth understanding on structure property relationship and to fulfill the target of low cost, durable and flexible solar cell for future source of energy.[30]

For polymer solar cell, designing CPs with a π-electron donor (D) and an π-electron acceptor (A), either as D-A/[42]D-A-D/[43]D-π-A[44] type of design has been of great interest.[45,46] π-Electron acceptors are generally a heterocyclic compound with C=N or N=S bond[47] such as 2,1,3-benzothiadiazole (BT), thieno[3,4-b]pyrazine (Tp), quinoxaline (Q) and π-electron donors are in general, sulphur containing heterocyclic and/or cyclic compound devoid of C=N and N=S bond such as thiophene (Th), cyclopentadithiophene (CPDT), benzo[1,2-b:4,5-b´]dithiophene (BDT), fluorene (FL), carbazole (Cz). Among various designs, D-A and D-A-D type of design has been proved to be very promising in achieving high solar cell performance with polymer based solar harvester and numerous report of such D-A design have guided understanding of structure property relationship between conjugated units and helps reaching the PCE to a number 11-13%.[29,48,49] Not only for solar cell, the above listed framework based CPs have been used for other organic electronic devices like polymer light emitting diodes (PLEDs)[50] and organic field effect transistor (OFET)[51,52] as well.

For any efficient and durable bulk heterojunction (BHJ) photovoltaic devices,[53,54] donor CPs synthesized from right combination of donor and acceptor having following property are highly desirable: (i) low dihedral angle along conjugation backbone, (a dihedral angle of $< 20^0$ are highly desirable)[55] for better ICT[56] from donor to acceptor, which results in bathochromic shift of absorption spectra to red-NIR (700-800 nm) region with high molar extinction coefficient[57] (need to make sure that minimum quantity of polymer is required to absorb high intensity of all solar spectrum); (ii) low band gap of less than 1.8 eV, with suitably positioned HOMO and LUMO level, for faster charge transfer from LUMO of

TH-1906_11615303

donor to LUMO of acceptor; (iii) deeper HOMO level, for better air stability[58] and high V_{oc} (as difference between HOMO of donor and LUMO of acceptor directly proportional to V_{oc}); (iv) hole mobility[59] in the order of 10^{-2} to 10^{-3} cm^2 V^{-1} s^{-1} with better solubility along with enhanced film forming property, for ease and faster charge transfer from donor to acceptor; (v) better π-π stacking in thin-film state between polymer backbone due to planarization[60] (rigidity), which leads to bi-continuous phase separation and reduces recombination in active layer, hence improves FF and J_{sc} and (vi) high tunability to external effect such as additives and high temperature annealing, which improves crystallinity of active layer.[61] All of the above characteristics within a CP directly affect J_{sc}, V_{oc}, FF and hence PCE.

1.1.3.1 Representative conjugated polymers for solar cell

Early research articles on PSC comprise of homo-polymers mainly of poly(3-alkyl-thiophene), P3AT. Later, D-A type of co-polymer was introduced which includes the combination of π-electron acceptor and π-electron donors with efficient ICT.

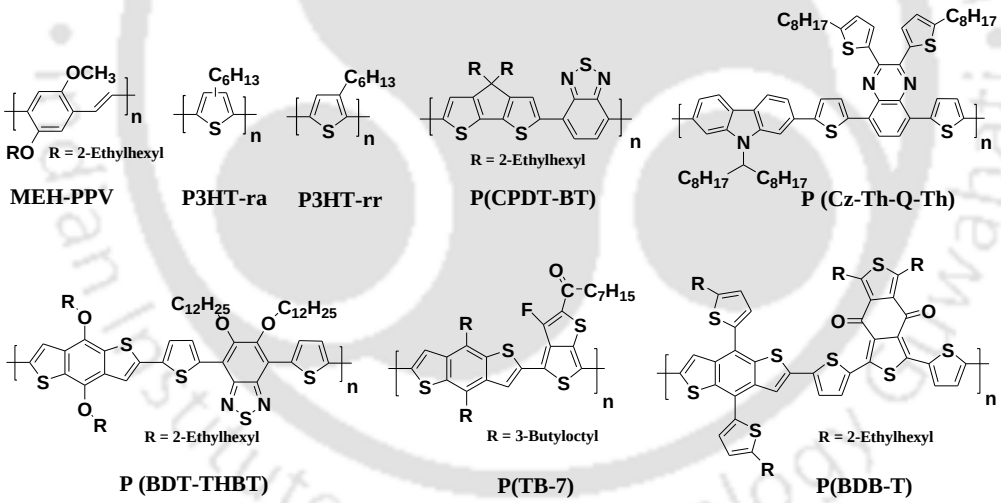

Figure 1.10 Representative conjugated polymers used for solar cell.

Using homo-polymers and D-A type of design, various polymers have been synthesized and fabricated as polymer solar cell, which are representative type and vastly studied polymers, commonly known as MEH-PPV,[26] P3HT-ra (regio-random),[62,63] P3HT-rr (regio-regular),[64] P(CPDT-BT),[65] [P(Cz-Th-BT-Th)],[66] P(BDT-THBT),[67] P(TB-7)[68] and P (BDB-T)[69] as shown in Figure 1.10.

TH-1906_11615303

Having P3AT type homo-polymer and D-A type of co-polymer as representative structure and taking advantage of fine tunability of polymer backbone, in last 10 to 15 years several CPs for solar cell have been synthesized which includes: (i) D-π-A type of design; (ii) to use different positions of various donors/acceptors as a site for main chain polymerization; (iii) two dimensional polymers, to extend the conjugation length further; (iv) fusing two near conjugated unit to bring planarity; (v) incorporating dipole moment changing electron withdrawing (EW) unit like fluorine, ester, aldehyde and ketone into the acceptor unit and varying combination among various donor and acceptors; (vi) substituting various non-conjugated functional group such as ester, alcohol and azide as side chain; (vii) varying alkyl chain, to change solubility; (viii) incorporating conjugated units to lower the dihedral angle along the polymer main chain; (ix) introducing alkyl chain on donor or acceptor side, to improve solubility in common organic solvents; (x) various newly designed CPs resulting from combinations of all those established structure-property relationship and concepts.

1.1.3.2 Donor-π-Acceptor (D-π-A) type of design (π refers to vinyl bond)

CPs with D-π-A framework have several advantages like: (i) additional π-bond that can extend conjugation to reduce the band gap which facilitates harvesting red-NIR radiation (ii) vinyl bond to reduce the dihedral angle between donor and acceptor, leading to more planar geometry in the conjugation main chain; (iii) moreover, incorporation of vinyl group into the polymer backbones provide rotational flexibility, which partially increases polymer solubility, allowing chromophore concentration to be increased (defined as the molecular weight ratio of conjugated backbone to solubilizing side chains). Generally D-π-A type of CPs comprise of poly-para-aryl (PPA) system and have been utilized in most of the commonly used D-A combination like P(Ph-π-Ph),[70] P(BDT-π-BT),[71] P(Cz-π-Tp),[72] P(Cz-π-Th),[73] P(Th-π-BT)[74] and P(CPDT-π-BT)[75] as shown in Figure 1.11.

In 2006 Leclerc and co-workers synthesized PPA type CPs for solar cell by Wittig reaction with carbazole as donor and thiophene as acceptor (P(Cz-π-Th)), where a PCE of 0.4% have been achieved with $PC_{61}BM$ as acceptor. Generally PPA polymers synthesized via Wittig polymerization suffers from low molecular weight leading to poor device performance. To address alternate approach to improve molecular weight, Stille coupling has also been performed by Reynolds group to synthesize P(Th-π-BT) in 2009 (PCE of

TH-1906_11615303

0.2% to 0.3% and Zhenan Bao group in 2010 to synthesized P(CPDT-π-BT) type polymer (PCE = 0.95%).

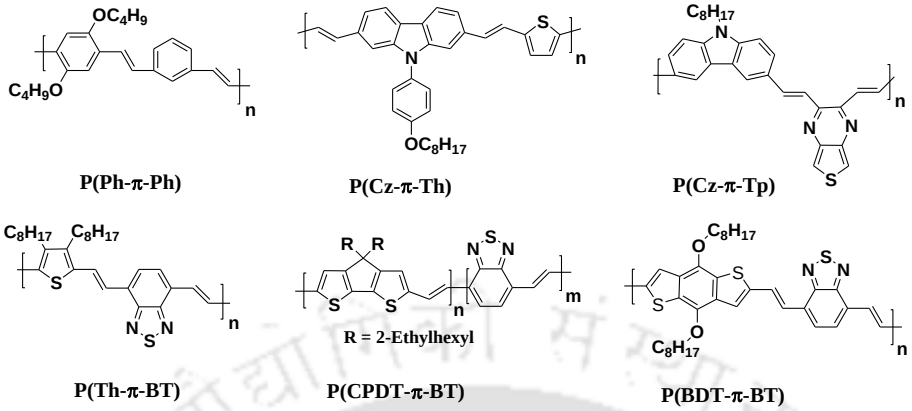

Figure 1.11 D-π-A-based polymers for solar cell (π refers to a vinyl bond).

Yet those high molecular weight polymers could not provide promising PCE for solar cell devices. So far the D-π-A based polymers for solar cell has not given any prominent PCE. Yet it remains in growing interest for researchers on D-π-A type of design for their advantages and need to be explored in future for better understanding of structure property relationship.

1.1.3.3 Use of different linkage position for polymerization

Changing position of aromatic conjugated unit for main chain polymerization also tune the optical property of CPs. This is very important to choose the right position, as ICT within D-A, planarity along conjugation backbone and the possibility of stabilization of polymer main chain by formation of quinoid structure can be varied by a change of position for co-polymerization in D-A polymers.

An important effort made by Zhen Li group in 2012, to understand linkage position influence on optical and optoelectronic properties of CPs. They have synthesized two monomers namely 10,13-bis(5-bromothiophen-2-yl)-11,12-bis(octyloxy)-dibenzo[a,c] phenazine **(M1)** and 2,7-bis(5-bromothiophen-2-yl)-11,12-bis(octyloxy)dibenzo-[a,c] phenazine **(M2),** followed by co-polymer of both the monomers with carbazole (Figure 1.12).[76] They found 120 nm red shift of absorbance in film for polymer (Cz-Th-M1-Th) compared to Cz-Th-M2-Th and PCE of 4.31% with Cz-Th-M1-Th compared to 0.64% with (Cz-Th-M2-Th). This happened because in M1, quinoid (Figure 1.12) structure was

TH-1906_11615303

more stabilized by the other aromatic groups but in M2 only one aromatic unit was stabilizing it (Figure 1.12).

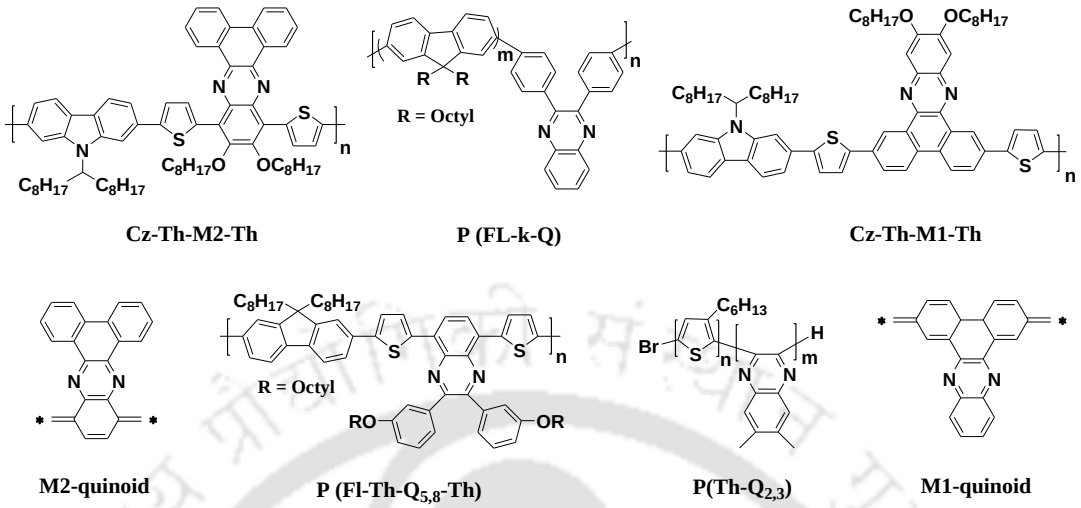

Figure 1.12 Designing D-A polymers by choosing different position for polymerization.

Likewise quinoxaline (Q) moiety has been used as an acceptor in D-A polymer with different linkage position for polymerization (as shown in Figure 1.12), which includes: (a) fluorene co-polymerized with quinoxaline group in a kinked position [P(FL-*k*-Q)][77] by Samson A. Jenekhe group in 2005, where because of kinked attachment of quinoxaline group the transport property improve without changing optical property (blue emission) of polyfluorene (PF); (b) rod-rod di-block copolymer by Zong Quan Wu et al. in 2013, with polymerization at 2,3-position of quinoxaline [P(Th-$Q_{2,3}$, Figure 1.12)],[78] where a tunable optical property with changing solvent has been established for the polymer; (c) the last one is the commonly chosen 5,8-position of quinoxaline and co-polymerized with fluorene[79] by Inganas et al. in 2006 (Figure 1.12, P(FL-Th-$Q_{5,8}$-Th).

1.1.3.4 Two-dimensional (2D) polymers

In a series of development of CPs for solar cell, two-dimensional (2D) polymers have been designed, with extended conjugation in side chain along with main chain conjugation. These extended conjugated structures contribute to the mobility and optical property for the polymers. The combination of donor and acceptor in D-A, D-A-D or D-π-A in linear fashion results in growing of conjugation in one direction (X-axis only) which is called one-dimensional (1D) polymer. 2D polymers used to have a main chain conjugation in X-axis and additional π-conjugation in Y-axis as well, together it works in two directional, to harvest more solar photons and have better hole-mobility.

TH-1906_11615303

In 2011 Songting Tan and co-workers synthesized a 2D-acceptor, where 2,5-dibromothiophene has been substituted on position '3' with a vinyl group followed by DTBT (dithiophene benzothiadiazole) group.[80] Polymer of this acceptor with BDT in D-A fashion gives a 2D-polymer (Figure 1.13.a), which has a broad absorption range (300 to 600 nm) and high hole-mobility ($2.2*10^{-4}$ cm^2 V^{-1} s^{-1}) compared to other BDT based polymer. Other representative 2D-polymers are BT-based polymer (Figure 1.13b)[81] synthesized by Zhi-Kuan Chen and Zhiyuan Xie group (Figure 1.13d)[82] in 2012.

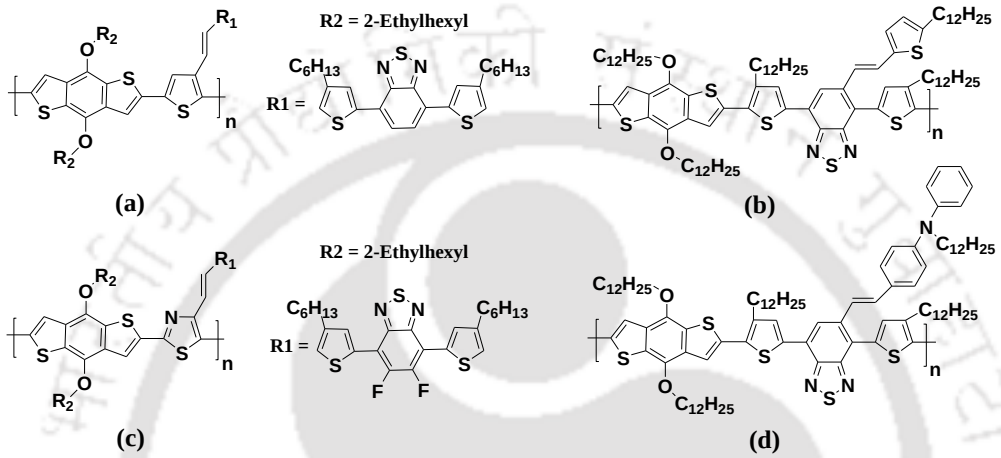

Figure 1.13 Two-dimensional (2D) polymers for solar cell.

Side conjugated unit of 2D-polymer can be modified to tune optoelectronic properties, as examined by Songting Tan et al. in 2013. They incorporated two fluorine atoms on the side conjugated unit of the 2D-system (Figure 1.12.c).[83] The PCE was improved to 3.75% compared to polymer with no fluorine atom on side conjugated unit. Moreover, design and use of CPs with extended conjugation does not limit to 2D polymers and solar cell only, rather star shaped polymers with extended conjugation in multi direction, has been used in solar cell (PSC)[84] and white polymer light emitting diode (WPLED) as well.[85]

1.1.3.5 Fusing two near conjugated unit to enhance rigidity/planarity

In addition, to existing donors and acceptors, newer donors and acceptors unit such as indaceno[1,2-b:5,6-b´]-dithiophene, indolo[3,2-b]carbazole, acenaphtho[1,2-b]quinoxaline and naphtho[1,2-c:5,6-c´]bis[1,2,5]thiadiazole have been synthesized, where aromatic units placed nearby have been fused by appropriate synthetic strategy, that leads to plane planarity in conjugation main chain. This is one the most important measures for improved ICT from D to A, with red shift of the absorbance and improved mobility.

TH-1906_11615303

8,11-Dibrormo-dithieno[2,3-a:3′,2′-c]phenazine is one such fused acceptors reported by Yong Cao et al. in 2011. Its co-polymer with fluorene as donor (Figure 1.14d) shows 74 nm red shift in UV-visible maxima (PCE = 4.4% and J_{sc} of 7.4 mA/cm^2) compared to non-fused counterpart, (Figure 1.14a) quinoxaline (PCE of 2.1% and J_{sc} of 4.7 mA/cm^2).[66] Again in 2011 Yong Cao group synthesized naphtho[1,2-c:5,6-c′]bis[1,2,5]thiadiazole-based new acceptor (having two BT ring fused, namely fused-2BT), (Figure 1.14.e) and co-polymerized with BDT as donor and compared its result with the BT counterpart (Figure 1.14b). They found a 150 nm red shift in absorption maximum in film casted from o-dichlorobenzene (DCB) with PCE of 6.0%, J_{sc} of 11.71 mA/cm^2, FF of 61% in D-A polymer with fused 2BT as acceptor compared to BT counterpart with PCE of 2.11%, J_{sc} of 5.8 mA/cm^2 and FF of 34.6%.[86]

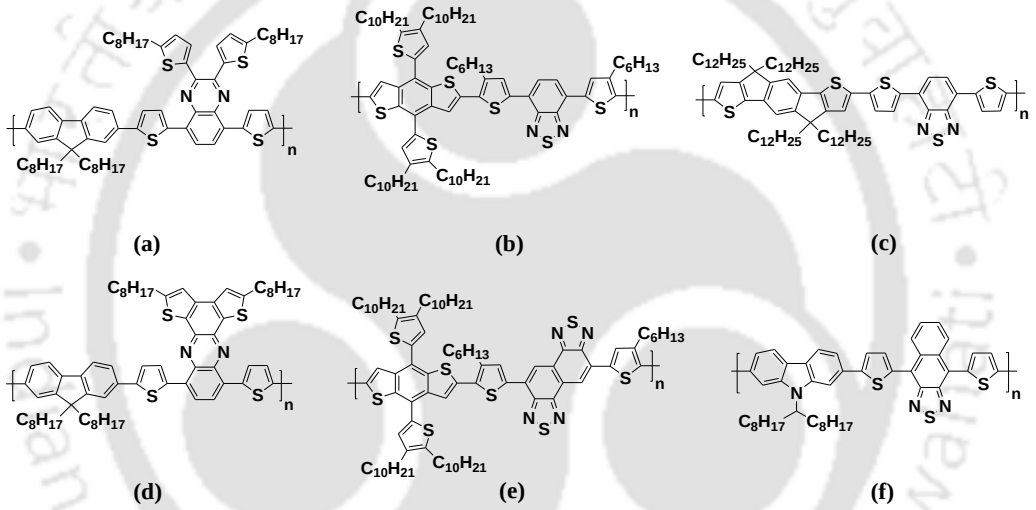

Figure 1.14 Fused donor and acceptor leading to rigidity of polymer backbone.

Other example of fused system are indaceno[1,2-b:5,6-b′]-dithiophene donor based polymer[87] (achieved PCE = 6.17%, with $PC_{71}BM$) by Yongfang Li group in 2011 as shown in Figure 1.14c and napthothiadiazole (BT with a fused benzene ring on 5,6 position) acceptor based polymer[88] (achieved PCE = 1.31%, with $PC_{71}BM$) by Changduk Yang group in 2012 as shown Figure 1.14.f.

1.1.3.6 Substituting EW group and choosing right combination of D and A

The most important part of all these strategy is to choose right combination of donor and acceptor in a D-A/D-π-A/D-A-D style of design, which affects optical and electronic properties of CPs. The right combination of D-A can be predetermined theoretically from density functional theory (DFT) and time dependent density functional theory (TDDFT)

TH-1906_11615303

calculation, such as: (i) in DFT, distribution of electron density on entire HOMO and concentrated electron density on acceptor side in LUMO is the ideal distribution for ICT from D to A; (ii) DFT calculations also gives insight for understanding the position of HOMO-LUMO and dihedral angle between conjugated units of CP; (iii) and from TDDFT one can estimate the possible absorption range as well. Apart from theoretical investigation of frontier orbitals another short hand tool to determine the right combination of donor and acceptor is: an electron donor should be weak and an electron acceptor should be strong. In line with choosing right combination of weak donor-strong acceptor for polymerization, many groups have synthesized various acceptors with electron withdrawing ketone or ester group attached to the ring (a strategy to enhance electron withdrawing (EW) ability of acceptors) and donors with various substituents.

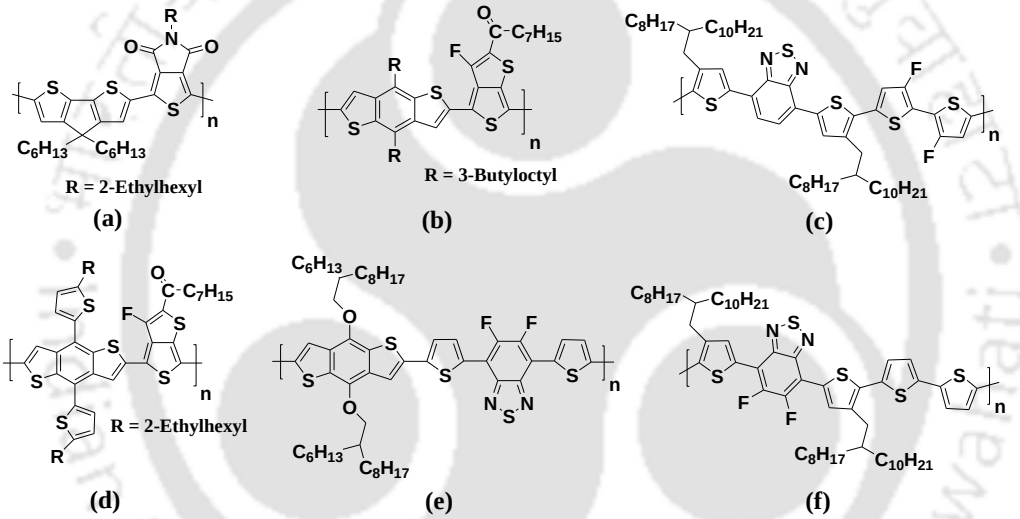

Figure 1.15 Conjugated polymer having electron withdrawing group on acceptor.

One important acceptor reported is thieno[3,4-c]pyrrole-4,6-dione, having an imide group fused at 3,4-position of thiophene. Co-polymerizing with cyclopenta[2,1-b;3,4-b´]dithiophene,[89] (Figure 1.15a) Jianfu Ding and co-workers in 2011 showed that polymer [P(CPDT-TPD)] absorbs maximum in red region of 650 nm and cover all over UV to red of the solar spectrum. With $PC_{71}BM$ as acceptor PCE of 6.41% (J_{sc} = 14.1 mA/cm^2, FF = 60.7%, V_{oc} = 0.75 V) has been achieved, which is improved result than P(CPDT-BT).

Similarly, Ye Tao group in 2011 synthesized thieno[3,4-b]thiophene based acceptor with a ketone and fluorine group attached to the ring. Both the substituent acts as an electron withdrawing group and makes thieno[3,4-b]thiophene group a strong acceptor.[90] Its copolymer with BDT unit gives a CP commonly known as PTB7 (Figure 1.15b) whose

TH-1906_11615303

absorption maximum (~700 nm) matches with maximum solar photon flux that reaches the earth most and has a PSC performance, with PCE of 4.8% (J_{sc} = 9.8 mA/cm^2, FF = 63% and V_{oc} = 0.78 V). Moreover, BDT unit was further substituted with two Th units, which gives BDT-Th as new donor unit. Polymerizing BDT-Th with fluorine and ketone substituted thieno[3,4-b]thiophene (acceptor used for PTB-7) as acceptor gives very promising polymer namely PTB7-Th. (Figure 1.15d). In 2013 Show-An-Chen group used both PTB-7/PTB7-Th as donor polymer with ZnO doped $PC_{61}BM$ as acceptor in an inverted geometry PSC device and achieved a PCE of 9.35% (J_{sc} of 15.73 mA/cm^2, FF of 74.3% and V_{oc} of 0.8 V) with PTB7-Th compared to a PCE of 8.21% (J_{sc} of 15.41 mA/cm^2, FF of 73% and V_{oc} of 0.73 V) with PTB-7 as donor polymer.[91] Use of BDT-Th as donor instead of BDT, improves absorption range as well, with 25 nm bathochromic shift.

Later, in 2016 Jianhui Hou et al. synthesized polymer with benzo[1′,2′-c:4′,5′-c′]dithiophene-4,8-dione (two ketone group inserted into BDT ring) as acceptor and BDT-Th as donor.[69] This polymer P(BDB-T) (as shown in Figure 1.10) along with ITIC as acceptor showed a PCE of 11.21% .

As like ketone, fluorine has remarkable influence on PSC performance, being able to increases dipole moment, improves mobility and crystalline nature in casted film of the polymer. One of the results by Won Ho Jo group in 2015, investigated that for bithiophe-co-ThBTTh polymer (Figure 1.15c and 1.1e), incorporating fluorine on donor (PCE = 7.10%) or on the acceptor (PCE = 6.41%) enhances PCE (no change in optical property but due to improved morphology of active layer) compared to the polymer without fluorine (PCE = 1.64%).[92] Achievement of PCE of 8.3% by Zhenhua Jiang et al. in 2013[93] with [BDT]-[Th-5,6-$DF_{5,6}$BT-Th] type D-A polymer (Figure 1.15 e) further confirms ability of fluorine group to tune the PCE in PSCs. Contrary to that the oxygen counter part of polymer (Figure 1.10) could only be able to result a maximum PCE of 5%.

1.1.3.7 Substituting non-conjugated functional group into the side chain of CPs

In addition, to main chain chemistry, many efforts have been given on side chain substitution with various functional groups such as (alcohol, ester, azide and phosphite) to understand importance of side chain substitution on polymer solubility, morphology of active layer of solar cell and stability (as these side chain functional group have crosslinking and anchoring property).

TH-1906_11615303

Wouter Maes and coworkers in 2015, reported side chain of CPDT functionalized with alcohol and ester group based (Figure 1.16a and 1.16b) P(CPDT-BT) type polymer with improved glass transition temperature (T_g) and reduced aggregation in casted film.[94] Due to high T_g, the polymer with OH group on side chain, showed improved solar cell stability (up to 85 hours with 85 °C PCE reduced from 1.98% to 1.82%), whereas with pristine P(CPDT-BT) it showed a reduction of PCE from 2.38% to 2.15% under similar condition.

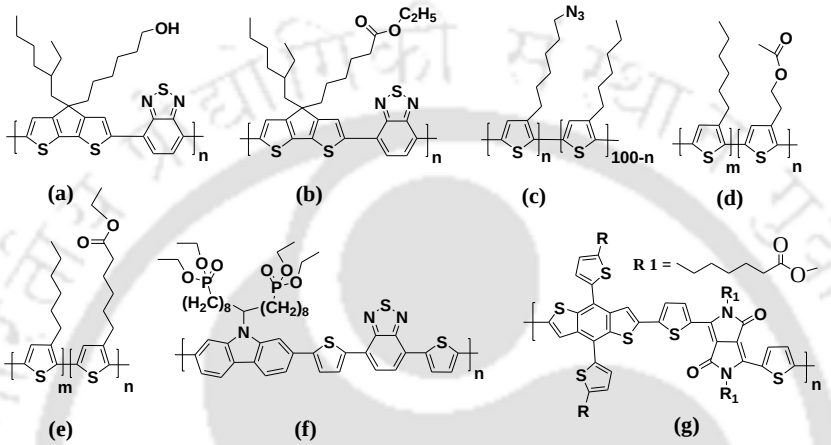

Figure 1.16 Improving solar cell performances by side chain functionalization.

Importance of non-conjugating ester group on CPs have been further demonstrated by Wouter Maes group in 2017, establishing side chain ester substituted polymers helps improving intrinsic stability[95] of active layer of fabricated PSCs with a side chain ester substituted PAT type block-co-polymer (Figure 1.16 d and 1.16e). Moreover, ester group further improves active layer morphology[96] as well in fabricated polymer solar cell, as demonstrated by Hoon Choi group in an article published in 2016, where improved phase separation was observed with side chain ester containing BDT-Th-DPP based D-A polymer (Figure 1.16g) and $PC_{71}BM$ acceptor (PCE of 2.04%) in PSC, compared to polymer without ester substitution (PCE of 0.99%).

Other example of side chain substitution is azide substituted block-co-polymer of 3-alkylthiophene[97] (Figure 1.16c) by Bumjoon J. Kim group in 2012, where azide group gets cross-linked with PCBM leading to improved PCE, mobility and stability. Similarly, side chain triethyl phosphite substituted polymer (Figure 1.16d)[98] was used by Lixiang Wang group in 2014 as additional interlayer in PSC, to improve device performance.

TH-1906_11615303

1.1.3.8 Improving solar cell performance by variation of side chain

PSC device performance also depends on choice of side chain on CP, as hydrophobic alkyl chain helps polymer soluble in common organic solvents. One of the literature by Barry C. Thompson group in 2012, where they have synthesized a poly(3-hexylthiophene-co-3-(2-ethylhexyl)thiophene) co-polymer (Figure 1.17a)[99] and showed that increasing 2-ethylhexyl content more than 25% in P3AT-based block co-polymer reduces the solar cell performance [PCE = 0.74%, J_{sc} = 2.52 mA/cm^2, FF = 35%, V_{oc} = 0.85 V for P($3HT_{50}$-co-PEH_{50})] compared to the P3AT with hexyl as side chain ((PCE = 3.84%, J_{sc} = 9.67 mA/cm^2, FF = 60%, V_{oc} = 0.6 V). This establishes hexyl chain is appropriate for PAT type of polymers. Similarly, G. C. Bazan group in 2007 established a high solar cell performance with PCE of 5.5%, J_{sc} of 16.2 mA/cm^2, FF of 55% and V_{oc} of 0.62 V for P(CPDT-BT) polymer (Figure 1.17b)[100] with 2-ethylhexyl side chain and using alkane di-thiol as additive. The main reason for such high performance was due to low aggregated morphology caused by 2-ethylhexyl chain and additive di-thiol.

Klaus Müllen group in 2011 showed that on P(CPDT-BT) (Figure 1.17c and 1.17d)[101] using long hexadodecyl chain, improves mobility of the polymer (μ = 0.5 cm^2 V^{-1} s^{-1}) but mobility reduces by the use of branched alkyl chain (2,7-dimethyloctyl) (μ = 0.34 cm^2 V^{-1} s^{-1}). They concluded that for P(CPDT-BT), the use of 2-ethylhexyl chain improves PCE but reduces the mobility.

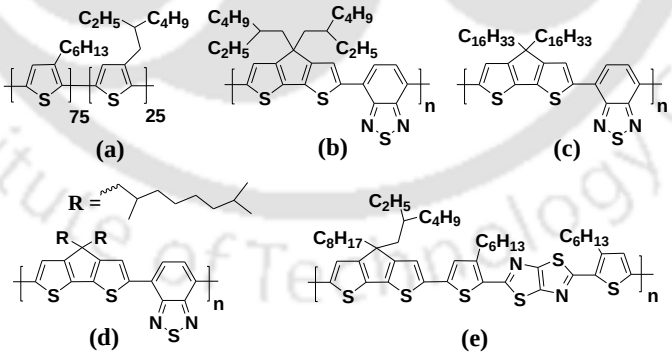

Figure 1.17 Improving solar cell performances by changing side chain.

Considering the above established results of Bazan group and Müllen group, in 2012 Wouter Maes group synthesized D-A based conjugated polymer with CPDT as donor and thiazolo[5,4-d]thiazole as acceptor (Figure 1.17e),[102] where instead of two 2-ethylhexyl chain (which would provide better solar cell performance) or two long straight chain

TH-1906_11615303

(which would provide better mobility) they have used combination of both, to balance solar cell performance and mobility of the polymer. They have achieved a mobility of $1.0*10^{-3}$ cm^2 V^{-1} s^{-1} and PCE of 4.03%, (J_{sc} =11.13 mA/cm^2, FF = 54%, V_{oc} = 0.67 V). This establishes importance of choice of alkyl chain and PSC performance.

1.1.3.9 Lowering of dihedral angle and introducing alkyl chain on D and A

Lowering of dihedral angle along the polymer main chain and within the other conjugated unit (a dihedral angle of < 20° are primarily essential) is one of the most important parameters, needed to achieve as the dihedral angle influences π-π stacking of polymer chains in film state, leading to improved absorption coefficient, mobility and nano-morphology.

Among various strategies implemented to reduce the dihedral angle between two conjugated units, introducing a thiophene unit between D and A is very common (synthesized polymers as shown in Figure 1.15e, 1.14a-f). A recent report by Jianhui Hou and co-workers in 2017 shows significant improvement of optical property, mobility and PCE due to lowering of dihedral angle by incorporation of a thiophene unit in between two ester substituted thiophene unit based polymer[49] (Figue 1.18d). Before incorporating Th unit (Figure 1.18a), dihedral angle between the two ester substituted Th unit was 78° (λ_{onset} film = 554 nm, ε = $3.62*10^4$ M^{-1} cm^{-1}, PCE = 0.01%) and after incorporating a Th unit (Figure 1.18d) dihedral angle reduced to 17° leading to improved performance (λ_{onset} film = 633 nm, ε = $3.57*10^4$ M^{-1} cm^{-1}, PCE = 11.9%).

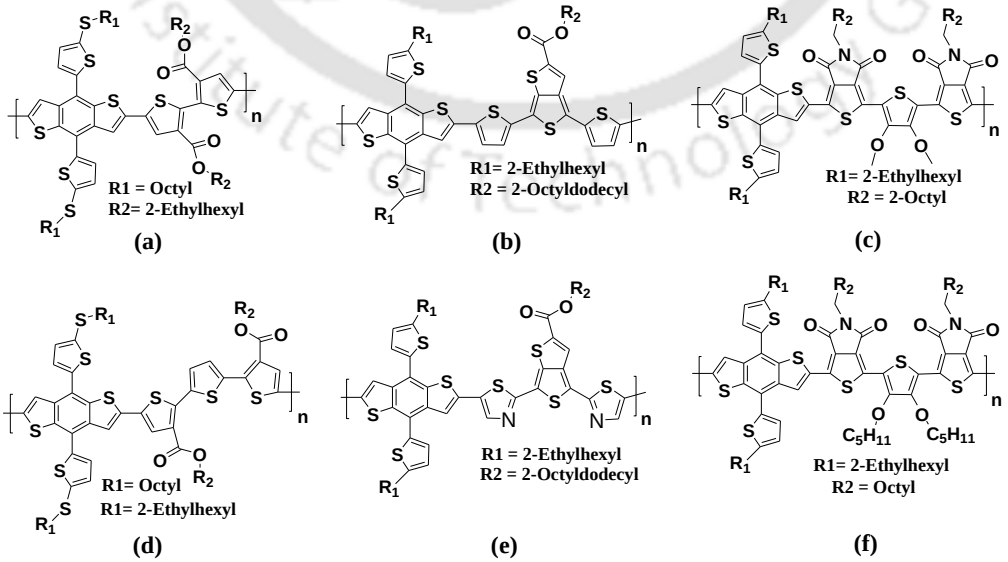

Figure 1.18 Improving solar cell performances by reducing dihedral angle.

TH-1906_11615303

Renqiang Yang group in 2017 established that thiophene, thiazole units have substantial ability to reduce the dihedral angle[103] further along the polymer main chain when replaced with Th unit in a BDT-Th and thienothiophene based D-A polymer (as shown Figure 1.18b and 1.18e). The PCE achieved from thiazole bridged polymer was 9.6% compared to its Th counterpart with PCE of 4.4% (thiophene bridged polymer, $\theta = 18^{o}$ and thiazole bridged polymer $\theta = 2^{o}$). In addition, introduction of alkyl chain to enhance the solubility and/or morphology without much change in dihedral angle is a further tool to achieve high PCE, as reported by Zhixiang Wei group in 2016.[104] Here they have achieved a PCE of 8.18% by introduction of pentyl group (polymer shown in Figure 1.18f) contrary to a PCE of 3.31% with methyl group (polymer shown in Figure 1.18c).

1.1.3.10 New D-A polymers using previous established concepts

It is worth noting that the newer design of polymers is being synthesized in recent times based upon the concept and understanding of structure property relationship for last decade. This includes donors such as benzotrithiophene (BTT, Figure 1.19a),[105] indenothiophene (IT, Figure 1.19b),[106] dithieno[3,2‑b:2′,3′‑d]pyran (DTP, Figure 1.19e)[107] and acceptors such as benzo[1,2-b:4,5-c′]dithiophene-4,8-dione (BDD, Figure 1.19f),[108] 2,2′-bithiophene-3,3′-imide (BTI, Figure 1.19d),[109] 6,7-difluoroquinoxaline (DFQ, Figure 1.19c).[110] With synthesized CPs using above listed donors and/or acceptors with suitable combination and with help of various device geometry significant PCE of 7.19%, 9.17%, 8%, 6.32%, 9.21% and 11.3% have been achieved respectively.

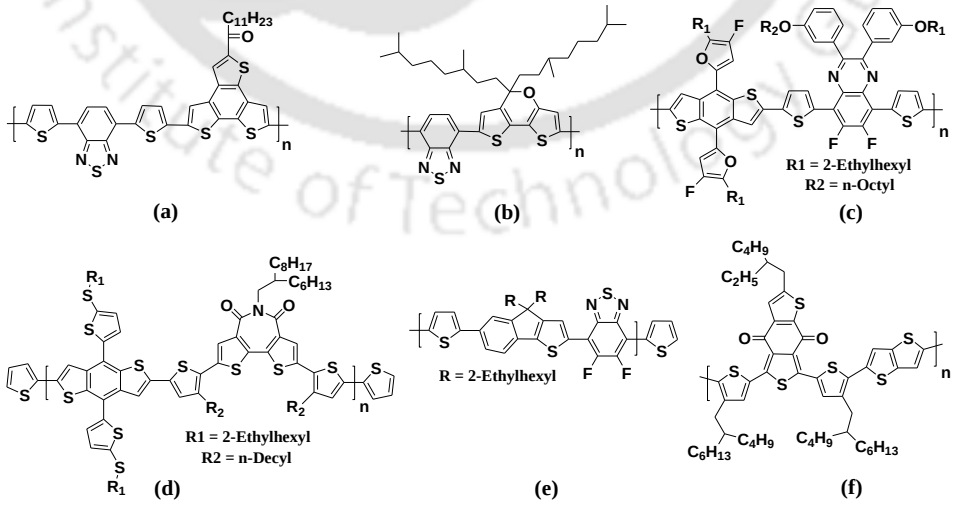

Figure 1.19 Recent trends in conjugated polymers for PSCs.

TH-1906_11615303

1.1.4 Further efforts to improve PSC performance

In addition, to designing strategy to synthesize efficient solar harvesting polymer, other approaches have also been experimented to improve performance of PSCs, such as: (i) new fullerene derivatives and non-fullerene based acceptors have been synthesized and fabricated with most efficient polymers for solar cell; (ii) use of solvent additive to improve morphology of active layer; (iii) there have been efforts to incorporate carbon nanotubes, graphene and similar π-electron rich entity into PSC, to improve PCE, stability of material and durability of PSC; (iv) modified device geometry and change of electrodes have also been implemented.

1.1.4.1 Major types of acceptors for PSC

Along with commonly used $PC_{61}BM$/$PC_{71}BM$ as acceptors, various derivatives of fullerene have also been synthesized (as shown in Figure 1.20) to modify its electron mobility, HOMO-LUMO position and to investigate polymer solar cell performance. Because V_{oc} for polymer solar cell is proportional to difference between HOMO of donor polymer and LUMO of acceptor, tuning of acceptor HOMO-LUMO position is another effective way to improve device performance. Two such important derivatives of PCBM are Bis-PCBM,[111] with two ester functionalized side chain on a fullerene molecule and indaceno-C_{60}bis-adduct (ICBA).[112]

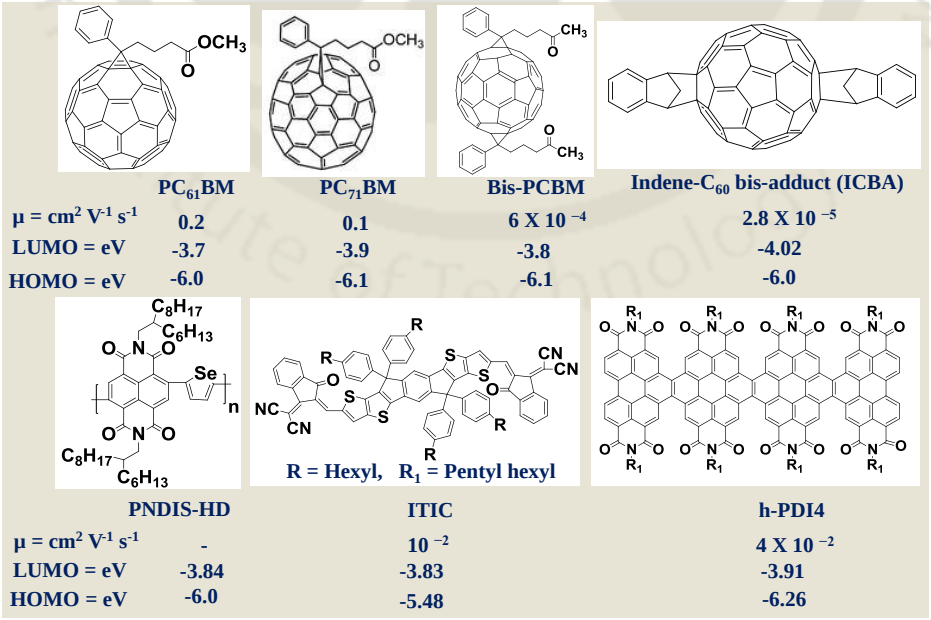

Figure 1.20 Various acceptors used in solar cell (figures of 1st row taken from e-source).

TH-1906_11615303

In addition, as fullerene derivatives are very expensive, so new n-type acceptor monomers and/or polymers have been synthesized (aiming to reduce cost of PSC) and have been as an exciting field of research since last few years. The strategies to design such non-fullerene-based acceptors are: it must have a non-planar geometry to achieve phase separation criteria when blend with donor polymer and should have similar HOMO-LUMO position and electron mobility as like PCBM. Some of those kind of acceptors are P(NDI-selenophene) polymer,[113] ITIC[114] and fused PDI (hPDI4) based acceptor (Figure 1.20).[69]

1.1.4.2 Morphology tuning by use additives in PSC

Morphology of D-A blend has a great impact on solar cell performance, as it influences exciton dissociation at active layer. An ideal polymer-PCBM blend morphology for solar cell must have: (i) phase separated state between donor polymer and acceptor PCBM (generally understood as ordered and directional arrangement of polymer and PCBM, which facilitate efficient charge transfer); (ii) low domain diameter; (iii) low root mean square roughness for the casted film; (iv) and since efficient exciton dissociation takes place within its exciton diffusion length of 10 nm, the ideal width of each D and A phase should be less than 20 nm. To achieve such requirements, various efforts have been made by researchers and can be listed as: (i) use of high boiling solvents like chlorobenzene (CB) and dichlorobenzene (DCB) with high dipole moment (high boiling solvents evaporates slow rate, hence allow the active layer to reorganize to the lowest possible energy state of uniform film); (ii) annealing of the casted film to temperature in the range of boiling point of the solvent used, because of the heat energy, the film gets orderly (crystalline) arranged rather that a random (amorphous) arrangement; (iii) use of additives along with high boiling primary solvent (additives are generally another high boiling solvent along with the primary solvent but in low feed ratio). Any high boiling solvent to be used as additives for PSCs must have two important properties such as: (a) high boiling point than primary solvent used; (b) dissolves any one of the donor or acceptor prudentially over other. Frequently used additives have been listed in Figure 1.21.

TH-1906_11615303

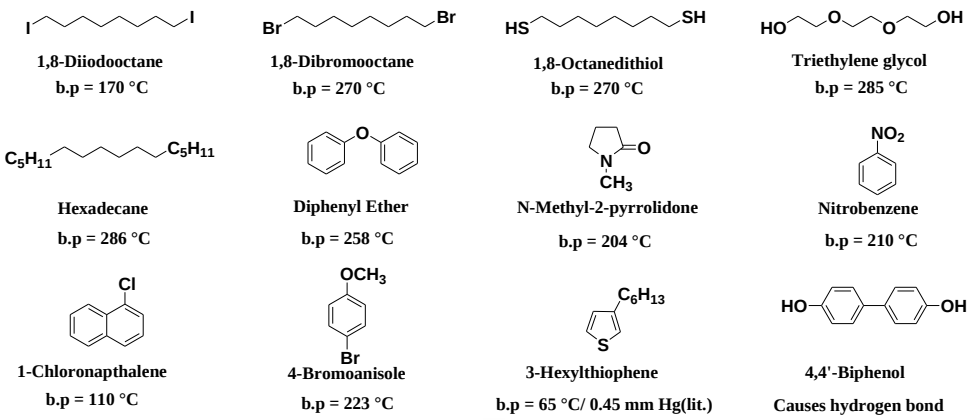

Figure 1.21 Additives used with active layer of PSC with their boiling point (b.p).

One interesting example of morphological change and PSC performance appeared from Mats R. Andersson group in 2010, where they fabricated solar cell using quinoxaline-co-thiophene polymer (TQ1) with $PC_{61}BM$/$PC_{71}BM$ as acceptor with $CHCl_3$ and DCB as solvent,[115] thoroughly investigating the change of morphology by AFM topography and correlate device performance with morphology of active layer. With $CHCl_3$ as solvent for TQ1-$PC_{61}BM$ as active layer a high domain diameter (200-400 nm) and RMS roughness 2.57 nm has been observed (Figure 1.122.a) with PCE of 3%. On changing solvent for deposition to o-DCB low domain diameter (1.09 nm) and RMS roughness (1.09 nm) has been witnessed, as can be seen from Figure 1.22.b, corresponding to PCE of 4.9%. Again with TQ1-$PC_{71}BM$ as active layer with o-DCB as solvent phase separated morphology (interpenetrating network with crystallinity) with domain diameter 3.2 nm has been realized leading to enhanced PCE up to 6% (Figure 1.22.c).

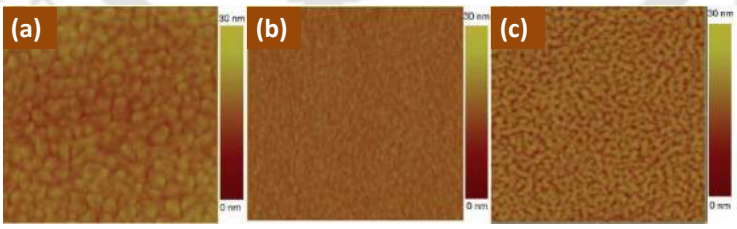

Figure 1.22 Morphology change in active layer of PSC with TQ1 polymer (a) TQ1-$PC_{61}BM$ in $CHCl_3$ (b) TQ1-$PC_{61}BM$ in o-DCB (c) TQ1-$PC_{71}BM$ in o-DCB. Figure taken from reference No. 115 with copyright permission.

TH-1906_11615303

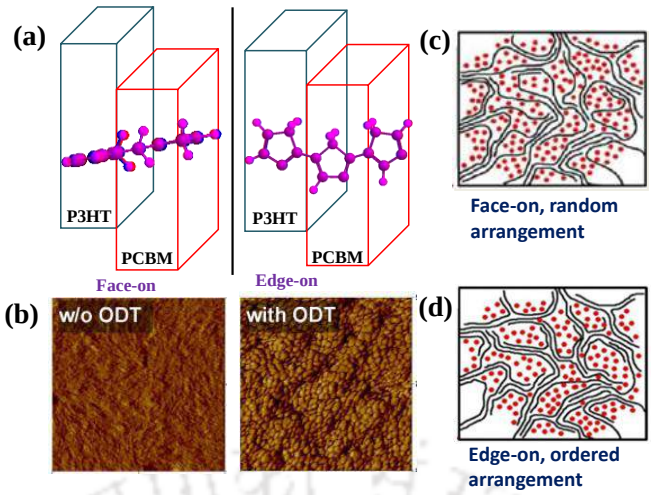

Figure 1.23 (a) Face-on and edge-on orientation of P3HT with additives in PSC, (b) AFM topography, (c, d) Graphical presentation of the active layer in edge-on and face-on arrangements in PSC. Figure taken from reference No. 116 with copyright permission.

In 2013 Wei Fang Su and group investigated the role of additives that brings enhancement in solar cell performances in P3HT-PCBM based devices.[116] They conclude from GIWAXS (grazing incidence wide angel X-ray scattering) that with additives, P3HT arrange themselves in a direction such that its alkyl chain becomes parallel to the substrate with polymer backbone aligning perpendicular to the substrate (this is the direction of charge transport from P3HT to PCBM and gives high PSC performance), this type of directional arrangement is called edge on arrangement, (Figure 1.23.a). On the other hand without additives P3HT arranges itself in a direction with alkyl chain perpendicular to the substrate and polymer backbone parallel to the substrate (opposite of charge transfer direction from P3HT to PCBM and displays reduced PSC performance). This type of arrangement is called face-on arrangement (Figure 1.23.a). The above directional phase separated arrangement can be correlated and seen easily in AFM image as well (Figure 1.23b, 1.23c,1.23d).

1.1.4.3 Ternary component used in active layer of polymer solar cell

Carbon nanotubes (CNTs) and grapheme oxide (GO) are another emerging class of organic materials having good conductivity (Figure 1.24), optical and physical properties which find wide application in multidisciplinary fields of optoelectronic devices. Over the past few years, CNTs and/or graphene oxide (GO) have received immense attention as an acceptor to replace PCBM,[117] to replace hole transporting layer (HTL)[118] and as an anode to replace ITO[119] in BHJ solar cells. Recently, few research groups have shown the

TH-1906_11615303

potential of these materials as an active layer in PSCs by incorporating both single walled and multi walled CNT into BHJ solar cell, where CNTs act as exciton dissociation center by transporting both holes and electrons, which otherwise lead to recombination of exciton and hence poor device performance.

S. Ravi P. Silva et al. in 2011 used a ternary blend of P3HT-PCBM and o-MWCNT (oxidized MWCNT) (Figure 1.24) and fabricated solar cell with improved PCE to 3.05% compared to pristine MWCNT counterpart (PCE = 1.39%) and without MWCNT (PCE = 2.86%).[120] On the other hand CNT and graphene were used to investigate their influence on BHJ solar cell stability and durability as well. A previous work by P. K. Iyer group in 2011, reported very high photo stability of P3HT by preparing composites with 10% (w/w) of MWCNT, in presence of oxygen and moisture which find application towards optoelectronic devices.[121] Later, in 2012 Zhaoyu Ren and co-workers improved stability of MEH-PPV,[122] polymer by adding 0.5% reduced graphene oxide (RGO). Use of π-electron rich CNT and graphene derivative have brought more opportunity of device engineering, optical tunability and stability measures to PSCs.

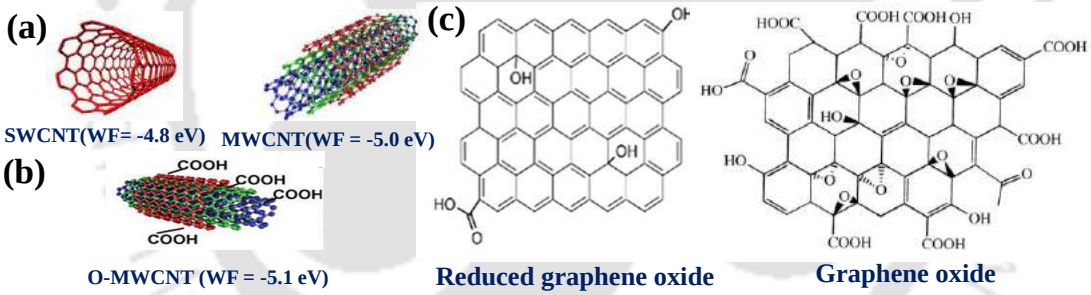

Figure 1.24 π-Electron rich entity in PSC (WF = work function). (a) figures taken from e-source (b, c) figures taken from reference No.120 and 122 respectively with copyright permission.

1.1.4.4 Device engineering in solar cell

Various types of device geometry (Figure 1.25) used for PSC has been listed below.

1.1.4.4.1 Bulk-heterojunction (BHJ) geometry

In BHJ geometry blend of solar harvesting polymer and acceptor such as PCBM is used as active layer. Blend active layer brings high surface contact between polymer and

TH-1906_11615303

PCBM with better charge transfer from polymer to PCBM and provide opportunity to tune nano-morphology compared to a bilayer active layer.

1.1.4.4.2 Polymer-polymer solar cell (all polymer solar cells)

Here expensive fullerene (acceptor) derivatives have been replaced by polymers with comparable electron mobility.[123] In all polymer solar cell, two CPs are blended and deposited as active layer.

1.1.4.4.3 Modifying Al cathode to Ca/Ba/Mg-Al

When Al as cathode is modified to Ca-Al or Mg-Al, due to low work function of Ca/Mg (generally a 20 nm is deposited followed by deposition of Al), high built in potential develops between the two electrodes and hence increases the V_{oc}, FF and overall device performance.[124,67]

1.1.4.4.4 Modifying Al cathode with LiF-Al

Due to quantum mechanical electron tunneling effect caused by thin film (0.5 to 1 nm) of wide band gap (13 eV) LiF, electron injection to cathode increases in devices fabricated with LiF as interfacial cathode layer.

1.1.4.4.5 Inverted geometry of solar cell

This geometry was implemented to overcome three major problems like: (a) as low work function metal such a Ca, Mg gets easily oxidized hence need to be replaced by high work function metal like silver (Ag); (b) commonly used PEDOT:PSS as hole transporting layer absorbs moisture hence reduces device efficiency and stability; (c) PSS present in HTL is a strong acid and hence able to etch ITO and dropping hole collection efficiency of anode. Hence silver (Ag) was used as cathode and MoO_3 has been used as a HTL in inverted geometry of polymer solar cell.[124,125]

1.1.4.4.6 Tandem solar cell

Tandem geometry is nothing but combination of two cells with a conducting layer in between. Two major challenges for solar cell fabrication have been addressed with tandem solar cell: (a) sub-band gap losses (high energy radiations cannot be absorbed by a low band gap material) and will be transmitted (b) thermalization losses, some of the excitons might get excited by high energy radiation to higher than S_1 state and while

TH-1906_11615303

coming back to S_0 excited electrons release their energy as unwanted heat energy. Above problems can be solved by fabricating a tandem cell with two devices connected with a conductor in between, generally the first one with a high band gap polymer and other one with low band gap, so that all of the solar photons can be absorbed from 400 to 800 nm.[126]

1.1.4.4.7 Ternary solar cell (three component active layer solar cell)

Three component active layer are being used instead of two to harvest more solar photons and to improve mobility. Three components can be two donor one acceptor or one donor two acceptor with suitably positioned HOMO-LUMO, complementary optical property and high mobility.[53,54,127]

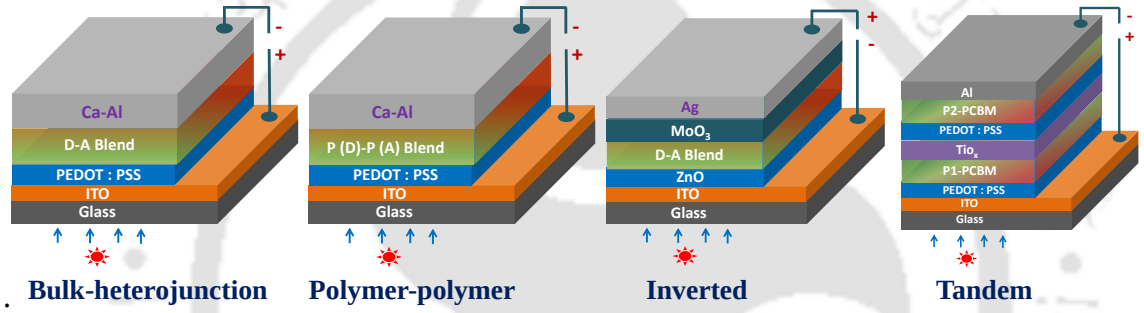

Figure 1.25 Commonly used device geometry for fabrication of polymer solar cell.

1.2 Objective of the present work and summary

A wide variety of CPs is being used for PSC and other optoelectronic devices. In PSC polymers suffer from low PCE and their photo degradation nature on exposure to UV light makes them less suitable and demands much extensive study in terms of structural changes and/or addition of other entity to solve it. In addition, extensive study in past decade on structural tunability on polymer main chain/side chain and along with device engineering helps researchers to achieve a PCE of 13%. Here efforts have been given to investigate further, on structural changes leading to a change in optoelectronic properties by synthesizing newer acceptors with 5,6-position of BT and durability measures for blend of thiophene containing donor polymer and acceptor (PCBM) used for solar cell, by preparing composites with MWCNT. Such systems can be used to bring high performance materials with improved photo stability for future optoelectronic application. This thesis is divided into 5 chapters, and summarized briefly below as:

TH-1906_11615303

Chapter 1 described progress in the respective research area, where design synthesis and fabrication of conjugated polymers, along with the scope and significance of the subsequent chapters are discussed.

Chapter 2 reports that the photo stability of P3HT-PCBM blend in chloroform and film, can be improved significantly by preparing composites of MWCNT having appropriate ratios of each component. This study establishes that P3HT-PCBM (7%) with MWCNT (3%) is a photo stable composite and displays good charge transfer characteristics for optoelectronic application such as BHJ-PSC under ambient conditions.

Chapter 3 reports two poly(o-arylene-vinylene) (POAV) type CP with polymer main chain alternating at 5,6-position of BT. POAV polymers have been synthesized, characterized, potential of POAV type of polymers as donor for PSC, thermal, optical, morphological properties and their structure property relationship have been investigated. This study gives an insight into polymers having 5,6-*alt*-benzothiadiazole as an acceptor in the D-π-A system and opens newer avenues of using o-arylene and explores use of 5,6-position of BT along with PAV or POAV type polymer towards newer designing opportunities for conjugated monomers/polymers for application of photovoltaic and other organic electronic devices.

In chapter 4 two non-conjugating ester group has been substituted on 5,6-position of BT and by use of commonly used donors its influence on PSC performance has been investigated. This established that non-conjugating ester group on side chain of acceptors lowers the dihedral angel, improves optical and electrochemical properties, enhances phase separation in active layer and PSC performance of side chain ester containing polymer compared to its methyl counterpart.

Chapter 5 describes using 5,6-position of BT, as a new acceptor has been developed by Wittig coupling namely 6,7-thiophene substituted napthothiadiazole (formed by C=C bond formation). Its structure property relationship towards fabrication of BHJ-PSC has been investigated. NT-derivative as new acceptor provides vast option of optical tunability on it. By suitable synthetic strategy and with appropriate combination to existing donor units, derivative of NT can be a promising candidate to achieve our target of low cost and efficient solar cell.

TH-1906_11615303

1.3 References

1. Shirakawa, H.; Louis, E. J.; Macdiarmid, A. G.; Chiang, C. K.; Heeger, A. J. *J. Chem. Soc. Chem. Commun*. **1977**, 578-580.
2. Patil, A. O.; Heeger, A. J.; Wudl, F. *Chem. Rev.* **1988**, *88*, 183-200.
3. Friedrich, K.; Burkhart, T.; Almajid, A. A.; Haupert, F. *Int. J. Polymer. Mater.* **2010**, *59*, 680-692.
4. Kraft, A.; Grimsdale, A. C.; Holmes, A. B. *Angew. Chem. Int. Ed.* **1998**, *37*, 402-428.
5. Bunz, U. H. F. *Chem. Rev.* **2000**, *100*, 1605-1644.
6. Perepichka, I. F.; Perepichka, D. F.; Meng, H.; Wudl, F. *Adv. Mater.* **2005**, *17*, 2281-2305.
7. MacDiarmid, A. G. *Angew. Chem. Int. Ed.* **2001**, *40*, 2581-2590.
8. Scherf, U.; List, E. J. W. *Adv. Mater.* **2002**, *14*, 477-487.
9. Zhang, L.; Hu, S.; Chen, J.; Chen, Z.; Wu, H.; Peng, J.; Cao, Y. *Adv. Funct. Mater.* **2011**, *21*, 3760-3769.
10. Pei, Q. B.; Yu, G.; Zhang, C.; Yang, Y.; Heeger, A. J. *Science* **1995**, *269*, 1086-1088.
11. Hide, F.; DiazGarcia, M. A.; Schwartz, B. J.; Heeger, A. J. *Acc. Chem. Res.* **1997**, *30*, 430-436.
12. McQuade, D. T.; Pullen, A. E.; Swager, T. M. *Chem. Rev*. **2000**, *100*, 2537-2574.
13. She, X. J.; Gustafsson, D.; Sirringhaus, H. *Adv. Mater.* **2017**, *29*, 1604769.
14. Gunes, S.; Neugebauer, H.; Sariciftci, N. S. *Chem. Rev.* **2007**, *107*, 1324-1338.
15. Liu, B.; Bai, L.; Li, T.; Wei, C.; Li, B.; Huang, Q.; Zhang, D.; Wang, G.; Ying, Z.; Zhang, X. *Energy Environ. Sci.* **2017**, *10*, 1134-1141.
16. Tan, H.; Furlan, A.; Li, W.; Arapov, K.; Santbergen, R.; Wienk, M. M.; Zeman, M.; Smets, A. H. M.; Janssen, R. A. J. *Adv. Mater.* **2016**, *28*, 2170-2177.
17. He, Z.; Xiao, B.; Liu, F.; Wu, H.; Yang, Y.; Xiao, S.; Wang, C.; Russell, T. P.; Cao, Y. *Nat. Photonics* **2015**, *9*, 174-179.
18. Kakiage, K.; Aoyama, Y.; Yano, T.; Oya, K.; Fujisawa, J. I.; Hanaya, M. *Chem. Commun.* **2015**, *51*, 15894-15897.
19. Ye, M.; Hong, X.; Zhang, F.; Liu, X. *J. Mater. Chem. A* **2016, *4,*** 6755-6771.

TH-1906_11615303

20. Liu, M.; Arquer, F. P. G. D.; Li, Y.; Lan, X.; Kim, G. H.; Voznyy, O.; Jagadamma, L. K.; Abbas, A. S.; Hoogland, S.; Lu, Z.; Kim, J. Y.; Amassian, A.; Sargent, E. H. *Adv. Mater.* **2016**, *28*, 4142-4148.
21. Lai, W. C.; Lin, K. W.; Wang, Y. T.; Chiang, T. Y.; Chen, P.; Guo, T. F. *Adv. Mater.* **2016**, *28*, 3290-3297.
22. He, J.; Gao, P.; Yang, Z.; Yu, J.; Yu, W.; Zhang, Y.; Sheng, J.; Ye, J.; Amine, J. C.; Cui, Y. *Adv. Mater.* **2017**, *29*, 1606321.
23. Kim, H.; Nam, S.; Jeong, J.; Lee, S.; Seo, J.; Han, H.; Kim, Y. *Korean J. Chem. Eng.* **2014**, *7*, 1095-1104.
24. Spanggaard, H.; Krebs, F. C. *Sol. Energy Mater. Sol. Cells* **2004**, *83*, 125-146.
25. Bagher, A. M. *Sustainable Energy*, **2014**, *2*, 85-90.
26. Yu, G.; Gao, J.; Hummelen, J. C.; Wudl, F.; Heeger, A. J. *Science* **1995**, *270* 1789-1791.
27. Padinger, F.; Rittberger, R. S.; Sariciftci, N. S. *Adv. Funct. Mater.* **2003**, *13*, 85-88.
28. Kim, J. Y.; Lee, K.; Coates, N. E.; Moses, D.; Nguyen, T. Q.; Dante, M.; Heeger A. J. *Science* **2007**, *217*, 222-225.
29. Zhao, W.; Li, S.; Yao, H.; Zhang, S.; Zhang, Y.; Yang, B.; Hou, J. *J. Am. Chem. Soc.* **2017**, *139*, 7148-7151.
30. Kang, H.; Kim, G.; Kim, J.; Kwon, S.; Kim, H.; Lee, K. *Adv. Mater.* **2016**, *28*, 7821-7861.
31. Yan, J.; Saunders, B. R. *RSC Adv.* **2014**, *4*, 43286-43314.
32. O'Regan, B.; Gratzel, M. *Nature* **1991**, *353*, 737-740.
33. Kojima, A.; Teshima, K.; Shirai, Y.; Miyasaka, T. *J. Am. Chem. Soc.* **2009**, *131*, 6050-6051.
34. Grancini, G.; Carmona, C. R.; Zimmermann, I.; Mosconi, E.; Lee, X.; Martineau D.; Narbey, S.; Oswald, F.; Angelis, F. D.; Graetzel, M.; Nazeeruddin, M. K. *Nat. Commun.* **2017**, *8*, 15684.
35. Berhe, T. A.; Su, W. N.; Chen, C. H.; Pan, C. J.; Cheng, J. H.; Chen, H. M.; Tsai, M. C.; Chen, L. Y.; Dubale, A. A.; Hwang, B. J. *Energy Environ. Sci.* **2016**, *9*, 323-356.
36. Etxebarria, I.; Ajuria, J.; Pacios, R. *Org. Electron.* **2015**, *19*, 34-60.
37. Liu, D.; Zhu, Q.; Gu, C.; Wang, J.; Qiu, M.; Chen, W.; Bao, X.; Sun, M.; Yang, R. *Adv. Mater.* **2016**, *28*, 8490-8498.

TH-1906_11615303

38. Kawashima, K.; Fukuhara, T.; Suda, Y.; Suzuki, Y.; Koganezawa, T.; Yoshida, H.; Ohkita, H.; Osaka, I.; Takimiya, K. *J. Am. Chem. Soc.* **2016**, *138*, 10265-10275.
39. Zhou, H.; Yang, L.; Stuart, A. C.; Price, S. C.; Liu, S.; You, W. *Angew. Chem. Int. Ed.* **2011**, *50*, 2995-2998.
40. Gao, M.; Subbiah, J.; Geraghty, P. B.; Chen, M.; Purushothaman, B.; Chen, X.; Qin, T.; Vak, D.; Scholes, F. H.; Watkins, S. E.; Skidmore, M.; Wilson, G. J.; Holmes, A. B.; Jones, D. J.; Wong, W. W. H. *Chem. Mater.* **2016**, *28*, 3481-3487.
41. Brabec, C. J.; Sariciftci, N. S.; Hummelen, J. C. *Adv. Funct. Mater.* **2001**, *11*, 15-26.
42. Xiao, S.; Stuart, A. C.; Liu, S.; Zhou, H.; You, W. *Adv. Funct. Mater.* **2010**, *20*, 635-643.
43. Li, P.; Fenwick, O.; Yilmaz, S.; Breusov, D.; Caruana, D. J.; Allard, S.; Scherf, U.; Cacialli, F. *Chem. Commun.* **2011**, *47*, 8820-8822.
44. Grisorio, R.; Allegretta, G.; Romanazzi, G.; Suranna, G. P.; Mastrorilli, P.; Mazzeo, M.; Cezza, M.; Carallo, S.; Gigli, G. *Macromolecules* **2012**, *45*, 6396-6404.
45. Yuan, J.; Dong, H.; Li, M.; Huang, X.; Zhong, J.; Li, Y.; Ma, W. *Adv. Mater.* **2014**, *26*, 3624-3630.
46. Chen, H. C.; Chen, Y. H.; Liu, C. C.; Chien, Y. C.; Chou, S. W.; Chou, P. T. *Chem. Mater.* **2012**, *24*, 4766-4772.
47. Huang, J.; Zhao, Y.; Ding, X.; Jia, H.; Jiang, B.; Zhang, Z.; Zhan, C.; He, S.; Pei, Q.; Li, Y.; Liu, Y.; Yao, J. *Polym. Chem.* **2012**, *3*, 2170-2177.
48. Zhao, W.; Qian, D.; Zhang, S.; Li, S.; Inganäs, O.; Gao, F.; Hou, J. *Adv. Mater.* **2016**, *28*, 4734-4739.
49. Liu, D.; Yang, B.; Jang, B.; Xu, B.; Zhang, S.; He, C.; Woo, H. Y.; Hou, J. *Energy Environ. Sci.* **2017**, *10*, 546-551.
50. Liu, J.; Chen, L.; Shao, S.; Xie, Z.; Cheng, Y.; Geng, Y.; Wang, L.; Jing, X.; Wang, F. *Adv. Mater.* **2007**, *19*, 4224-4228.
51. Fei, Z.; Chen, L.; Han, Y.; Gann, E.; Chesman, A. S. R.; McNeill, C. R.; Anthopoulos, T. D.; Heeney, M.; Pietrangelo, A. *J. Am. Chem. Soc.* **2017**, *139*, 8094-8097.
52. Sun, J.; Liu, Z.; Luo, H.; Yang, S.; Yao, J.; Zhang, G.; Zhang, D. *J. Mater. Chem. C* **2016**, *4*, 9359-9365.

TH-1906_11615303

53. Zhang, G.; Zhang, K.; Yin, Q.; Jiang, X. F.; Wang, Z.; Xin, J.; Ma, W.; Yan, H.; Huang, F.; Cao, Y. *J. Am. Chem. Soc.* **2017**, *139*, 2387-2395.
54. Kang, H.; Kim, K. H.; Kang, T. E.; Cho, C. H.; Park, S.; Yoon, S. C.; Kim, B. J. *ACS Appl. Mater. Interfaces* **2013**, *5*, 4401-4408.
55. Zhu, D.; Bao, X.; Zhu, Q.; Gu, C.; Qiu, M.; Wen, S.; Wang, J.; Shahid, B.; Yang, R. *Energy Environ. Sci.* **2017**, *10*, 614-620.
56. Huo, L.; Liu, T.; Sun, X.; Cai, Y.; Heeger, A. J.; Sun. Y. *Adv. Mater.* **2015**, *27*, 2938-2944.
57. Yoon, W. S.; Kim, D. W.; Park, J. M.; Cho, I.; Kwon, O. K.; Whang, D. R.; Kim, J. H.; Park, J. H.; Park, S. Y. *Macromolecules* **2016**, *49*, 8489-8497.
58. Alem, S.; Wakim, S.; Lu, J.; Robertson, G.; Ding, J.; Tao, Y. *ACS Appl. Mater. Interfaces* **2012**, *4*, 2993-2998.
59. Deng, P.; Wu, B.; Lei, Y.; Cao, H.; Ong, B. S. *Macromolecules* **2016**, *49*, 2541-2548.
60. Lee, J.; Ko, H.; Song, E.; Kim, H. G.; Cho, K. ACS *Appl. Mater. Interfaces* **2015**, *7*, 21159-21169.
61. Yuan, L.; Zhao, Y.; Zhang, J.; Zhang, Y.; Zhu, L.; Lu, K.; Yan, W.; Wei, Z. *Adv. Mater.* **2015**, *27*, 4229-4233.
62. Gao, J.; Niles, E. T.; Grey, J. K. *J. Phys. Chem. Lett.* **2013**, *4*, 2953-2957.
63. Dang, M. T.; Hirsch, L.; Wantz, G.; Wuest, J. D. *Chem. Rev.* **2013**, *113*, 3734-3765.
64. Li, G.; Shrotriya, V.; Yao, Y.; Huang, J.; Yang, Y. *J. Mater. Chem.* **2007**, *17*, 3126-3140.
65. Mühlbacher, D.; Scharber, M.; Morana, M.; Zhu, Z.; Waller, D.; Gaudiana, R.; Brabec, C. *Adv. Mater.* **2006**, *18*, 2884-2889.
66. Zhang, J.; Cai, W.; Huang, F.; Wang, E.; Zhong, C.; Liu, S.; Wang, M.; Duan, C.; Yang, T.; Cao, Y. *Macromolecules* **2011**, *44*, 894-901.
67. Chen, H. Y.; Yeh, S. C.; Chen, C. T.; Chen, C. T. *J. Mater. Chem.* **2012**, *22*, 21549-21559.
68. Wakim, S.; Alem, S.; Li, Z.; Zhang, Y.; Tse, S. C.; Lu, J.; Ding, J.; Tao, Y. *J. Mater. Chem.* **2011**, *21*, 10920-10928.
69. Zhao, W.; Qian, D.; Zhang, S.; Li, S.; Inganäs, O.; Gao, F.; Hou, J. *Adv. Mater.* **2016**, *28*, 4734-4739.
70. Liao, L.; Pang, Y. *Macromolecules* **2001**, *34*, 6756-6760.

TH-1906_11615303

71. Leclerc, N.; Michaud, A.; Sirois, K.; Morin, J. F.; Leclerc, M. *Adv. Funct. Mater.* **2006**, *16*, 1694-1704.
72. Zou, Y.; Wan, M.; Sang, G.; Ye, M.; Li, Y. *Adv. Funct. Mater.* **2008**, *18*, 2724-2732.
73. Mei, J.; Heston, N. C.; Vasilyeva, S. V.; Reynolds, J. R. *Macromolecules* **2009**, *42*, 1482-1487.
74. Ko, S.; Mondal, R.; Risko, C.; Lee, J. K.; Hong, S.; McGehee, M. D.; Bredas, J. L.; Bao, Z. *Macromolecules* **2010**, *43*, 6685-6698.
75. Abbotto, A.; Seri, M.; Dangate, M. S.; Angelis, F. D.; Manfredi, N.; Mosconi, E.; Bolognesi, M.; Ruffo, R.; Salamone, M. M.; Muccini, M. *J. Polym. Sci., Part A: Polym. Chem.* **2012**, *50*, 2829-2840.
76. Li, S.; He, Z.; Yu, J.; Chen, S.; Zhong, A.; Tang, R.; Wu, H.; Qin, J.; Li, Z. *J. Mater. Chem.* **2012**, *22*, 12523-12531.
77. Kulkarni, A. P.; Zhu, Y.; Jenekhe, S. A. *Macromolecules* **2005**, *38*, 1553-1563.
78. Wu, Z. Q.; Liu, D. F.; Wang, Y.; Liu, N.; Yin, J.; Zhu, Y. Y.; Qiu, L. Z.; Ding, Y. S. *Polym. Chem.* **2013**, *4*, 4588-4595.
79. Gadisa, A.; Mammo, W.; Andersson, L. M.; Admassie, S.; Zhang, F.; Andersson, M. R.; Inganäs, O. *Adv. Funct. Mater.* **2007**, *17*, 3836-3842.
80. Gu, Z.; Shen, P.; Tsang, S. W.; Tao, Y.; Zhao, B.; Tang, P.; Nie, Y.; Fang, Y.; Tan, S. *Chem. Commun.* **2011**, *47*, 9381-9383.
81. Peng, Q.; Lim, S. L.; Wong, I. H. K.; Xu, J.; Chen, Z. K. *Chem. Eur. J.* **2012**, *18*, 12140-12151.
82. Peng, Q.; Fu, Y.; Liu, X.; Xu, J.; Xie, Z. *Polym. Chem.* **2012**, *3*, 2933-2940.
83. Liu, X.; Huang, Y.; Cao, Z.; Weng, C.; Chen, H.; Tan, S. *Polym. Chem.* **2013**, *4*, 4737-4745.
84. Chakraborty, C.; Layek, A.; Ray, P. P.; Malik, S. *European Polymer Journal* **2014,** *52*, 181-192.
85. Liu, J.; Cheng, Y.; Xie, Z.; Geng, Y.; Wang, L.; Jing, X.; Wang, F. *Adv. Mater.* **2008**, *20*, 1357-1362.
86. Wang, M.; Hu, X.; Liu, P.; Li, W.; Gong, X.; Huang, F.; Cao, Y. *J. Am. Chem. Soc.* **2011**, *133*, 9638-9641.
87. Zhang, M.; Guo, X.; Wang, X.; Wang, H.; Li, Y. *Chem. Mater.* **2011**, *23*, 4264-4270.

TH-1906_11615303

88. Kim, J.; Yun, M. H.; Kim, G. H.; Kim, J. Y.; Yang, C. *Polym. Chem.* **2012**, *3*, 3276-3281.
89. Li, Z.; Tsang, S. W.; Du, X.; Scoles, L.; Robertson, G.; Zhang, Y.; Toll, F.; Tao, Y.; Lu, J.; Ding, J. *Adv. Funct. Mater.* **2011**, *21*, 3331-3336.
90. Wakim, S.; Alem, S.; Li, Z.; Zhang, Y.; Tse, S. C.; Lu, J.; Ding, J.; Tao, Y. *J. Mater. Chem.* **2011**, *21*, 10920-10928.
91. Liao, S. H.; Jhuo, H. J.; Cheng, Y. S.; Chen, S. A. *Adv. Mater.* **2013**, *25*, 4766-4771.
92. Jo, J. W.; Bae, S.; Liu, F.; Russell, T. P.; Jo, W. H. *Adv. Funct. Mater.* **2015**, *25*, 120-125.
93. Wang, N.; Chen, Z.; Wei, W.; Jiang, Z. *J. Am. Chem. Soc.* **2013**, *135*, 17060-17068.
94. Kesters, J.; Verstappen, P.; Raymakers, J.; Vanormelingen, W.; Drijkoningen, J.; D'Haen, J.; Manca, J.; Lutsen, L.; Vanderzande, D.; Maes, W. *Chem. Mater.* **2015**, *27*, 1332-1341.
95. Kesters, J.; Kudret, S.; Bertho, S.; Brande, N. V. D.; Defour, M.; Mele, B. V.; Penxten, H.; Lutsen, L.; Manca, J.; Vanderzande, D.; Maes, W. *Org, Electron.* **2014**, *15*, 549-562.
96. Kim, J. Y.; Kim, Y. U.; Kim, H. J.; Um, H. A.; Shin, J.; Cho, M. J.; Choi, D. H. *Macromol. Res.* **2016**, *24*, 980-985.
97. Kim, H. J.; Han, A. R.; Cho, C. H.; Kang, H.; Cho, H. H.; Lee, M. Y.; Fréchet, J. M. J.; Oh, J. H.; Kim, B. J. *Chem. Mater.* **2012**, *24*, 215-221.
98. Meng, B.; Fu, Y.; Xie, Z.; Liu, J.; Wang, L. *Macromolecules* **2014**, *47*, 6246-6251.
99. Burkhart, B.; Khlyabich, P. P.; Thompson, B. C. *Macromolecules* **2012**, *45*, 3740-3748.
100. Peet, J.; Kim, J. Y.; Coates, N. E.; Ma, W. L.; Moses, D.; Heeger, A. J.; Bazan, G. C. *Nat. Mater.* **2007**, *6*, 479-500.
101. Tsao, H. N.; Cho, D. M.; Park, I.; Hansen, M. R.; Mavrinskiy, A.; Yoon, D. Y.; Graf, R.; Pisula, W.; Spiess, H. W.; M€ullen, K. *J. Am. Chem. Soc.* **2011**, *133*, 2605-2612.
102. Mierloo, S. V.; Hadipour, A.; Spijkman, M. J.; Brande, N. V. D.; Ruttens, B.; Kesters, J.; D'Haen, J.; Assche, G. V.; Leeuw, D. M. D.; Aernouts, T.; Manca, J.; Lutsen, L.; Vanderzande, D. J.; Maes, W. *Chem. Mater.* **2012**, *24*, 587-593.

TH-1906_11615303

103. Zhu, D.; Bao, X.; Zhu, Q.; Gu, C.; Qiu, M.; Wen, S.; Wang, J.; Shahid, B.; Yang, R. *Energy Environ. Sci.* **2017**, *10*, 614-620.
104. Xia, B.; Lu, K.; Yuan, L.; Zhang, J.; Zhu, L.; Zhu, X.; Deng, D.; Li, H.; Wei, Z. *Polym. Chem.* **2016**, *7*, 1323-1329.
105. Keshtov, M. L.; Khokhlov, A. R.; Kuklin, S. A.; Chen, F. C.; Koukaras, E. N.; Sharma, G. D. *ACS Appl. Mater. Interfaces* **2016**, *8*, 32998-33009.
106. Wang, M.; Cai, D.; Yin, Z.; Chen, S. C.; Du, C. F.; Zheng, Q. *Adv. Mater.* **2016**, *28*, 3359-3365.
107. Dou, L.; Chen, C. C.; Yoshimura, K.; Ohya, K.; Chang, W. H.; Gao, J.; Liu, Y.; Richard, E.; Yang, Y. *Macromolecules* **2013**, *46*, 3384-3390.
108. Zhao, X.; Qian, L.; Cao, J.; Yan, S.; Ding, L. *Polym. Chem.* **2016**, *7*, 1226-1229.
109. Yang, D.; Li, Z.; Li, Z.; Zhao, X.; Zhang, T.; Wu, F.; Tian, Y.; Ye, F.; Sun, Z.; Yang, X. *Polym. Chem.* **2017**, *8*, 4332-4338.
110. Zheng, Z.; Awartani, O. M.; Gautam, B.; Liu, D.; Qin, Y.; Li, W.; Bataller, A.; Gundogdu, K.; Ade, H.; Hou, J. *Adv. Mater.* **2017**, *29*, 1604241.
111. Ye, L.; Zhang, S.; Qian, D.; Wang, Q.; Hou, J. *J. Phys. Chem. C* **2013**, *117*, 25360-25366.
112. Gao, D.; Djukic, B.; Shi, W.; Bridges, C. R.; Kozycz, L. M.; Seferos, D. S. *ACS Appl. Mater. Interfaces* **2013**, *5*, 8038-8043.
113. Hwang, Y. J.; Courtrigh, B. A. E.; Ferreira, A. S.; Tolbert, S. H.; Jenekhe, S. A. *Adv. Mater.* **2015**, *27*, 4578-4584.
114. Lin, Y.; Zhao, F.; He, Q.; Huo, L.; Wu, Y.; Parker, T. C.; Ma, W.; Sun, Y.; Wang, C.; Zhu, D.; Heeger, A. J.; Marder, S. R.; Zhan, X. *J. Am. Chem. Soc.* **2016**, *138*, 4955-4961.
115. Wang, E.; Hou, L.; Wang, Z.; Hellström, S.; Zhang, F.; Inganäs, O.; Andersson, M. R. *Adv. Mater.* **2010**, *22*, 5240-5244.
116. Liao, H. C.; Ho, C. C.; Chang, C. Y.; Jao, M. H.; Darling, S. B.; Su, W. F. *Mater. Today* **2013**, *16*, 326-336.
117. Kymakis, E.; Alexandrou, I.; Amaratunga, G. A. J. *J. Appl. Phys.* **2003**, *93*, 1764-1768.
118. Ago, H.; Petritsch, K.; Shaffer, M. S. P.; Windle, A. H.; Friend, R. H. *Adv. Mater.* **1999**, *11*, 1281-1285.
119. Saran, N.; Parikh, K.; Suh, D. S.; Munoz, E.; Kolla, H.; Manohar, S. K. *J. Am. Chem. Soc.* **2004**, *126*, 4462-4463.

TH-1906_11615303

120. Nismy, N. A.; Jayawardena, K. D. G. I.; Adikaari, A. A. D. T.; Silva, S. R. P. *Adv. Mater*. **2011**, *23*, 3796-3800.
121. Goutam, P. J.; Singh, D. K.; Giri, P. K.; Iyer, P. K. *J. Phys. Chem. B* **2011**, *115*, 919-924.
122. Ran, C.; Wang, M.; Gao, W.; Ding, J.; Shi, Y.; Song, X.; Chen, H.; Ren, Z. *J. Phys. Chem. C* **2012**, *116*, 23053-23060.
123. Kim, H.; Shin, M.; Kim, Y. *EPL* **2008**, *84*, 58002.
124. Guo, X.; Zhou, N.; Lou, S. J.; Smith, J.; Tice, D. B.; Hennek, J. W.; Ortiz, R. P.; Navarrete, J. T. L.; Li, S.; Strzalka, J.; Chen, L. X.; Chang, R. P. H.; Facchetti, A.; Marks, T. J. *Nat. Photonics* **2013**, *7*, 825-833.
125. Zhou, N.; Guo, X.; Ortiz, R. P.; Li, S.; Zhang, S.; Chang, R. P. H.; Facchetti, A.; Marks, T. J. *Adv. Mater*. **2012**, *24*, 2242-2248.
126. You, J.; Dou, L.; Yoshimura, K.; Kato, T.; Ohya, K.; Moriarty, T.; Emery, K.; Chen, C. C.; Gao, J.; Li, G.; Yang, Y. *Nat. Commun.* **2012**, *4*, 1446.
127. Gasparini, N.; Jiao, X.; Heumueller, T.; Baran, D.; Matt, G. J.; Fladischer, S.; Spiecker, E.; Ade, H.; Brabec, C. J.; Ameri, T. *Nat. Energy* **2016**, *1*, 16118.

TH-1906_11615303

Chapter 2

Photo Stability Enhancement of Poly(3-hexylthiophene)-PCBM Nano-composites by Addition of Multi Walled Carbon Nanotubes Under Ambient Conditions

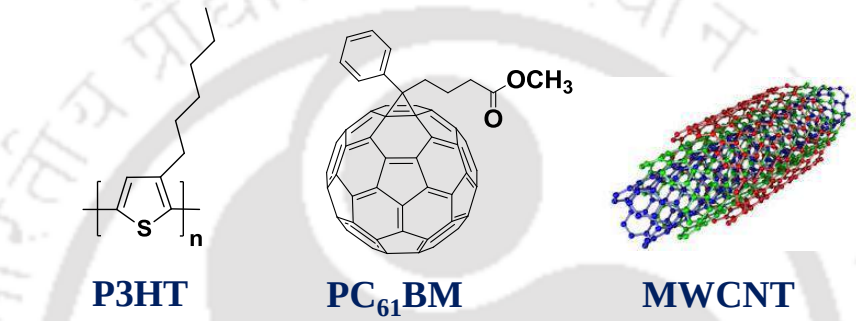

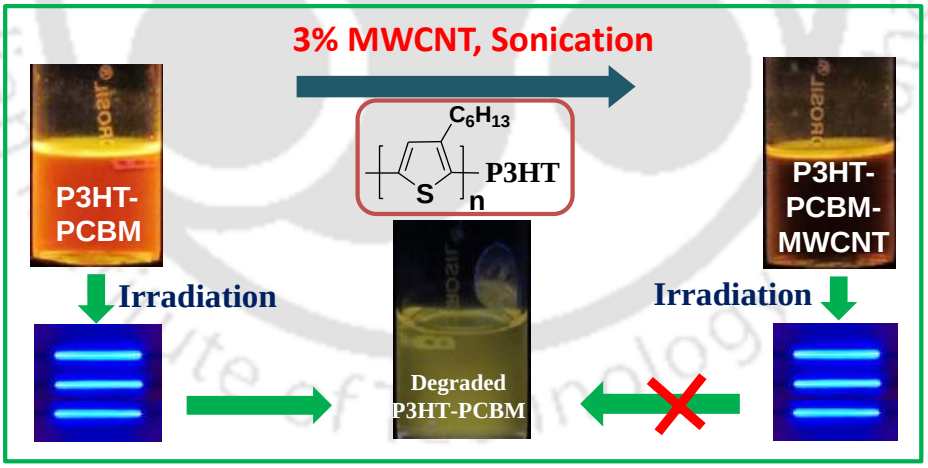

Org. Electron. **2014**, *15*, 1650-1656.

TH-1906_11615303

Abstract

Poly(3-hexylthiophene):phenyl-C61-butyric acid methyl ester (P3HT-PCBM) composites find wide application in optoelectronic devices, especially bulk-hetero junction (BHJ) solar cells. These composites, even though could give efficient polymer solar cells with ~4-5% power conversion efficiencies (PCE), a major problem of photo stability is associated with it and remains unsolved. P3HT-PCBM composite was found to be degrading on irradiation with ultraviolet radiation or a solar simulator providing AM 1.5G illumination (1000 W m^{-2}, 72 ± 2 °C or 330 W m^{-2}, 25 °C), in presence of oxygen and moisture. The photo stability of P3HT-PCBM under ambient conditions has been studied to observe that a new ternary composite, P3HT-PCBM-MWCNT (multi walled carbon nanotube) has superior photo stability even on extended UV-visible exposure. A total of 7% (w/w) PCBM and 3% (w/w) MWCNT with respect to P3HT resulted in optimum stability. UV-visible and fluorescence spectral analysis have been used to study the photo stability, both in solution state and solid/film state. Transmission electron micrograph (TEM) along with selected area electron diffraction (SAED) pattern and field emission scanning electron microscopy (FE-SEM) micrographs have been used to show the well coating of MWCNT on P3HT-PCBM composite. Since MWCNT is one of the very important carbon based nano-material with several supreme characteristics, this new ternary composite has great importance for optoelectronic applications.

2.1 Introduction

Composite of poly(3-hexylthiophene) with PCBM has been studied extensively as a donor-acceptor combination in bulk-heterojunction solar cells,[1] where P3HT acts as a donor and PCBM an acceptor. P3HT and its composites with PCBM are reported to degrade under UV-irradiation due to the presence of dissolved molecular oxygen and moisture.[2-4] Yet the application of this composite material is continuing and has been used as a standard material for fabricating bulk-heterojunction (BHJ) solar cells. Although several alternative materials are also being developed, the most promising materials still comprise of thiophene, substituted thiophenes[5,6] and cyclopentadithiophene (CPDT) type molecules. Over the past few years, CNTs with good conductivity, optical and physical properties[7,8] have received immense attention as an acceptor to replace PCBM,[9] as an anode to replace ITO[10,11] and incorporating into active layer of BHJ solar cell as exciton dissociation enhancer.[12-15] In active layer, CNTs act as exciton dissociation center by

TH-1906_11615303

transporting both holes and electrons, which otherwise lead to recombination of exciton and hence poor device performance. Moreover it has been reported that MWCNT gives best polymer solar cell in presence of P3HT and PCBM than SWCNT.[16]

The major efforts in most reports has been on the enhancement of PCE, by synthesizing newer conjugated polymer structures having low band gap to harvest efficient solar energy with deep HOMO level to improve the V_{oc} and synthesizing various acceptor moieties as well.[17,18] Other important study for BHJ solar cell is its stability and durability. Hence, a detailed study on photo stability and its enhancement is highly essential (as BHJs are known to degrade in presence of oxygen and moisture) which brings in-depth study on PSCs to sustain the aim of achieving affordable, clean and green energy for future generations.[19] In a previous report very high photo stability of P3HT was reported by Goutam et al. by preparing composites with MWCNT, where total of less than 10% (w/w) MWCNT composite with P3HT was found to be a photo stable composite towards optoelectronic application.[20] The mechanism for the high PL quenching of P3HT observed in the P3HT-MWCNT composite due to the electron transfer from photo-excited P3HT to MWCNT involves not just a simple collision-induced quenching but also π-π and CH-π interactions. It was further realized that, with the above knowledge, it is also important to stabilize the P3HT-PCBM binary mixture which is the most frequently used composite for BHJ solar cells. Yet, no meticulous reports are available that explain the appropriate ratios of stabilizing components for P3HT-PCBM under ambient conditions. Herein, a systematic study has been performed on the photo stability of this binary mixture in the presence of MWCNT at various ratios and optimized the conditions that could be utilized for fabricating photovoltaic devices even under ambient conditions. The P3HT-PCBM binary mixture was converted to a ternary composite by sonicating with MWCNT, maintaining the total amount of carbon nanomaterial (PCBM-MWCNT) within 10% (w/w). It was found that P3HT-PCBM (7%)-MWCNT (3%) is a better photo stable composite than P3HT and P3HT-PCBM (10%) composite. The reasons for enhancement of photo stability are CH-π and π-π interactions between P3HT and MWCNT along with PCBM within P3HT-PCBM-MWCNT nano-composites. For P3HT-PCBM (7%)-MWCNT (3%), 3% MWCNT might have been the optimum amount to be able to coat over polymer surface appropriately (established using FE-SEM images), leading to better CH-π and π-π interaction with in the composite.

TH-1906_11615303

2.2 Results and discussion

2.2.1 Solution state photo-degradation study via UV-visible spectra

UV-visible spectroscopy of P3HT-PCBM (10%) w/w composite shows a wavelength maximum of 440 nm for π-π* transition of P3HT,[21] due to the extended conjugated backbone of the polymer P3HT and a peak at around 330 nm due to π-π* transition of PCBM. On UV-irradiation a gradual blue shift (Table 2.1) and decrease in intensity is observed for the π-π* transition of P3HT (Figure 2.1a) for 12 minute exposure time (absorption spectra recorded up to 15 minute irradiation, but spectra shown only for 0, 3, 6, 9, 12 minute irradiation for comparison). In order to compare the changes in wavelength due to the blue shift in all the composites, the spectra were plotted in normalized mode. The cause for the degradation of P3HT-PCBM composite is the disruption of π-conjugation in the backbone and shortening of this conjugated backbone followed by complete degradation of polymer P3HT.[22] At the same time intensity of π-π* transition for PCBM gets increased, because degradation of P3HT brings PCBM molecules closer to each other leading to their enhanced intensity (Figure 2.1a to 2.1g).

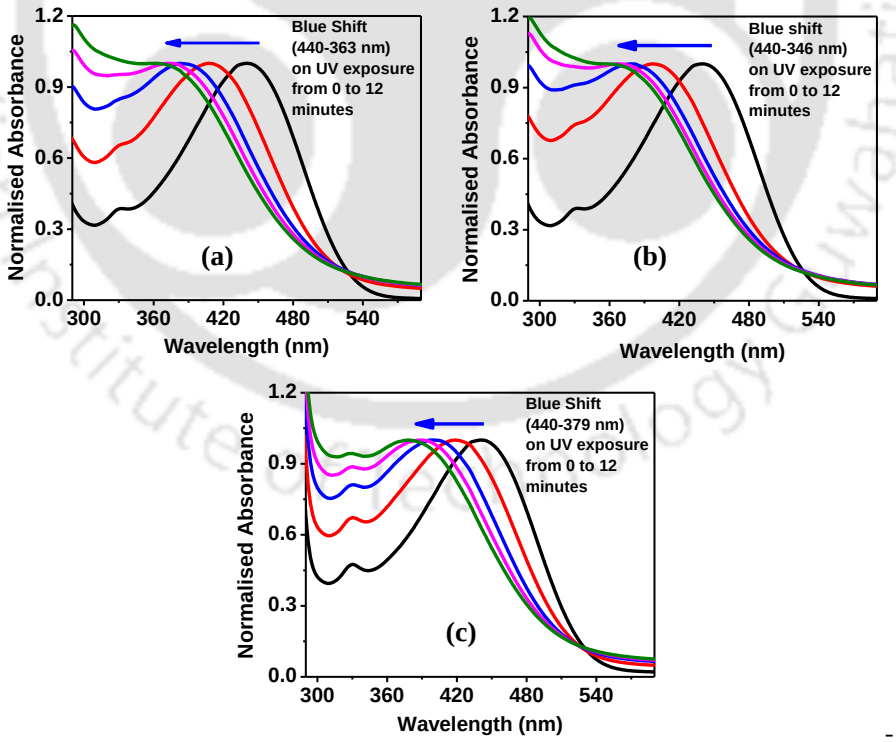

Figure 2.1 Photo-degradation under UV radiation of composites in dry chloroform causes blue shift in UV-visible spectra (a) P3HT-PCBM (10%) (b) P3HT-PCBM (10%) with 5 µl H2O in 3 ml chloroform (c) P3HT-PCBM (9%)-MWCNT (1%).

TH-1906_11615303

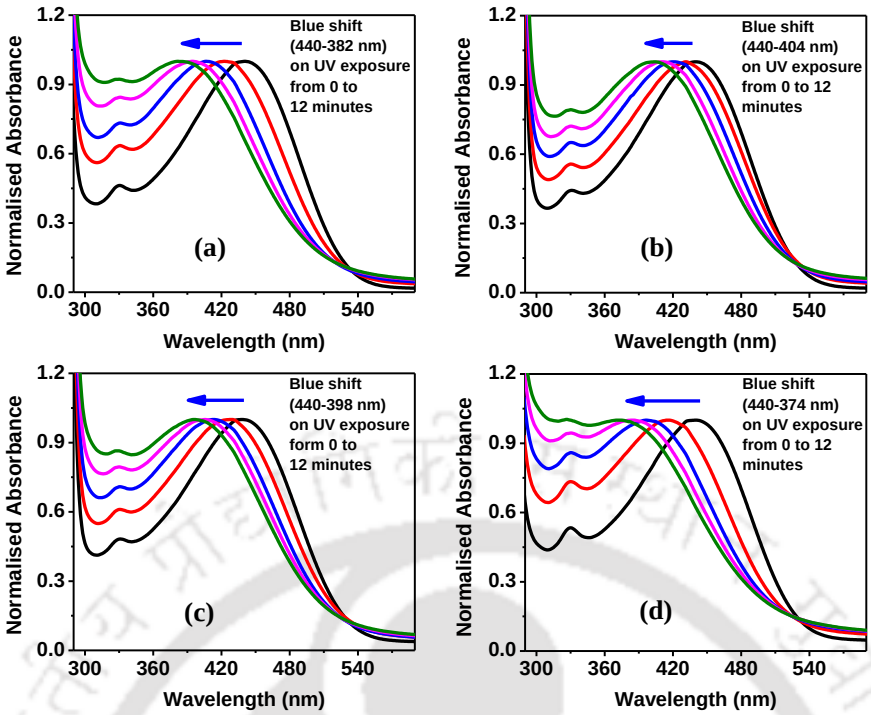

Figure 2.2 Photo-degradation under UV radiation of composites in dry chloroform, causes blue shift in UV-Visible spectra (a) P3HT-PCBM (8%)-MWCNT (2%) (b) P3HT-PCBM (7%)-MWCNT (3%) (c) P3HT-PCBM (6%)-MWCNT (4%) (d) P3HT-PCBM (5%)-MWCNT (5%).

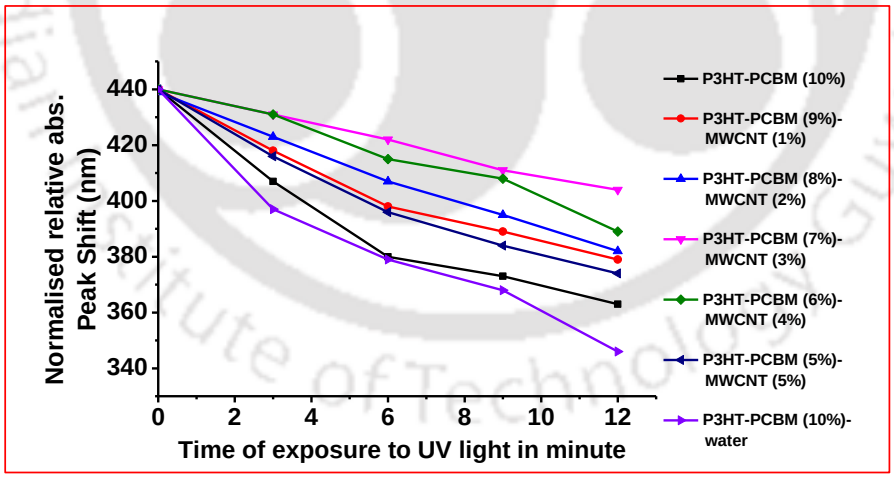

Figure 2.3 Comparison of photo-degradation of all the composites and composite with moisture in solution state.

Although all the above studies were performed at ambient conditions (relative humidity during the time of experiments is 55-60%), the effect of moisture on the composite has also been studied additionally by diffusing 5 µL water in 3 mL (out of 5 mL standard

TH-1906_11615303

solution) solution of P3HT-PCBM (10%) composite in the UV-Cuvette. In presence of additional amount of water, the observed huge blue shift of 94 nm, under 12 min exposures is much higher, indicating faster degradation of the P3HT-PCBM (Figure 2.1b) binary mixture. Better stability is observed in case of P3HT-PCBM (9%) - MWCNT (1%) composite (Figure 2.1c) in comparison to the binary P3HT-PCBM composite. Stability further increases in the P3HT-PCBM (9%)-MWCNT (3%) composite (Figure 2.2b) with much less photo-degradation on exposure to UV-irradiation up to 12 minutes. This indicates that on preparing composites with 1% MWCNT's, a large part of the P3HT remains uncoated, exposing them to UV-irradiation which results in photo-degradation, whereas increasing the quantity to 3% MWCNT in the composites, results in lesser exposure to UV irradiation. However, on further increasing the amount of MWCNT as in the case of P3HT-PCBM (5%)-MWCNT (5%) (Figure 2.1d), the photo stability decreases again due to presence of excess of MWCNT. Overall these studies confirm that P3HT-PCBM (7%)-MWCNT (3%) were shown to have optimum photo stability (Figure 2.3) under ambient conditions. On carefully scrutinizing the observed results of regular increase in photo stability among the composites having 1% MWCNT to 2% MWCNT and from 2% MWCNT to 3% MWCNT and the regular decrease in photo stability of the composite having 3% MWCNT to 4% and from 4% MWCNT to 5% MWCNT (Figure 2.1, 2.2 and 2.3), three out of the six nano-composites [P3HT-PCBM (9%)-MWCNT (1%), P3HT-PCBM (7%)-MWCNT (3%), P3HT-PCBM (5%)-MWCNT (5%)] were chosen and further studied for their photo stability.

2.2.2 Thin-film state photo-degradation study via UV-visible spectra

As like in $CHCl_3$, similar UV degradation experiments were also performed in solid state films for four different composites (Figure 2.4a to 2.4d) namely, P3HT-PCBM (10%), P3HT-PCBM (9%)-MWCNT (1%), P3HT-PCBM (7%)-MWCNT (3%), P3HT-PCBM (5%)- MWCNT (5%) by spin coating dry chloroform solutions of composites on a clean glass slide and baked for 1 hour at 80 °C, to let the solvent evaporate.

The absorption of pristine P3HT film as well as the P3HT-PCBM film was found to be at 463 nm (Figure 2.4a). The absorption maxima of P3HT-PCBM-MWCNT was 473 nm which is approximately 10 nm red shifted compared to the P3HT-PCBM composite. The below study confirms that the thin film degradation studies were in agreement with the

TH-1906_11615303

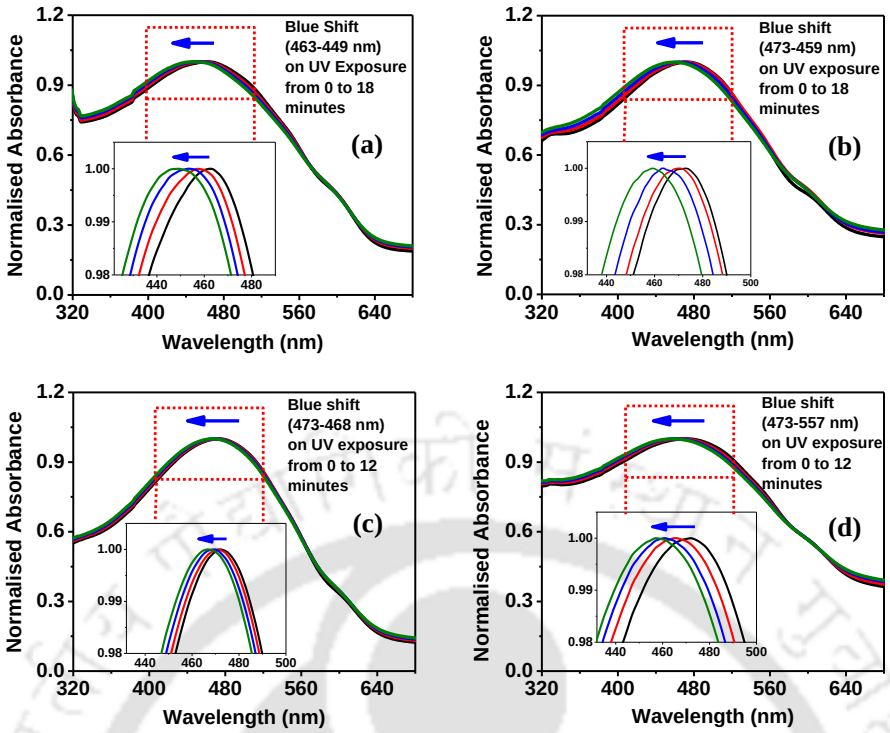

Figure 2.4 solid state UV-degradation studies of composites (a) P3HT-PCBM (10%) (b) P3HT-PCBM (9%)-MWCNT (1%) (c) P3HT-PCBM (7%)-MWCNT (3%) (d) P3HT-PCBM (7%)-MWCNT (3%).

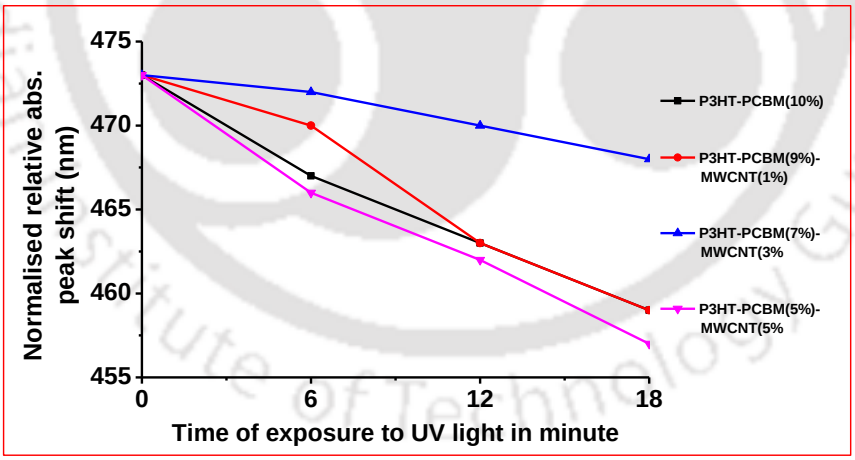

Figure 2.5 Photo stability comparison shows better stability of P3HT-PCBM (7%)-MWCNT (3%) in solid state too.

solution state data leading to better stability of P3HT-PCBM (7%)-MWCNT (3%), (Figure 2.4b-d and Figure 2.5). The above shift observed for the absorption maxima (for comparison, all the spectra were normalized to 473 nm) of the composites films are common and are in well agreement with earlier reports in literature for composites with

TH-1906_11615303

P3HT.[23,24] The absorption maxima is higher (463 nm) in solid state compared to solution state (440 nm), which may be due to the formation of *J*-aggregates in solid state where molecular aggregation occurs. Also the change in wavelength on UV-irradiation in case of solid state under ambient conditions was very less compared to solution state (Table 2.1). Hence, figures were shown in enlarged format for better clarity. The reason behind less change in solid state may be due to higher molecular stacking in solid state

Table 2.1 Details of wavelength change caused by photo-degradation and comparison of stability among the composites.

Composites	Degradation in Solution state, λ_{max} in nm			Degradation in Solid state, λ_{max} in nm		
	At '0' min.	At '12' min	Change	At '0' min.	At '12' min	Change
P3HT - PCBM (10%)	440	363	77	463	449	14
P3HT-PCBM 10(%)-5 µL water.	440	346	94	-	-	-
P3HT - PCBM (9%) - MWCNT (1%)	440	379	61	473	459	14
P3HT - PCBM (8%) - MWCNT (2%)	440	382	58	-	-	-
P3HT - PCBM (7%) - MWCNT (3%)	440	404	36	473	468	5
P3HT - PCBM (6%) - MWCNT (4%)	440	398	42	-	-	-
P3HT - PCBM (5%) - MWCNT (5%)	440	374	66	473	457	16

2.2.3 FE-SEM and TEM analysis of composites

In order to prove the presence of MWCNT and PCBM with their various ratios in composites with P3HT and to have a better understanding and representation into the degraded and un-degraded composites, TEM (Figure 2.6) and FE-SEM (Figure 2.7) micrographs have been used as a tool to characterize these mixtures. TEM microscopic analysis of composites shows the morphology of binary P3HT-PCBM composite (Figure 2.6a),[25] the crystalline nature of the 5 minutes degraded sample of P3HT-PCBM (10%) (Figure 2.6b), and ternary composite of P3HT-PCBM-MWCNT (Figure 2.6c to e) having MWCNT in cylindrical shape.[26] With SAED patterns presented in the manuscript confirms that the composites degrade (as amorphous composite converted to crystalline) and rates of their degradation can be compared form observed amount of crystallinity. SAED pattern of P3HT-PCBM (10%) composite shows crystalline nature in the 5 minutes UV light exposed sample (Figure 2.6b), compared to the non-exposed sample (Figure 2.6a), which can be clearly distinguished and interpreted from the morphology

TH-1906_11615303

difference of the degraded sample under exposure to UV irradiation. Similar SAED pattern of P3HT-PCBM (7%)-MWCNT (3%) (Figure 2.6f) shows less crystalline nature than P3HT-PCBM (9%)-MWCNT (1%), (Figure 2.6d). Because of the optimum stability observed for the P3HT-PCBM (7%)-MWCNT (3%), the polymer P3HT wrapped on the nanotubes did not degrade with due cause of reduction in photooxidation and shortening in conjugation length, as a result the amorphous nature remains intact before and after the UV exposure. The dispersion of MWCNTs in conjugated polymers has been one of the major problems in processing it.[27] It is likely that the interaction between P3HT and MWCNTs via π-π and CH-π forces overcomes the van der Waals interaction between MWCNT, resulting in uniform dispersion within the solution that stays stable for several weeks.[28]

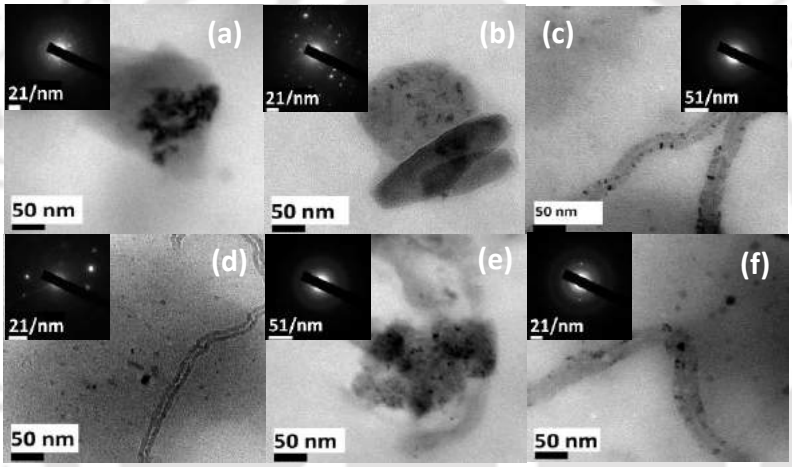

Figure 2.6 TEM images and SAED pattern of composites (a) P3HT-PCBM (10%) (b) 5 minutes degraded sample of P3HT-PCBM (10%) shows crystalline nature (c) P3HT-PCBM (9%)-MWCNT (1%) (d) P3HT-PCBM (9%)-MWCNT (1%), degraded up to 20 minutes shows crystalline behavior (e) P3HT-PCBM(7%)-MWCNT(3%) (f) P3HT-PCBM (7%)-MWCNT (3%) degraded for 20 minutes shows no crystalline nature.

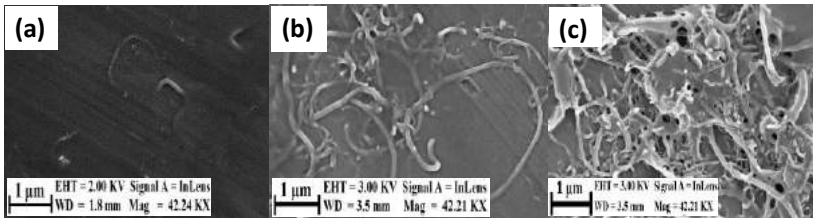

Figure 2.7 FE-SEM images shows ratio of MWCNT in composites (a) P3HT-PCBM (9%)-MWCNT (1%) (b) P3HT-PCBM (7%)-MWCNT (3%) (c) P3HT-PCBM (5%)-MWCNT (5%).

TH-1906_11615303

2.2.4 Charge transfer investigation with in prepared nano-composites

It is well known that both MWCNT and PCBM are capable of accepting or donating electrons from the excited state or ground state of P3HT,[29] (band diagram given in Appendix A2).

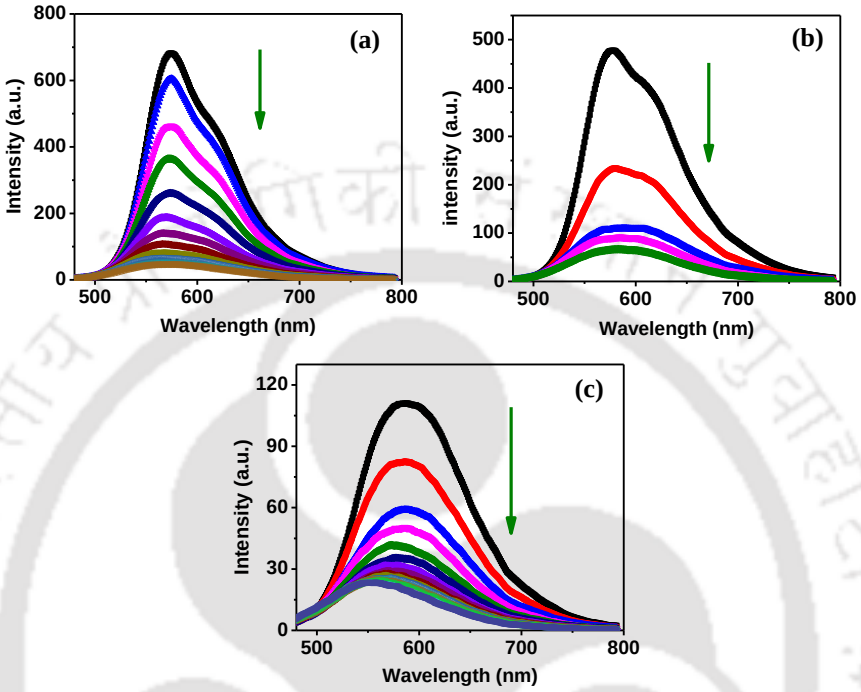

Figure 2.8 PL spectra of composites recorded in steps of 1 minute exposure of UV-radiation (a) P3HT-PCBM (9%)-MWCNT (1%) (b) P3HT-PCBM (7%)-MWCNT (3%) (c) P3HT-PCBM (5%)-MWCNT (5%).

In order to investigate the effect of charge transfer with respect to the loading of MWCNT and UV-exposure, photoluminescence spectra were recorded with steps of 1 minute UV-irradiation intervals under ambient conditions. The charge transfer from P3HT to PCBM and MWCNT has been confirmed by photoluminescence quenching of P3HT (λ_{emis}= 575 nm, I_{arb} = 734 (Figure attached in Appendix A2), whereas in case of 1% MWCNT composite a regular fluorescence quenching up to ~22% (step wise reduction of $I_{arb.}$= 680 to $I_{arb.}$= 149) occurred with UV-irradiation for 8 minutes (Figure 2.8a) and a quenching of ~51% ($I_{arb.}$= 477 to $I_{arb.}$= 232) in case of composite having 3% MWCNT only in 1 minute exposure (Figure 2.8b), which confirms faster charge transfer from P3HT to PCBM and MWCNT. In case of 5% MWCNT composite the charge transfer is so fast that the emission intensity remains below 110 arbitrary units at the same concentration used for 1% and 3% MWCNT which is evident in Figure 2.8c. Possibly

TH-1906_11615303

charge transfer occurs from LUMO of P3HT to LUMO of PCBM and from Fermi level of MWCNT to HOMO of P3HT leading to the observed quenching in fluorescence in all the composites (Appendix A2). Also reduction in photo oxidation is observed in all composites is caused by the above two phenomenon.

2.2.5 Understanding the reason for photo stability

According to earlier reports[30] it was suggested that both reduced π-conjugation and chain scission are responsible for the photo-degradation of P3HT. Chain scissions occur via a classical route of photooxidation where scission is initiated by residual trace amount of transition metal salt impurities used in the preparation of CNTs.[31] Therefore, adding more than 3% CNTs with P3HT is responsible for the reduction in stability of P3HT due to higher quantities of metal impurities. CH-π and π-π interaction between P3HT and MWCNT along with PCBM results in the enhancement of photo-stability of P3HT-PCBM (9%)-MWCNT (1%) nano-composite. The main reason for better photo stability in P3HT-PCBM (7%)-MWCNT (3%) compared to the P3HT-PCBM (9%)-MWCNT (1%) might be due to the better CH-π and π-π interaction between P3HT-PCBM-MWCNT and 3% MWCNT might be able to coat on polymer surface appropriately, establishing that 3% MWCNT is an optimum amount, leading to better wrapping on P3HT, which have been established using FE-SEM (Figure 2.7). With the help of optical and microscopic experiments it has been shown that the P3HT-PCBM (7%)-MWCNT (3%) ternary mixture has highest photo stability under ambient conditions under UV exposure as compared to the photo stability of pristine P3HT-PCBM composites or any other composite ratios.

2.3 Conclusion

This study described that the photo stability of a ternary composite comprising P3HT-PCBM-MWCNT prepared by sonicating various ratios of PCBM and MWCNT in chloroform, can be improved significantly by preparing composites having appropriate ratios of each component. This study establishes that P3HT-PCBM (7%) with MWCNT (3%) as a photo stable composite for optoelectronic application such as BHJ solar cells under ambient conditions, which has further been confirmed by solid state experiments. In all the composites, fast charge transfer from P3HT to PCBM and MWCNT occurs resulting in quenching of fluorescence even at low concentrations of the CNTs. Materials

TH-1906_11615303

and composites that display good charge transfer characteristics are desired for BHJ solar cell applications. Hence, the above photo stable composite comprising a thiophene based donor polymer, an acceptor and a photo stabilizing additive such as MWCNT in low concentrations can be applied for future optoelectronic application.

2.4 Experimental procedures

2.4.1 Synthesis of poly(3-hexylthiophene)

P3HT used in these studies were synthesized by a known oxidative polymerization method using $FeCl_3$ as catalyst with high molecular weight and good PDI value.[32,33] Gel permeation chromatographic analysis of the synthesized P3HT (THF, Polystyrene standard) showed weight average molecular weight, M_w = 50,439 with PDI-1.05.

2.4.2 Preparation of P3HT-PCBM and P3HT-PCBM-MWCNT nano-composites

All six composites namely, P3HT-PCBM (10%), P3HT-PCBM (9%)-MWCNT (1%), P3HT-PCBM (8%)-MWCNT (2%), P3HT-PCBM (7%)-MWCNT (3%), P3HT-PCBM (6%)-MWCNT (4%) P3HT-PCBM and (5%)-MWCNT (5%) were prepared by ultrasonication for 30 minutes at ambient conditions. In all the composites the standard solution was 7 mg P3HT in 3 mL dry chloroform, to which mentioned w/w percentages of PCBM and MWCNT were added. The weight percentages of PCBM and MWCNT are according to the weight of P3HT taken.

2.4.3 Degradation studies in UV chamber

Stability studies of composites were performed by irradiating inside the UV chamber in steps of 1 minute and subsequent UV-visible spectra were recorded for every exposure at ambient conditions. Similar concentration of composites was mentioned for degradation study, with necessary equivalent dilution. This experiment was also done in solid state by spin coating the composites on a glass substrate cleaned in acetone by sonicating at ambient conditions.

TH-1906_11615303

2.5 References

1. Thompson, B. C.; Frechet, J. M. J. *Angew. Chem. Int. Ed.* **2008,** *47*, 58-77.
2. Cook, S.; Furube, A.; Katoh, R. *J. Mater. Chem.* **2012**, *2*, 4282-4289.
3. Tromholt, T.; Madsen, M. V.; Carle, J. E.; Helgesen, M.; Krebs, F. C. *J. Mater. Chem.* **2012**, *22*, 7592-7601.
4. Lee, J. U.; Jung, J. W.; Jo, J. W.; Jo, W. H. *J. Mater. Chem.* **2012**, *22*, 24265-42283.
5. Miyanishi, S.; Tajima, K.; Hashimoto, K. *Macromolecules* **2009**, *42*, 1610-1618.
6. Bijleveld, J. C.; Shahid, M.; Gilot, J.; Wienk, M. M.; Janssen, R. A. J. *Adv. Funct. Mater.* **2009**, *19*, 3262-3270.
7. Baughman, R. H.; Zakhidov, A. A.; Heer, W. A. D. *Science* **2002**, *297*, 787-792.
8. Dresselhaus, M. S.; Dresselhaus, G.; Charlier, J. C.; Hernandez, E. *Phil. Trans. R. Soc. Lond. A* **2004**, *362*, 2065-2098.
9. Kymakis, E.; Alexandrou, I.; Amaratunga, G. A. J. *J. Appl. Phys.* **2003**, *93*, 1764-1768.
10. Ago, H.; Petritsch, K.; Shaffer, M. S. P.; Windle, A. H.; Friend. R. H. *Adv. Mater.* **1999**, *11*, 128-1285.
11. Saran, N.; Parikh, K.; Suh, D. S.; Munoz, E.; Kolla, H.; Manoha, S. K. *J. Am. Chem. Soc.* **2004**, *126*, 4462-4463.
12. Berson, S.; Bettignies, R. D.; Bailly, S.; Guillerez, S.; Jousselme, B. *Adv. Funct. Mater.* **2007**, *17*, 3363-3370.
13. Kymakis, E.; Koudoumas, E. *SPIE Digital Library* **2008**, *6999*, 69991N1-69991N6.
14. Sgobba, V.; Guldi, D. M. *J. Mater. Chem.* **2008**, *18*, 153-157.
15. Nismy, N. A.; Jayawardena, K. D. G. I.; Adikaari, A. A. D. T.; Silva, S. R. P. *Adv. Mater.* **2011**, *23*, 3796-3800.
16. Sgobba, V.; Rahman, G. M. A.; Guldi, D. M.; Jux, N.; Campidelli, S.; Prato, M. *Adv. Mater.* **2008**, *18*, 2264-2269.
17. Li, Z.; Tsang, S. W.; Du, X.; Scoles, L.; Robertson, G.; Zhang, Y.; Toll, F.; Tao, Y.; Lu, J.; Ding, J. *Adv. Funct. Mater.* **2011**, *21*, 3331-3336.
18. Mühlbache, D.; Scharbe, M.; Morana, M.; Zhu, Z.; Waller, D.; Gaudiana, R.; Brabec, C. *Adv. Mater.* **2006**, *18*, 2884-2889.
19. Norrman, K.; Madsen, M. V.; Gevorgyan, S. A.; Krebs, F. C. *J. Am. Chem. Soc.* **2010**, *132*, 16883-16892.

TH-1906_11615303

20. Goutam, P. J.; Singh, D. K.; Giri, P. K.; Iyer, P. K. *J. Phys. Chem. B* **2011**, *115*, 919-924.
21. Shrotriya, V.; Ouyang, J.; Tseng, R. J.; Li, G.; Yang, Y. *Chem. Phys. Lett.* **2005**, *411*, 138-143.
22. Holdcroft, S. *Macromolecules* **1991**, *24*, 2119-2121.
23. Kuila, B. K.; Nandi, A. K. *Macromolecules* **2004** *37*, 8577-8584.
24. Kuila, B. K.; Nandi, A. K. *J. Phys. Chem. B* **2006**, *110*, 1621-1631.
25. Lee, J. U.; Jung, J. W.; Emrick, T.; Russell, T. P.; Jo, W. H. *J. Mater. Chem.* **2010**, *20*, 3287-3294.
26. Liu, C. D.; Shu, D. Y.; Tsao, C. T.; Han, J. L.; Tsai, F. Y.; Chen, F. C.; Chen, W. C.; Hsieh, K. H. *Compos. Sci. Technol.* **2010**, *70*, 1242-1248.
27. Bahr, J. L.; Mickelson, E. T.; Bronikowski, M. J.; Smalley, R. E.; Tour, J. M. *Chem. Commun.* **2001**, *2*, 193-194.
28. Geng, J.; Kong, B. S.; Yang, S. B.; Youn, S. C.; Park, S.; Joo, T.; Jung, H. T. *Adv. Funct. Mater.* **2008**, *18*, 2659-2665.
29. Sariciftci, N. S.; Smilowitz, L.; Heeger, A. J.; Wudl, F. *Science* **1992**, *258*, 1474-1476.
30. Abdou, M. S. A.; Holdcroft, S. *Macromolecules* **1993**, *26*, 2954-2962.
31. Kumar, M.; Ando, Y. *J. Nanosci. Nanotechnol.* **2010**, *10*, 3739-3758.
32. Pomerantz, M.; Liu, L.; Zhang, X. *Arkivoc*, **2003**, *12*, 119-137.
33. Reddy, P. K.; Goutam, P. J.; Singh, D. K.; Ghoshal, A. K.; Iyer, P. K. *Poly. Degrad. Stab.* **2009**, *94*, 1839-1848.

TH-1906_11615303

Chapter 3

Insight into The Synthesis and Fabrication of 5,6-*alt*-Benzothiadiazole Based D-π-A Conjugated Co-polymers for Bulk-heterojunction Solar Cell

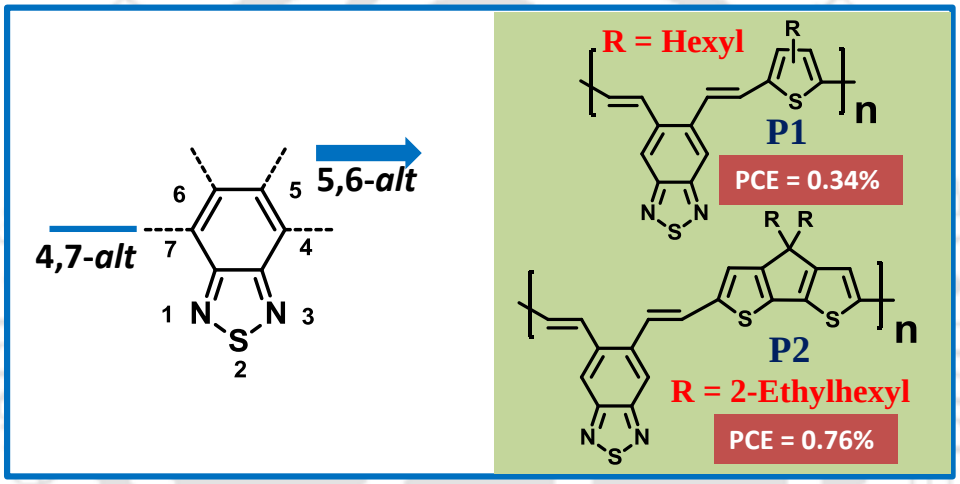

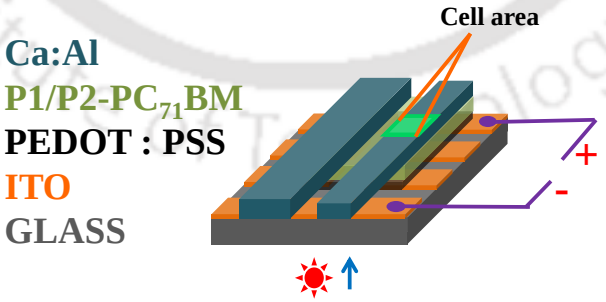

Polym. Bull. **2017**, DOI:10.1007/s00289-017-2193-x.

TH-1906_11615303

Abstract

Herein, two new 5,6-*alt*-benzothiadiazole based poly(o-arylene-vinylene) (POAV) type of D-π-A conjugated copolymers, namely P1 and P2 have been synthesized by using Horner-Wittig reaction and characterized by UV-visible, ^{1}H-NMR, ^{13}C-NMR and CV. With a deeper HOMO level of ≈5.95 eV, these two polymers have been used as donor with [6,6]-phenyl C61-butyric acid methyl ester, $PC_{61}BM$ and $PC_{71}BM$ as an acceptor to fabricate solar cells with a device structure ITO/PEDOT:PSS/P1orP2-PCBM/Al or Ca:Al. Without annealing or use of additives, maximum V_{oc} of 0.68, fill factor of 30.2%, quantum efficiency of 22% and maximum power conversion efficiency (PCE) of 0.76% have been achieved yet with P2. Morphology of blended active layer, P1/P2 with $PC_{61}BM$ and $PC_{71}BM$ has been investigated using AFM images.

3.1 Introduction

D-A[1] type of polymers have been proved to be very promising apart from other designs such as D-A-D/[2]D-π-A/[3]D-A_{2D} used for designing CPs for PSCs. Using D-A type of design, various polymers have been synthesized and fabricated as BHJ solar cell, which includes a vastly studied polymer PCPDTBT with a PCE of ~5.5%.[4] So far the D-π-A based strategy has not given any prominent results to enhance PCE in P(CPDT-π-BT)[5] and other D-π-A system.[6-9] Yet it remains of growing interest for researchers on D-π-A type of design,[10,11] and need to be explored more, as it has advantages like additional π-bond that can extend conjugation to the red-NIR region (lowering band gap)[12,13] and lowering of dihedral angle between donor and acceptor, thereby leading to more planar geometry. In addition to D-A or D-π-A, an alternate approach such as to use different positions of various donors/acceptors like fluorene,[14,15] quinoxaline,[16,17] carbazole,[18,19] thienopyrazine[16,20] and benzene[21,22] as a site for main chain polymerization has been another important method to design similar type of polymer, not only for PSCs but also for PLED and sensor applications.

One of the above discussed type of design, by using different position for substitution are ortho-arylenes, which is of growing interest in present research[23-25] where various polymers[19,26] have been synthesized using closely spaced ortho position. A recent report[23] suggests that o-phenylenes have helical arrangement and sterically congested structures, which can be eliminated to larger extents in a POAV (poly-o-arylene vinylene) type of

TH-1906_11615303

polymer having two vinyl bonds at the o-position (vinyl-bond reduces the dihedral angle between donor and acceptor and distances the closely spaced rings). This approach makes o-arylene kind of (POAV) polymer useful for optoelectronic application with commonly used fullerene/non-fullerene derivatives as acceptor, where an appropriate phase separation between donor and acceptor is an important factor for charge separation.[27,28]

Among various acceptors listed above, for benzothiadaizole, it is always 4 and 7 position that has been chosen as site for designing various main chain polymers.[10,29] Yet there has been no effort to synthesize polymers using 5 and 6 position of benzthiadiazole as a site for main chain polymerization. This approach shows synthesis of two poly(o-arylene-vinylene) (POAV) type polymers, where BT has been attached alternatively to donor via two vinyl-bond in 5 and 6 position rather than commonly chosen 4 and 7. Two extensively used hole transporting donor units: 3-hexylthiophene[30,31] and 4,4-bis-(2-ethylhexyl)-4H-cyclopenta[2,1-b;3,4-b′]-dithiophene[4,5] have been chosen, to obtain 5,6-*alt*-BT based D-π-A type polymers and to give an insight into its potential as a donor in a BHJ solar cell. The noticeable irregularity in the position of hexyl chain in P1 is not a limiting factor, as is a vastly used strategy to design various polymers.[32,33]

3.2 Results and discussion

3.2.1 Reaction scheme

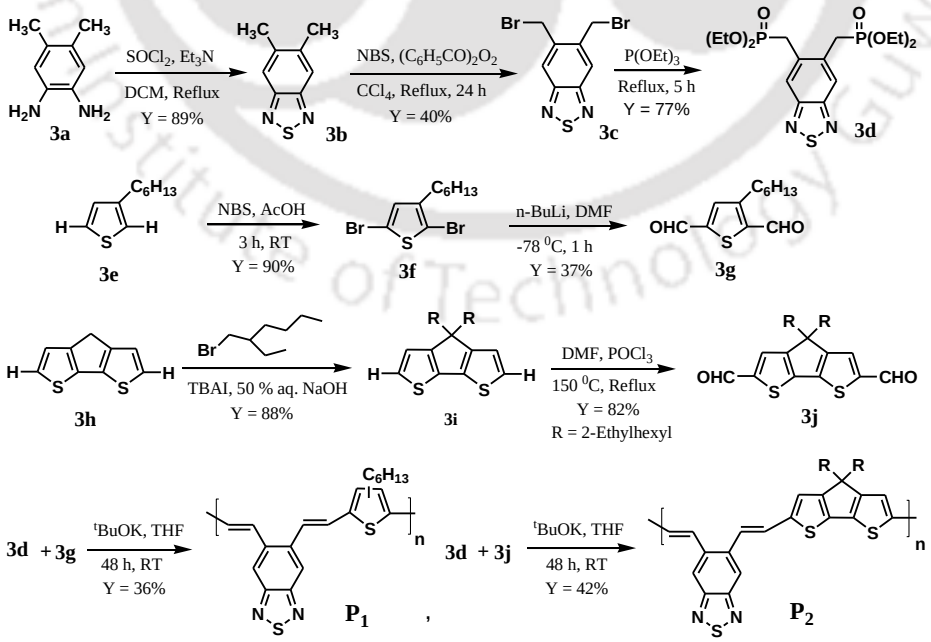

Figure 3.1 Reaction scheme for synthesis of polymer P1 and P2.

TH-1906_11615303

3.2.2 Thermal properties

Thermo gravimetric analysis (TGA) under nitrogen atmosphere shows high thermal stability with a degradation temperature of ~340 ^{0}C for P1 and ~346 ^{0}C for P2 (Figure 3.2a). This degradation temperature in range of 340 ^{0}C is adequate for solar cell fabrication and ensures thermal stability of polymers with in device as well. Differential scanning calorimetry (DSC) was recorded in N_2 flow to find out a phase change in the polymer with respect to change in temperature, which shows a glass transition temperature (T_g) of 158 ^{0}C for P1 and 148 ^{0}C for P2 (Figure 3.2b) in the exothermic cycle. Low height peaks/small humped peaks for T_g indicates amorphous nature of both the polymers. Thermal properties (TGA/DSC) for both P1 and P2 shows similar behavior with small change, indicating POAV skeleton hold high thermal behavior even with different donor here as in case of P1 (3HT) and P2 (CPDT-Eth).

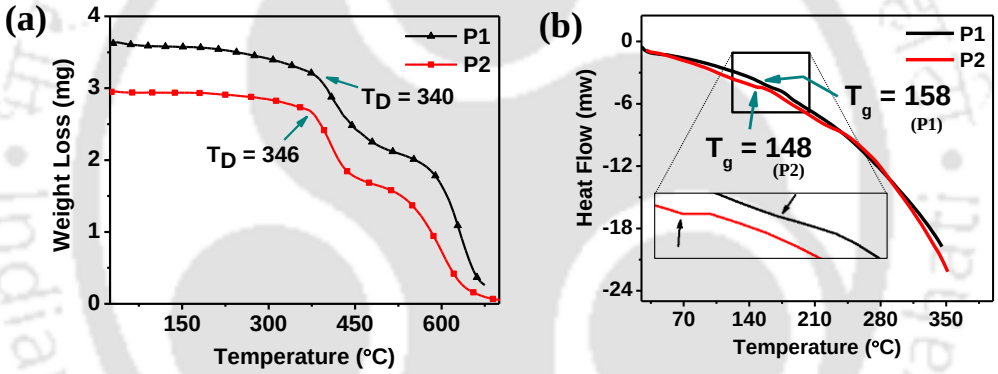

Figure 3.2 Thermal properties for P1 and P2 (a) TGA (b) DSC.

3.2.3 Optical properties

Solution state UV-visible spectra in chlorobenzene shows two characteristic peaks for both the polymers; the low wavelength corresponds to π-π* transition (P1; 375 nm, P2; ca. 430 nm) for polymer backbone and a low energy (P1; 443 nm, P2; 482 nm) (Table 3.1, Figure 3.3a) transition corresponds to the transition for internal charge transfer from the donor (P1; 3HT, P2; CPDT-di(ethyl hexyl)) to the acceptor (benzthiadiazole) via π-bridge with in main polymer backbone.[34] Very high energy ICT spectra is obvious from short conjugation length in a low molecular weight[35] polymer and partially might be due to the kinked[17] position of attachment, which decreases the effective resonance in a o-arylene system (vinyl bond reduces dihedral angle between moieties at ortho position, bringing enhanced planar geometry). In chlorobenzene, highest intensity peak in

TH-1906_11615303

absorption spectra is of high energy for P1 and low energy for P2, with an onset of 533 nm for P1 and 586 nm for P2 as observed (Figure 3.3a). A broadening in the absorption spectra[36] has been observed in solid state with a change in onset of 586 nm solution state to 606 nm (Table 3.1, Figure 3.3a) in film, casted form chlorobenzene for P2. This small (20 nm) red shift indicates similar conformation of P2 in solid and solution state.[3]

Table 3.1 Optical properties of P1 and P2.

P	λ_{max} Solution (nm)	λ_{onset} (nm)	λ_{max} film (nm)	λ_{onset} film (nm)
P1	375, 443	533	456	571
P2	~430, 482	586	490	606

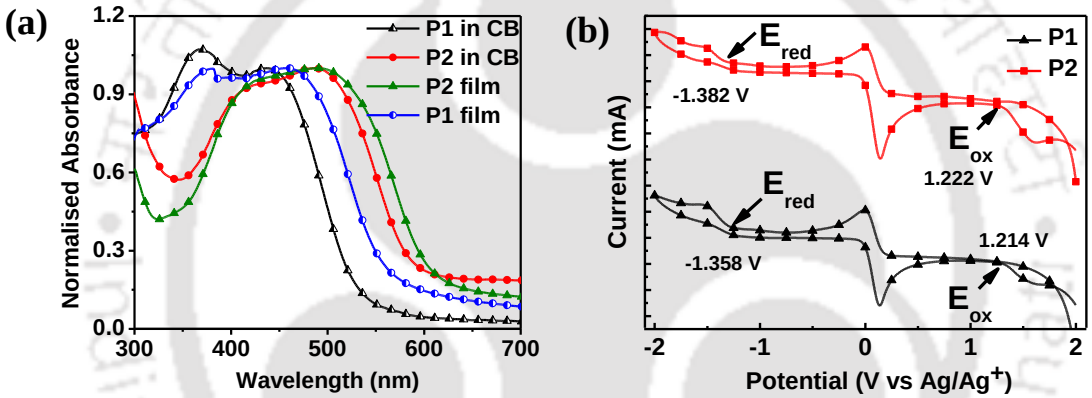

Figure 3.3 Optical properties of P1 and P2 (a) UV-visible spectra in chlorobenzene and in film casted from same solvent. (b) cyclic-voltammetry showing oxidation and reduction potential for both the polymers.

Table 3.2 Optical properties of P1 and P2.

P	E_{ox} (Volt)	HOMO (eV)	E_{red} (Volt)	LUMO (eV)	Band gap (E_g)	Optical gap (E_{opt})	$LUMO^{opt}$
P1	+1.21	-5.95	-1.35	-3.37	2.57	2.17	-3.78
P2	+1.22	-5.95	-1.38	-3.35	2.60	2.04	-3.91

This small change in absorbance in film state compared to solution also confirms negligible impact of zig-zag arrangement of POAV structure of P1 and P2 on its optical property in film state, as compared to its reported analogues PAV type polymers,[5,10]

TH-1906_11615303

where a similar change has been observed. Cyclic voltammetry analysis shows a deeper HOMO (P1; 5.95 eV, P2; 5.95 eV) (Table. 3.2, Figure. 3.3b) for both the polymers, which is one of the desired parameters for designing solar cell material, as open circuit voltage (V_{oc}) is directly proportional to difference between HOMO of donor and LUMO of acceptor.[4] Higher HOMO for polymer corresponds to higher V_{oc} and hence enhanced PCE for solar cell. Here HOMO levels of both P1 and P2 are similar even though its donor part is different, this shows POAV type structure on 5,6-*alt*-BT restricts electrochemical property irrespective of use of donor. Determined optical band gap for P1 and P2 using absorption onset in film state using formula $E_{opt} = 1240/\lambda_{onset}$ gives better insight for band positions (optical LUMO) of POAV type polymer (Table 3.1) (P1: -3.78 eV, P2: -3.91eV).

3.2.4 Theoretical calculation

As POAV represents a cross conjugated system[37,38] and o-arylenes have helical arrangement,[20] DFT calculations have been carried out at B3LYP/6-31G (*d,p*), aiming to address linearity in the POAV system and whether the entire polymeric backbone is conjugated with the present cross conjugated arrangement. Ground state frontier orbital of both HOMO and LUMO for CPs, P1 and P2 have been calculated taking a dimer model of the polymer. The distribution of electron density all over the polymer backbone in HOMO and concentrated at acceptor in LUMO is considered as ideal distribution for internal charge transfer from donor to acceptor in the polymeric backbone.

Here for both the polymers electron density for HOMO is distributed all over the backbone and LUMO is concentrated mostly on the acceptor side with partial distribution on donor as well (Figure 3.4), which suggests ICT is hampered due to the kinked position of attachment in POAV system. The polymer backbone as such is not linear, as obvious due to o-alternation, which makes the growth of polymer chain in two different directions, differing in only a normal linear arrangement. To address more into the arrangement, here 3 units of monomer have also been used and ground state frontier molecular orbital have been determined by using DFT-B3LYP/6-31G (*d.p*) (Figure 3.4), where it was observed that 3 units of backbone in both polymers form a zig-zag arrangement rather than a helical structure as observed in o-arylenes. These results confirm that the vinyl bridge helps in making a zig-zag arrangement, which distances the donor and acceptor.

TH-1906_11615303

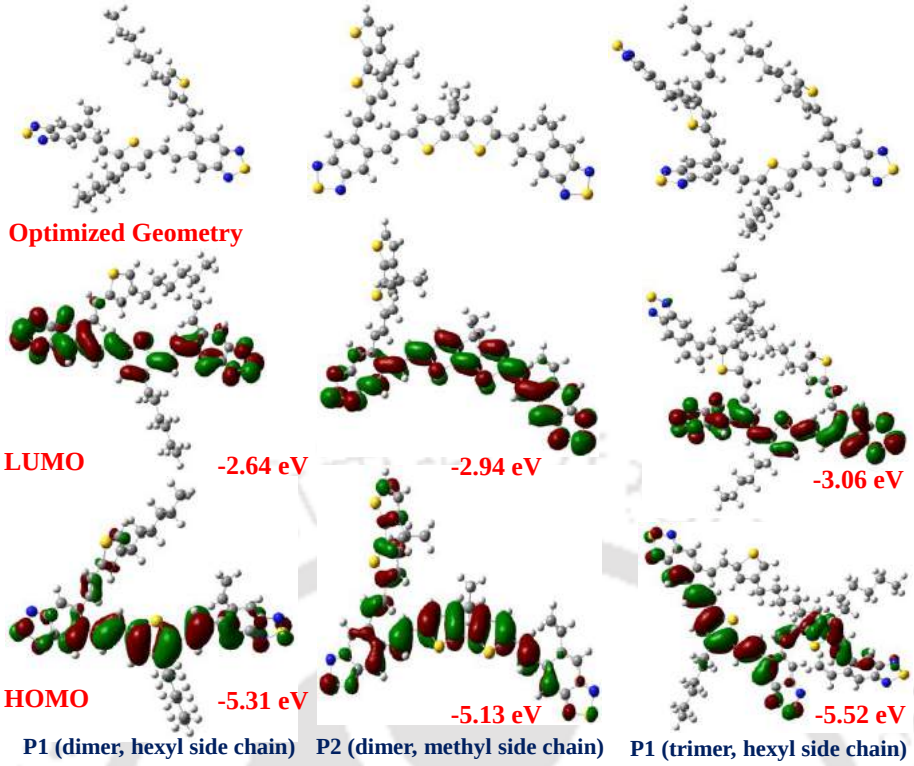

Figure 3.4 DFT calculations for P1 and P2, addressing linearity for the polymer backbone.

3.2.5 Solar cell performance

Under illumination of an Air mass 1.5 solar stimulator, P2 shows better result in 1:4 ratio with $PC_{71}BM$ as acceptor and Ca-Al as cathode. Open circuit voltage (V_{oc}) of 0.68 V (Table 3.3, Figure 3.5a) was recorded. In similar conditions with Al as cathode maximum V_{oc} recorded was 0.46 V. Similarly for P1-$PC_{71}BM$ (1:2) maximum V_{oc} achieved was 0.46 V with Ca-Al as cathode, compared to a V_{oc} of 0.34 V with Al as cathode. The reason for high V_{oc} in case of Ca-Al as cathode is due to high built in potential caused by low work function metal calcium in fabricated PSC. However, a maximum current density J_{sc} of 3.67 mA/cm^2 (Table 3.3, Figure 3.5a) was recorded for P2-$PC_{71}BM$ (1:4), which is very low. The reason for the low photocurrent may be due to the less coverage of absorption spectra in solid state (from 350 to 606 nm) and quenching of generated excitons in the active layer due to deeper HOMO level of -5.95 eV for P1 and P2.[39] Holes do not get separated easily as the offset between HOMO of PCBM and polymers (P1 and P2) is less. It has also been established by calculating ideality factor of the dark current for the fabricated devices (Appendix A3, ideality factor) which showed an ideality factor (n) of 6.5 (P1:$PC_{71}BM$, 1:2) and 4.07 (P2:$PC_{71}BM$, 1:4). High ideality factor of diode (more

TH-1906_11615303

than 2) further confirms high recombination of excited electron and holes at the bulk-heterojunction of polymer and $PC_{71}BM$ blend.[40,41] The fill factor (FF) was found to be 32.2% in case of P2-$PC_{61}BM$ (1:4) (Table 3.3, Figure 3.5a). Under these conditions, PCE of 0.47% has been achieved from P2 (Table 3.3)

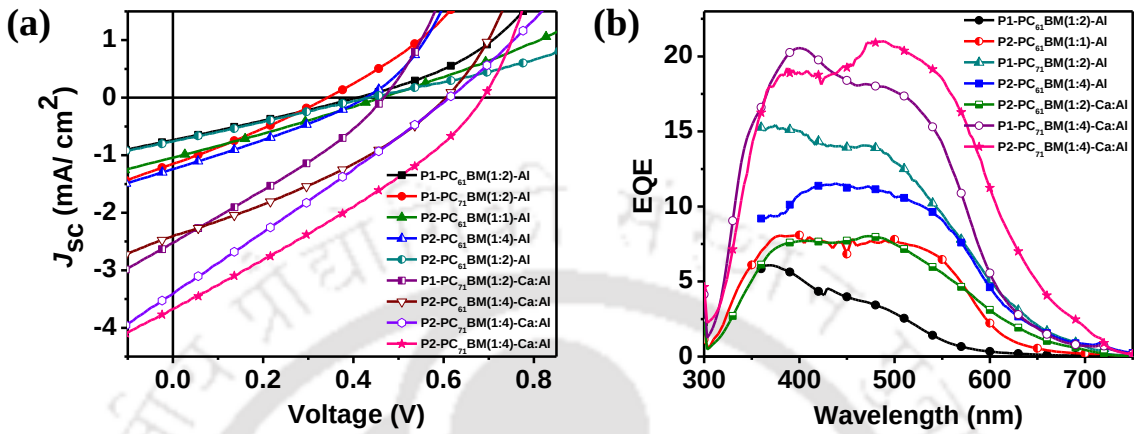

Figure 3.5 Solar cell properties (a) current density-voltage curve (J-V) (b) external quantum efficiency.

PCE of 0.34% has been achieved using P1 (Table 3.2, Figure 3.5a) for 1:2 ratio with $PC_{71}BM$ as an acceptor and a maximum PCE of 0.76% yet with P2-$PC_{71}BM$ (1:4) as active layer. The low PCE of P1 compared to P2 might be due to the low absorption range and a poor film forming ability. Increase in PCE in P2 in 1:4 ratio with $PC_{71}BM$ is attributed to faster charge transfer from donor to acceptor and high absorption range of $PC_{71}BM$ with increased $PC_{71}BM$ concentration. For P1 negligible result was obtained with 1:4 ratio with $PC_{61}BM$, which might be caused due to low molar coefficient of P1, limiting its minimum concentration to be present to absorb solar photons. Observed enhancement in PCE in P1:$PC_{71}BM$ (1:2) compared to P1:$PC_{61}BM$ (1:2) and P2:$PC_{71}BM$ (1:4) compared to P2:$PC_{61}BM$ (1:4) is obvious from faster charge transport property and higher wavelength coverage of absorption spectra of $PC_{71}BM$ over $PC_{61}BM$. Although P2 has more planar (CPDT) donor structure, the solar cell performances are not much superior as compared to P1, which may be due to the bulkiness of CPDT ring and kinked position of attachment through a vinyl bond that might have restricted the large change. Fill factor recorded in all the devices were in the range of 25% to 32%. The reason might be due to low charge carrier extraction from both the polymers due to zig-zag molecular structure of POAV type polymers, limiting its photo current as well. The low work function metal calcium also helps in increasing FF from 25% to 32% in case of P2-

TH-1906_11615303

$PC_{61}BM$ (1:4) (Table 3.3, Figure 3.5b). The external quantum efficiency (EQE) for the device with a spectral coverage from 300 to 700 nm was recorded to be approximately 22% for P2:$PC_{71}BM$ (1:4) with Ca-Al as cathode (Figure 3.5b). The recorded low percentage (20%) EQE is also another reason for low PCE. The spectral coverage in the EQE spectra beyond 600 nm (absorption onset of P2) to 700 nm is due to absorption of $PC_{71}BM$, which starts absorbing in 700 nm region with low intensity.

Table 3.3 Photovoltaic performance for P1 and P2.

Active layer, (rpm, thickness in nm)-Cathode	Open circuit voltage (V_{oc}) in Volt	Current density (J_{sc}) in mA/cm^2	Fill factor (FF) (%)	Power conversion efficiency (PCE) (%)
P1 : $PC_{61}BM$ (1: 2), (1000)-Al	0.48	0.73	26.6	0.08
P1 : $PC_{71}BM$ (1: 2), (2000, 80)-Al	0.34	1.14	27.3	0.108
P2 : $PC_{61}BM$ (1: 1), (2500)-Al	0.46	1.04	26.8	0.13
P2 : $PC_{61}BM$ (1: 2), (2000, 105)-Al	0.56	0.77	24.9	0.107
P2 : $PC_{61}BM$ (1: 4), (2500, 68)-Al	0.43	1.24	28.1	0.15
P1 : $PC_{71}BM$ (1: 2), (2000, 80)-Ca: Al	**0.46**	**2.52**	**29.2**	**0.34**
P2 : $PC_{61}BM$ (1: 4), (2000, 88)-Ca: Al	0.60	2.40	32.2	0.47
P2 : $PC_{71}BM$ (1: 4), (1000,150)-Ca: Al	0.61	3.41	25.9	0.54
P2 : $PC_{71}BM$ (1: 4), (2000)-Ca: Al	**0.68**	**3.67**	**30.2**	**0.76**

3.2.6 Morphology of active layer

Morphology of active layer has a prominent effect on device performances both in phase separation and charge transport, which further affects the fill factor efficiency and PCE. AFM topography shows both desired parameters that is a low domain diameter (small particle size) and low root mean square (RMS) roughness 0.43 nm in P2:$PC_{61}BM$ (1:1) (Figure 3.6c).[27] Topography of polymer-$PC_{61}BM$ blend shows good mixing nature between both polymer and $PC_{61}BM$, with bi-continuous phase separation, indicating that the low PCE is largely due to limited absorption range for the polymer that matches with the UV-blue range of solar spectrum rather than inappropriate morphology of polymer-PCBM blend (which excludes any negative impact of zig-zag arrangement of polymer backbone on film morphology).[42] In case of P1 the domain size was larger than P2 with RMS roughness that are in the similar range of 0.57 nm and 1.2 nm. The reason for large domain size in case of P1:$PC_{71}BM$ (1:2) might be due to aggregation caused by

TH-1906_11615303

randomness and presence of one alkyl chain on donor unit, rather than presence of two 2-ethylhexyl chain on P2.[43]

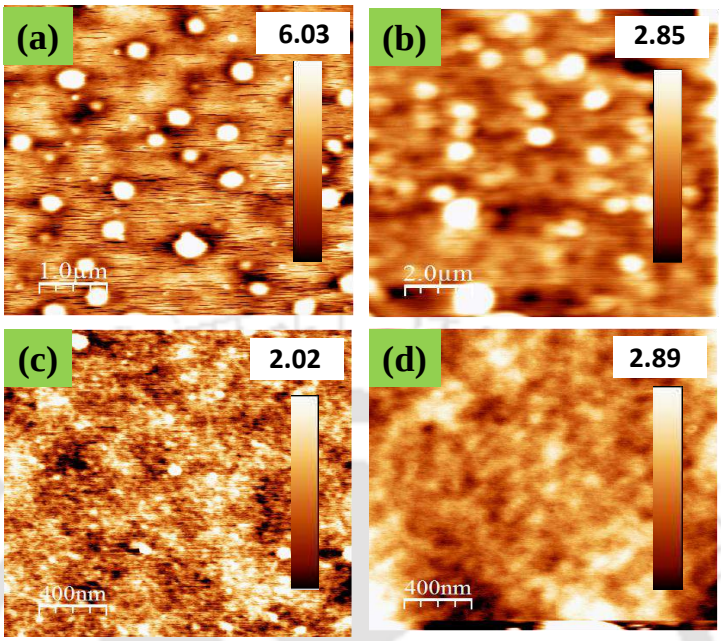

Figure 3.6 Topography of AFM images with scale bar in nm (RMS roughness) (a) P1:$PC_{61}BM$-1:4 (1.24 nm) (b) P1:$PC_{71}BM$-1:2 (0.57 nm) (c) P2:$PC_{61}BM$-1:1 (0.43 nm) (d) P2:$PC_{61}BM$-1:4 (0.56 nm). 3D view of AFM images given in appendix A3.

3.3 Conclusion

Two poly(o-arylene-vinylene) (POAV) type polymers namely P1 and P2, with polymer main chain alternating at 5,6-position of BT have been synthesized and characterized. It has been established here that both D-π-A polymers P1 and P2 have deeper HOMO levels, good thermal stability and good solubility in $CHCl_3$, THF, CB and DCB (which are frequently used in fabricating PSCs). By fabricating BHJ solar cell using $PC_{61}BM$ and $PC_{71}BM$ as an acceptor, potential of POAV type of polymers as donor and their structure property relation have been investigated which gives a power conversion efficiency of 0.76% for P2 and 0.34% for P1. The reason for low PCE might be due to low molecular weight for both the polymers and weak intermolecular charge transfer from donor to acceptor limiting its absorption range to UV-blue region. This study gave an insight into the thermal, optical and morphological properties of polymers having 5,6-*alt*-benzothiadiazole as an acceptor in the D-π-A system and opens newer avenues of using o-arylene and 5,6-*alt*-Benzothiadiazole acceptor for application of photovoltaic and for other organic electronic devices . The zig-zag arrangement of POAV type of polymer at

TH-1906_11615303

5,6-*alt*-benzothiadiazole can be used as revolutionary approach, for designing polymer based π-electron acceptor for cost effective solar cell, where non-planarity/globular arrangement of polymer back bone is highly essential to achieve appropriate phase separation with in active layer to bring enhanced charge separation. The approach of designing PAV, POAV or 5,6-*alt*-benzothiadiazole type polymer provides newer design opportunities for conjugated polymer systems and monomeric units as well. A further attempt to improve the solar cell performance by introducing the additional double bond that leads to extended conjugation makes it an upright approach for future research.

3.4 Experimental Procedures

3.4.1 Synthetic procedures of monomers, polymer P1 and P2

Detail reaction scheme for synthesis of all monomers and polymers shown in Figure 3.1.

5,6-Dimethyl-benzo[1,2,5]thiadiazole (**3b)**

Monomer **3b** was synthesized according to the literature procedure.[44] To a 50 mL round bottom flask 4,5-dimethyl-1,2-phenylenediamine, **3a** (0.3 g, 2.2 mmol), triethylamine (1.229 mL, 8.81 mmol), DCM (30 mL) were added and stirred under argon atmosphere for 3 hours. Using a liquid addition funnel, thionyl chloride (0.4 mL, 5.5 mmol) was added dropwise. The solution turned orange-brown and triethylamine hydrochloride salt precipitated out. Reaction mixture was refluxed overnight, cooled to room temperature and the solvent was removed under reduced pressure. Later combined organics were extracted with DCM and water, dried over Na_2SO_4 and the solvent was again removed under reduced pressure to get solid red-brown colored product **3b** (0.32 g, 89% yield).^{1}H-NMR (600 MHz, $CDCl_3$, δ in ppm): 7.728 (s, 2H), 2.44 (s, 6H). ^{13}C-NMR (150 MHz, $CDCl_3$, δ in ppm): 154.49, 140.76, 119.98, 21.02. HRMS (+APCI): m/z $[M+H]^+$ calcd for $C_8H_8N_2S$ 165.0486, found 165.0466.

5,6-Bis-bromomethyl-benzo[1,2,5]thiadiazole (**3c)**

5,6-Dimethyl-benzo[1,2,5]thiadiazole, **3b** (0.4 g, 2.435 mmol) was dissolved in 30 mL CCl_4. To this NBS (1.07 g, 6.0875 mmol) and benzoyl peroxide (0.059 g, 0.24 mmol) was added as a free radical initiator. The reaction mixture was refluxed overnight under argon atmosphere. The completion of reaction was indicated by the appearance of succinimide on the surface of the reaction solution. After cooling to room temperature, the mixture

TH-1906_11615303

was diluted with DCM and neutralized with 1N aqueous NaOH. Further the combined solution was extracted using brine. The organic phase was dried with anhydrous Na_2SO_4 and concentrated in vacuum to give crude product, which after chromatographic separation (SiO_2, Hexane: $CHCl_3$= 90:10) gives 0.31 g of compound **3c**[45] (cream colored solid) with a yield of 40%. ^{1}H-NMR (400 MHz, $CDCl_3$, δ in ppm): 8.058 (s, 2H), 4.852 (s, 4H). ^{13}C NMR (150 MHz, $CDCl_3$, δ in ppm): 154.72, 138.43, 123.74, 30.28. HRMS (ESI): m/z $[(M+2)+H]^+$ calcd for $C_8H_6Br_2N_2S$ 322.8676, found 322.8680.

5,6-Bis[(diethoxyphosphoryl)methyl] benzo[c][1,2,5]thiadiazole (3d)

5,6-Bis-bromomethyl-benzo[1,2,5]thiadiazole **3c** (0.2 g, 0.621 mmol) and triethyl phosphite (0.825 g, 4.968 mmol) was added in a Schlenk tube and heated 156 ^{0}C to reflux under argon atmosphere for 5 hours. The crude product was purified (along with removal of excess of triethyl phosphite used) by column chromatography (SiO_2, ethyl acetate), giving a yield of 77% (0.2 g) of compound **3d** (colorless oil). ^{1}H-NMR (600 MHz, $CDCl_3$, δ in ppm): 7.904-7.898 (d, 2H), 4.059-4.023 (m, 8H), 3.636-3.600 (d, 4H), 1.260-1.237 (t, 12H). ^{13}C-NMR (150 MHz, $CDCl_3$, δ in ppm): 154.1, 134.35, 134.28, 123.24, 123.20, 62.73, 62.69, 32.52, 31.60, 29.85, 20.88, 16.52 (many peaks arises due to carbon coupling with phosphorous). HRMS (+APCI): m/z $[M+H]^+$ calcd for $C_{10}H_{26}N_2O_6P_2S$ 437.1065, found 437.1874.

2,5-Diformyl-3-hexylthiophene (3g)

Compound **3g** was synthesized from 3-hexylthiophene by brominating at 2,5-position[26] followed by formylation using literature procedure.[46]

4,4-Bis-(2-ethylhexyl)-4H-cyclopenta[2,1-b;3,4-b′]-dithiophene (3i)

4H-cyclopenta[2,1-b;3,4-b′]-dithiophene (0.2 g, 1.12 mmol), freshly prepared 50% aq. NaOH, and tetrabutylammonium iodide (0.08 g, 20 mol%) were added into a round bottom flask. The flask was degassed thrice by applying freeze–thaw cycles to remove trace amount of oxygen completely, followed by alkyl halide (2.8 mmol) addition via syringe (degassed) and the mixture was heated at 75 ^{0}C continuously for 4 hours. The reaction mixture was cooled to room temperature and extracted with ethyl acetate. The organic layer was washed with water and dried over anhydrous Na_2SO_4. The solvent was removed under vacuum, and the crude was purified via column chromatography over silica/hexane to get product **3i** as a light yellow color liquid. (yield 0.397 g, 88%). ^{1}H-

TH-1906_11615303

NMR (600 MHz, $CDCl_3$, δ in ppm): 7.11 (d, 2H), 6.93 (d, 2H), 1.89 (m, 4H), 0.99 (m, 18H), 0.77 (t, 6H), 0.61 (t, 6H); ^{13}C-NMR (150 MHz, $CDCl_3$, δ in ppm): 157.83, 137.01, 124.16, 122.55, 53.44, 43.45, 35.21, 34.35, 29.04, 27.48, 23.05, 14.33, 11.08; HRMS (ESI): m/z $[M+H]^+$ calcd for $C_{25}H_{38}S_2$ 403.2493, found 403.2493.

2,6-Diformyl-4,4-bis-(2-ethylhexyl)-4H-cyclopenta[2,1-b;3,4-b′]-dithiophene (3j)

Monomer **3j** was synthesized according to the literature procedure.[47] A flask containing anhydrous DMF (1.46 mL) was prepared in ice bath. After 1 hour $POCl_3$ (2.28 g, 14.925 mmol) was then added drop wise with stirring. 4,4-bis-(2-ethylhexyl)-4H-cyclopenta[2,1-b;3,4-b′]-dithiophene (0.2 g, 0.4975 mmol) was then added with stirring to the flask. The solution was heated to reflux for 5 hours. The reaction mixture was then cooled, poured into crushed ice and neutralized with aqueous NaOH. The mixture was extracted with DCM and washed with water, dried over anhydrous Na_2SO_4 and concentrated. The residue was purified with column chromatography using silica gel/n-hexane: chloroform (80:20) as the eluent to yield 0.186 g (82%) of the compound **3j**. ^{1}H-NMR (400 MHz, $CDCl_3$, δ in ppm): 9.904 (s, 1H), 7.637-7.619 (t, 2H), 1.975-1.245 (t, 4H), 0.971-0.870 (m, 18H), 0.749-0.716 (t, 6H), 0.617-0.564 (t, 6H). ^{13}C-NMR (150 MHz, $CDCl_3$, δ in ppm): 183.01, 182.94, 161.18, 146.52, 145.52, 130.38, 54.59, 43.22, 35.56, 34.40, 28.68, 27.55, 22.89, 14.19, 10.77. HRMS (+APCI): m/z $[M+H]^+$ calcd for $C_{27}H_{38}O_2S_2$ 459.2391, found 459.2599.

Poly[3-hexylthiopheneylenevinylene)-alt-5,6-(2,1,3-benzothiadiazole) (P1)

Horner-Wittig polymerization was carried out according to the literarure procedure.[48] In 50 mL flask, 5,6-bis[(diethoxyphosphoryl)methyl] benzo[c][1,2,5]thiadiazole **3d** (0.1 g, 0.229 mmol), 2,5-diformyl-3-hexylthiophene **4g** (0.051 g, 0.229 mmol) and anhydrous THF (15 mL) were mixed inside a glove box. Then potassium tert-butoxide (0.2057 g, 1.833 mmol) was slowly added and the solution was stirred at room temperature under Ar atmosphere (inside glove box) for 48 hours. The resulting solution was poured into 300 mL of methanol and the precipitate was centrifuged to get yellowish red colored solid (100 mg, yield 36%) ^{1}H-NMR (600 MHz, $CDCl_3$, δ in ppm): 8.074-8.053 (br, 2H),7.330-7.172 (br, CH-vinyl), 6.952 (br, 1H), 2.712-2.688 (br, 2H), 1.651-1.627 (br, 2H), 1.325-1.315 (br, 6H), 0.854-0.837 (br, 3H). ^{13}C-NMR (150 MHz, $CDCl_3$, δ in ppm): 155.00, 144.16, 140.86, 136.38, 132.26, 127.82, 125.44, 124.68, 117.65, 31.88, 31.15, 29.31,

TH-1906_11615303

28.72, 22.83, 14.29. GPC: M_n = 6090 g/mol; M_w = 10589 g/mol; PDI = 1.738. In THF at λ_{max} = 447 nm ε = 1.0158*10^4 L mol^{-1} cm^{-1}.

Poly[2,6-(4,4-bis(2-ethylhexyl)-4H-cyclopenta[2,1-b:3,4-b']-dithiopheneylenevinylene)-alt-5,6-(2,1,3-benzothiadiazole) (P2)

P2 was synthesized following same procedure as for P1 taking bis[(diethoxyphosphoryl)methyl] benzo[c][1,2,5]thiadiazole **3d** (0.1 g, 0.229 mmol), 2,6-(4,4-bis-(2-ethylhexyl)-4H-cyclopenta[2,1-b;3,4-b′]dithiophene **3j** (0.105 g, 0.229 mmol), potassium tert-butoxide (0.411 g, 3.666 mmol) and dry THF (15 mL), to get 218 mg of dark orange colored solid (yield= 43%). ^{1}H-NMR (600 MHz, $CDCl_3$, δ in ppm): 8.101-8.073 (br, 2H), 7.367-7.175 (br, CH-vinylic), 7.024-7.010 (br, 2H), 1.962-1.896 (br, 4H), 1.259 (br, 4H), 1.079-0.683 (br, 26H). ^{13}C-NMR (150 MHz, $CDCl_3$, δ in ppm): 159.11, 154.49, 143.55, 139.64, 137.90, 129.66, 128.0, 124.33, 116.92, 43.42, 34.41, 30.41, 29.91, 29.89, 27.64, 23.06, 14.39, 10.09. GPC: M_n = 6079 g/mol; M_w = 10422 g/mol; PDI = 1.714. In THF at λ_{max} = 485 nm, ε = 2.5885*10^4 L mol^{-1} cm^{-1}.

3.4.2 Procedure and spectra

Device fabrication procedure and method of UV-visible spectra and cyclic voltammetry were given in Appendix A1. NMR spectra of all monomers and polymer synthesized and GPC spectra have been given in Appendix A3.

TH-1906_11615303

3.5 References

1. Xiao, S.; Stuart, A. C.; Liu, S.; Zhou, H.; You, W. *Adv. Funct. Mater.* **2010**, *20*, 635-643.
2. Li, P.; Fenwick, O.; Yilmaz, S.; Breusov, D.; Caruana, D. J.; Allard, S.; Scherf, U.; Cacialli, F. *Chem. Commun.* **2011**, *47*, 8820-8822.
3. Leclerc, N.; Michaud, A.; Sirois, K.; Morin, J. F.; Leclerc, M. *Adv. Funct. Mater.* **2006**, *16*, 1694-1704.
4. Bijleveld, J. C.; Shahid, M.; Gilot, J.; Wienk, M. M.; Janssen, R. A. J. *Adv. Funct. Mater.* **2009**, *19*, 3262-3270.
5. Ko, S.; Mondal, R.; Risko, C.; Lee, J. K.; Hong, S.; McGehee, M. D.; Bredas, J. L.; Bao, Z. *Macromolecules* **2010**, *43*, 6685-6689.
6. Mei, J.; Heston, N. C.; Vasilyeva, S. V.; Reynolds, J. R. *Macromolecules* **2009**, *42*, 1482-1487.
7. Abbotto, A.; Seri, M.; Dangate, M. S.; Angelis, F. D.; Manfredi, N.; Mosconi, E.; Bolognesi, M.; Ruffo, R.; Salamone, M. M.; Muccini, M. *J. Polym. Sci., Part A: Polym. Chem.* **2012**, *50*, 2829-2840.
8. Colladet, K.; Fourier, S.; Cleij, T. J.; Lutsen, L.; Gelan, J.; Vanderzande, D. *Macromolecules* **2007**, *40*, 65-72.
9. David, T. M. S.; Arasho, W.; Sun, S. S. *J. Polym. Sci., Part A: Polym. Chem.* **2015**, *53*, 2202-2213.
10. Grisorio, R.; Allegretta, G.; Romanazzi, G.; Suranna, G. P.; Mastrorilli, P.; Mazzeo, M.; Cezza, M.; Carallo, S.; Gigli, G. *Maromolecules* **2012**, *45*, 6396-6404.
11. Qing, F.; Sun, Y.; Wang, X.; Li, N.; Li, Y.; Li, X.; Wang, H. *Polym. Chem.* **2011**, *2*, 2102-2106.
12. Harris, J. D.; Liu, J.; Carter, K. R. *Macromolecules* **2015**, *48*, 6970-6977.
13. Liang, X.; Gu, S.; Cai, Z.; Sun, W.; Tan, L.; Dong, L.; Wang, L.; Liu, Z.; Chen, W.; Li, J. *Chem. Commun.* **2017**, *53*, 8176-8179.
14. Wu, Z.; Xiong, Y.; Zou, J.; Wang, L.; Liu, J.; Chen, Q.; Yang, W.; Peng, J.; Cao, Y. *Adv. Mater.* **2008**, *20*, 2359-2364.
15. King, S. M.; Perepichka, I. I.; Perepichka, I. F.; Dias, F. B.; Bryce, M. R.; Monkman, A. P. *Adv. Funct. Mater.* **2009**, *19*, 586-591.
16. Inganäs, O.; Zhang, F.; Tvingstedt, K.; Andersson, L. M.; Hellström, S.; Andersson, M. R. *Adv. Mater.* **2010**, *22*, E100-E116.

TH-1906_11615303

17. Kulkarni, A. P.; Zhu, Y.; Jenekhe, S. A. *Macromolecules* **2005**, *38*, 1553-1563.
18. Blouin, N.; Michaud, A.; Leclerc, M. *Adv. Mater.* **2007**, *19*, 2295-2300.
19. Niu, Y. H.; Huang, J.; Cao, Y. *Adv. Mater.* **2003**, *15*, 807-811.
20. Zou, Y.; Wan, M.; Sang, G.; Ye, M.; Li, Y. *Adv. Funct. Mater.* **2008**, *18*, 2724-2732.
21. Liao, L.; Pang, Y. *Macromolecules* **2001**, *34*, 6756-6760.
22. Krebs, F. C.; Jørgensen, M. *Macromolecules* **2002**, *35*, 10233-10237.
23. Mathew, S. M.; Engle, J. T.; Ziegler, C. J.; Hartley, C. S. *J. Am. Chem. Soc.* **2013**, *135*, 6714-6722.
24. Ito, S.; Takahashi, K.; Nozaki, K. *J. Am. Chem. Soc.* **2014**, *136*, 7547-7550.
25. He, J.; Mathew, S. M.; Cornett, S. D.; Grundy, S. C.; Hartley, C. S. *Org. Biomol. Chem.* **2012**, *10*, 3398-3405.
26. Wu, Z. Q.; Liu, D. F.; Wang, Y.; Liu, N.; Yin, J.; Zhu, Y. Y.; Qiu, L. Z.; Ding, Y. S. *Polym. Chem.* **2013**, *4*, 4588-4595.
27. Wang, E.; Hou, L.; Wang, Z.; Hellström, S.; Zhang, F.; Inganäs, O.; Andersson, M. R. *Adv. Mater.* **2010**, *22*, 5240-5244.
28. Hwang, Y. J.; Courtright, B. A. E.; Ferreira, A. S.; Tolbert, S. H.; Jenekhe, S. A. *Adv. Mater.* **2015**, *27*, 4578-4584.
29. Mühlbacher, D.; Scharber, M.; Morana, M.; Zhu, Z.; Waller, D.; Gaudiana, R.; Brabec, C. *Adv. Mater.* **2006**, *18*, 2884-2889.
30. Burkhart, B.; Khlyabich, P. P.; Thompson, B. C. *Macromolecules* **2012**, *45*, 3740-3748.
31. Mierloo, S. V.; Hadipour, A.; Spijkman, M. J.; Brande, N. V. D.; Kesters, B. R. J.; D'Haen, J.; Assche, G. V.; Leeuw, D. M. D.; Aernouts, T.; Manca, J.; Lutsen, L.; Vanderzande, D. J.; Maes, W. *Chem. Mater.* **2012**, *24*, 587-593.
32. Liu, J.; Zhang, R.; Sauve, G.; Kowalewski, T.; McCullough, R. D. *J. Am. Chem. Soc.* **2008**, *130*, 13167-13176.
33. Lu, K.; Di, C. A.; Xi, H.; Liu, Y.; Yu, G.; Qiu, W.; Zhang, H.; Gao, X.; Liu, Y.; Qi, T.; Du, C.; Zhu, D. *J. Mater. Chem.* **2008**, *18*, 3426-3432.
34. Gunbas, G. E.; Durmus, A.; Toppare, L. *Adv. Mater.* **2008**, *20*, 691-695.
35. Liu, C.; Wang, K.; Hu, X.; Yang, Y.; Hsu, C. H.; Zhang, W.; Xiao, S.; Gong, X.; Cao, Y. *ACS Appl. Mater. Interfaces* **2013**, *5*, 12163-12167.
36. Hou, J.; Tan, Z.; He, Y.; Yang, C.; Li, Y. *Macromolecules* **2006**, *39*, 4657-4662.
37. Phelan, N. F.; Orchin, M. *J. Chem. Educ.* **1968**, *45*, 633-637.

TH-1906_11615303

38. Pruissen, G. W. P. V.; Brebels, J.; Hendriks, K. H.; Wienk, M. M.; Janssen, R. A. J. *Macromolecules* **2015**, *48*, 2435-2443.
39. Fan, M.; Du, Z.; Chen, W.; Liu, D.; Wen, S.; Sun, M.; Yang, E. *Asian J. Org. Chem.* **2016**, *5*, 1273-1279.
40. Gündüza, B.; Turan, N.; Kaya, E.; Colak, N. *Synth. Met.* **2013**, *184*, 73-82.
41. Wetzelaer, G. J. A. H.; Blom, P. W. M. *NPG Asia Mater.* **2017**, *6*, e110.
42. Chiu, C. Y.; Wang, H.; Phan, H.; Shiratori, K.; Nguyen, T. Q.; Hawker, C. J. *J. Polym. Sci., Part A: Polym. Chem.* **2016**, *54*, 889-899.
43. Li, Y.; Chen, Y.; Liu, X.; Wang, Z.; Yang, X.; Tu, Y.; Zhu, X. *Macromolecules* **2011**, *44*, 6370-6381.
44. Speros, J. C.; Paulsen, B. D.; Slowinski, B. S.; Frisbie, C. D.; Hillmyer, M. A. *ACS Macro, Lett.* **2012**, *1*, 986-990.
45. Neidlein, R.; Knecht, D. *Chem. Ber.* **1987**, *120*, 1593-1595.
46. Tsai, F. C.; Chang, C. C.; Liu, C. L.; Chen, W. C.; Jenekhe, S. A. *Macromolecules* **2005**, *38*, 1958-1966.
47. Padhy, H.; Sahu, D.; Patra, D.; Pola, M. K.; Huang, J. H.; Chu, C. W.; Wei, K. H.; Lin, H. C. *J. Polym. Sci., Part A: Polym. Chem.* **2011**, *49*, 3417-3425.
48. Tasch, S.; List, E. J. W.; Ekström, O.; Graupner, W.; Leising, G.; Schlichting, P.; Rohr, U.; Geerts, Y.; Scherf, U.; Müllen, K. *Appl. Phys. Lett.* **1997**, *71*, 2883-2885.

TH-1906_11615303

Chapter 4

Substituting Non-conjugating Ester Group into Side Chain of Benzothiadiazole Improves Optical, Electrochemical Properties, Morphology of Active Layer and Solar Cell Performance of D-A Polymer for Photovoltaics

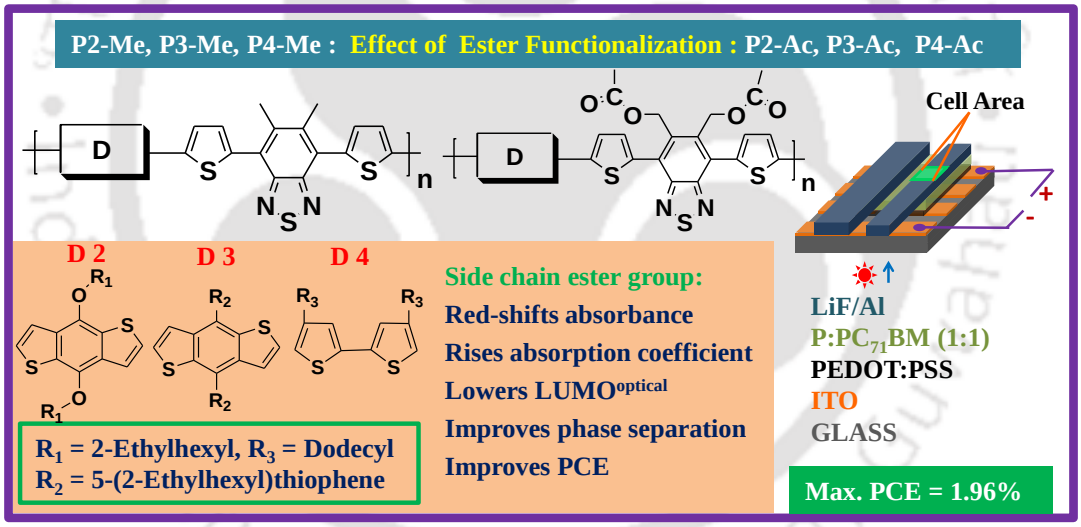

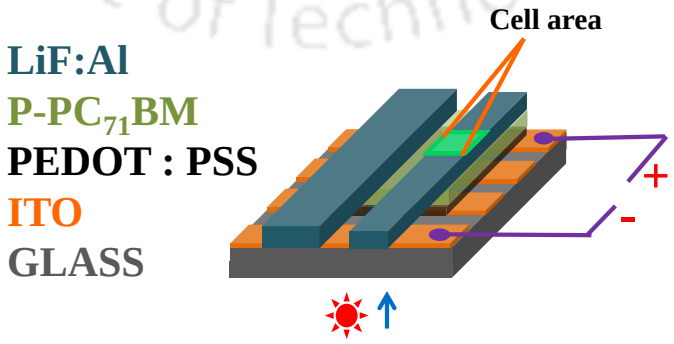

TH-1906_11615303

Abstract

Herein, the effect of non-conjugated ester functionalization at 5,6-position of 2,1,3-benzothiadaizole (BT) in donor (D)-acceptor (A) polymer used for photovoltaic devices have been investigated. Position 5 and 6 of BT have been functionalized with methyl acetate group and its structure property relationship have been compared with BT having methyl group at 5,6-positions using four types of D-A polymers. Alternate co-polymers of methyl and methyl acetate derivatives of BT and Th-BT-Th with commonly used donors such as dithiophene (DTh) and benzodithiophene (BDT) have been synthesized using Stille coupling reaction namely P(1,2,3,4)-Me and P(1,2,3,4)-Ac. All polymers have been characterized by GPC, UV-visible, ^{1}H-NMR, ^{13}C-NMR, TGA and CV. Optimized geometry along with change of dihedral angle on substitution of acetate group have been investigated using density functional theory (DFT) at B3LYP/6-31G (*d,p*). It has been studied that side chain ester group lowers the dihedral angle, improves optical and electrochemical properties of CPs used for PSC, improves phase separation of active layer and solar cell performance of fabricated PSC compared to its methyl counterpart, as investigated between P(1,2.3,4)-Me and P(1,2,3,4)-Ac. On fabrication of BHJ solar cell with device configuration **ITO/PEDOT:PSS/P-PC$_{71}$BM/LiF/Al**, polymer having methyl acetate functionalization such as P2-Ac, P3-Ac and P4-Ac results in higher PCE of 1.36%, 1.17% and 0.35% compared to their methyl counterpart polymer P2-Me, P3-Me and P4-Me with PCE of 0.9%, 0.54% and 0.17% respectively. With 1,8-diiodooctane (DIO) as additive, a PCE of 1.96% has been achieved from P3-Ac as well. Thin film X-ray diffraction and atomic force microscopy (AFM) has been used to determine impact of side chain ester group on π-π stacking distance among polymer main chain in film state and morphology of active layer of fabricated PSCs respectively.

4.1 Introduction

In line with the discussion of designing CPs as solar harvester (with good photo-physical property, mobility and having functional group which improves morphology of active layer), it is worth mentioning that CPs with substituted functional groups such as fluorine, oxygen, sulphur, ester, ketone, cyanide and azide[1-6] into main chain/side chain of polymer backbone, are often being synthesized to improve solar cell performance to a great number. Such functional groups lower dihedral angle within polymers and bring planarity

TH-1906_11615303

and linearity into it,[7] which leads to improved π-π stacking in film state with desired morphology of active layer of PSC.[8] The reason for improvement of PSC performance in case of main chain/side chain functionalized polymers are enhanced intra-molecular/inter-molecular oxygen-sulphur (O-S)/fluorine-hydrogen (F-H)/nitrogen(N)-hydrogen(H)/oxygen-hydrogen (O-H) interaction of polymers chains in film state.[9-12] This improves optical property in film state and segregation between polymer and PCBM, for the reason of enhanced interaction within polymer-polymer chain, which repels the PCBM and gives the most anticipated morphology called segregation rather than undesired morphology called aggregation.

Ester group is one of such important functional group among all, being used both in side chain and main chain of conjugated polymers for solar cell. It has been reported that ester group improves thermal stability of fabricated devices due to cross linking property,[13,14] thermo cleavable nature of ester group helps the active layer of PSC resistant to solvent during multilayer device fabrication,[15] impart promising solubility, along with mobility[16] and improves morphology of active layer in PSC as well.[17]

In this approach BT has been modified to design and synthesize acceptor unit with methyl acetate group substituted as side chain at 5,6-position of BT. D-A type of polymers have been synthesized (namely P1-Ac, P2-Ac, P3-Ac, P4-Ac) from corresponding ester functionalized BT-based acceptors with commonly used donors (D1, D2, D3 and D4, Figure 4.2) using Stille coupling. Corresponding methyl counterpart polymers (namely P1-Me, P2-Me, P3-Me and P4-Me) have also been synthesized to compare influence of ester group at 5,6-position of BT. Herein, it has been established that side chain ester group at 5,6-position of BT, (i) can lower the dihedral angle along the conjugation main chain resulting in the increase in molar absorption coefficient (ii) red-shifts in the absorption spectra in film state (iii) lowers optical LUMO level due to electron withdrawing nature and (iv) enhances the solar cell performance of polymer compared to its methyl counterpart. All these enhanced property of side chain ester groups are due to oxygen-sulphur (O-S)/π-π and CH-π interactions both within the polymer chain and/or inter-molecularly in film state of polymer and/or polymer PCBM blend.

TH-1906_11615303

4.2 Results and discussion

4.2.1 Reaction scheme

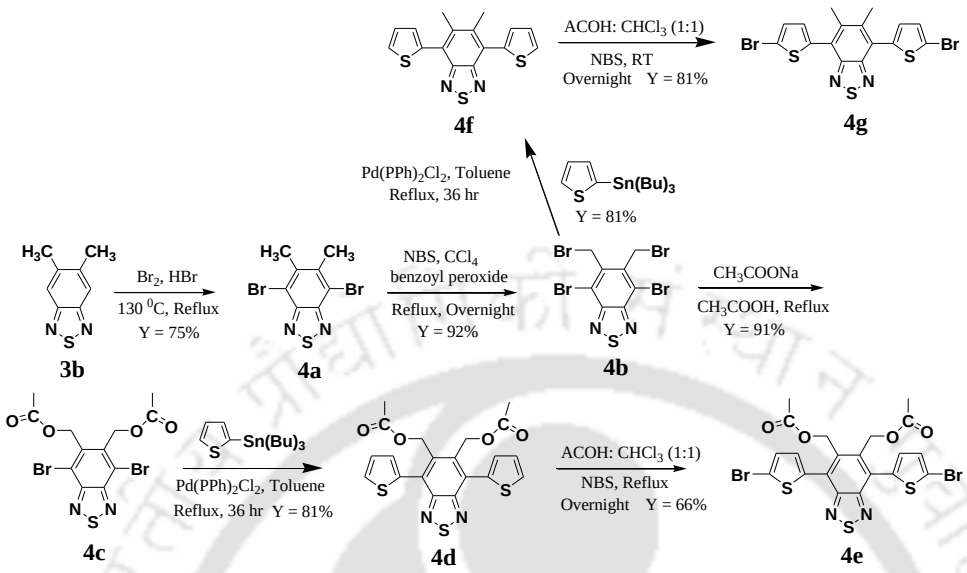

Figure 4.1 Reaction scheme for synthesis of monomers.

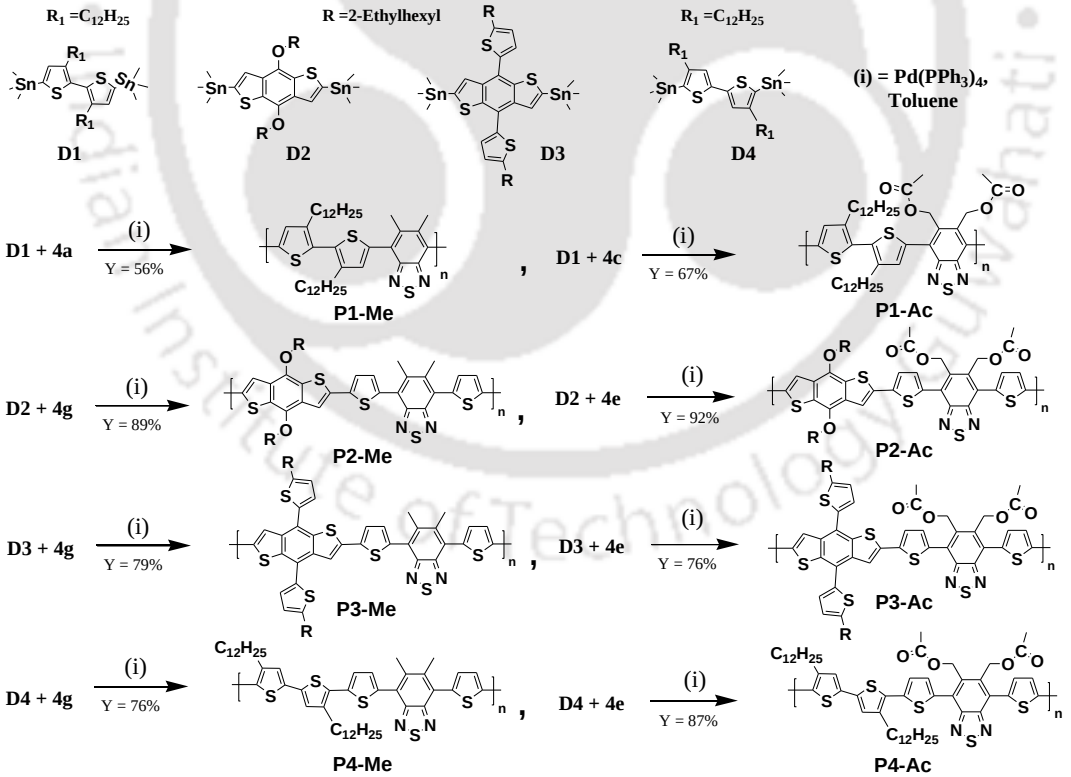

Figure 4.2 Reaction scheme for synthesis of polymers.

TH-1906_11615303

4.2.2 Theoretical calculation

Influence of ester group on HOMO-LUMO levels and dihedral angle between conjugated units of polymers have been investigated using DFT calculation at B3LYP/6-31G (*d,p)*. For simplifying calculations methyl chain have been taken for any kind of alkyl chain and investigation on all polymers have been carried out taking 1 unit of each polymer. Ester functionalised polymers displayed required distribution of charge density for intramolecular charge transfer (ICT) between donor and acceptor (distribution of charge density all over HOMO and localization of charge density on acceptor only in LUMO)[18] in all four polymers [P(1,2,3,4)-Ac] with 4 different donors (D1 to D4).

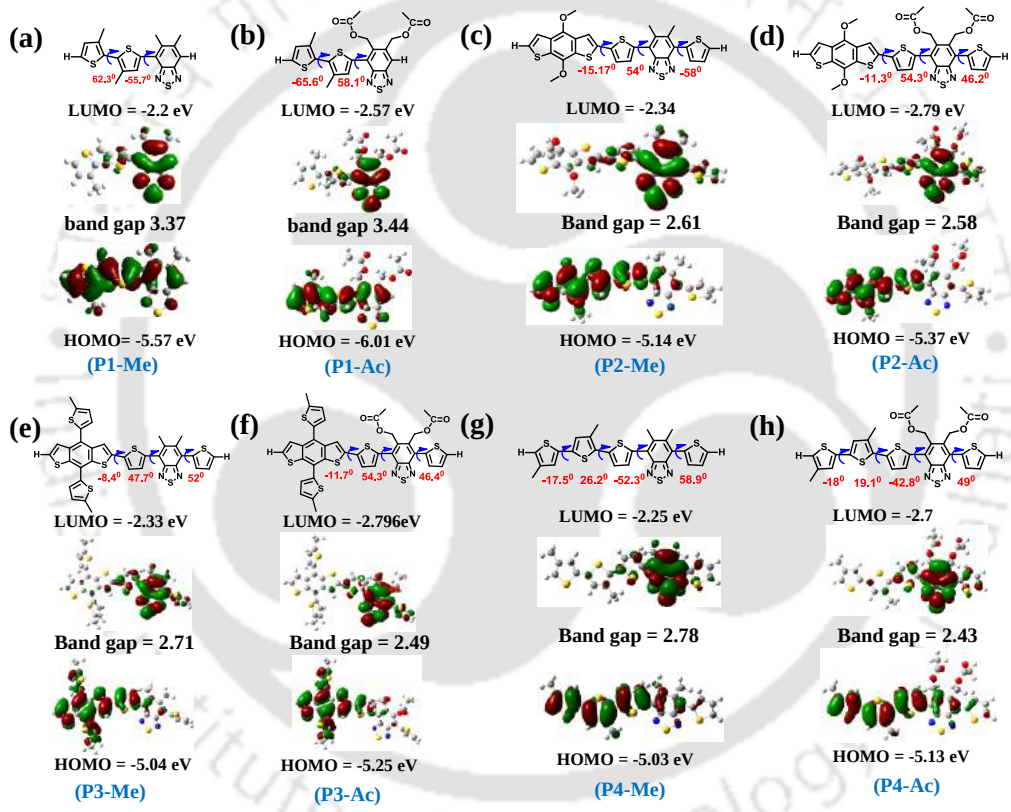

Figure 4.3 DFT calculation showing lowering of LUMO on functionalization of methyl acetate at 5,6-positon of BT-based CPs (model is a monomer).

Ester functionalized polymer has low dihedral angle in case of D2 and D4 compared to their methyl counterpart (Figure 4.3c,d,g,h), due to possible oxygen (negatively charged in ester group)-sulphur (positively charges in thiophene ring) interactions. But in case of D1 and D3 dihedral angle increases in ester functionalized polymers (Figure 4.3a,b and 4.3e,f) compared to its methyl counterpart because of steric hindrance caused by D1 with

TH-1906_11615303

two dodecyl chains in close position (at 3,3′) and bulkiness of D3 (due to two thiophene substituted ethylhexyl unit on BDT), which predominates over any possible oxygen sulphur interactions. In case of D2 and D4 dihedral angle reduced by 10° in ester substituted polymer.

4.2.3 Optical properties

UV-visible spectra for both methyl acetate substituted polymers [P(1,2,3,4)-Ac] and methyl substituted polymers [P(1,2,3,4)-Me] at 5,6-position of BT have been recorded from dilute $CHCl_3$ solution and in film state (drop casted from chlorobenzene). A comparison of absorption property for both solution and as film shows bathochromic shift of both absorption maximum of ICT transition and absorption onset with broadening of UV-visible spectra for ester functionalized polymers compared to their methyl counterpart (Table 4.1, Figure 4.4a to 4.4d). All polymers exhibit tri-humped peak (Figure 4.4a to 4.4d) in general both in solution and film state, which referes to high energy intrinsic band for donor only, moderate energy π-π* trsnsition for polymer backbone and low energy ICT band.[19] In film state, intrinsic band for P1-Me, P1-Ac and P2-Me is not clearly visible due to broadening of spectra (Figure 4.4a and 4.4b). In solution state, in addition, to small variation in intrinsic band and π-π* band a red-shift in ICT transition has been observed for methyl acetate substituted polymers compared to their methyl counterpart. In film state a significant bathochromic shift of absorption spectra has been obsorved along with peak broadening for λ_{max} (ICT band) and/or UV-visible (onset), signifying a substantial π-π stacking of polymer main chain (Figure 4.4a to 4.4d),[20] when side chain ester was introduced into it, due to enhanced CH-π, π-π and oxygen-sulphur interaction (intamolecular and intermolecular). Molar absorption coefficienct (ε) of π-π* band and ICT band in $CHCl_3$ was higher for ester substituted polymers P2-Ac (27373, 26197 L mol^{-1} cm^{-1}) and P4-Ac (29827, 20113 L mol^{-1} cm^{-1}) compared to methyl substituted polymer P2-Me (13820, 15372 L mol^{-1} cm^{-1}) and P4-Me (18124, 19819 L mol^{-1} cm^{-1}) respectively (Table 4.1), due to lowering of dihedral angle. However for similar instance, ester substituted polymer P1-Ac and P3-Ac molar absorption coefficient gets lowered compared to their methyl counterpart P1-Me and P3-Me due to higher dihedral angle in ester substituted polymers caused due to steric hindered donor D1 (P1-Me) (Figure 4.2) with closely positioned dodecyl chain[21] in case of P1-Ac and bulky 2-ethylhexylthiophene substituted BDT donor D3 (Figure 4.2) in case

TH-1906_11615303

of P3-Ac, which predominantly controls the structure, eliminating possible oxygen-sulphur interactions by ester group with near Th-units which could stabilize the structure.

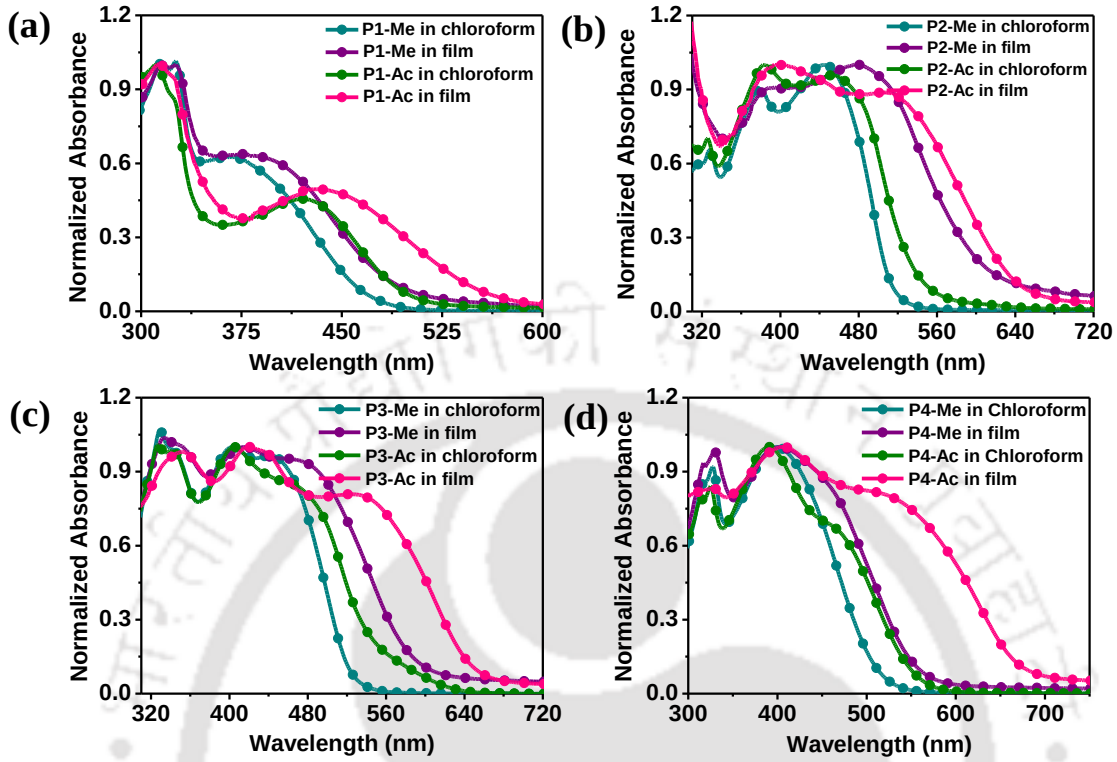

Figure 4.4 Absorption spectra for synthesized polymers, showing red-shift and broadening of spectra for methyl acetate substituted polymers compared to their methyl counterpart.

4.2.4 Electrochemical properties

Cyclic voltammetry was carried out for all synthesized polymers and they exhibited only an oxidation potential within -0.6 Volt to -1.04 Volt (Figure 4.5a and 4.5b). Calculated HOMO of all polymers is in the range from -5.36 to -5.6 eV. HOMO of P1-Ac is 0.11 eV deeper than P1-Me (Table 4.1), which might have caused due to high sterically hindered donor D1, leading to weak donating tendency to the acceptor BT having methyl acetate group (higher the π-electron donating tendency of donor in D-A polymer, higher the HOMO). Minor fluctuation (maximum observed change 0.03 eV) of HOMO levels has been observed[22] in P2-Ac, P3-Ac and P4-Ac compared to their methyl counterpart, indicating less control of ester group on HOMO of synthesized polymers and influence of methyl acetate group on polymer photo physical property purely due to contribution to LUMO only. None of the polymers exhibited a reduction potential, hence their

TH-1906_11615303

LUMO^{optical} have been calculated from absorption onset using formula (band gap = λ_{onset}/1240 and LUMO^{opt} = HOMO + band gap). As all ester substituting polymers show a high absorption onset, hence all ester functionalized polymers showed a low LUMO^{opt} compared to its methyl counterpart. Low lying LUMO^{opt} in ester functionalized polymers will help improve charge separation in active layer of fabricated PSC due to small energy difference between LUMO of polymer and LUMO of $PC_{71}BM$.[23]

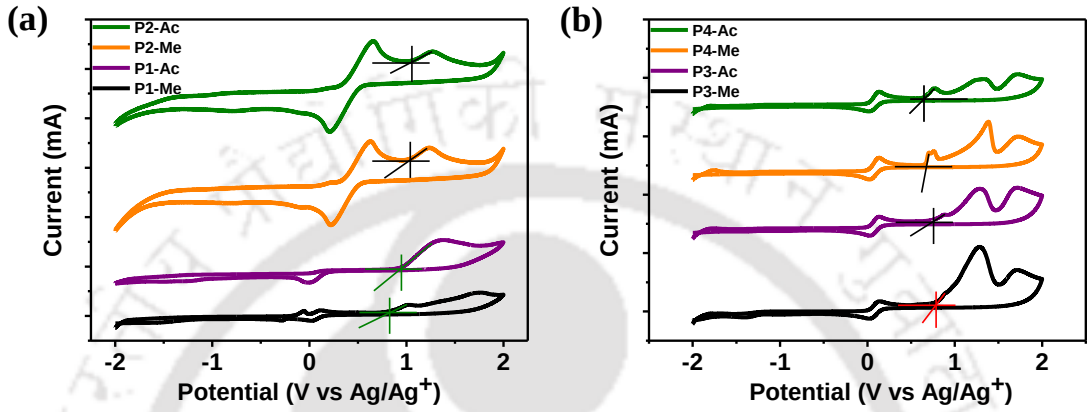

Figure 4.5 CV for polymers, showing oxidation potential (a) P1-Me, P1-Ac, P2-Me, P2-Ac (b) P3-Me, P3-Ac, P4-AMe, P4-Ac.

Table 4.1 Optical properties and voltammetry for synthesized polymers.

P	λ_{max} [nm]	λ_{onset} [nm]	λ_{max} film [nm]	λ_{onset} film [nm]	E_{ox} [Volt]	HOMO^{el} [eV]	LUMO^{opt} [eV]	ε (π-π*, ICT) [L mo^{-1} cm^{-1}]
P1-Me	316, 326, 369	470	327, 374	490	+0.801	-5.49	-2.94	16757, 10282
P1-Ac	312, 324, 421	496	326, 433	558	+0.92	-5.609	-3.32	16942, 8247
P2-Me	328, 379, 445	511	388, 480	602	+1.03	-5.39	-3.33	13820, 15372
P2-Ac	326, 382, 454	543	400, 515	644	+1.04	-5.40	-3.47	27373, 26197
P3-Me	329, 404, 440	526	333, 416, 462	586	+0.77	-5.49	-3.38	41536, 40772
P3-Ac	339, 404, ~470	555	352, 420, 523	648	+0.74	-5.46	-3.55	23934, 20532
P4-Me	327, 401,	510	330, 404, 460	557	+0.66	-5.38	-3.16	18124, 19819
P4-Ac	325, 390, ~457	554	327, 401, 512	670	+0.64	-5.36	-3.51	29827, 20113

TH-1906_11615303

4.2.5 Thermal stability of polymers

Thermal stability for all side chain ester and methyl functionalized polymers have been investigated using TGA under nitrogen atmosphere. All polymers are stable up to 250 °C corresponding to 5% weight loss of polymer (Table 4.2, Figure 4.6a and 4.6b) on a constant heating rate of 10K per minute, which is adequate temperature for device fabrication.[24,25] With exception, sticky natured polymer P1-Me starts degrading at less than 100 °C (Figure 4.6a) corresponding to 5% weight loss and might have occurred due to the presence of moisture (which might have responsible for its sticky nature). In Table 4.2 for P3 T_{10D} (degradation corresponding to 10% weight loss) was at 368 °C. All ester functionalized polymers have low T_{5D} and show bi-humped degradation pattern compared to their methyl counterpart (Figure 4.6a and 4.6b), which might have occurred due to fragileness/thermocleavable nature of side chain ester group (here methyl acetate).[15]

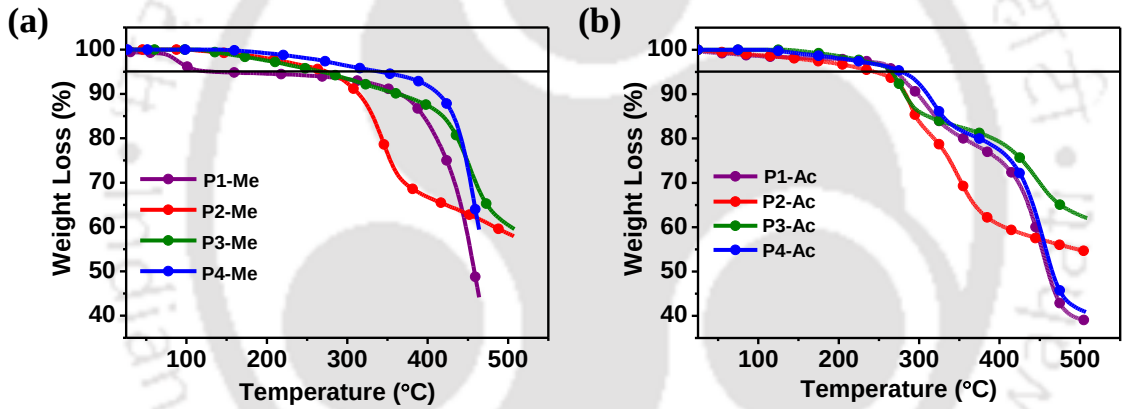

Figure 4.6 TGA spectra for polymers showing T_{5D} (corresponding to 5% weight loss) (a) methyl substituted at 5,6-position of BT-based CPs (b) methyl acetate counterpart polymer.

Table 4.2 Degradation temperature for synthesized polymers.

Polymer	P1-Me	P1-Ac	P2-Me	P2-Ac	P3-Me	P3-Ac	P4-Me	P4-Ac
T_{5D} [°C]	368 ($T_{10\,D}$)	272	275	244	275	265	348	279

4.2.6 Solar cell performance

Both methyl ester and methyl functionalized on BT-based polymers have been used as donor polymer with $PC_{71}BM$ as acceptor to fabricate PSC and similar device

TH-1906_11615303

configuration (ITO/PEDOT:PSS/Polymer:$PC_{71}BM$(1:1)/LiF/Al) have been chosen to establish influence of side chain ester group on solar cell performance. It has been established that ester substituted polymers [P(2,3,4)-Ac] show high solar cell performance (PCE, V_{oc} and J_{sc}) than their methyl counterpart polymer [P(2,3,4)-Me]]. With P2-Me:$PC_{71}BM$ (1:1) as active layer a PCE of 0.9% (J_{sc} = 5.09 mA/cm^{2,} V_{oc} = 0.68 V and FF = 26.2%) have been achieved, whereas ester functionalized polymer P2-Ac in similar device configuration results in a PCE of 1.36% with photo current density of 7.4 mA/cm^2, V_{oc} of 0.69 V and FF of 26.5% (Table 4.3, Figure 4.7a). Similarly with ester functionalized polymer P3-Ac a PCE of 1.17% (J_{SC} = 7.65 mA/cm^{2,} V_{oc} = 0.63 V, FF = 29.3%) was achieved compared to a PCE of 0.54% (J_{sc} = 3.5 mA/cm^{2,} V_{oc} = 0.57 V, FF = 27.1%) for its methyl counterpart (P3-Me). PSC performance for P3-Ac has further improved to a PCE of 1.96% by the use of 3% 1,8-diiodooctane (DIO) as additive into active layer (Table 4.3, Figure 4.7a).[26] The reason for improvement of PSC performance with DIO is mainly due to film reorganization and better phase separation (Figure 4.8c).[27]

P4-Me and P4-Ac follow similar pattern as like P2-Me and P2-Ac in fabricated devices with PCE of 0.35% (P4-Ac) and 0.31% (P4-Me). Solar cell performance with P4-Me and P4-Ac (polymer with DTh as donor) was very poor (PCE in the range of 0.3%) compared to BDT based polymers. This is due to poor film forming ability of P9 and P10 with high dihedral angle (~18°) between two thiophene units (Figure 4.3d) of the donor dithiophene (DTh), this leads to low rigidity of polymer backbone and hence poor film forming property.[28] Moreover, maximum external quantum efficiency of 37% (Table 4.3, Figure 4.7b) have been achieved with P3-Ac:$PC_{71}BM$ (1:1)-3% (DIO) as active layer for fabricated solar cells and improvement of EQE values have been observed subsequently with PCE in case of ester functionalized polymers compared to their methyl counterpart. This establishes side chain ester group at 5,6-position of BT improves solar cell performance, as studied in three different set of polymers with varying three donors (D2, D3, D4). In addition, P1-Ac:$PC_{71}BM$ (2:1) showed a PCE of 0.02% (J_{SC} = 0.50 mA/cm^2, V_{oc} = 0.17 V and FF = 26.2%), which is too low to study any comparison with its methyl counterpart P1-Me. Both P1-Me and P1-Ac have very poor film forming property, due to high dihedral angle along the conjugation main chain.[29] The cause of improvement of solar cell performances in case of ester substituted polymers are due to higher absorption range (red-region), better phase separation in active layer due to cross linking nature of

TH-1906_11615303

ester group with in polymer and/or $PC_{71}BM$, improved ICT due to lowering in dihedral angle along conjugation main chain and lowering of LUMO which facilitates ease of separation of exciton from LUMO of polymer to LUMO of $PC_{71}BM$.

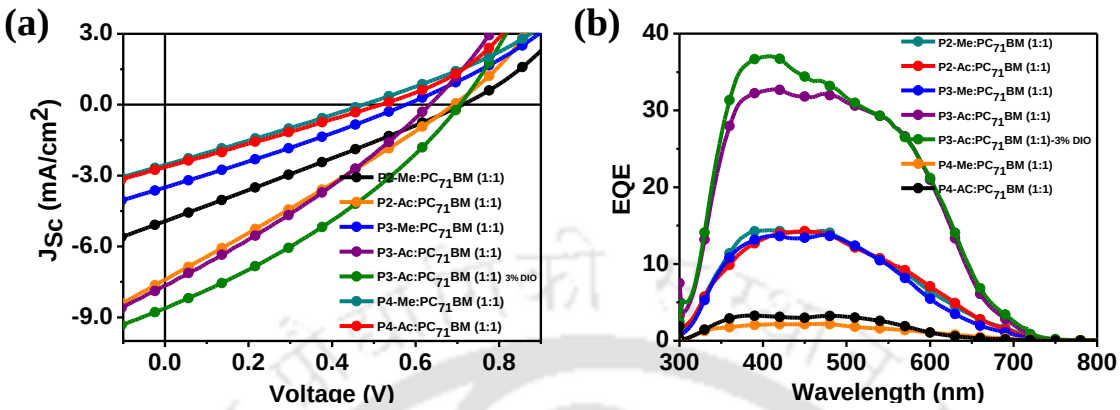

Figure 4.7 Solar cell performance for side chain methyl acetate and methyl containing BT- based polymers (a) J-V curve (b) external quantum efficiency.

Table 4.3 Solar cell parameter for fabricated bulk-heterojunction devices.

Active layer	V_{oc} [Volt]	J_{sc} [mA/cm^2]	FF [%]	Max. PCE [Avg. PCE, from 3 cells] %	Max. EQE [%]
P2-Me : $PC_{71}BM$ (1: 1)-LiF/Al	0.68	5.09	26.2	0.90 [0.85]	14
P2-Ac : $PC_{71}BM$ (1:1)-LiF/Al	0.69	7.4	26.5	1.36 [1.17]	14
P3-Me : $PC_{71}BM$ (1: 1)-LiF/Al	0.57	3.5	27.1	0.54 [0.54]	13
P3-Ac : $PC_{71}BM$ (1: 1)-LiF/Al	0.63	7.65	29.3	1.17 [1.16]	32
P3-Ac : $PC_{71}BM$ (1: 1)-LiF/Al-3% DIO	0.70	8.62	32.3	1.96 [1.94]	37
P4-Me : $PC_{71}BM$ (1: 1)-LiF/Al	0.47	2.54	26.3	0.31 [0.28]	2
P4-Ac : $PC_{71}BM$ (1: 1)-LiF/Al	0.51	2.62	26.2	0.35 [0.32]	3

4.2.7 Morphology of active layer of fabricated PSCs

Tapping mode AFM images have been recorded to investigate nano-morphology of active layer for fabricated devices by spin coating polymer:$PC_{71}BM$ blend on a pre cleaned ITO coated glass slide. As compared for P3-Me:$PC_{71}BM$ (1:1), P3-Ac:$PC_{71}BM$ (1:1) and P3-Ac:$PC_{71}BM$ (1:1)-3% DIO, it was observed that both the polymer-$PC_{71}BM$ blend have proper miscibility in the active layer with RMS (root mean square) roughness less than 3

TH-1906_11615303

nm.[19] Ester functionalized polymer P3-Ac results in better phase separation between P3-Ac and $PC_{71}BM$ in the blend film compared to its methyl counterpart P3-Me (Figure 4.8a and 4.8b). When 3% DIO was added into the P3-Ac:$PC_{71}BM$ (1:1) a significant improvement of phase separation[27,30] has been observed (Figure 4.8c) allowing distinguished path for electron and hole to travel and reducing recombination of generated excitons (as can be seen in the height and 3D view of height images in Figure 4.8). As a result PCE improved to 1.96% with P3-Ac:$PC_{71}BM$ (1:1)-3% DIO as active layer. This further confirms the positive influence of side chain ester group in gaining crtystallinity[31] in the active layer of fabricated PSC with tunability to external effects like additives and various solvent processing.

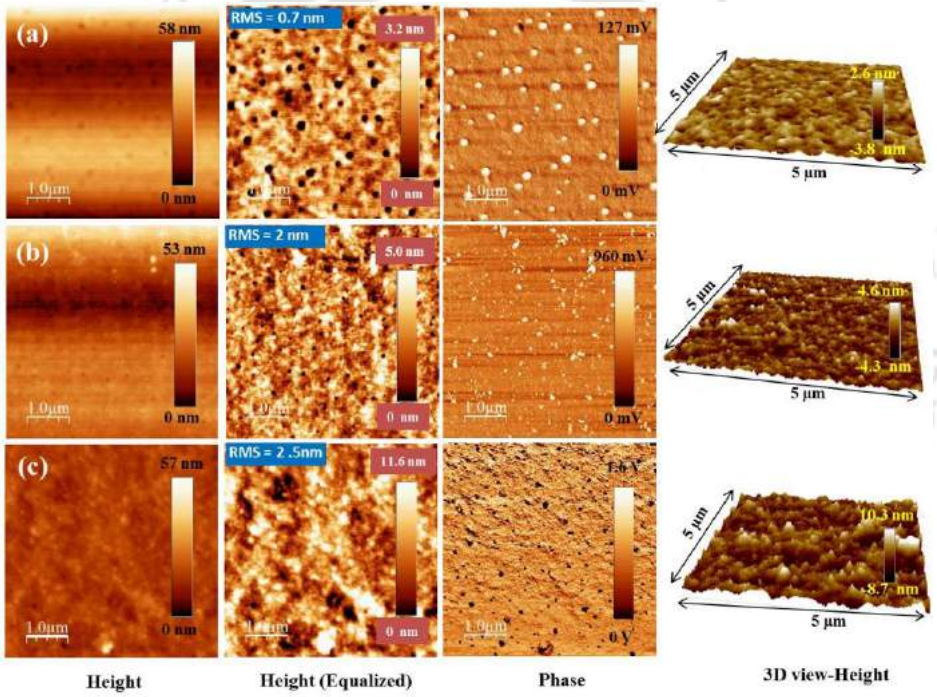

Figure 4.8 Morphology of active layer (polymer:$PC_{71}BM$ blend) of fabricated PSCs shows improvement of phase separation with ester substituted polymers and the phase separation further improved to large extent when 3% DIO was added to P3-Ac:$PC_{71}BM$ (1:1). (a) P3-Me:$PC_{71}BM$ (1:1) (b) P3-Ac:$PC_{71}BM$ (1:1) (c) P3-Ac:$PC_{71}BM$ (1:1)-3% DIO.

TH-1906_11615303

4.2.8 Thin film X-ray diffraction pattern

Thin film X-ray diffraction has been carried out by spin coating equal concentration of methyl and corresponding ester substituted polymers in order to investigate influence on π-π stacking distance in thin-film state with side chain ester substitution at 5,6-position of BT. For P4-Me and P4-Ac the diffraction peaks were observed at 2θ = 24.21° and 25.2° corresponding to π-π stacking distance of 0.3673 nm and 0.3531 nm respectively (Figure 4.9c). Close π-π stacking distance in case of ester substituted polymer P4-Ac compared to P4-Me further confirms improved π-π stacking within polymer chain in film state and hence better solar cell performance.[32,33] In addition, among P3-Me and P3-Ac, ester substituted at 5,6-position of BT polymer P3-Ac exhibited a similar/small incease in π-π stacking distance (2θ = 23.16°, π-π stacking distance = 0.3837 nm) as obvious due to small increase in dihedral angle (Figure 4.9b) (determined by DFT) compared to its methyl counterpart P3-Me (2θ = 23.25°, π-π stacking distance = 0.3822 nm). Similarly in case of P2-Me and P2-Ac no change in π-π distance was observed (Figure 4.9a).

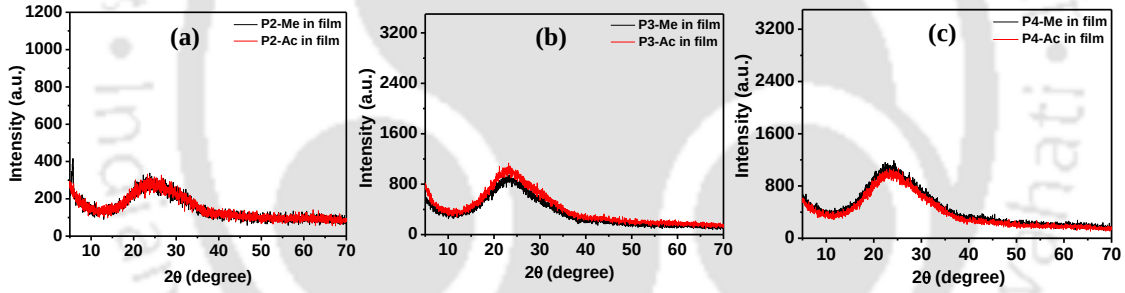

Figure 4.9 Thin film X-ray diffraction patterns confirming better π-π stacking in ester functionalized polymers with low dihedral angle along conjugation main chain (a) P2-Me and P2-Ac (b) P3-Me and P3-Ac (c) P4-Me and P4-Ac. Fit file of T-XRD given in appendix 4A.

4.3 Conclusion

In conclusion 5,6-position of BT have been synthetically modified to introduce two methyl acetate groups into it and co-polymer synthesized with commonly used donors, (BDT, DT and BDT-Th) resulting in newer conjugated polymers having methyl acetate group at 5,6-position of BT. All newly synthesized methyl and methyl acetate substituted 5,6-BT-based polymers are well soluble in commonly used solvent for device fabrication (CB, DCB $CHCl_3$, THF) and

TH-1906_11615303

additionally the ester substituted polymers are stable up to 250 °C. With this study it has been established that functionalizing ester group at 5,6-position of BT: reduces the dihedral angle in the polymer backbone due to oxygen-sulphur interaction, improves π-π stacking in film leading to red-shift and broadening of absorption spectra, lowers $LUMO^{optical}$ for polymer, improves phase separation of active layer of fabricated solar cell and hence improves solar cell performance compared to methyl counterpart. Ester substituted polymers are prone to external effect as well, such as with P3-Ac as donor polymer and $PC_{71}BM$ as acceptor that achieved PCE of 1.14% and have been improved to 1.96% via addition of 3% DIO as additive. Such side chain ester group with good photo-physical and morphological influence on polymer film state can be introduced into side chain of synthetically feasible conjugated units to be used to synthesize polymer with superior properties for solar cells and other optoelectronic devices.

4.4 Experimental procedures

4.4.1 Synthetic procedures

Detail reaction scheme for stepwise synthesis of monomers and polymers have been given in Figure 4.1 and Figure 4.2 respectively.

5,6-Dimethyl-benzo[1,2,5]thiadiazole (3b). Monomer **3b** was synthesized according to the literature procedure.[34]

4,7-Dibromo-5,6-dimethylbenzo[c][1,2,5]thiadiazole (4a). Monomer **3b** (0.5g, 1.55 mmol) and concentrated HBr (48 wt% ca. 30 mL) was added to a two neck round bottom flask, equipped with a condenser at one neck. The flask was fitted with an addition funnel at other neck to which Br_2 (0.470 mL, 9.134 mmol) solution in concentrated HBr (ca. 15 mL) was added slowly (2-3 drops per second) while stirring at room temperature. After few drops of addition the solution turns orange and a precipitate appears. After completion of addition the suspension was refluxed for 6 hours at 130 ^{0}C. To the reaction mixture, excess amount of H_2O was added to quench excess of bromine present. It was then filtered washed with H_2O repeatedly to give crude product, upon further purification by column chromatography (SiO_2, 50% $CHCl_3$ in hexane) yields 75% cream colored solid **4a**. ^{1}H-NMR (400 MHz, $CDCl_3$, δ in ppm): 2.672 (s, 6H). ^{13}C-NMR (150 MHz, $CDCl_3$, δ

TH-1906_11615303

in ppm): 152.12, 140.61, 114.68, 22.03. HR-MS: m/z $[M+H]^+$ calcd for $C_8H_6Br_2N_2S$ 322.868, found 322.868.

4,7-Dibromo-5,6-bis(bromomethyl)benzo[c][1,2,5]thiadiazole (4b). Monomer **4b** was synthesized following free radical bromination procedure as per literature procedure[34] using 4,7-Dibromo-5,6-dimethylbenzo[c][1,2,5]thiadiazole **4a** (0.5 g, 1.553 mmol), NBS (0.683 g, 3.883 mmol), benzoyl peroxide (0.037 g, 0.155 mmol) and 30 ml CCl_4. After chromatographic purification (SiO_2, 50% $CHCl_3$ in hexane) to crude product, gives compound **4b** (cream colored solid) with a yield of 92%. ^{1}H-NMR (400 MHz, $CDCl_3$, δ in ppm): 5.047 (s, 4H). ^{13}C-NMR (150 MHz, $CDCl_3$, δ in ppm): 152.81, 138.41, 118.14, 29.87. MALDI-TOF: m/z $[M]^+$ calcd for $C_8H_4Br_4N_2S$ 479.68 (requires), found 480.15.

4,7-Dibromobenzo[c][1,2,5]thiadiazole-5,6-diyl)bis(methylene)diacetate (4c). Monomer **4b** 0.9 g (1.87 mmol) and anhydrous sodium acetate 2.55 g (5.6 mmol) was mixed in a round bottom flask containing 25 ml of glacial acetic acid and refluxed for overnight at 120 ^{0}C. The reaction mixture was transfered into water and neutralized with sodium bicarbonate solution in water. It was further extracted with $CHCl_3$ and water. The organic portion was dried and desired product was separated with column chromatography using eluent (10% ethyl acetate in hexane) to get **4c** (0.75 g, yield = 91.7%) as white colored solid. ^{1}H-NMR (600 MHz, $CDCl_3$, δ in ppm): 5.58 (s, 4H), 2.1 (s, 6H). ^{13}C-NMR (150 MHz, $CDCl_3$, δ in ppm): 170.44, 152.88, 137.28, 118.01, 63.83, 20.84. HRMS (ESI): m/z $[M+H]^+$ calcd for $C_{12}H_{10}Br_2N_2O_4S$ 438.878, found 439.215.

4,7-Di(thiophen-2-yl)benzo[c][1,2,5]thiadiazole-5,6-diyl)bis(methylene) diacetate (4d). To a 50 ml round bottom flask monomer **4c** (0.3 g 0.687 mmol), tributyl(thiophen-2-yl)stannane 0.77 g (2.06 mmol) and 25 ml of dry toluene was added. The flask was purged for 5 minutes with argon before adding $Pd(PPh_3)_2Cl_2$ 0.024 g (0.034 mmol). It was then refluxed at 100 ^{0}C for 40 hours under argon flow. After cooled to RT, solvent was evaporated and the crude product was purified with column chromatography using eluent (5% ethyl acetate in hexane), to get 0.25 g of greenish yellow colored product (**4d**) with 81% yield. ^{1}H-NMR (600 MHz, $CDCl_3$, δ in ppm): 7.61-7.60 (d, 2H), 7.31-7.30 (d, 2H), 7.26-7.23 (dd, 2H), 5.30 (s, 4H), 2.13 (s, 6H). ^{13}C-NMR (75 MHz, $CDCl_3$, δ in ppm): 170.15, 154.39, 135.03, 134.80, 130.08, 129.77, 128.16, 127.16, 61.81, 20.91. HRMS (ESI): m/z $[M+H]^+$ calcd for $C_{20}H_{16}N_2O_4S_3$ 445.038, found 445.0336.

TH-1906_11615303

4,7-Bis(5-bromothiophen-2-yl)benzo[c][1,2,5]thiadiazole-5,6-diyl)bis(methylene) diacetate (4e). Inside a round bottom flask, monomer **4d** (0.1 g, 0.22 mmol) was dissolved in $CHCl_3$:glacial acetic acid (1:1) and NBS (0.12 g, 0.675 mmol) was added to it in one portion. It was refluxed in dark for overnight and then evaporated to get crude product. Further column chromatographic (SiO_2, eluent 5% EtOAc in hexane) purification of the crude gives 0.09 g of monomer **4e** (yellow colored solid, 66% yield). ^{1}H-NMR (600 MHz, $CDCl_3$, δ in ppm): 7.19-7.18 (d, 2H), 7.06-7.05 (d, 2H), 5.30 (s, 4H), 2.13 (s, 6H). ^{13}C-NMR (75 MHz, $CDCl_3$, δ in ppm): 170.10, 154.02, 136.31, 135.28, 130.25, 130.12, 129.40, 115.54, 61.65, 20.94. HRMS (ESI): m/z $[M+H]^+$ calcd for $C_{20}H_{14}Br_2N_2O_4S_3$ 602.858, found 602.858.

5,6-Dimethyl-4,7-di(thiophen-2-yl)benzo[c][1,2,5]thiadiazole (4f). Monomer **4f** was synthesized as like monomer **4d** using monomer **4b** (0.4 g, 1.24 mmol), tributyl(thiophen-2-yl)stannane (1.39 g 3.7 mmol) and $Pd(PPh)_2Cl_2$ 0.043 g (0.0621 mmol). The reaction mixture was purified by column chromatography (eluent 15% $CHCl_3$ in hexane) to give 0.33 g of compound **4f** as greenish yellow colored solid (yield = 81%). ^{1}H-NMR (600 MHz, $CDCl_3$, δ in ppm): 7.56-7.55 (d, 2H), 7.24-7.23 (dd, 2H), 7.129-7.123 (d, 2H), 2.48 (s, 6H). ^{13}C-NMR (75 MHz, $CDCl_3$, δ in ppm): 153.79, 139.78, 137.41, 128.74, 127.04, 126.79, 125.50, 18.99. HRMS (ESI): m/z $[M+H]^+$ calcd for $C_{16}H_{12}N_2S_3$ 329.028, found 329.024

4,7-Bis(5-bromothiophen-2-yl)-5,6-dimethylbenzo[c][1,2,5]thiadiazole (4g). Monomer **4g** was synthesized as like monomer **4e,** by taking monomer **4f** (0.25 g, 0.75 mmol) and NBS (0.4 g, 2.28 mmol) with room temperature stirring in dark. The reaction mixture was purified using column chromatography with 10% $CHCl_3$ in hexane as eluent to yield monomer **4g** as yellow colored solid (0.3 g, 81% yield). ^{1}H-NMR (600 MHz, $CDCl_3$, δ in ppm): 7.182-7.76 (d, 2H), 6.954-6.948 (d, 2H), 2.50 (s, 6H). ^{13}C-NMR (75 MHz, $CDCl_3$, δ in ppm): 153.34, 140.02, 138.79, 129.90, 129.26, 124.92, 113.71, 19.01. HRMS (ESI): m/z $[M+H]^+$ calcd for $C_{16}H_{10}Br_2N_2S_3$ 486.848, found 486.846.

General synthetic procedure for polymerization using Stille coupling. Donor monomer **(D1/D2/D3/D4)** and acceptor monomer **(4a/4c/4e/4g)** in equivalents of 1:1 were taken into a 50 ml round bottom flask and 25 mL of dry toluene was added to it. Before addition of 0.2 equivalent of $Pd(PPh_3)_4$, it was purged with argon for 5 minutes.

TH-1906_11615303

The reaction mixture was then degassed three times and filled with argon at each stage. It was then refluxed at 100 ^{0}C for 72 hours under argon atmosphere. After cooling to room temperature, the reaction mixture was concentrated and poured into 400 ml of methanol. The precipitates were collected washed with methanol, dried and then dissolved in chloroform. The insoluble portion was then filtered off twice and chloroform portion was concentrated and again precipitated with 300 ml of methanol. The precipitates were carefully collected to get desired polymer.

P1-Me. It was synthesized using monomer **D1** (0.1 g, 0.1207 mmol), monomer **4a** (0.038 g, 0.1207 mmol) and $Pd(PPh_3)_4$ (14 mg, 0.02414 mmol). **P1-Me** was formed as yellow colored sticky solid (45 mg, yield 56%). ^{1}H-NMR (600 MHz, $CDCl_3$, δ in ppm): 7.14-7.12 (br, 1H), 7.09-7.07 (br, 1H), 2.71-2.69 (br, 2H), 2.62-2.55 (br, 6H), 1.78-1.68 (br, 4H), 1.43-1.38 (br, 2H), 1.26-1.25 (br. 36H), 0.88-0.86 (br, 6H). GPC: M_n = 12600 g/mol.; M_w = 15883 g/mol.; PDI = 1.26; degree of polymerization, n = 16.

P1-Ac. It was synthesized using monomer **D1** (0.1 g, 0.1207 mmol), monomer **4c** (0.0526 g, 0.1207 mmol) and $Pd(PPh_3)_4$ (27.8 mg, 0.02414 mmol). **P1-Ac** was formed as reddish yellow colored powder (60 mg, yield 67.3%). ^{1}H-NMR (600 MHz, $CDCl_3$, δ in ppm): 7.26-7.25 (br, 1H), 7.20-7.17 (br, 1H), 5.39 (br, 4H), 2.78-2.68 (br, 2H), 2.23-1.98 (br, 6H), 1.74-1.62 (br, 4H), 1.44-1.37 (br, 2H), 1.37-1.12 (br, 36H), 0.91-0.80 (br, 6H). GPC: M_n = 4986 g/mol.; M_w = 5396 g/mol.; PDI = 1.08; degree of polymerization, n = 7.

P2-Me. It was synthesized using monomer **D2** (0.07 g, 0.09042 mmol), monomer **4g** (0.04385 g, 0.09042 mmol) and $Pd(PPh_3)_4$ (20.8 mg, 0.018 mmol). **P2-Me** was formed as red colored powder (62 mg, yield 89%). ^{1}H-NMR (600 MHz, $CDCl_3$, δ in ppm): 7.69-7.66 (br, 1H), 7.63-7.59 (br, 1H), 7.51-7.46 (br, 2H), 7.26-7.20 (br, 2H), 4.31-4.23 (br, 4H), 2.67-2.58 (br, 6H), 1.95-1.83 (br, 2H), 1.62-1.54 (br, 4H), 1.53-1.39 (br, 12H), 1.16-0.94 (br, 12H). GPC: M_n = 11580 g/mol.; M_w = 15300 g/mol.; PDI = 1.29; degree of polymerization, n = 15.

P2-Ac. It was synthesized using monomer **D2** (0.07 g, 0.09042 mmol), monomer **4e** (0.0544 g, 0.09042 mmol) and $Pd(PPh_3)_4$ (20.8 mg, 0.018 mmol). **P2-Ac** was formed as deep red colored solid (74 mg, yield 92%). ^{1}H-NMR (600 MHz, $CDCl_3$, δ in ppm): 7.71-7.65 (br, 1H), 7.60-7.51 (br, 1H), 7.45-7.36 (br, 2H), 7.30-7.28 (br, 2H), 5.48-5.39 (br, 4H), 4.32-4.21 (br, 4H), 2.24-2.15 (br, 6H), 1.95-1.85 (br, 2H), 1.64-1.53 (br, 4H), 1.53-

TH-1906_11615303

1.40 (br, 12H), 1.16-1.09 (br, 12H). ^{13}C-NMR (150 MHz, $CDCl_3$, δ in ppm): 170.18, 154.16, 144.5, 144.33, 140.55, 136.07, 135.31, 135.21, 132.54, 130.99, 130.17, 129.73, 129.46, 125.28, 124.54, 118.25, 116.79, 114.09, 76.24, 62.0, 40.64, 31.94, 30.46, 29.23, 23.99, 20.99, 14.21, 11.37. GPC: M_n = 11581 g/mol.; M_w = 11959 g/mol.; PDI = 1.03; degree of polymerization, n = 13.

P3-Me. It was synthesized using monomer **D3** (0.07 g, 0.077 mmol), monomer **4g** (0.037 g, 0.077 mmol) and $Pd(PPh_3)_4$ (17.8 mg, 0.015 mmol). **P3-Me** was formed as red colored solid (55 mg, yield 79%). ^{1}H-NMR (600 MHz, $CDCl_3$, δ in ppm): 7.69-7.59 (br, 2H), 7.36-7.29 (br, 2H), 7.22-7.12 (br, 2H), 7.12-7.02 (br, 2H), 6.91-6.79b (br, 2H), 2.87-2.75 (br, 4H), 2.55-2.39 (br, 6H), 1.70-1.59 (br, 2H), 1.59-1.45 (br, 4H), 1.33-1.21 (br, 12H), 0.92-0.78 (br, 12H). ^{13}C-NMR (150 MHz, $CDCl_3$, δ in ppm): 153.45, 146.14, 139.91, 139.18, 138.77, 137.69, 137.37, 137.19, 136.83, 130.13, 129.32, 128.89, 127.87, 125.54, 125.29, 125.18, 124.04, 123.52, 121.19, 119.49, 114.11, 41.46, 34.33, 32.51, 28.95, 25.80, 23.07, 19.29, 14.23, 10.95. GPC: M_n = 11142 g/mol.; M_w = 13924 g/mol.; PDI = 1.24; degree of polymerization, n = 12.

P3-Ac. It was synthesized using monomer **D3** (0.07 g, 0.077 mmol), monomer **4e** (0.0466 g, 0.077 mmol) and $Pd(PPh_3)_4$ (17.8 mg, 0.015 mmol). **P3-Ac.** was formed as deep red colored solid (60 mg, yield 76%). ^{1}H-NMR (600 MHz, $CDCl_3$, δ in ppm): 7.72-7.63 (br, 2H), 7.37-7.30 (br, 2H), 7.30-7.24 (br, 2H), 7.24-7.15 (br, 2H), 6.91-6.81 (br, 2H), 5.36-5.22 (br, 4H), 2.86-2.76 (br, 4H), 2.12-2.03 (br, 6H), 1.68-1.61 (br, 2H), 1.61-1.47 (br, 4H), 1.32-1.23 (br, 12H), 0.94-0.78 (br, 12H). ^{13}C-NMR (150 MHz, $CDCl_3$, δ in ppm): 170.14, 154.17, 146.14, 140.58, 139.28, 138.95, 138.12, 137.41, 136.71, 135.29, 135.17, 130.85, 130.15, 129.66, 127.94, 125.55, 125.34, 124.51, 123.68, 119.97, 115.54, 114.08, 61.98, 34.33, 32.53, 28.94, 25.77, 23.10, 20.98, 14.20, 10.95. GPC: M_n = 9937 g/mol.; M_w = 10605 g/mol.; PDI = 1.06; degree of polymerization, n = 9.

P4-Me. It was synthesized using monomer **D4** (0.07 g, 0.0844 mmol), monomer **4g** (0.0409 g, 0.0844 mmol) and $Pd(PPh_3)_4$ (19.5 mg, 0.0169 mmol). **P4-Me** was formed as deep red colored solid (53 mg, yield 76%). ^{1}H-NMR (600 MHz, $CDCl_3$, δ in ppm): 7.20-7.16 (br, 2H), 7.16-7.08 (br, 2H), 7.01-6.93 (br, 2H), 2.78-2.70 (br, 2H), 2.55-2.40 (br, 6H), 1.69-1.59 (br, 4H), 1.41-1.31 (br, 2H), 1.25-1.06 (br, 36H), 0.84-0.74 (br, 6H). ^{13}C-NMR (150 MHz, $CDCl_3$, δ in ppm): 153.60, 143.48, 140.45, 139.79, 138.62, 137.79,

TH-1906_11615303

137.01, 136.74, 134.97, 129.94, 129.52, 126.62, 125.39, 123.93, 114.02, 31.96, 31.94, 30.58, 29.70-29.38 (many peaks), 22.72, 19.24, 14.17. GPC: M_n = 15325 g/mol.; M_w = 17370 g/mol.; PDI = 1.33; degree of polymerization, n = 18.

P4-Ac. It was synthesized using monomer **D4** (0.06 g, 0.0724 mmol), monomer **4e** (0.0436 g, 0.0724 mmol) and $Pd(PPh_3)_4$ (16.7 mg, 0.0144 mmol). **P4-Ac** was formed as deep red colored solid (59 mg, yield 87%). ^{1}H-NMR (600 MHz, $CDCl_3$, δ in ppm):7.27-7.15 (br, 4H), 7.04-6.93 (br, 2H), 5.37-5.27 (br, 4H), 2.80-2.69 (br, 2H), 2.14-2.04 (br, 6H), 1.69-1.61 (br, 4H), 1.40-1.32 (br, 2H) 1.25-1.06 (br, 36H), 0.84-0.74 (br, 6H). ^{13}C-NMR (150 MHz, $CDCl_3$, δ in ppm): 170.24, 154.28, 140.98, 139.31, 135.24, 135.0, 134.55, 130.88, 130.50, 129.72, 129.20, 129.0, 126.77, 125.62, 124.51, 114.08, 62.1, 31.94, 31.92, 30.58, 29.7-29.39 (many peaks), 22.65, 21.04, 14.20. GPC: M_n = 14008 g/mol.; M_w = 18199 g/mol.; PDI = 1.29; degree of polymerization, n = 14.

4.4.2 Methods, procedure and spectra

Device fabrication procedure and method of UV-visible spectra and cyclic voltammetry were given in Appendix A1. NMR spectra of all monomers and polymer synthesized and GPC spectra have been given in appendix A4.

TH-1906_11615303

4.5 References

1. Li, A.; Amonoo, J.; Huang, B.; Goldberg, P. K.; McNeil, A. J.; Green, P. F. *Adv. Funct. Mater.* **2014**, *24*, 5594-5602.
2. Shi, S.; Liao, Q.; Tang, Y.; Guo, H.; Zhou, X.; Wang, Y.; Yang, T.; Liang, Y.; Cheng, X.; Liu, F.; Guo, X. *Adv. Mater.* **2016**, *28*, 9969-9977.
3. Ouyang, D.; Xiao, M.; Zhu, D.; Zhu, W.; Du, Z.; Wang, N.; Zhou, Y.; Bao, X.; Yang, R. *Polym. Chem.* **2015**, *6*, 55-63.
4. Cui, C.; He, Z.; Wu, Y.; Cheng, X.; Wu, H.; Li, Y.; Cao, Y.; Wong, W. Y. *Energy Environ. Sci.* **2016**, *9*, 885-891.
5. Hou, J.; Chen, H. Y.; Zhang, S.; Chen, R. I.; Yang, Y.; Wu, Y.; Li, G. *J. Am. Chem. Soc.* **2009**, *131*, 15586-15587.
6. Kim, H. J.; Han, A. R.; Cho, C. H.; Kang, H.; Cho, H. H.; Lee, M. Y.; Fréchet, J. M. J.; Oh, J. H.; Kim, B. J. *Chem. Mater.* **2012**, *24*, 215-221.
7. Wang, X.; Sun, Y.; Chen, S.; Guo, X.; Zhang, M.; Li, X.; Li, Y.; Wang, H. *Macromolecules* **2012**, *45*, 1208-1216.
8. Xia, B.; Lu, K.; Yuan, L.; Zhang, J.; Zhu, L.; Zhu, X.; Deng, D.; Li, H.; Wei, Z. *Polym. Chem.* **2016**, *7*, 1323-1329.
9. Guo, X.; Zhou, N.; Lou, S. J.; Smith, J.; Tice, D. B.; Hennek, J. W.; Ortiz, R. P.; Navarrete, J. T. L.; Li, S.; Strzalka, J.; Chen, L. X.; Chang, R. P. H.; Facchetti, A.; Marks, T. J. *Nat. Photonics*, **2013**, *7*, 825-833.
10. Li, Y.; Zou, J.; Yip, H. L.; Li, C. Z.; Zhang, Y.; Chueh, C. C.; Intemann, J.; Xu, Y.; Liang, P. W.; Chen, Y.; Jen, A. K. Y. *Macromolecules* **2013**, *46*, 5497-5503.
11. Duan, C.; Franeker, J. J. V.; Wienk, M. M.; Janssen, R. A. J. *Polym. Chem.* **2016**, *7*, 5730-5738.
12. Dou, J. H.; Zheng, Y. Q.; Yao, Z. F.; Lei, T.; Shen, X.; Luo, X. Y.; Yu, Z. A.; Zhang, S. D.; Han, G.; Wang, Z.; Yi, Y.; Wang, J. Y.; Pei, J. *Adv. Mater.* **2015**, *27*, 8051-8055.
13. Kesters, J.; Kudret, S.; Bertho, S.; Brande, N. V. D.; Defour, M.; Mele, B. V.; Penxten, H.; Lutsen, L.; Manca, J.; Vanderzande, D.; Maes, W. *Org. Electro.* **2014**, *15*, 549-562.
14. Kesters, J.; Verstappen, P.; Raymakers, J.; Vanormelingen, W.; Drijkoningen, J.; D'Haen, J.; Manca, J.; Lutsen, L.; Vanderzande, D.; Maes, W. *Chem. Mater.* **2015**, *27*, 1332-1341.

TH-1906_11615303

15. Helgesen, M.; Gevorgyan, S. A.; Krebs, F. C.; Janssen, R. A. J. *Chem. Mater.* **2009**, *21*, 4669-4675.
16. He, Y.; Guo, C.; Sun, B.; Quinn, J.; Li, Y. *Polym. Chem.* **2015**, *6*, 6689-6697.
17. Kim, J. Y.; Kim, Y. U.; Kim, H. J.; Um, H. A.; Shin, J.; Cho, M. J.; Choi, D. H. *Macromol. Res.* **2016**, *24*, 980-985.
18. Mei, C.Y.; Liang, L.; Zhao, F. G.; Wang, J. T.; Yu, L. F.; Li, Y. X.; Li, W. S.; *Macromolecules* **2013**, *46*, 7920-7931.
19. Li, Y.; Chen, Y.; Liu, X.; Wang, Z.; Yang, X.; Tu, Y.; Zhu, X. *Macromolecules* **2011**, *44*, 6370-6381.
20. Wang, X.; Chen, S.; Sun, Y.; Zhang, M.; Li, Y.; Li, X.; Wang, H. *Polym. Chem.* **2011**, *2*, 2872-2877.
21. Liu, D.; Yang, B.; Jang, B.; Xu, B.; Zhang, S.; He, C.; Woo, H. Y.; Hou, J. *Energy Environ. Sci.* **2017**, *10*, 546-551.
22. Chen, H. Y.; Hou, J.; Zhang, S.; Liang, Y.; Yang, G.; Yang, Y.; Yu, L.; Wu, Y.; Li, G. *Nat. Photonics* **2009**, *3*, 649-653.
23. Nguyen, T. L.; Choi, H.; Ko, S. J.; Kim, T.; Uddin, M. A.; Hwang, S.; Kim, J. Y.; Woo, H. Y. *Polymer Journal* **2017**, *49*, 141-148.
24. Chen, L.; Shen, P.; Zhang, Z. G.; Li, Y. *J. Mater. Chem. A* ***2015***, *3*, 12005-12015.
25. Lee, C. H.; Lai, Y. Y.; Cao, F. Y.; Hsu, J. Y.; Lin, Z. L.; Jeng, U. S.; Su, C. J.; Cheng, Y. J. *J. Mater. Chem. C* **2016**, *4*, 11427-11435.
26. Liang, Y.; Xu, Z.; Xia, J.; Tsai, S. T.; Wu, Y.; Li, G.; Ray, C.; Yu, L. *Adv. Mater.* **2010**, *22*, E135-E138.
27. Li, S.; Yuan, Z.; Yuan, J.; Deng, P.; Zhang, Q.; Sun, B. *J. Mater. Chem.* A, **2014**, *2*, 5427-5433.
28. Jiang, J. M.; Yang, P. A.; Hsieh, T. H.; Wei, K. H. *Macromolecules* **2011**, *44*, 9155-9163.
29. Zhou, H.; Yang, L.; Xiao, S.; Liu, S.; You, W. *Macromolecules* **2010**, *43*, 811-820.
30. Liu, D.; Zhao, W.; Zhang, S.; Ye, L.; Zheng, Z.; Cui, Y.; Chen, Y.; Hou, J. *Macromolecules* **2015**, *48*, 5172-5178.
31. Wakim, S.; Alem, S.; Li, Z.; Zhang, Y.; Tse, S. C.; Lu, J.; Ding, J.; Tao, Y. *J. Mater. Chem.* **2011**, *21*, 10920-10928.
32. Cui, C.; He, Z.; Wu, Y.; Cheng, X.; Wu, H.; Li, Y.; Cao, Y.; Wong, W. Y. *Energy Environ. Sci.* **2016**, *9*, 885-891.

TH-1906_11615303

33. Kim, H.; Lee, H.; Seo, D.; Jeong, Y.; Cho, K.; Lee, J.; Lee, Y. *Chem. Mater*. **2015**, *27*, 3102-3107.
34. Ratha, R.; Singh, A.; Raju, T. B.; Iyer, P, K. *Polym. Bull.* **2017**, DOI 10.1007/s00289-017-2193-x.

TH-1906_11615303

Chapter 5

6,7-Di(thiophen-2-yl)naphtho[2,3-c][1,2,5]thiadiazole and 4,6,7,9-Tetra(thiophen-2-yl)naphtho[2,3-c][1,2,5]thiadiazole as New Acceptor Units for D-A Type Co-polymer Towards Fabrication of Polymer Solar Cell

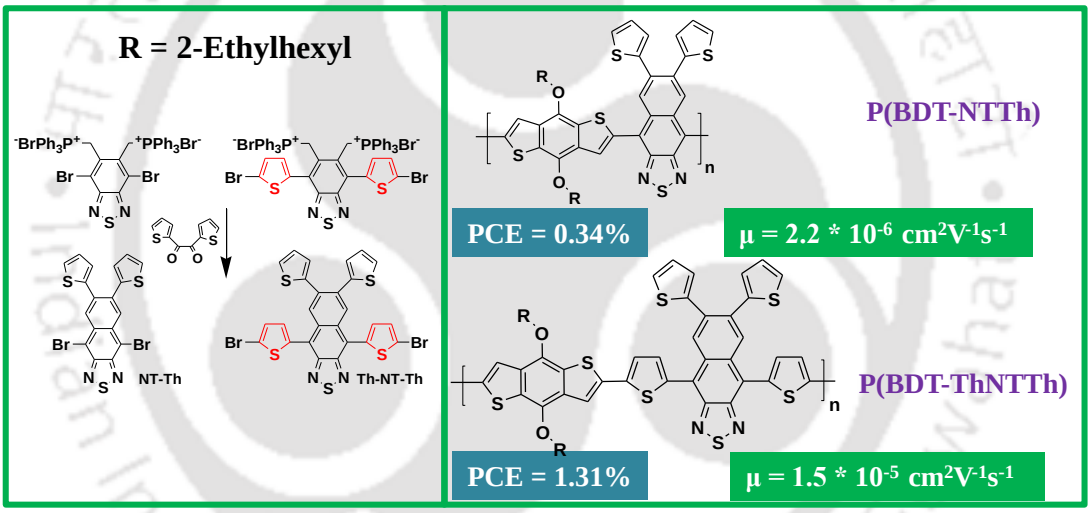

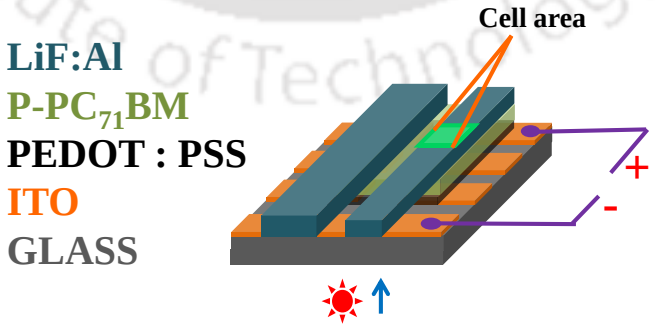

Abstract

This work emphasize on the synthesis of two new acceptor units for donor (D)-acceptor (A)-based polymers used in photovoltaic devices, namely 4,9-dibromo-6,7-di(thiophen-2-yl)naphtho[2,3-c][1,2,5]thiadiazole [a derivative of naphtho[2,3-c][1,2,5]thiadiazole (NT), substituted with two thiophene (Th) units on 6 and 7 position of it (NT-Th)] and 4,9-bis(5-bromothiophen-2-yl)-6,7-di(thiophen-2-yl)naphtho[2,3-c][1,2,5]thiadiazole (Th-NT-Th) with two additional Th units substituted at 4,7 position of NT-Th. Both the NT-based acceptors have been designed using 5,6-position of benzothiadiazole (BT) and synthesized by Wittig coupling reaction. Alternate D-A co-polymer of new NT-based acceptors with commonly used donor 4,8-bis((2-ethylhexyl)oxy)benzo[1,2-b:4,5-b´]dithiophene (BDT) via Stille coupling results new conjugated polymers (CPs) namely **P(BDT-NTTh)** and **P(BDT-ThNTTh)**. Newly synthesized acceptor units distinguishes itself from existing literature of naphtho[2,3-c][1,2,5]thiadiazole (NT) acceptor in having additional two Th units attached at 6,7 position of NT, imparting into it a 2-dimensional (2D) type of conjugated structure. Both **P(BDT-NTTh)** and **P(BDT-ThNTTh)** were characterized by GPC, UV-visible, ^{1}H-NMR, ^{13}C-NMR, TGA and CV. Dihedral angle for optimized geometry and ICT of newly synthesized NT-based polymers have also been investigated using DFT. PSC performance of synthesized polymers has been examined by fabricating BHJ solar cell with configuration **ITO/PEDOT:PSS/Polymer-$PC_{71}BM$/LiF/Al**, which results a PCE of 0.34% and 1.31% with **P(BDT-NTTh)** and **P(BDT-ThNTTh)** respectively. Hole-mobility for blend of **P(BDT-NTTh)** and **P(BDT-ThNTTh)** with $PC_{71}BM$ have been calculated using SCLC (space charge limited current) method by fabricating hole only devices of configuration **ITO/PEDOT:PSS/Polymer-$PC_{71}BM$/Cu** and mobility of $2.2*10^{-6}$ and $1.5*10^{-5}$ cm^2 V^{-1} s^{-1} respectively were found. Morphology of active layer of fabricated PSC has been studied with atomic force microscopy (AFM).

5.1 Introduction

Conjugated polymers synthesized from representative class of donors and acceptors as mentioned in page 9 (chapter 1) could only be able to result a PCE of 4 to 6%.[1-3] Again newer derivatives of representative donors and acceptors (as listed in section 1.1.3.10, chapter 1, page no 21) in suitable combination to synthesize D-A polymers have been

TH-1906_11615303

proved to be very encouraging in producing PCE of 7-9%.[4-11] Moreover in a recent literature[12] PCE of 11.3% have been achieved using fluorine substituted quinoxaline derivative (difluoro quinoxaline, DFQ) as acceptor unit in D-A polymer. Contrary to DFQ acceptor-based CP, representative Quinoxaline (Q) acceptor-based polymer could only result a PCE of < 5%. In addition to the design that have been followed to synthesize D-A, CPs using donors and acceptors are not only 1-dimensinal (1D) polymers (co-polymer of 'D' and 'A' in D-A/D-A-D/D-π-A fashion, with conjugation units only in polymer main chain), (2D) polymers have also been synthesized and fabricated into PSCs. In 2-dimensional structure π-electron donor such as Th)/BDT[13,14] and π-electron acceptor such as BT[15] have been substituted with a conjugated unit as side chain, which can enhance optical/electrochemical/transport property and/or improves rigidity of the polymer.[16]

This article aim to explore use of derivatives of NT as innovative 2D acceptor unit for D-A CPs in BHJ solar cell. NT is among various acceptors used to design D-A polymers/monomers for several optoelectronic applications and has gained momentum in recent photovoltaic research articles. Recent literatures demonstrate potential of NT as acceptor unit in designing both monomers and co-polymers having promising application in all types of optoelectronic devices such as: NT as an acceptor unit for D-A polymer used for solar cell (PSC);[17,18] as an conjugate spacer in dye used for dye sensitized solar cell (DSSC);[19] as an narrow band gap dopant unit for designing CPs for light emitting diode (PLED);[20] and designing monomeric emitter for organic light emitting diode (OLED).[21,22] Although NT alone has been used as an acceptor in D-A type co-polymer for photovoltaic devices, yet there is no report which establishes design and synthesis of 2D derivatives of NT as acceptor unit for D-A CPs, unlike other reported and much studied acceptor units such as benzothiadiazole (BT).[2] thienopyrazine (Tp),[23] benzopyrazine (Bz)/quinoxaline (Q).[1]

Earlier existing literature demonstrating use of Q/Bz/Tp and their derivatives as an acceptor unit in D-A CPs used as active layer for optoelectronic devices have been possible and/or synthesized by formation of two C=N bond at nearby ortho-position of corresponding core conjugated unit of the acceptor.[1,24] But there has been no report of C=C bond formation of similar kind which could result in the formation of derivatives of NT from BT. Herein, two derivative of NT have been synthesized namely NT-Th and Th-NT-Th. These derivatives in another way can be consider as two vinyl thiophene units

TH-1906_11615303

attached to 5,6-position of BT, which have been fused and became 6,7-thiophene substituted naphtho[2,3-c][1,2,5]thiadiazole as well, giving it a 2D structured conjugated unit. Alternate co-polymer of new NT-based acceptors with commonly used donor BDT (D) in D-A fashion results polymer namely **P(BDT-NTTh)** and **P(BDT-ThNTTh)**. Thiophenes attached as side conjugated units will enhance both optical property and hole-mobility of synthesized CPs.[13-16]

5.2 Results and discussion

5.2.1 Reaction scheme

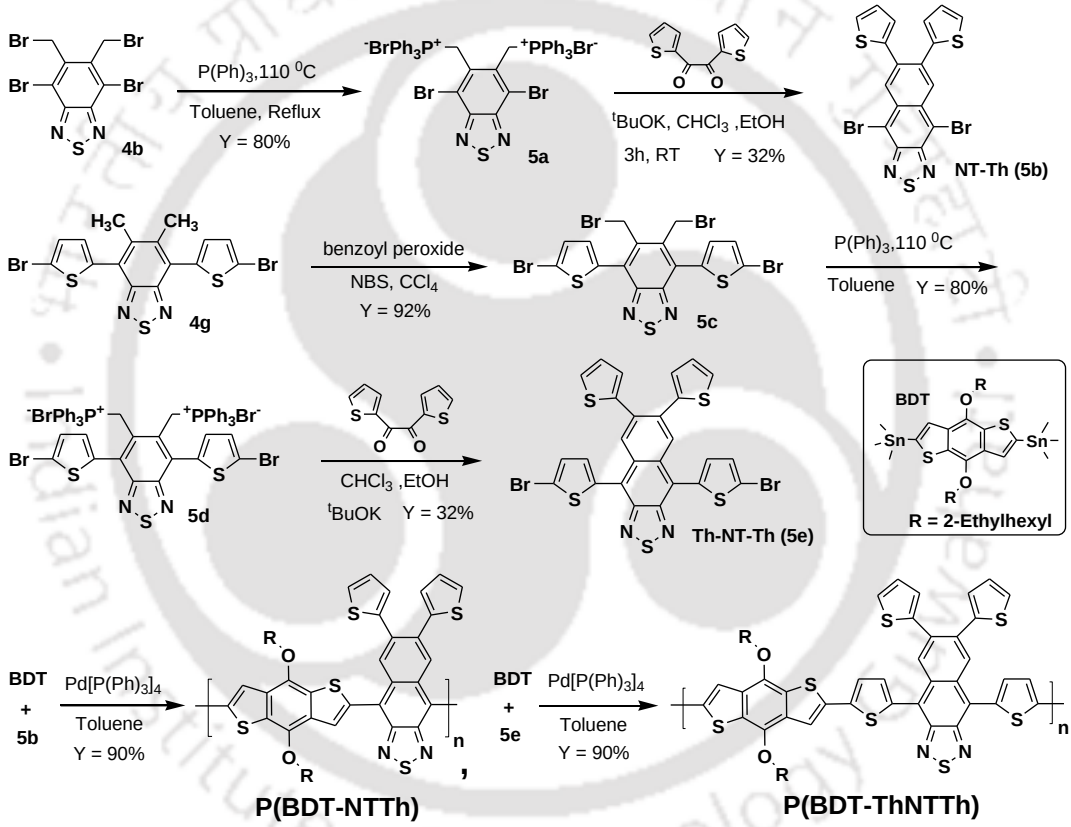

Figure 5.1 Reaction scheme for synthesis of napthothiadiazole derivative and its polymer with Benzodithiophene.

TH-1906_11615303

5.2.2 Thermal properties

Thermal stability of synthesized polymers have been investigated using thermo gravimetric analysis (TGA) under nitrogen flow. Both the polymer **P(BDT-NTTh)** and **P(BDT-ThNTTh)** are stable up to 253 ^{0}C corresponding to a 5% weight loss (Figure 5.2). This degradation temperature (T_{5D}) is adequate for device fabrication[25] from solution processed polymer-PCBM blend. In addition, after 253 °C further 5% weight loss was witnessed up to 300 °C and then the polymer starts degrading. This might be due to degradation of small length polymers or small amount of monomers left and commonly observed for conjugated polymers.[17]

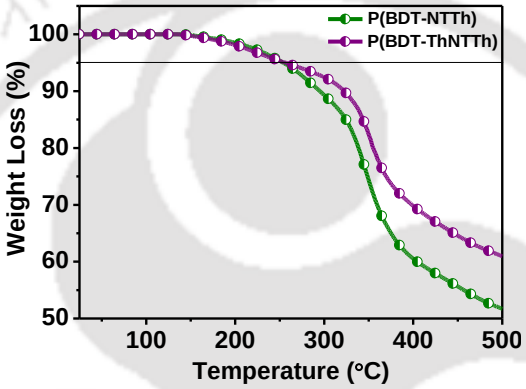

Figure 5.2 TGA showing degradation temperature for 5% weight loss (T_{5D}) in range of 250 ^{0}C, which is adequate for device fabrication.

5.2.3 Optical properties

Absorbance spectra of polymers **P(BDT-NTTh)** and **P(BDT-ThNTTh)** have been investigated from chloroform solution and in film state (by spin coating from chlorobenzene solution on a pre-cleaned glass substrate). In chloroform solution both the polymers show three significant intense peaks at λ_{max} 358, 422, 589 nm [**P(BDT-NTTh)**] and ~348, 410, 596 nm [**P(BDT-ThNTTh)**]. Peak at higher wavelength or low energy transition corresponding to ICT band. The π-π* transition for polymer backbone appears at 422 nm for **P(BDT-NTTh)** and 410 nm for **P(BDT-ThNTTh)** (Table 5.1, Figure 5.3a).[26] The high energy peak corresponds to intrinsic peak for BDT donor unit for both the CPs. Molar absorption coefficient (ε) have been determined from chloroform solution for both the polymers, with **P(BDT-ThNTTh)** having higher absorption coefficient both for π-π* transition (41051 L mol^{-1} cm^{-1}) and ICT band (16688 L mol^{-1} cm^{-1}) compared to

TH-1906_11615303

P(BDT-NTTh) with absorption coefficient for π-π* transition (11413 L $mol^{-1}cm^{-1}$) and ICT band (5722 L mol^{-1} cm^{-1}) transition (Table 5.1). Solid state absorbance for both the CPs were red-shifted compared to solution state, both at λ_{max} and absorption onset, with tri-humped peak as like solution state (Figure 5.3a). This indicates substantial change in conformation or formation of *J*-aggregates of CPs in film state.[27] However **P(BDT-ThNTTh)** demonstrates more red-shift in solid state compared to **P(BDT-NTTh)**, indicating large change in conformation in solid state due to linear geometry with maximum dihedral angle of 40° (due to incorporation of thiophene unit on both side of acceptor NT-Th) for **P(BDT-ThNTTh)** compared to **P(BDT-NTTh)** having maximum dihedral angle of 53° (Figure 5.4) along conjugation main chain.[28]

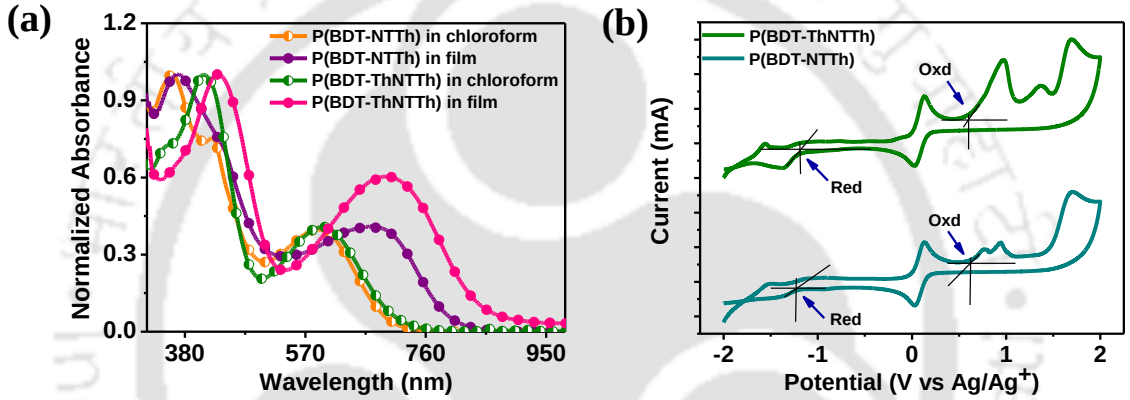

Figure 5.3 Photophysical properties for NT-based CPs (a) absorption spectra in solution (from $CHCl_3$) and film (chlorobenzene) (b) oxidation and reduction potentials from cyclic voltammetry.

Table 5.1 Optical properties of NT-based polymers.

P	λ_{max} [nm]	λ_{onset} [nm]	λ_{max} film [nm]	λ_{onset} film [nm]	E_{ox} [Volt]	E_{red} [Volt]	$HOMO^{el}$ [eV]	$LUMO^{el}$ [eV]	$LUMO^{opt}$ [eV]	ε L. $mo^{-1}.cm^{-1}$
P11	358, 422, 589	699	368, ~440, 682	802	+0.62	-1.19	-5.34	-3.53	-3.79	11413, 5722
P12	410, 596	716	425, 701	846	+0.69	-1.44	-5.4	-3.28	-3.69	41051, 16688

Both oxidation and reduction peaks were observed for NT-based polymers in CV with HOMO and LUMO levels calculaed to be -5.34 eV and -3.50 eV for **P(BDT-NTTh)** and -5.33 eV, -3.54 eV for **P(BDT-ThNTTh)** respectively (Table 5.2, Figure 5.3b). Optical

TH-1906_11615303

LUMO in film state have also been calculated using absorption onset and results for **P(BDT-NTTh)** -3.79 eV) and for **P(BDT-ThNTTh)** -3.86 eV respectively.

5.2.4 DFT calculation

Ground state geometry optimization have been carried out by Gaussian 03W software at B3LYP/6-31G (*d*,*p*,) to investigate dihedral angle along polymer main chain, intra-molecular charge transfer (ICT) from D to A and frontier molecular orbitals for HOMO and LUMO. NT-based polymers displayed continuous distribution of charge density on entire conjugated units in HOMO with localization of charge density largely on acceptor (NT-Th) in LUMO, which are the ideal distributions for ICT between D and A in a D-A based CPs (Figure 5.4).[28] In **P(BDT-NTTh)** maximum dihedral angle between donor and acceptor unit was 53.8° (Figure 5.4) due to close vicinity of donor (BDT) and acceptor (NT-Th). Incorporating two Th-units, distances the donor and acceptor as in case of **P(BDT-ThNTTh)** leading to lowering of dihedral angle, with maximum value of 42° and more planar geometry has been attained.[29]

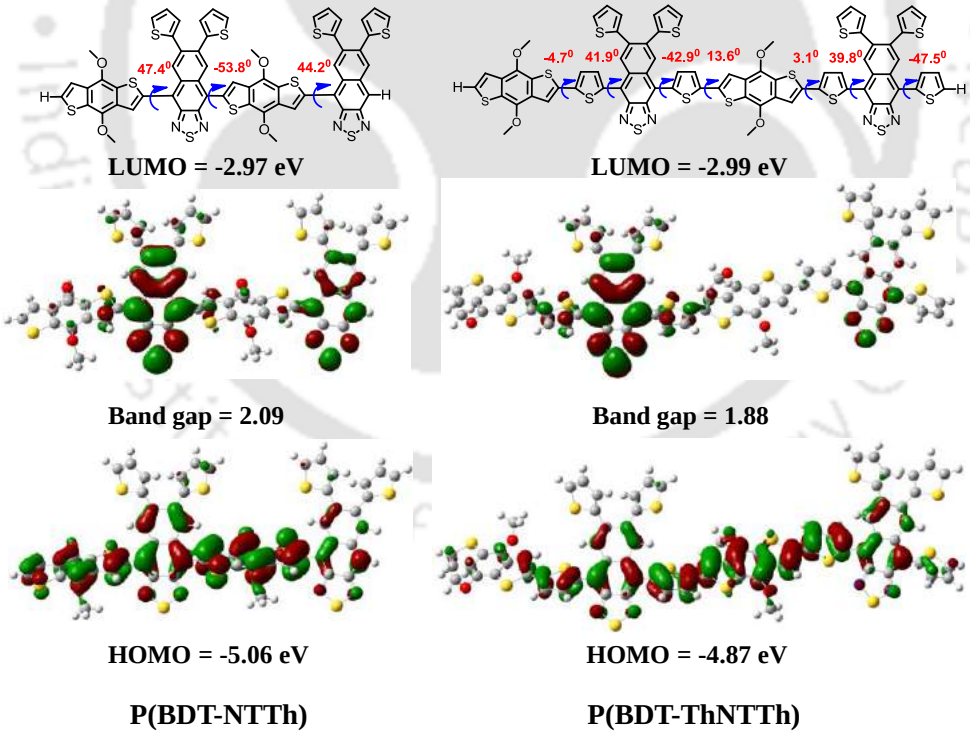

Figure 5.4 Molecular orbitals of HOMO and LUMO shows ideal distribution for ICT between donor (BDT) and acceptor (NT-Th/ThNTTh) with lowering of dihedral angle in case of P(BDT-ThNTTh) compared to P(BDT-NTTh) (model is a dimer).

TH-1906_11615303

5.2.5 Solar cell performance

Solar cell performance of synthesized 2D polymers a donor with $PC_{71}BM$ as acceptor have been studied with device geometry **ITO/PEDOT:PSS/Polymer/$PC_{71}BM$/LiF/Al**. **P(BDT-NTTh):$PC_{71}BM$** as active layer in 1:1 ratio showing a PCE of 0.34% (J_{sc} =2.04 mA/cm^2, V_{oc} = 0.67 V, FF = 25.2%). In similar device geometry **P(BDT-ThNTTh)** results a PCE of 0.7% with J_{sc} = 4.49 mA/cm^2, V_{oc} = 0.59 V, FF = 26.7%. Solar cell performance with **P(BDT-ThNTTh)** is superior to **P(BDT-NTTh)**, which is obvious due to high absorption coverage of solar spectrum with high absorption coefficient of **P(BDT-ThNTTh)** over **P(BDT-NTTh)** (Figure 5.3a) and blend film **P(BDT-ThNTTh):$PC_{71}BM$** has low roughness (Figure 5.6) along with higher hole-mobility (Figure 5.7) compared to **P(BDT-NTTh):$PC_{71}BM$**. With **P(BDT-ThNTTh)** a PCE of 1.31% have been achieved when blend of polymer and $PC_{71}BM$ was 1:1.5 respectively (Table 5.3, Figure 5.5a), which is due to increase in electron extraction of active layer with increasing $PC_{71}BM$ feed ratio, resulting superior PSC performance with current density 9.81 mA/cm^2, V_{oc} = 0.51 V and FF = 26.3%.[30]

On further increase in ratio to **P(BDT-ThNTTh):$PC_{71}BM$ (1:2)** no major change in PCE was observed but average PCE (average of three cells) of fabricated solar cell (Table 5.3) was superior (1.19%) compared to 1.10% in case of **P(BDT-ThNTTh):$PC_{71}BM$ (1:1.5).** Fill factor of all the fabricated devices were in range of 26%. Reason for Low FF and low PCE for fabricated devices are due to low molecular weight NT-based polymers caused due to steric congestion with in conjugation backbone leading to dihedral angle more than 40°.[17,18,31] Although PCE in case of **P(BDT-ThNTTh):$PC_{71}BM$ (1:2)** was not higher but maximum external quantum efficiency (EQE) was higher (15%) compared to **P(BDT-ThNTTh):$PC_{71}BM$ (1:1.5**) due to high loading of $PC_{71}BM$ having ultrafast electron mobility.[30] With **P(BDT-ThNTTh):$PC_{71}BM$ (1:1.5)** and **P(BDT-ThNTTh):$PC_{71}BM$ (1:1)** as active layer, maximum EQE value was 13% and 9% respectively (Table 5.3, Figure 5.5b), where as in case of **P(BDT-NTTh):$PC_{71}BM$ (1:1)** blend used for PSC it is lowest of all value (5%), indicating very low charge separation in active layer.

TH-1906_11615303

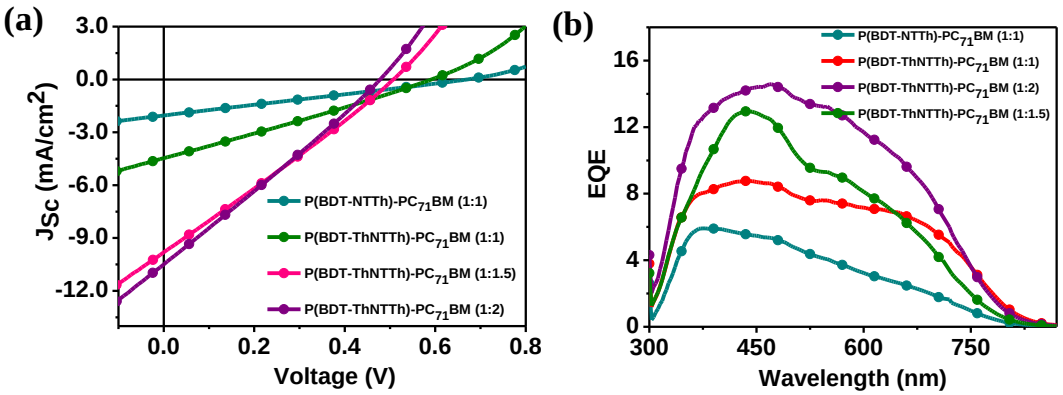

Figure 5.5 Solar cell performance of napthothiadiazole-based polymers, P(BDT-NTTh) and P(BDT-ThNTTh) (a) current density-voltage curve (b) external quantum efficiency (EQE).

Table 5.2 PSC parameters for devices with NT-based polymers as solar harvester.

Active layer	V_{oc} [Volt]	J_{sc} [mA/cm^2]	FF [%]	Max. PCE [Avg. PCE] %	EQE [%]
P11 : $PC_{71}BM$ (1: 1)-LiF/Al	0.67	2.04	25.2	0.34 [-]	5
P12 : $PC_{71}BM$ (1: 1)-LiF/Al	0.59	4.49	26.7	0.70 [0.64]	9
P12 : $PC_{71}BM$ (1: 1.5)-LiF/Al	0.51	9.81	26.3	1.31 [1.10]	13
P12 : $PC_{71}BM$ (1: 2)-LiF/Al	0.48	10.49	26.2	1.31 [1.19]	15

5.2.6 Morphology of active layer

Tapping mode AFM analysis has been performed to understand morphology of active layer for the fabricated solar cells with NT-based polymers (**P(BDT-NTTh)** and **P(BDT-ThNTTh).** Both the polymers exhibited homogeneous mixing with $PC_{71}BM$. **P(BDT-NTTh):PC_{71}BM (1:1)** showed large domain sized (Figure 5.6a)[32] long ordered film[33] with low (2.4 nm) root mean square (RMS) roughness. **P(BDT-ThNTTh):PC_{71}BM (1:1)** blend displayed better morphology (Figure 5.6b) compared to **P(BDT-NTTh):PC_{71}BM (1:1)** with lower RMS roughness of 1.6 nm and smaller aggregated states as well. In addition **P(BDT-ThNTTh):PC_{71}BM (1:2)** have similar morphology with close RMS roughness (1.5 nm) as like **P(BDT-ThNTTh):PC_{71}BM (1:1)** (Figure 5.6c). Moreover no distinguished phase separation (crtystallinity) between NT-based polymers and $PC_{71}BM$ was observed for the blend films (Figure 5.6a to 5.6c).[34] The reason for smaller

TH-1906_11615303

aggregation as can be seen from AFM images with dark depths on a homogeneous film[35] might be due to high surface energy[36] of blend film upon spin coating and absence of alkyl chain on the acceptor unit (NT-Th and Th-NT-Th) in both the CPs, which could have reduced the aggregation by virtue of improved solubility. The higher aggregation and roughness for **P(BDT-NTTh): $PC_{71}BM$ (1:1)** blend might be due to high dihedral angle along the polymer main chain leading to poor film forming ability and hence low PCE as well.[37]

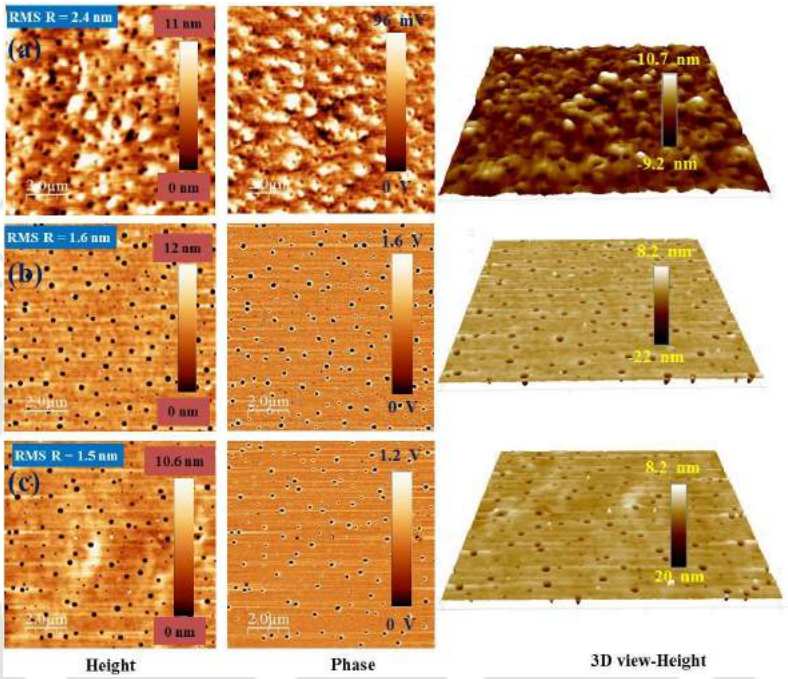

Figure 5.6 Morphology of active layer for fabricated PSC casted from chlorobenzene on pre-cleaned ITO substrate with tapping mode AFM image (10 μm X 10 μm) (height-left, phase-center, 3D view of height-right) (a) P(BDT-NTTh): $PC_{71}BM$ (1:1) (b) P(BDT-ThNTTh): $PC_{71}BM$ (1:1) (c) P(BDT-ThNTTh): $PC_{71}BM$ (1:2).

5.2.7 Hole-mobility of active layer

To compare change in mobility due to differences in dihedral angle within **P(BDT-NTTh)** and **P(BDT-ThNTTh)**, hole-mobility for blend of each polymer with $PC_{71}BM$ in 1:1 ratio have been calculated using SCLC method and Mott-Gurney relationship.[38,39] Fabricated hole only device configuration was **ITO/PEDOT:PSS/Polymer-$PC_{71}BM$ (1:1)/Cu** and resulted in mobility value of $2.2*10^{-6}$ and $1.5*10^{-5}$ cm^2 V^{-1} s^{-1} for **P(BDT-NTTh):$PC_{71}BM$ (1:1)** and **P(BDT-ThNTTh):$PC_{71}BM$ (1:1)** respectively (detail

TH-1906_11615303

procedure has been given in appendix A1). Dark current with forward bias characteristics for SCLC region were shown in Figure 5.7. Polymer **P(BDT-ThNTTh)** with low dihedral angle (42° between D and A unit) blend with $PC_{71}BM$ results higher hole-mobility compared to **P(BDT-NTTh)** with high dihedral angle (53^0 between D and A unit), due to better film forming property and low roughness of blend film (Figure 5.6).

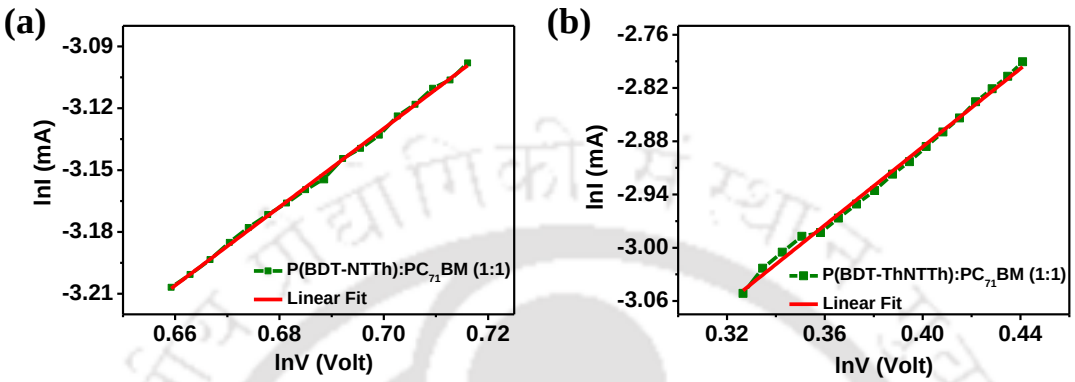

Figure 5.7 Determination of hole-mobility by SCLC method for blend of NT-based polymers and $PC_{71}BM$ (a) P(BDT-NTTh): $PC_{71}BM$ (1:1) (b) P(BDT-ThNTTh): $PC_{71}BM$ (1:1).

5.2.8 Thin film X-ray diffraction patterns

Thin film X-ray diffraction patterns study has been performed by spin coating equal concentration of both NT-based polymers on pre-cleaned galss slide, in order to determined π-π stacking distance in thin-film state. For both the polymers broad peak around $2\theta = 23.28^0$ was observed, confirming amorphous nature of both the NT-based polymeres and has similar π-π stacking distance[9] of 0.3817 nm (Figure 5.8).

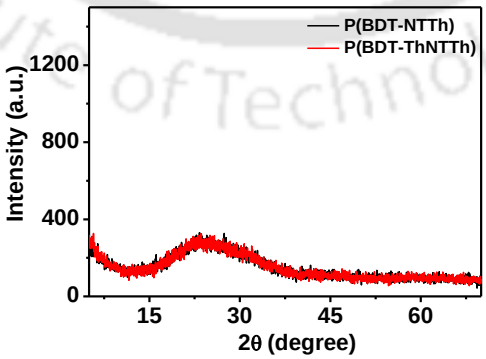

Figure 5.8 Thin film X-ray diffraction pattern study for newly synthesized NT-based polymers, P(BDT-NTTh) and P(BDT-ThNTTh).

TH-1906_11615303

5.3 Conclusion

In summary two new NT-based 2D acceptors (NT-Th and Th-NT-Th) has been synthesized via C=C bond formation at 5,6-position of BT using Witting reaction. With BDT as donor D-A polymers namely **P(BDT-NTTh)** and **P(BDT-ThNTTh)** have been synthesized. NT-based 2-D polymers are thermally stable up to 250 °C, well soluble in common organic solvents ($CHCl_3$, CB, DCB, THF) used for device fabrication and have good film forming property as well. NT as an acceptor unit have good ICT with commonly used donor BDT with polymers showing absorption maxima in the near 700 nm (an area of maximum solar photo flux) makes this acceptor very promising for polymer based solar cell application. When fabricated as solar harvesting polymer with $PC_{71}BM$ as acceptor, a PCE of 1.31% with **P(BDT-ThNTTh)** and 0.34% with **P(BDT-NTTh)** has been achieved. This NT derivative along with other synthetic unit gives possibility to modify it to newer derivatives and suitable selection of π-electron donor will open innovative pathway to synthesize new monomers and polymers for solar cell and other optoelectronic applications.

5.4 Experimental procedure

Detail reaction scheme for synthesis of all monomers and polymers shown in Figure 5.1

5.4.1 Synthetic procedures

4,7-Dibromo-5,6-bis(bromomethyl)benzo[c][1,2,5]thiadiazole (4b):

Synthetic procedure for monomer **4b** has been as mentioned in chapter 4.

((4,7-Dibromobenzo[c][1,2,5]thiadiazole-5,6-diyl)bis(methylene))bis(triphenylphosphonium) bromide (5a): Monomer **4b** (1.3 g, 2.71 mmol) and triphenylphosphine (2.84 g, 10.84 mmol) were dissolved in toluene and then refluxed at 110 ^{0}C for 55 hours. It was cooled to RT, filtered, dried and then the residue was dissolved in a boiling ethanol and kept for precipitation in deep freeze. White colored compound will precipitate out with a yield of 70%. ^{1}H-NMR (400 MHz, $CDCl_3$, δ in ppm): 8.15-8.09 (m, 6H), 7.67-7.56 (m, 9H), 5.44 (d, 2H). ^{13}C-NMR (150 MHz, $CDCl_3$, δ in ppm): 151.26 (s), 135.21 (s), 134.37 (d), 133.54 (s) 130.75 (d), 118.92 (s), 118.05 (s), 117.52 (s), 34.70 (d, J = 46.5 Hz).

TH-1906_11615303

4,9-Dibromo-6,7-di(thiophen-2-yl)naphtho[2,3-c][1,2,5]thiadiazole (NT-Th, 5b): Monomer **5a** (0.15 g, 0.149 mmol), 2,2´-thenil (0.33 g, 3.98 mmol) were dissolved in 3 ml of chloroform. Potassium tertiary butoxide (0.166 g, 1.49 mmol) dissolved in 1 ml of dry ethanol was added drop wise into it, with continuous stirring and followed by addition of another 15 ml of ethanol into the reaction mixture. Reaction mixture was stirred for another 3 hours at room temperature followed by extraction with chloroform and water. Later organic phase was dried in vacuum followed by column chromatography (SiO_2, using 15% $CHCl_3$ in hexane). Pure reddish solid product (**NT-Th, 5b**) can be recovered as 32% yield (23 mg) by washing with hexane two times and collecting the insoluble part. ^{1}H-NMR (600 MHz, $CDCl_3$, δ in ppm): 8.51 (s, 2H), 7.43-7.42 (m, 2H), 7.08-7.07 (m, 4H). ^{13}C-NMR (75 MHz, $CDCl_3$, δ in ppm): 150.92, 140.92, 135.39, 132.30, 129.28, 128.34, 127.34, 127.26, 112.58. MALDI-TOF: m/z $[M]^+$ calcd for $C_{18}H_8Br_2N_2S_3$ 507.82, found 507.38

4,7-Bis(5-bromothiophen-2-yl)-5,6-dimethylbenzo[c][1,2,5]thiadiazole (4g)

Synthesis of monomer **4g** was discussed in chapter 4.

5,6-Bis(bromomethyl)-4,7-bis(5-bromothiophen-2-yl)benzo[c][1,2,5]thiadiazole (5c). Monomer **5c** was synthesized as like monomer **4b,** by using monomer **4g** (0.55 g, 1.13 mmol), NBS (0.9 g, 5.1 mmol) and 0.112 g (0.027 mmol) of benzoyl peroxide. The reaction mixture after chromatographic purification (SiO_2, 10% $CHCl_3$ in hexane) provides compound **5c** 0.7 g (deep yellow colored solid) with a yield of 92%. ^{1}H-NMR (600 MHz, $CDCl_3$, δ in ppm): 7.33-7.32 (d, 2H), 7.24-7.23 (d, 2H), 4.96 (s, 4H). ^{13}C-NMR (75 MHz, $CDCl_3$, δ in ppm): 154.08, 137.24, 136.00, 130.15, 129.87, 128.54, 115.49, 28.39. HRMS (ESI): m/z $[M+H]^+$ calcd for $C_{16}H_8Br_4N_2S_3$ 644.65, found 644.47.

((4,7-Bis(5-bromothiophen-2-yl)benzo[c][1,2,5]thiadiazole-5,6-diyl)bis(methylene))bis(triphenylphosphonium) bromide (5d). Wittig salt **5d** was synthesized following procedure used for synthesis of Wittig salt **5a** and using monomer **5c** (0.7 g, 1.086 mmol) and triphenylphosphine (1.14 g, 4.34 mmol). The product was yellow colored with yield of 70% (0.9 g). ^{1}H-NMR (600 MHz, $CDCl_3$, δ in ppm): 7.87-7.83 (m, 12H), 7.66-7.64 (m, 6H), 7.54-7.52 (m, 18H), 7.27-7.26 (d, 2H), 7.19-7.18 (d, 2H), 6.45 (t, 2H), 4.14 (t, 2H). ^{13}C-NMR (75 MHz, $CDCl_3$, δ in ppm): 135.49, 134.48,

TH-1906_11615303

133.59, 133.45, 131.70, 131.55, 130.64, 130.46, 128.77, 128.69, 117.87, 116.83, 116.75, 29.50, 28.90.

4,9-Bis(5-bromothiophen-2-yl)-6,7-di(thiophen-2-yl)naphtho[2,3-c][1,2,5]thiadiazole (Th-NT-Th). Acceptor **Th-NT-Th** was synthesized as like monomer **NT-Th** by using Wittig salt **5d** (0.15 g, 0.128 mmol) and 2,2′-thenil (0.0285 g, 0.1284 mmol). The crude product was purified with column chromatographic technique (SiO_2, 15% $CHCl_3$ in hexane). Pure wine colored solid product can be recovered as 32% yield (28 mg) by washing with hexane two times and collecting the insoluble part. ^{1}H-NMR (600 MHz, $CDCl_3$, δ in ppm): 8.49 (s, 2H), 7.34-7.33 (d, 2H), 7.31-7.29 (m, 4H), 7.01-7.0 (d, 2H), 6.95-6.94 (d, 2H). ^{13}C-NMR (75 MHz, $CDCl_3$, δ in ppm): 151.70, 141.60, 137.54, 133.79, 131.68, 131.06, 130.31, 128.32, 127.99, 127.26, 126.79, 122.55, 115.54. MALDI-TOF: m/z $[M]^+$ calcd for $C_{26}H_{12}Br_2N_2S_5$ 671.80, found 672.185.

General synthetic procedure used for polymerization

For synthesis of polymer P(BDT-NTTh) and P(BDT-ThNTTh) similar procedure of polymerization was followed as like in chapter 4.

Polymer P(BDT-NTTh): It was synthesized using monomer **BDT** (0.811 g, 0.1047 mmol), monomer **NT-Th** (0.053 g, 0.1047 mmol) and $Pd(PPh_3)_4$ (24 mg, 0.0209 mmol). **P(BDT-NTTh** was formed as greenish black colored powder (75 mg, yield 90%). ^{1}H-NMR (600 MHz, $CDCl_3$, δ in ppm): 8.67-8.58 (br, 2H), 8.0-7.94 (br, 1H), 7.72-7.58 (br, 1H), 7.49-7.38 (br, 1H), 7.27-7.20 (br, 2H), 7.08-6.98 (br, 1H), 6.95-6.89 (br, 2H), 4.40-4.25 (br, 4H), 1.90-1.79 (br, 2H), 1.55-1.47 (br, 4H), 1.47-1.40 (br, 12H), 0.99-0.88 (br, 12H). ^{13}C-NMR (150 MHz, $CDCl_3$, δ in ppm): 152.12, 144.78, 141.82, 139.21, 136.36, 133.85, 132.09, 131.29, 128.80, 128.03, 127.54, 127.28, 126.61, 124.64, 123.97, 123.52, 119.12, 118.29, 115.92, 76.55, 40.69, 30.46, 29.22, 23.89, 23.14, 14.14, 11.39. GPC: M_n = 5657 g/mol.; M_w = 7393 g/mol.; PDI = 1.3; degree of polymerization, n = 7.

Polymer P(BDT-ThNTTh): It was synthesized using monomer **BDT** (0.953 g, 0.13 mmol), monomer **Th-NT-Th** (0.0828 g, 0.13 mmol) and $Pd(PPh_3)_4$ (28.4 mg, 0.0246 mmol). **P(BDT-ThNTTh)** was formed as deep-green colored powder (100 mg, yield 90%). ^{1}H-NMR (600 MHz, $CDCl_3$, δ in ppm): 8.61-8.42 (br, 2H), 7.7-7.22 (br, 10H), 6.98-6.90 (br, 2H), 4.20-4.12 (br, 4H), 1.85-1.74 (br, 2H), 1.52-1.44 (br, 4H), 1.44-1.28

TH-1906_11615303

(br, 12H), 1.10-0.88 (br, 12H). ^{13}C-NMR (150 MHz, $CDCl_3$, δ in ppm): 149.17, 141.71, 139.44, 138.06, 133.82, 131.08, 129.46, 129.18, 126.92, 126.45, 126.24, 126.02, 125.94, 125.47, 124.76, 124.17, 123.06, 121.89, 120.96, 120.13, 115.59, 114.17, 113.20, 73.65, 38.18, 27.83, 26.74, 21.35, 20.64, 11.70, 8.85. GPC: M_n= 9544 g/mol.; M_w = 11116 g/mol.; PDI = 1.16; degree of polymerization, n = 9.

5.4.2 Methods, procedure and spectra

Device fabrication procedure and method of UV-visible spectra and cyclic voltammetry were given in Appendix A1. NMR spectra of all monomers and polymer synthesized and GPC spectra have been given in appendix A5.

TH-1906_11615303

5.5 References

1. Wang, E.; Hou, L.; Wang, Z.; Hellström, S.; Zhang, F.; Inganäs, O.; Andersson, M. R. *Adv. Mater.* **2010**, *22*, 5240-5244.
2. Zhou, E.; Cong, J.; Hashimoto, K.; Tajima, K. *Macromolecules* **2013**, *46*, 763-768.
3. Li, Z.; Tsang, S. W.; Du, X.; Scoles, L.; Robertson, G.; Zhang, Y.; Toll, F.; Tao, Y.; Lu, J.; Ding, J. *Adv. Funct. Mater.* **2011**, *21*, 3331-3336.
4. Zhang, M.; Guo, X.; Wang, X.; Wang, H.; Li, Y. *Chem. Mater.* **2011**, *23*, 4264-4270.
5. Keshtov, M. L.; Khokhlov, A. R.; Kuklin, S. A.; Chen, F. C.; Koukaras, E. N.; Sharma, G. D. *ACS Appl. Mater. Interfaces* **2016**, *8*, 32998-33009.
6. Wang, M.; Cai, D.; Yin, Z.; Chen, S. C.; Du, C. F.; Zheng, Q. *Adv. Mater.* **2016**, *28*, 3359-3365.
7. Dou, L.; Chen, C. C.; Yoshimura, K.; Ohya, K.; Chang, W. H.; Gao, J.; Liu, Y.; Richard, E.; Yang, Y. *Macromolecules* **2013**, *46*, 3384-3390.
8. Wang, J.; Bao, X.; Ding, D.; Qiu, M.; Du, Z.; Wang, J.; Liu, J.; Sun, M.; Yang, R. *J. Mater. Chem. A* **2016**, *4*, 11729-11737.
9. Zhao, X.; Qian, L.; Cao, J.; Yan, S.; Ding, L. *Polym. Chem.* **2016**, *7*, 1226-1229.
10. Yang, D.; Li, Z.; Li, Z.; Zhao, X.; Zhang, T.; Wu, F.; Tian, Y.; Ye, F.; Sun, Z.; Yang, X. *Polym. Chem.* **2017**, *8*, 4332-4338.
11. Wang, M.; Hu X.; Liu, P.; Li, W.; Gong, X.; Huang, F.; Cao, Y. *J. Am. Chem. Soc.* **2011**, *133*, 9638-9641.
12. Zheng, Z.; Awartani, O. M.; Gautam, B.; Liu, D.; Qin, Y.; Li, W.; Bataller, A.; Gundogdu, K.; Ade, H.; Hou, J. *Adv. Mater.* **2017**, *29*, 1604241.
13. Gu, Z.; Shen, P.; Tsang, S. W.; Tao, Y.; Zhao, B.; Tang, P.; Nie, Y.; Fang, Y.; Tan, S. *Chem. Commun.* **2011**, *47*, 9381-9383.
14. Liu, C.; Yi, C.; Wang, K.; Yang, Y.; Bhatta, R. S.; Tsige, M.; Xiao, S.; Gong, X. *ACS Appl. Mater. Interfaces* **2015**, *7*, 4928-4935.
15. Peng, Q.; Lim, S. L.; Wong, I. H. K.; Xu, J.; Chen, Z. K. *Chem. Eur. J.* **2012**, *18*, 12140-12151.
16. Lee, J.; Kim, J. H.; Moon, B.; Kim, H. G.; Kim, M.; Shin, J.; Hwang, H.; Cho, K. *Macromolecules* **2015**, *48*, 1723-1735.
17. Kim, J.; Yun, M. H.; Kim, G. H.; Kim, J. Y.; Yang, C. *Polym. Chem.* **2012**, *3*, 3276-3281.
18. Nakanishi, T.; Shirai, Y.; Han, L. *J. Mater. Chem. A* **2015**, *3*, 4229-4238.

TH-1906_11615303

19. Yen, Y. S.; Ni, J. S.; Hung, W. I.; Hsu, C. Y.; Chou, H. H.; Lin, J. T. *ACS Appl. Mater. Interfaces* **2016**, *8*, 6117-6126.
20. Guo, X.; Qin, C.; Cheng, Y.; Xie, Z.; Geng, Y.; Jing, X.; Wang, F.; Wang, L. *Adv. Mater.* **2009**, *21*, 3682-3688.
21. Liu, T.; Zhu, L.; Zhong, C.; Xie, G.; Gong, S.; Fang, J.; Ma, D.; Yang, C. *Adv. Funct. Mater.* **2017**, *27*, 1606384.
22. Zhang, M.; Xue S.; Dong, W.; Wang, Q.; Fei, T.; Gu, C.; Ma, Y. *Chem. Commun.* **2010**, *46*, 3923-3925.
23. Zhou, E.; Cong, J.; Yamakawa, S.; Wei, Q.; Nakamura, M.; Tajima, K.; Yang, C.; Hashimoto, K. *Macromolecules* **2010**, *43*, 2873-2879.
24. Gadisa, A.; Mammo, W.; Andersson, L. M.; Admassie, S.; Zhang, F.; Andersson, M. R.; Inganäs, O. *Adv. Funct. Mater.* **2007**, *17*, 3836-3842.
25. Keshtov, M. L.; Khokhlov, A. R.; Kuklin, S. A.; Ostapov, I. E.; Nikolaev, A. Y.; Konstantinov, I. O.; Sharma, A.; Koukaras, E. N.; Sharma, G. D. *Polym. Chem.* **2016**, *7*, 5849-5861.
26. Zhou, P.; Yang, Y.; Chen, X.; Zhang, Z. G.; Li, Y. *J. Mater. Chem. C* **2017**, *5*, 2951-2957.
27. Park, G. E.; Kim, H. J.; Lee, D. H.; Cho, M. J.; Choi, D. H. *Polym. Chem.* **2016**, *7*, 5069-5078.
28. Huang, Y.; Liu, F.; Guo, X.; Zhang, W.; Gu, Y.; Zhang, J.; Han, C. C.; Russell, T. P.; Hou, J. *Adv. Energy Mater.* **2013**, *3*, 930-937.
29. Duan, X.; Xiao, M.; Chen, J.; Wang, X.; Peng, W.; Duan, L.; Tan, H.; Lei, G.; Yang, R.; Zhu, W. *ACS Appl. Mater. Interfaces* **2015**, *7*, 18292-18299.
30. Lee, J.; Sin, D. H.; Clement, J. A.; Kulshreshtha, C.; Kim, H. G.; Song, E.; Shin, J.; Hwang, H.; Cho, K. *Macromolecules* **2016**, *49*, 9358-9370.
31. Li, S.; Zhao, B.; He, Z.; Chen, S.; Yu, J.; Zhong, A.; Tang, R.; Wu, H.; Li, Q.; Qin, J.; Li, Z. *J. Mater. Chem. A* **2013**, *1*, 4508-4515.
32. Li, S.; Yuan, Z.; Yuan, J.; Deng, P.; Zhang, Q.; Sun, B. *J. Mater. Chem. A* **2014**, *2*, 5427-5433.
33. Lee, J.; Sin, D. H.; Moon, B.; Shin, J.; Kim, H. G.; Kim, M.; Cho, K. *Energy Environ. Sci.* **2017**, *10*, 247-257.
34. Dang, D.; Zhou, P.; Duan, L.; Bao, X.; Yang, R.; Zhu, W. *J. Mater. Chem. A* **2016**, *4*, 8291-8297.

TH-1906_11615303

35. Wang, J. L.; Liu, K. K.; Yan, J.; Wu, Z.; Liu, F.; Xiao, F.; Chang, Z. F.; Wu, H. B.; Cao, Y.; Russell, T. P. *J. Am. Chem. Soc.* **2016**, *138*, 7687-7697.
36. Li, Z.; Lu, J.; Tse, S. C.; Zhou, J.; Du, X.; Tao, Y.; Ding, J. *J. Mater. Chem.* **2011**, *21*, 3226-3233.
37. Zhang, Z.; Liu, Y.; Zhang, J.; Feng, S.; Wu, L.; Gong, X.; Xu, X.; Chen, X.; Bo, Z. *ACS Appl. Mater. Interfaces* **2017**, *9*, 23775-23781.
38. Kang, Z.; Chen, S. C.; Ma, Y.; Wang, J.; Zheng, Q. P. *ACS Appl. Mater. Interfaces* **2017**, *9*, 24771-24777.
39. Zhang, Z.; Liu, W.; Rehman, T.; Ju, H. X.; Mai, J.; Lu, X.; Shi, M.; Zhu, J.; Li, C. Z.; Chen, H. *J. Mater. Chem. A* **2017**, *5*, 9649-9654.

TH-1906_11615303

A1.1 Device fabrication method for polymer solar cell

Chapter 2

Solar cells were fabricated for the polymers in the configuration of **Glass/ITO/PEDOT: PSS/Active Layer (P1 or P2 and PCBM)/Al or Ca: Al.** ITO coated glass was etched with Zn dust and dilutes HCl (1:1), then ITO substrates were cleaned by sonicating for 15 minute with detergent solution in Mili-Q water, followed by sonication in Mili-Q water, acetone, and isopropyl alcohol. After the substrate cleaning, the substrates were dried under argon and treated using oxygen plasma cleaner for 20 minute. As a buffer layer, the conductive polymer PEDOT:PSS (filtered through 0.45 µm nylon filters) was spin-coated onto ITO-coated glass substrates at 3000 rpm for 60 s using ~200 µL of solution (thickness ~40 nm) followed by annealing in vacuum at 150 °C for 30 minute to remove water.

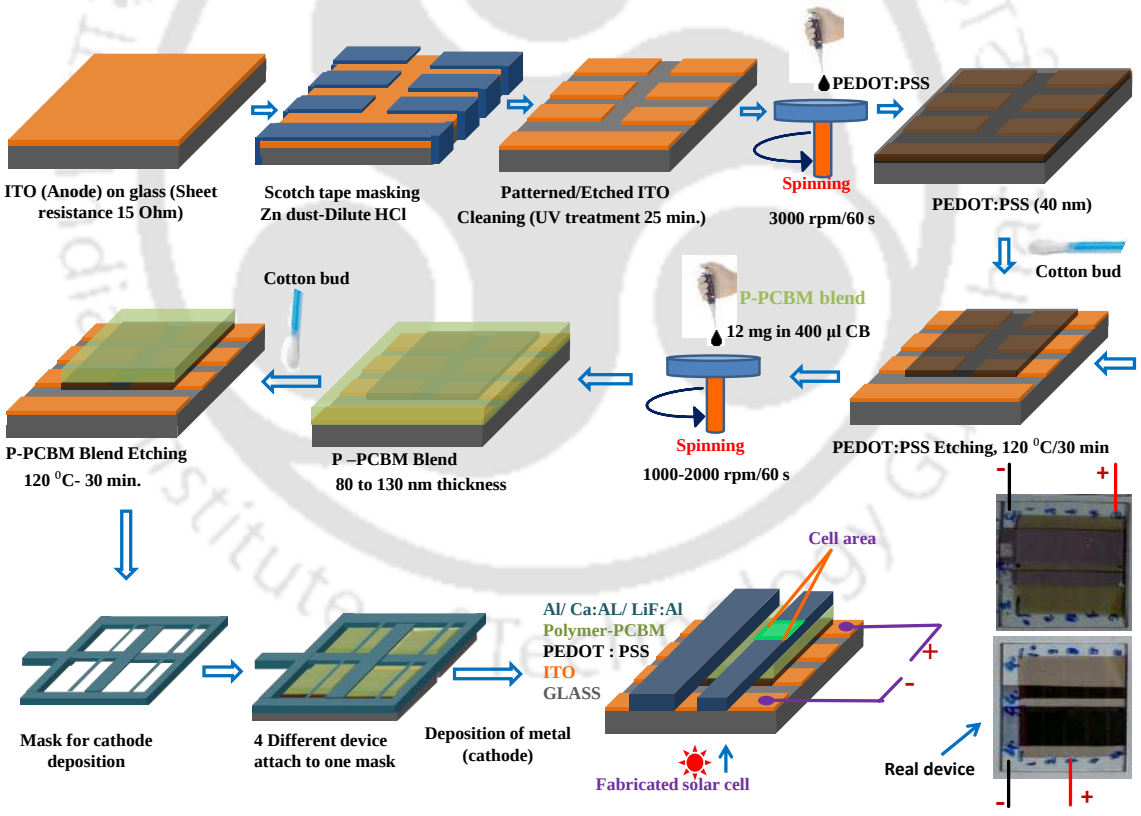

Figure A1.1 Solar cell fabrication methods.

Inside the glove box, the (w/w) ratio of (concentration 12mg/ 400 µL) polymer:PCBM respectively were dissolved in chlorobenzene 24 hours prior to device fabrication. Active layers were deposited (filtered through a 0.45 µm PTFE filter) on top of the PEDOT:PSS

TH-1906_11615303

layer by spin-coating (1000-2500 rpm) for 60 s (the thickness of the blend films ranged from 80 to 110 nm. Al (80-100 nm) was evaporated on top of the active layers to form the top electrode, i.e., the cathode under pressure of $1*10^{-6}$ mbar. The active areas of the devices were 20 mm^2 in general and we the cell size was reduced to to 8 mm^2 to achieve a PCE of 0.15 in P2. In case of devices with Ca-Al as cathode, Ca was deposited 20 nm and then 75 nm-thickness Al was deposited on top of calcium for both the polymers. The cell size in case of device with Ca-Al as cathode was 6 mm^2. Fabricated solar cell was tested under simulated air mass (AM) 1.5 solar irradiation (100 mW cm^{-2}) inside the glove box. The photovoltaic cells with no protective encapsulation were removed from glove box for EQE measurement.

Chapter 4

Here **Glass/ITO/PEDOT:PSS/Active Layer(Polymer and $PC_{71}BM$)/LiF-Al** were taken as standard to fabricated polymer solar cell for all synthesized methyl ester substitutes polymers and their results have been compared with their methyl counterpart. Similar device configuration and method has been used as like chapter 3. As cathode LiF 1 nm and Al (80 nm) was evaporated using a thermal evaporator one after another respectively. In case of devices fabricated with additives (1,8-diiodooctane), 3% volume ratio with respect to the active layer was added prior deposition of active layer.

Chapter 5

Solar cells were fabricated for NT-based polymers in chapter 5 with device configuration **Glass /ITO/PEDOT:PSS/Active Layer(polymer and $PC_{71}BM$)/LiF:Al** and following similar device configuration and method as like chapter 4.

A1.2 Absorbance Spectra

Solid state UV-visible analysis were carried out with films prepared by drop coating (spin coating in case of P1) from chlorobenzene (CB) solutions of polymers on precleaned glass substrates and were dried on a hot plate upto 110 ^{0}C for 1 hour.

A1.3 Cyclic voltammetry

Electrochemical measurements were carried out using a CH instrument Model 700D with polymer film coated on a glassy carbon working electrode. Platinum wire was used as a

TH-1906_11615303

counter electrode, Ag/Ag^{+} (0.01M $AgNO_3$) as a reference electrode and ferrocene/ferrocenium ion (Fc/Fc^{+}) as the internal standard. These experiments were carried out under argon atmosphere in a solution of tetra-n-butyl ammonium perchlorate (0.1M) in acetonitrile. Both oxidation and reduction potentials were determined from the intersection of two tangents drawn at the rising and background currents of the cyclic voltammogram. Using the formulae $E_{HOMO} = -e({}_{onset}E^{ox} - E_{1/2}(Ferrocene)+4.8)$ and $E_{LUMO} = -e({}_{onset}E^{red} - E_{1/2}(Ferrocene)+4.8)$ with $E_{1/2}$ of ferrocene determined from voltammogram (as $(E_{cathodic} + E_{anodic})/2$),[1] highest occupied molecular orbital (HOMO) and lowest unoccupied molecular orbital (LUMO) energy levels of the polymers have been estimated . $LUMO^{opttical}$ have been calculated from absorption onset using the fromula $E_{LUMO(optical)} = E_{HOMO} +$ Bandgap (where band gap = $1240/ \lambda_{onset\ film\ (UV\text{-}visible)}$).

A1.4 SCLC method for determination of hole-mobility

Hole mobility was measured using the space charge limited current model (SCLC), using a diode configuration of ITO/PEDOT:PSS/Polymer:$PC_{70}BM$(1:1)Cu, and taking current-voltage measurements in the range of 0-10 V in the dark. The SCLC mobilities were estimated by fitting the results to Mott-Gurney relationship [$J = (9/8)\varepsilon_0\varepsilon r\mu(V^2/L^3)$] in the conduction region of the dark current(J)-voltage (V) curve.

where ε_0 is the permittivity of free space (8.85×10^{-12} F m^{-1}), ε_r is the dielectric constant of the active layer material (assumed to be 3, which is a typical value for organic semiconductors), μ is the hole mobility, V is the voltage drop across the device and the L is the active layer thickness.[2,3]

A.1.5 References

1. Liu, J.; Zhou, Q.; Cheng, Y.; Geng, Y.; Wang, L.; Ma, D.; Jing, X.; Wang, F. *Adv. Funct. Mater.* **2006**, *16*, 957-965.
2. Kang, Z.; Chen, S. C.; Ma, Y.; Wang, J.; Zheng, Q. *ACS Appl. Mater. Interfaces*, **2017**, *9*, 24771-24777.
3. Wu, J.; Chen, J.; Huang, Hao.; Li, S.; Wu, H.; Hu, C.; Tang, J.; Zhang, Q. *Macromolecules* **2016**, *49*, 2145-2152.

TH-1906_11615303

1. Energy level band diagram for charge transfer in ternary composite.

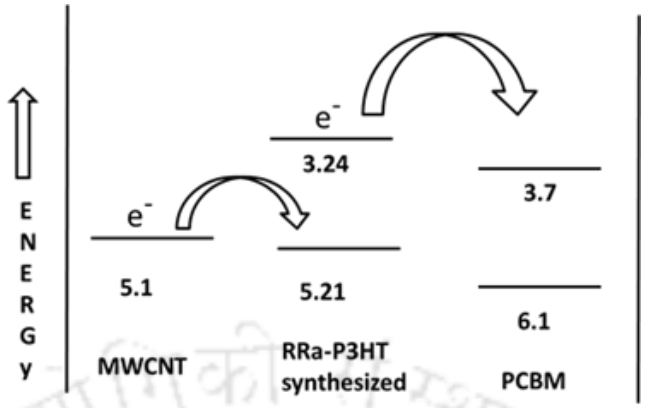

Figure A2.1. Energy level diagram for P3HT, $PC_{61}BM$ and MWCNT.

2. PL spectra of pure P3HT recorded in the same conditions (before and after irradiation).

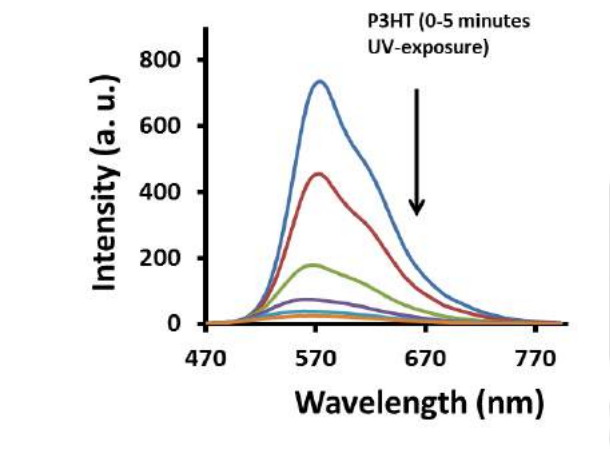

Figure A2.2. Pl quenching experiment for P3HT in air, from 0-5 minute UV-exposure.

TH-1906_11615303

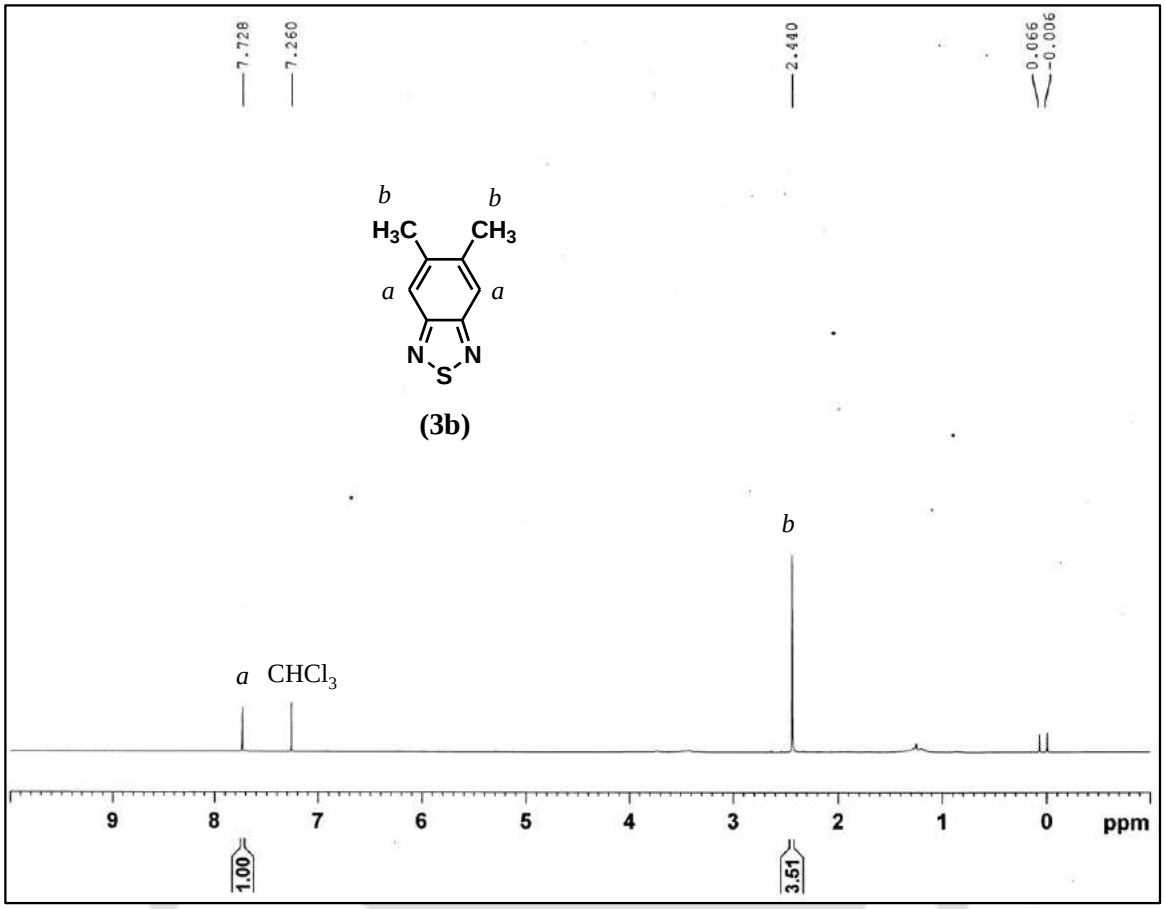

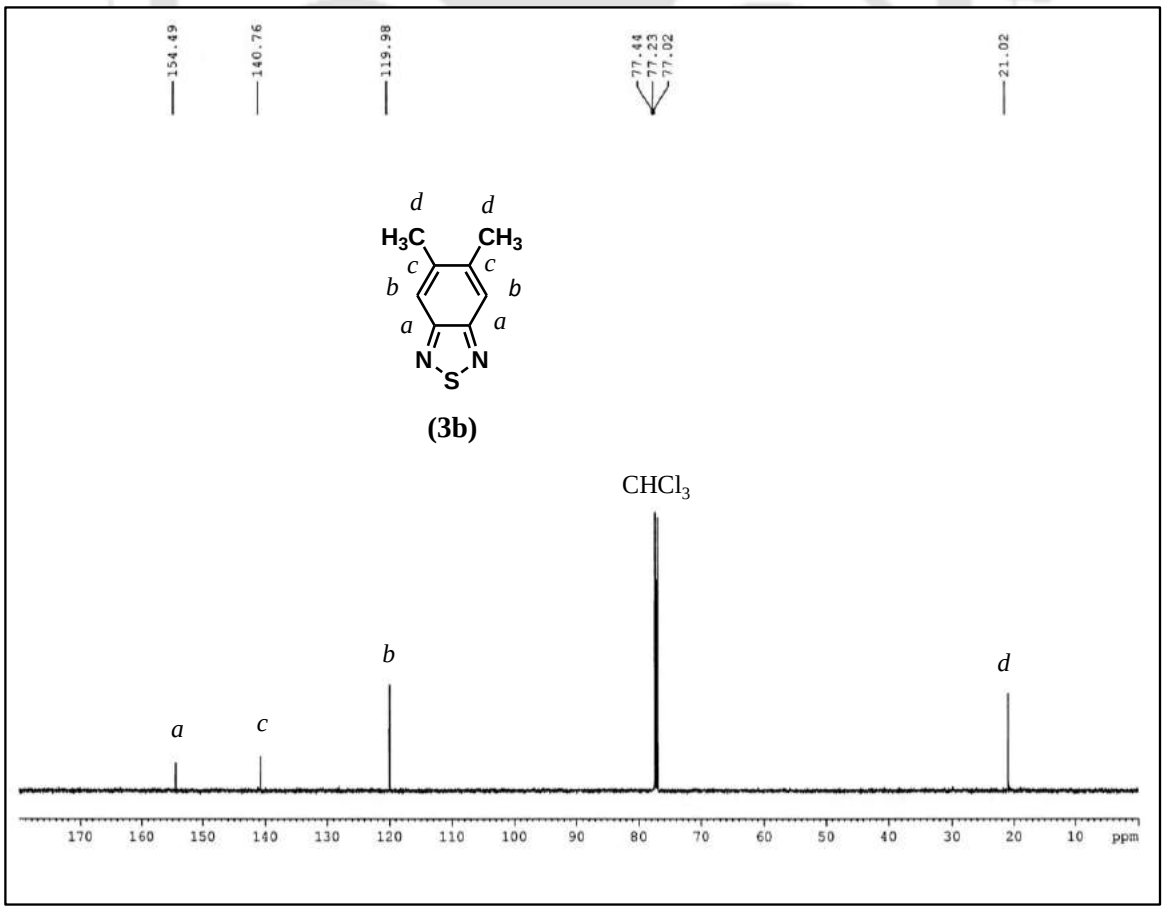

TH-1906_11615303

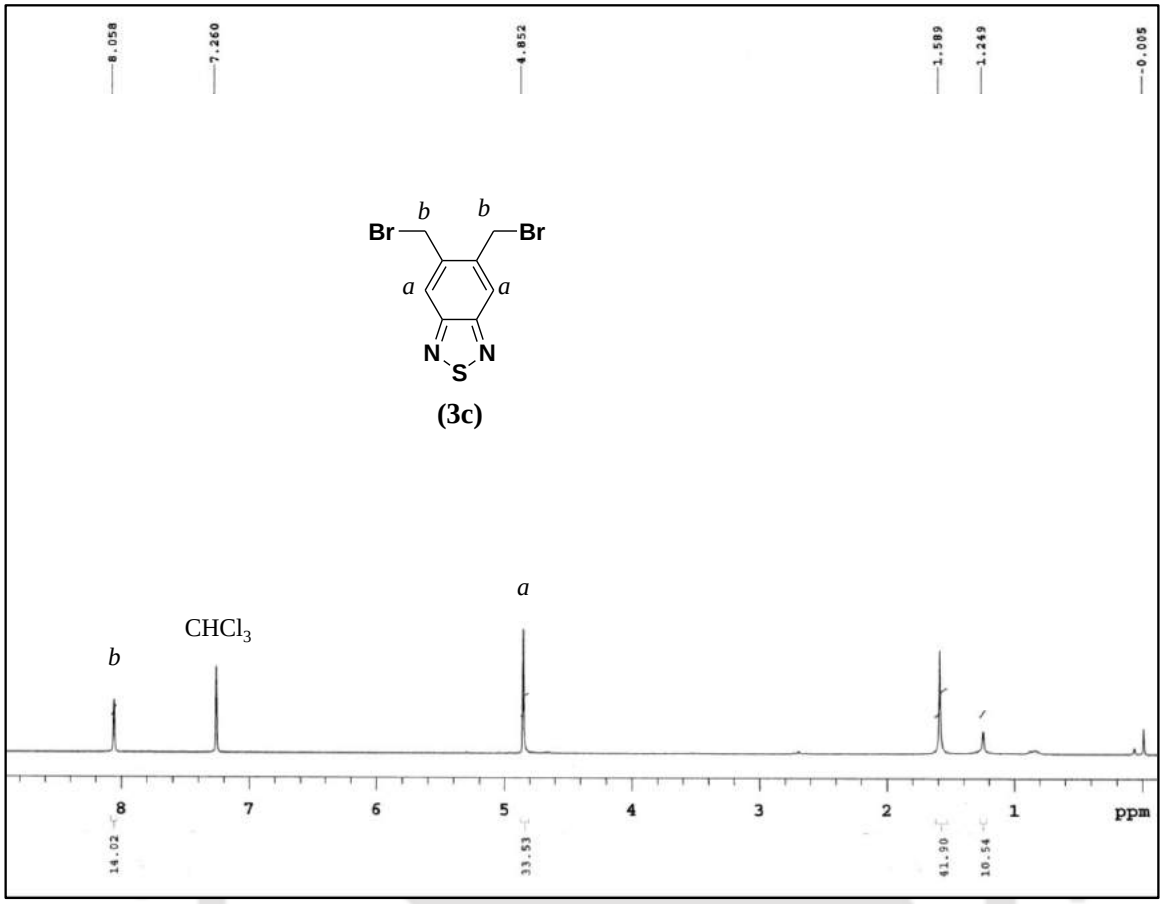

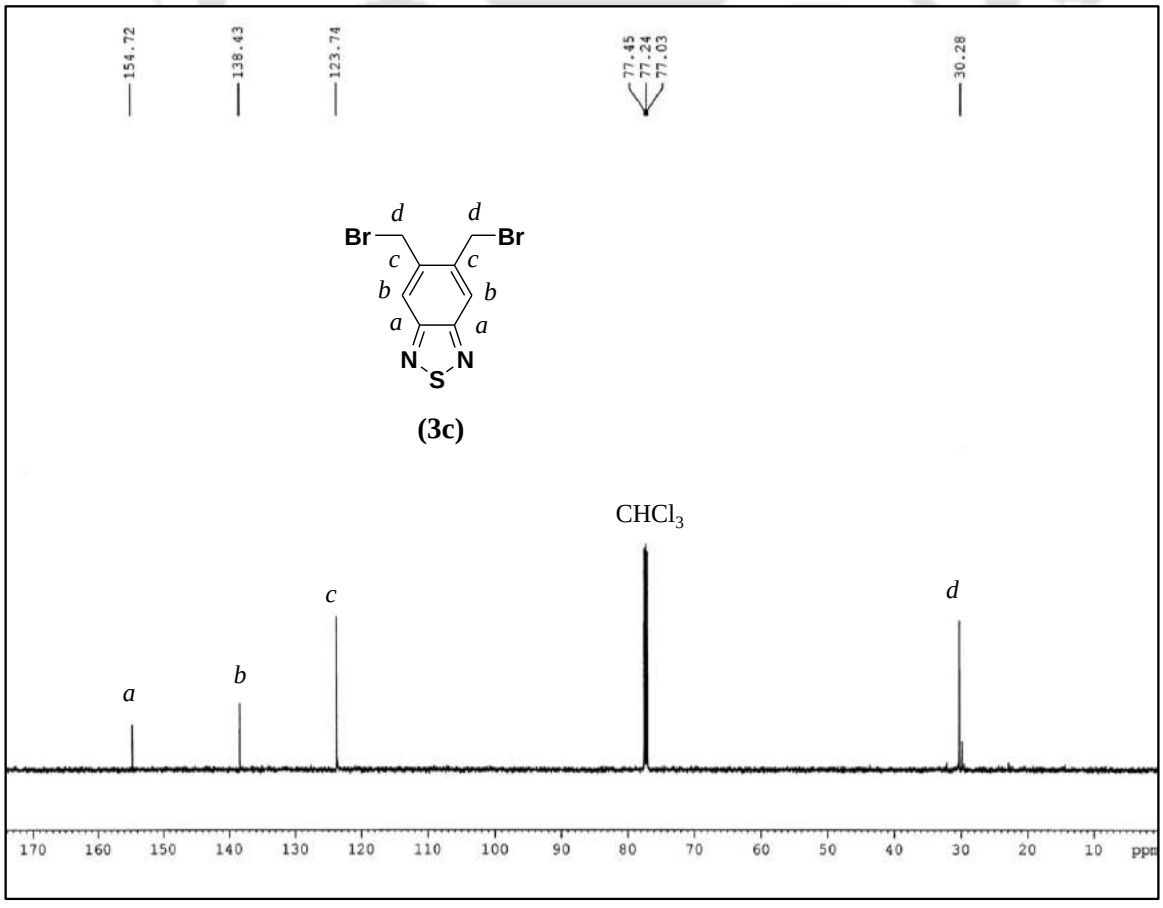

TH-1906_11615303

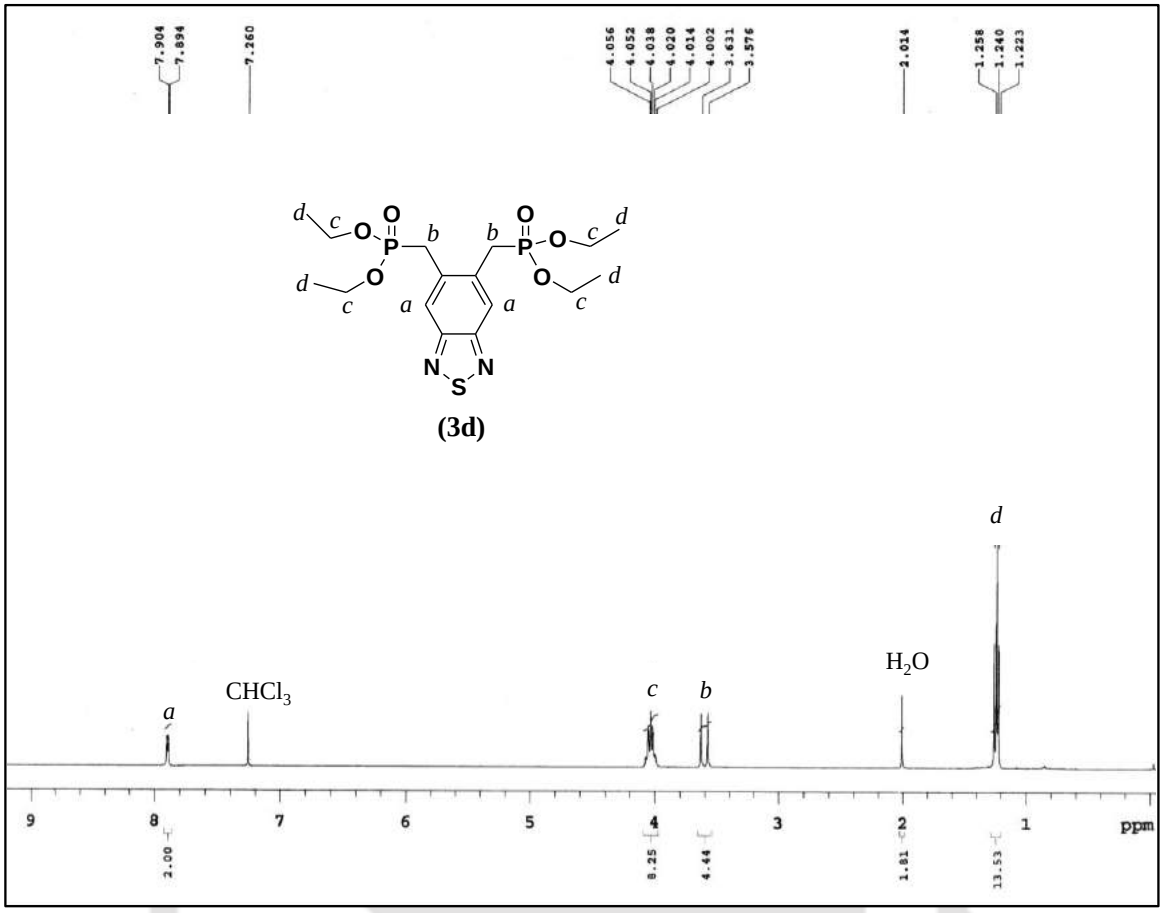

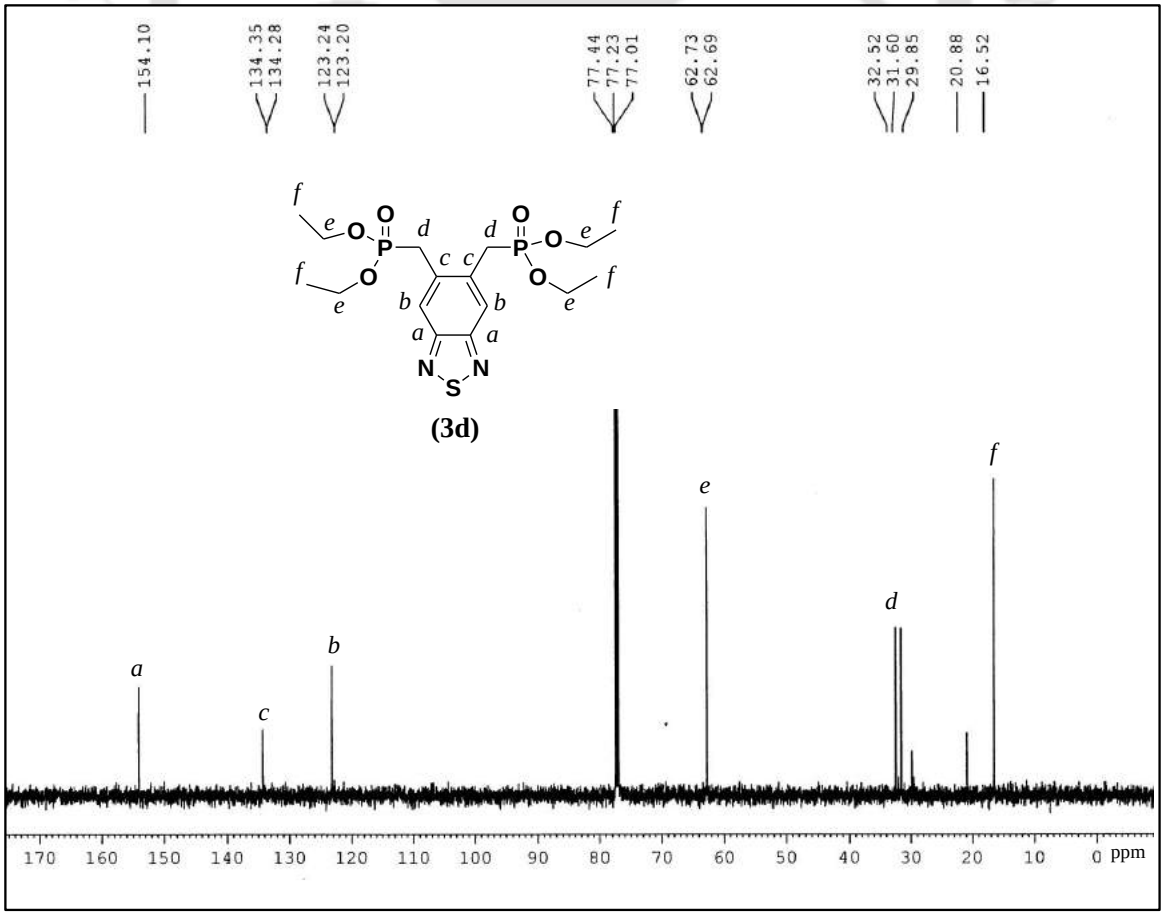

TH-1906_11615303

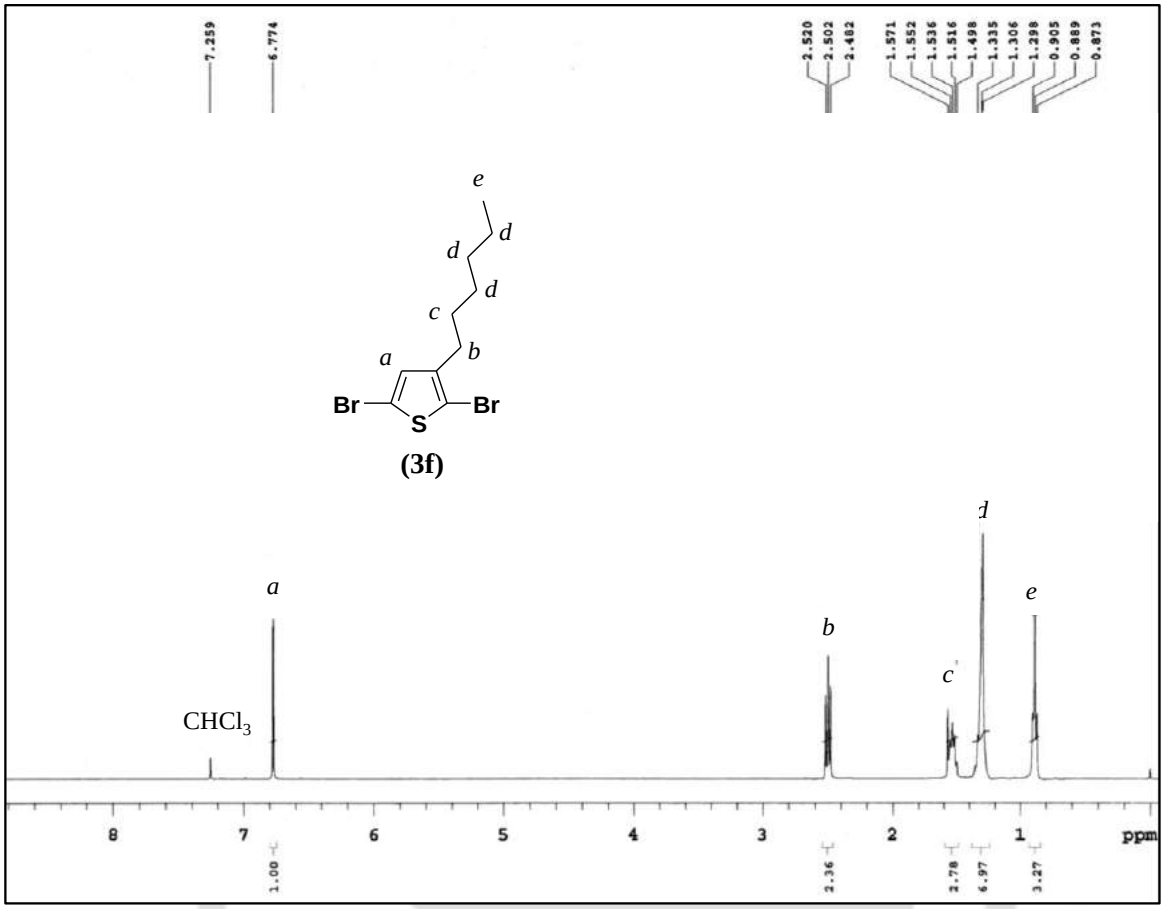

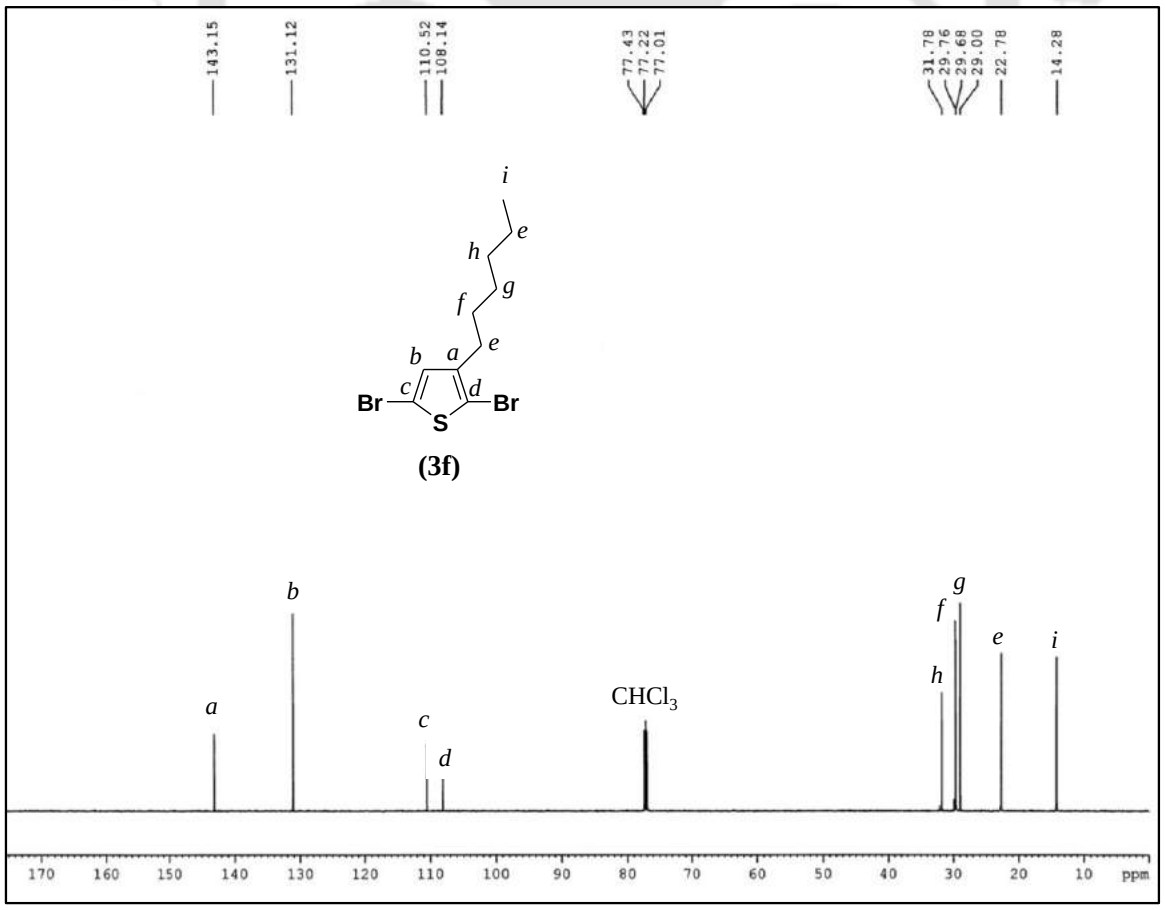

TH-1906_11615303

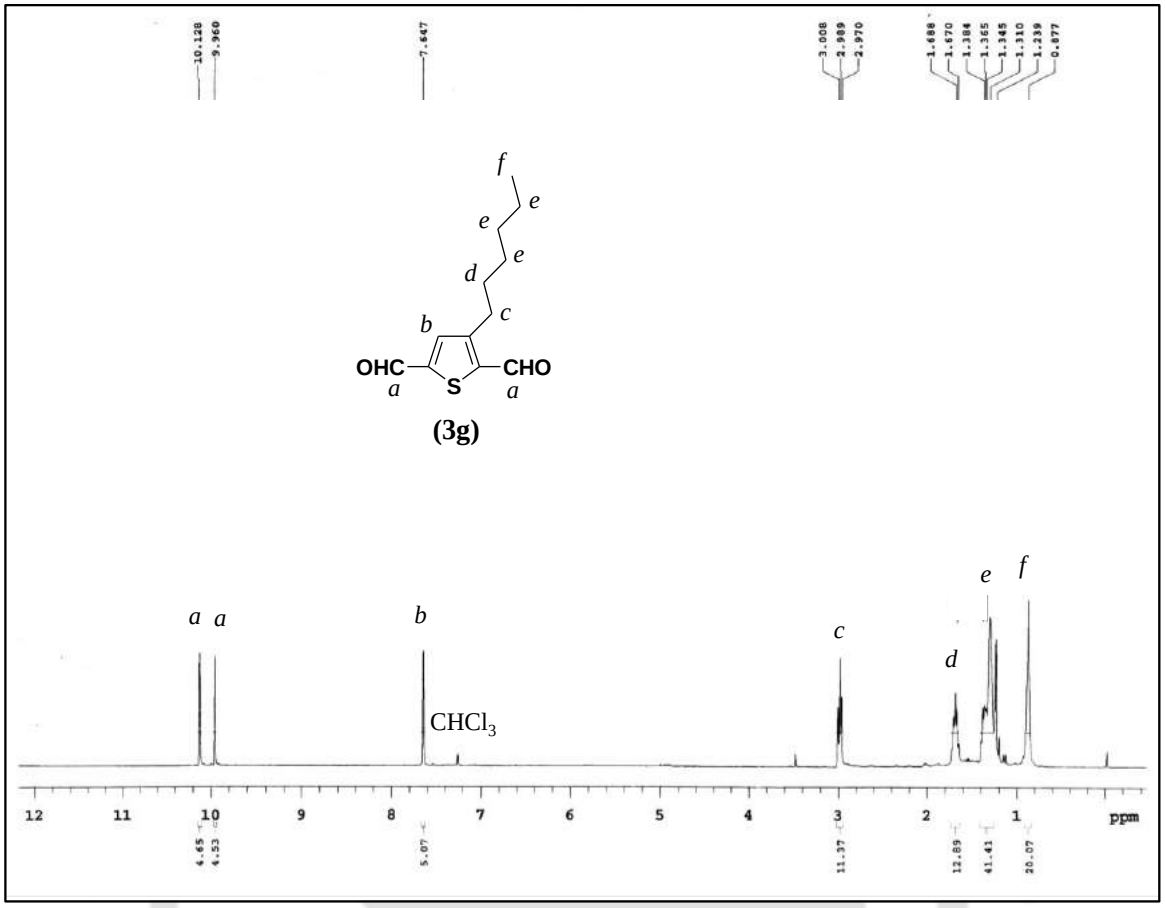

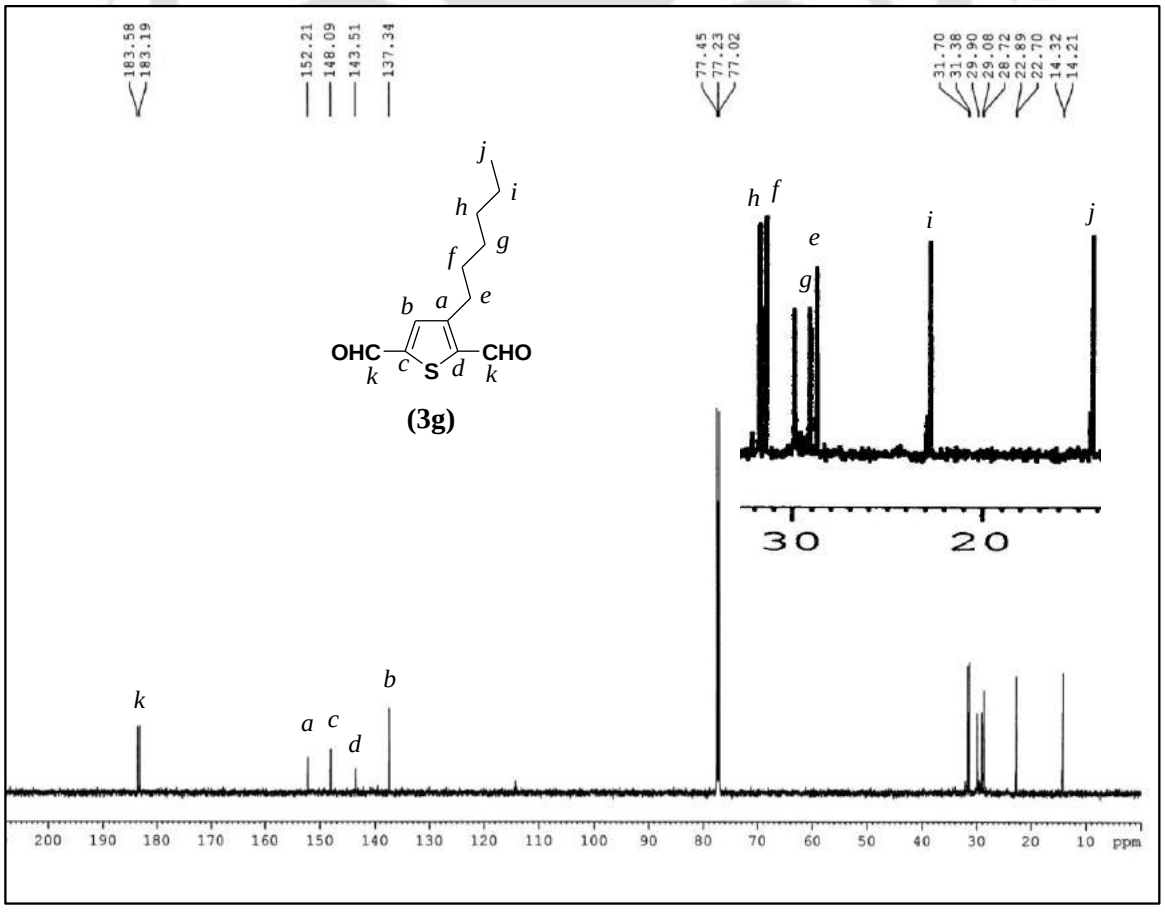

TH-1906_11615303

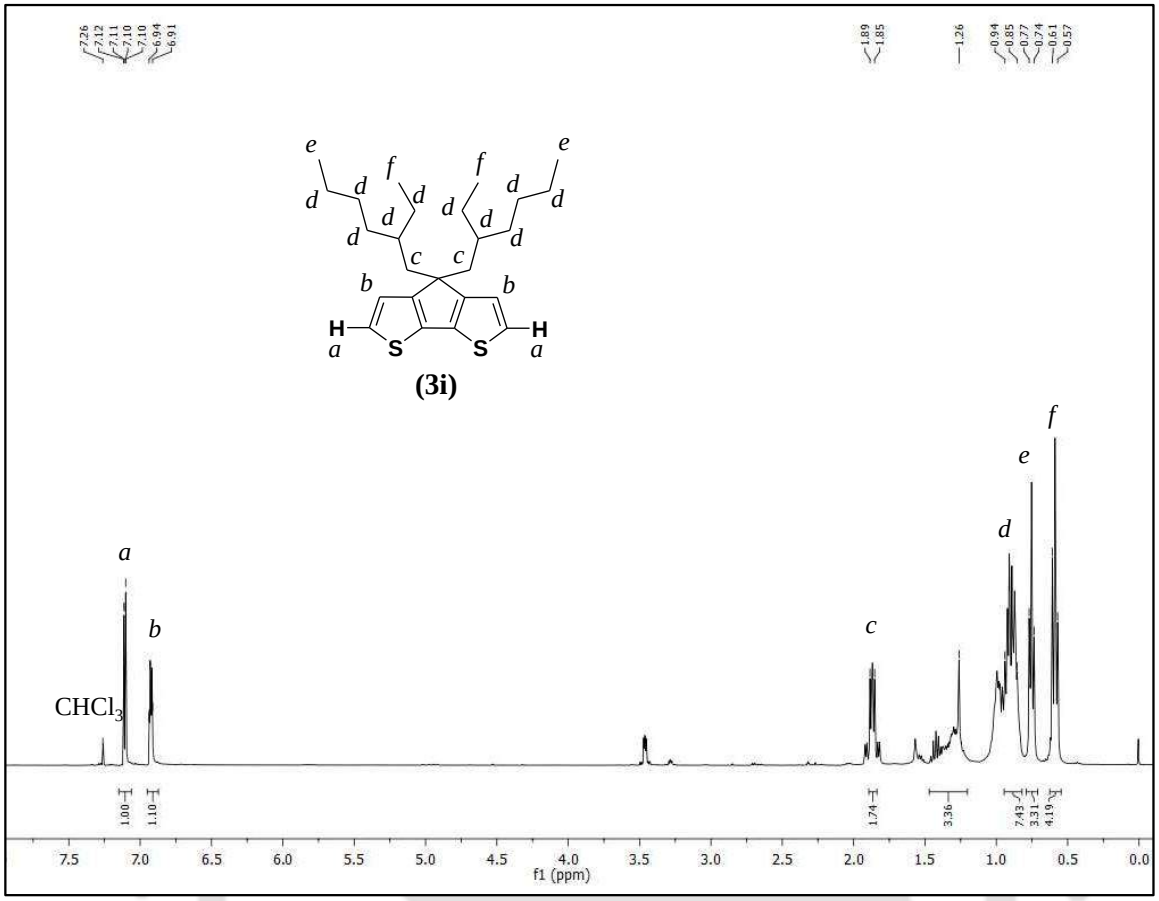

(3i)

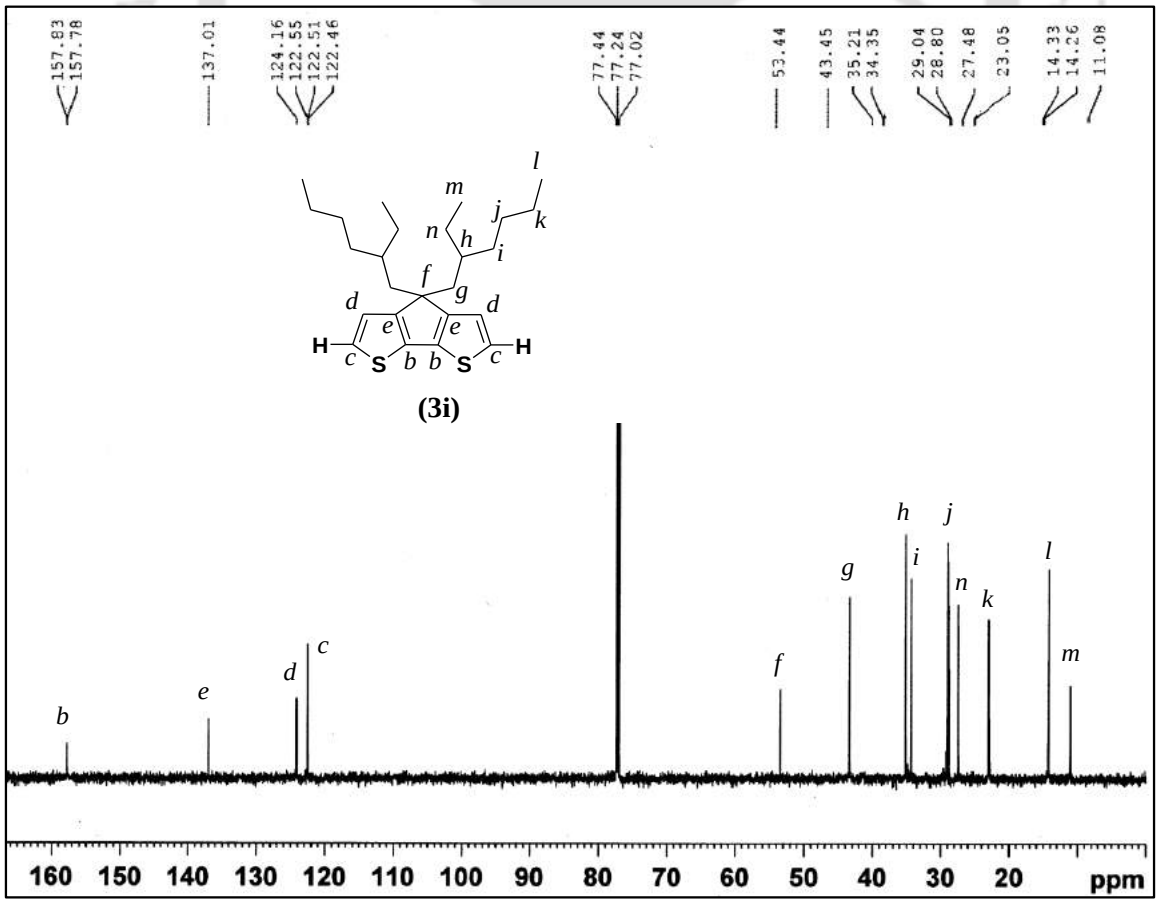

(3i)

TH-1906_11615303

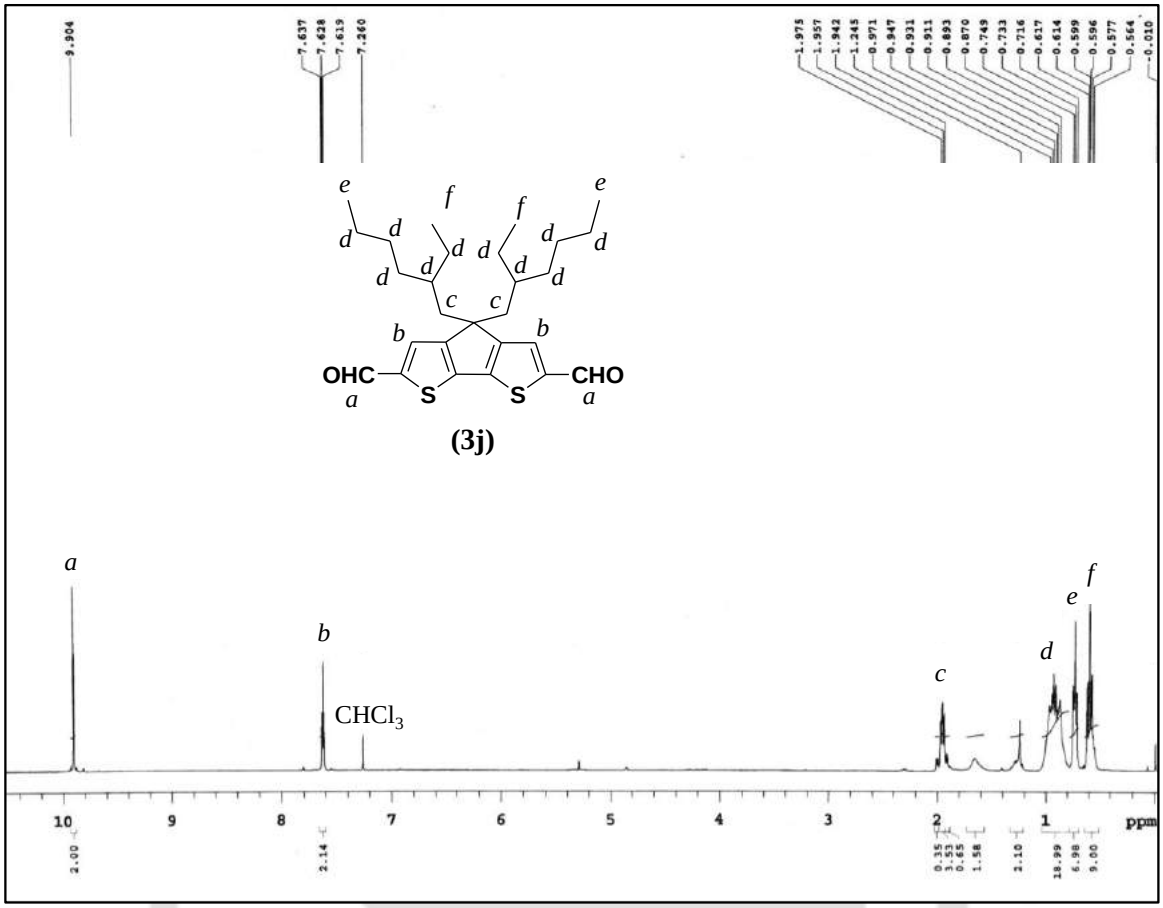

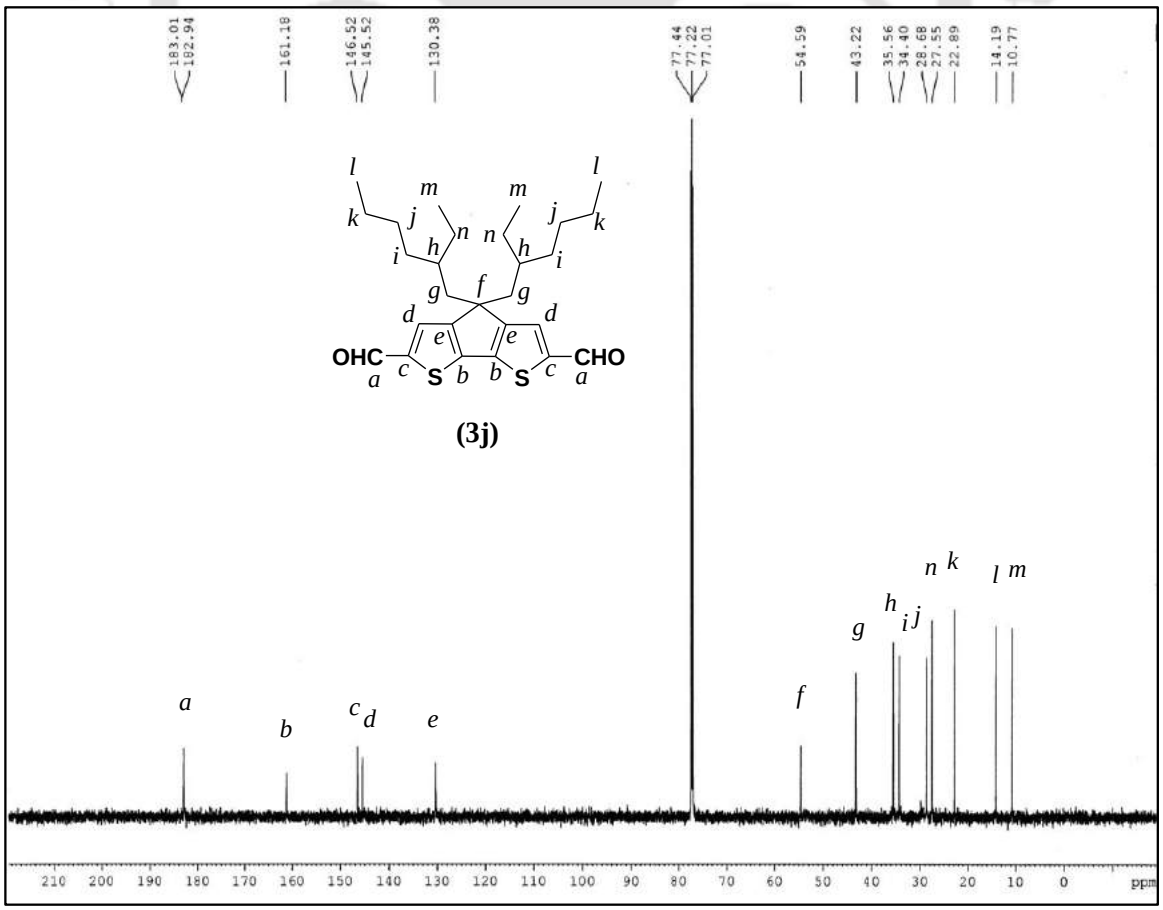

TH-1906_11615303

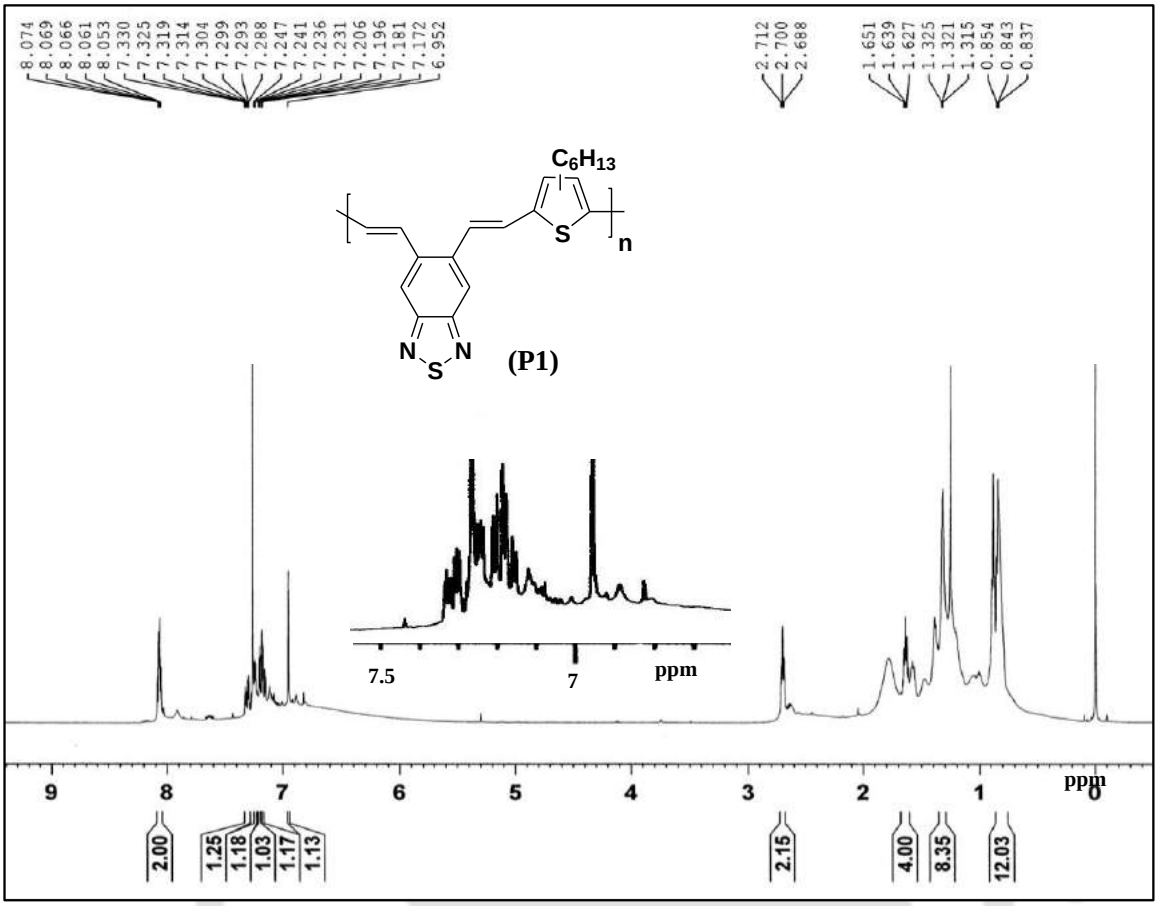

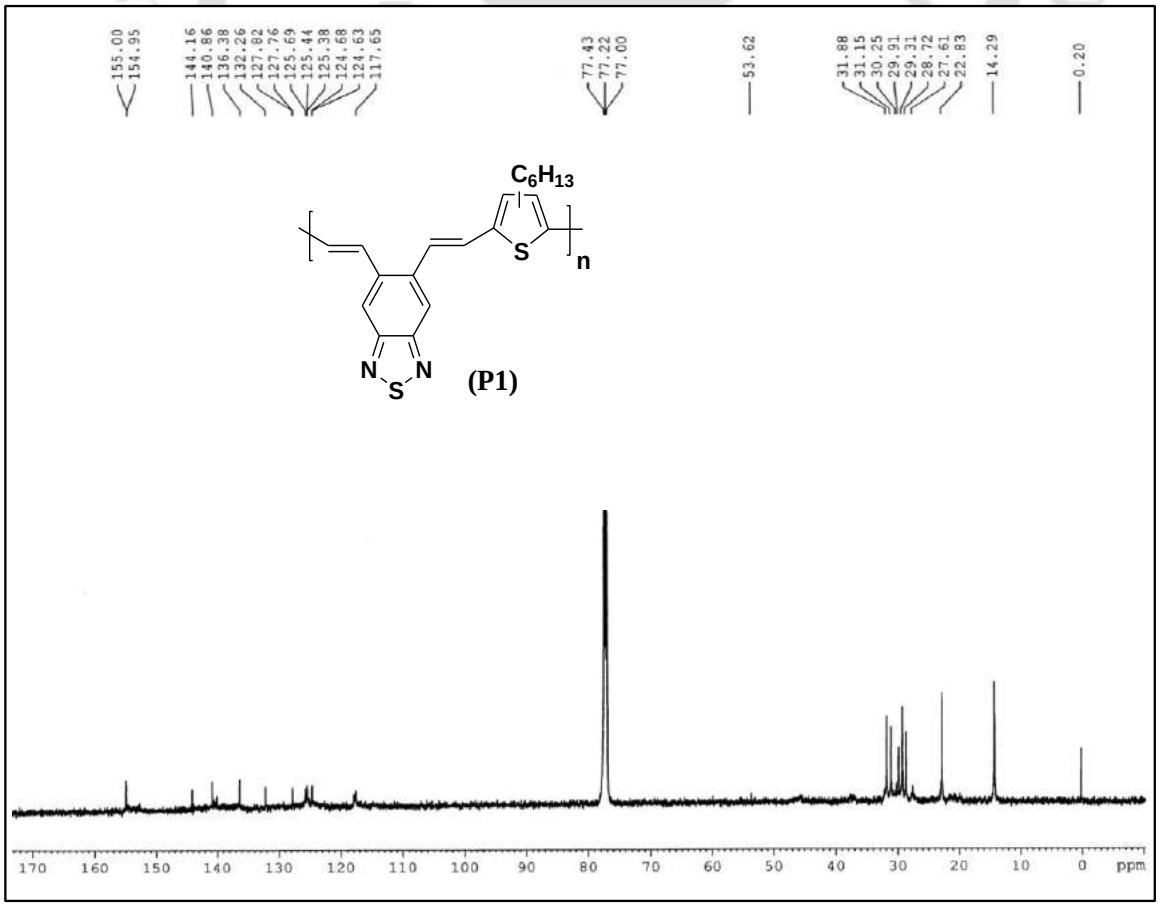

TH-1906_11615303

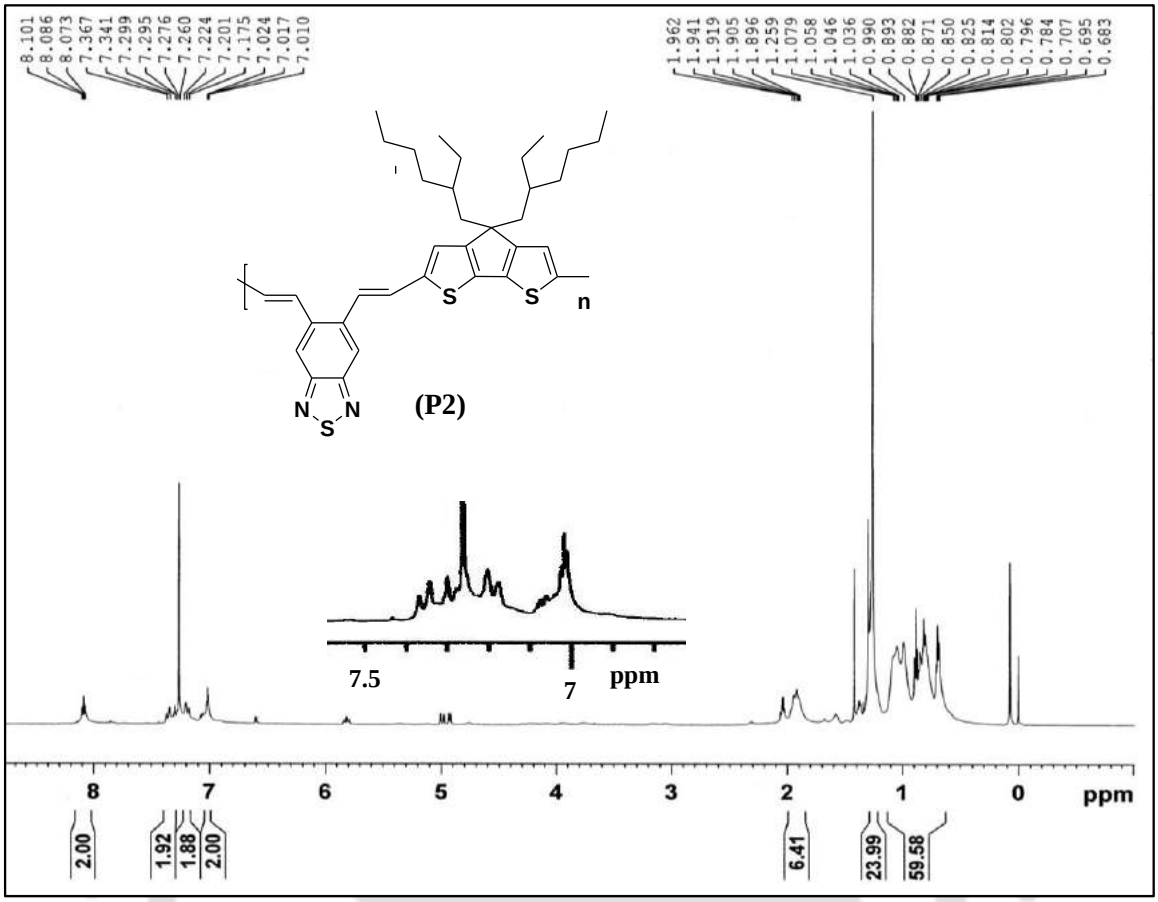

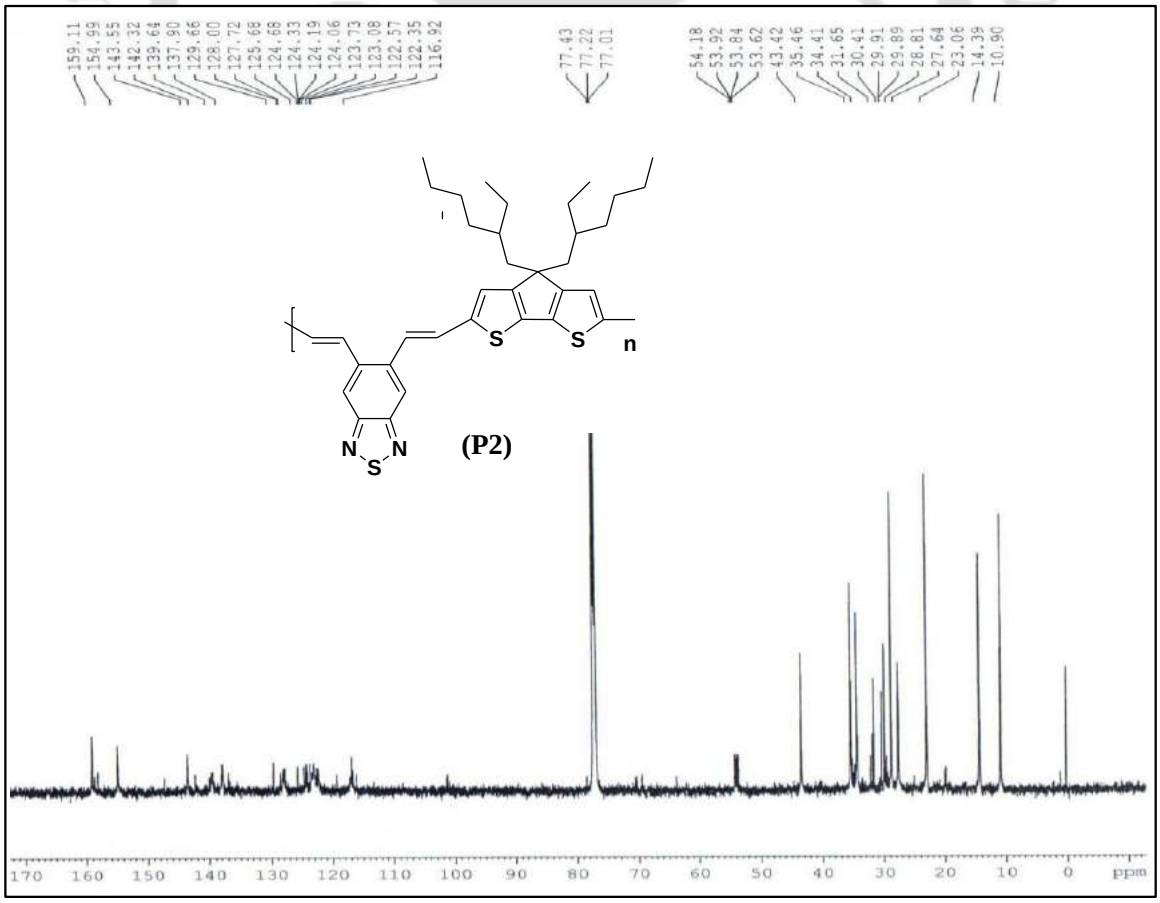

TH-1906_11615303

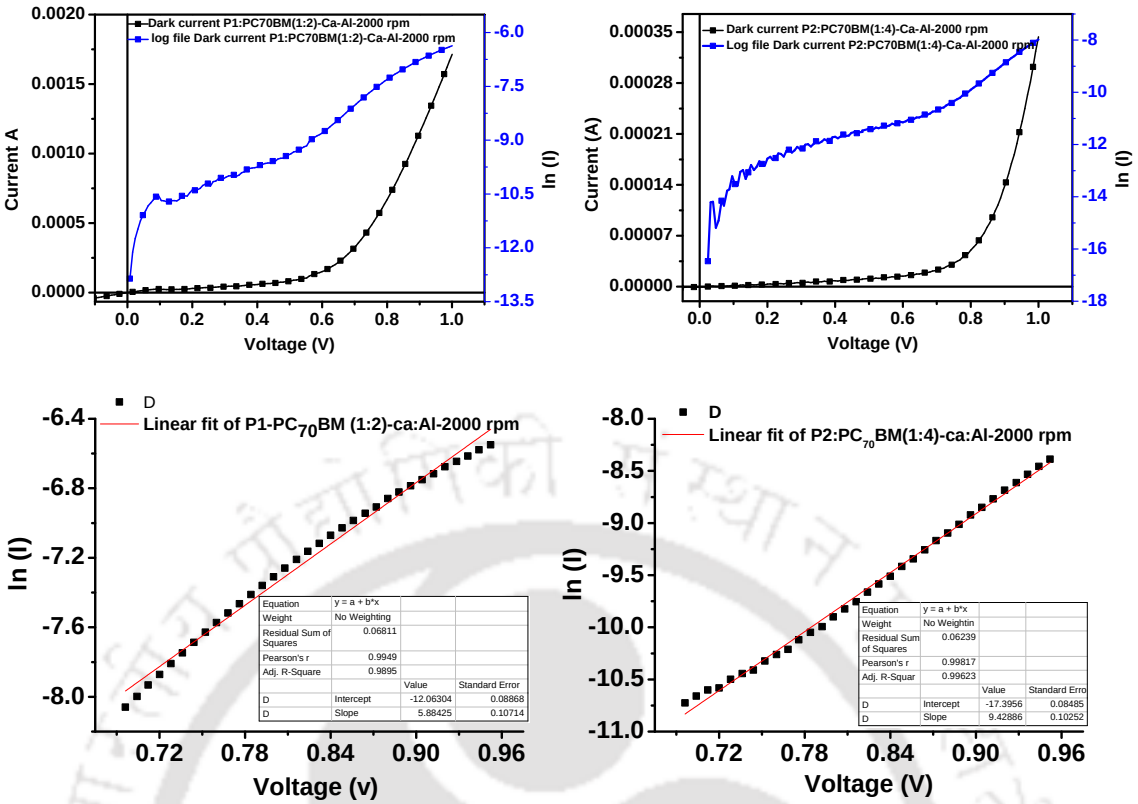

Figure A3.1 Determination of ideality factor from log file of dark current of fabricated solar cells of high efficiency with P1 and P2.

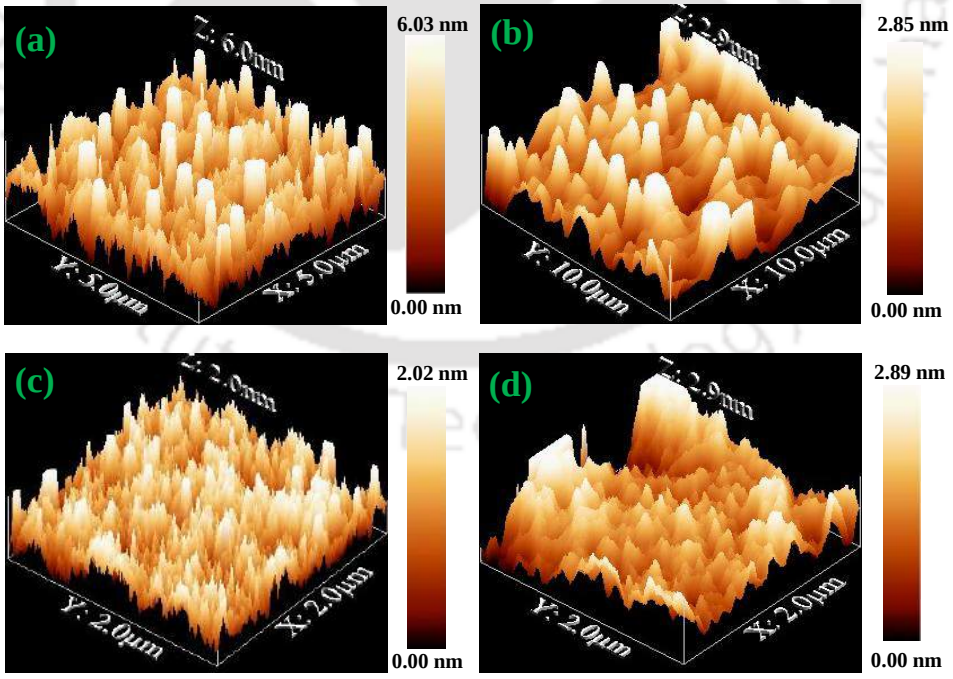

Figure A3.2 Topography of AFM images in 3D view (RMS roughness) (a) P1:PC_{61}BM-1:4 (1.24 nm) (b) P1:PC_{71}BM-1:2 (0.57 nm) (c) P2:PC_{61}BM-1:1 (0.43 nm) (d) P2:PC_{61}BM-1:4 (0.56 nm).

TH-1906_11615303

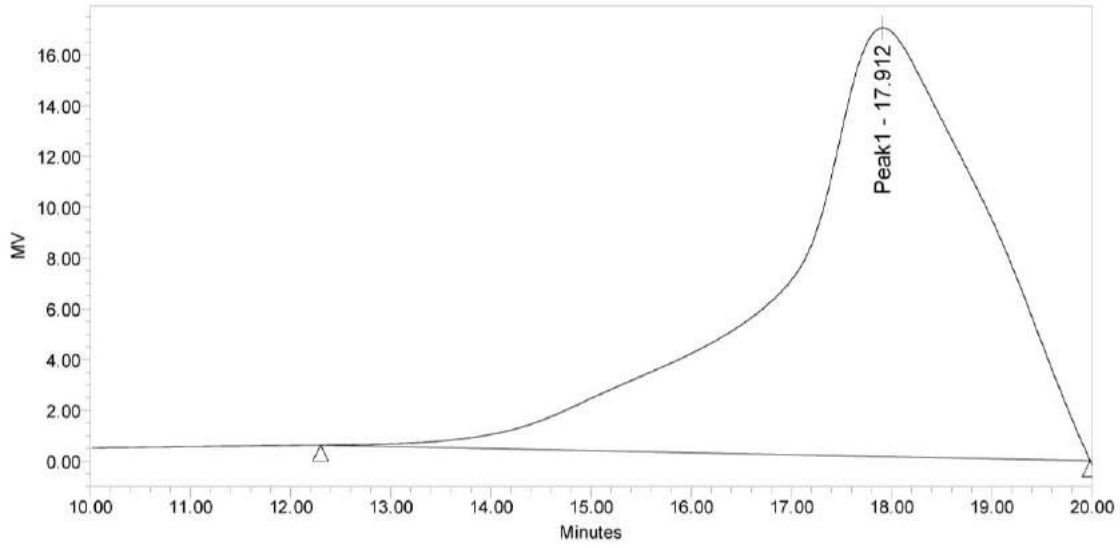

GPC Results

	SampleName	Mn	Mw	MP	Mz	Mz+1	Polydispersity
1	BT-Vinyl-3HT-P	6090	10589		21505	35681	1.738791

Figure A3.2 Determination molecular weight for polymer P1.

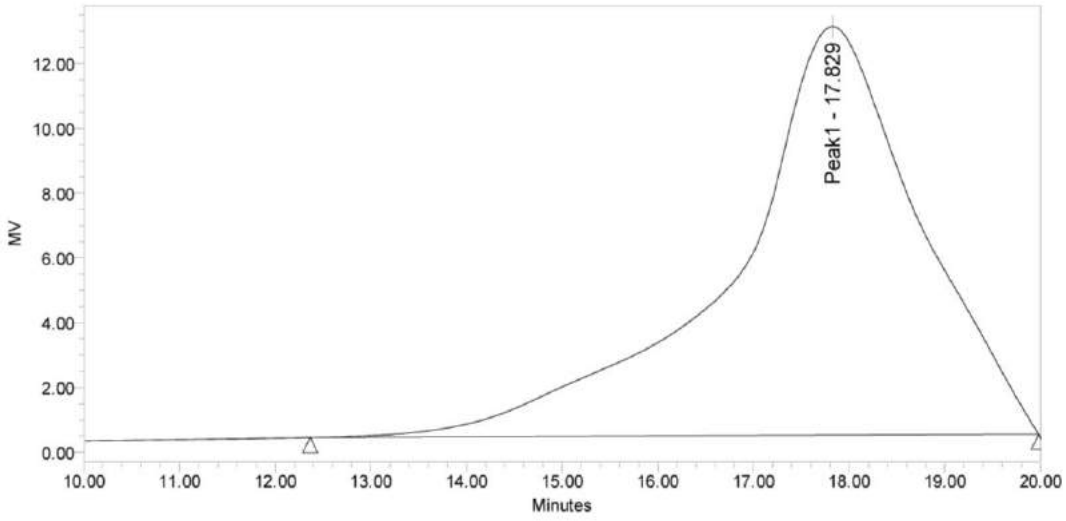

GPC Results

	SampleName	Mn	Mw	MP	Mz	Mz+1	Polydispersity
1	BT-Vinyl-CPDT-Et-P	6079	10422		20733	34393	1.714411

Figure A3.3 Determination molecular weight for polymer P2.

TH-1906_11615303

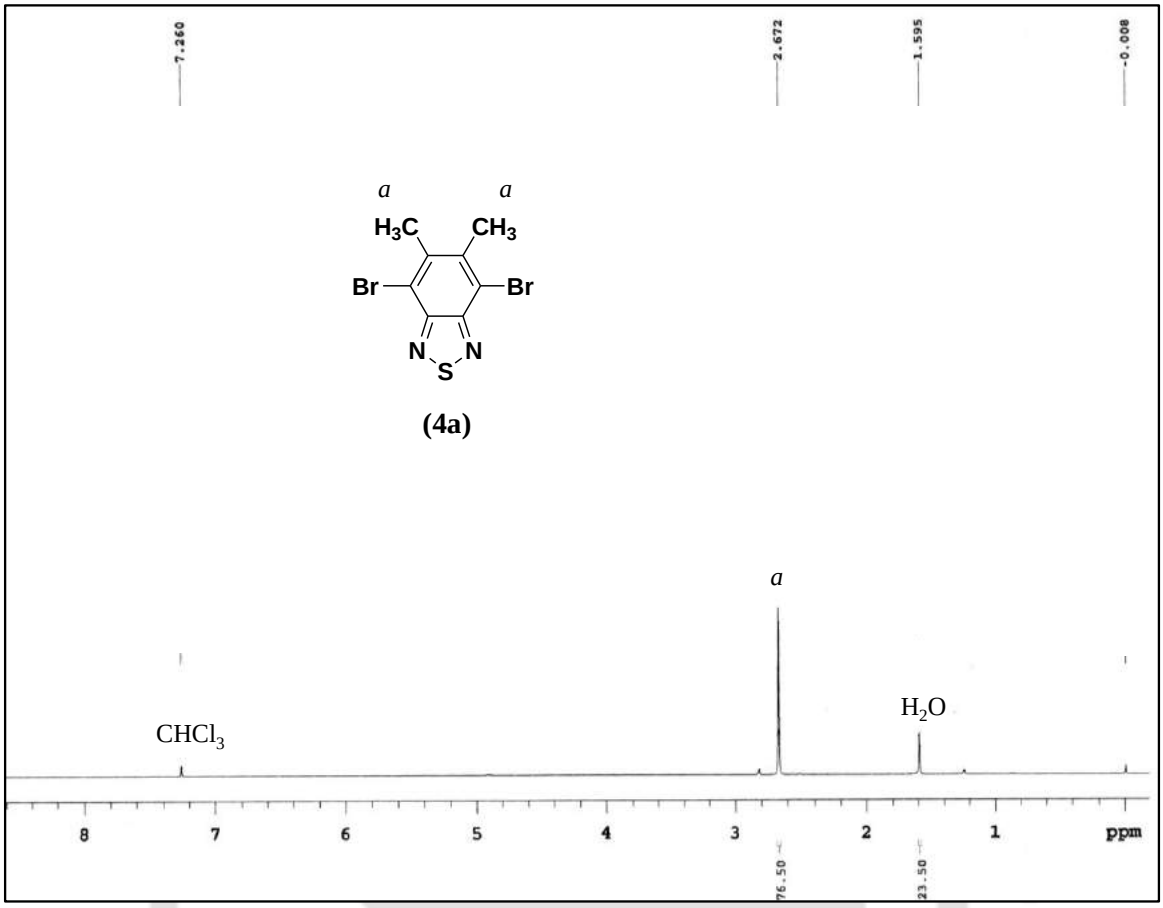

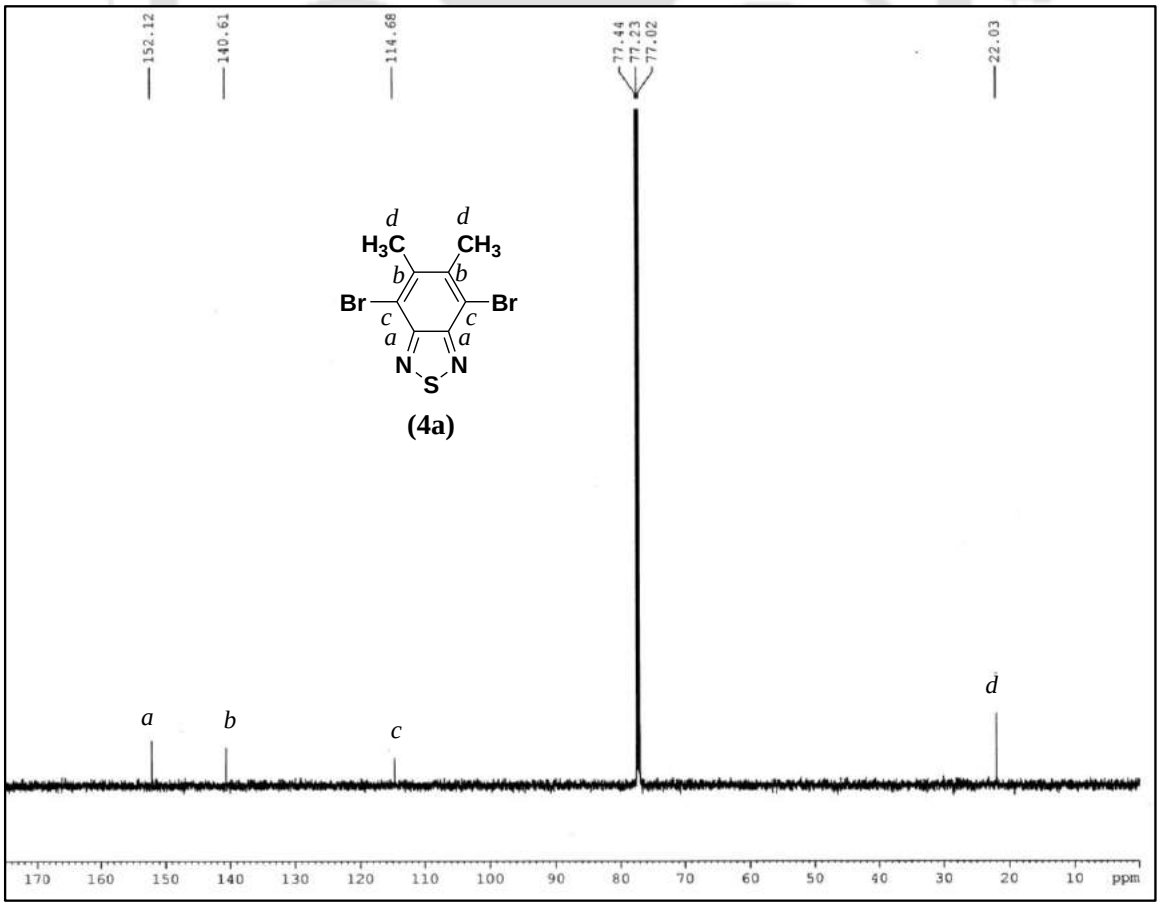

TH-1906_11615303

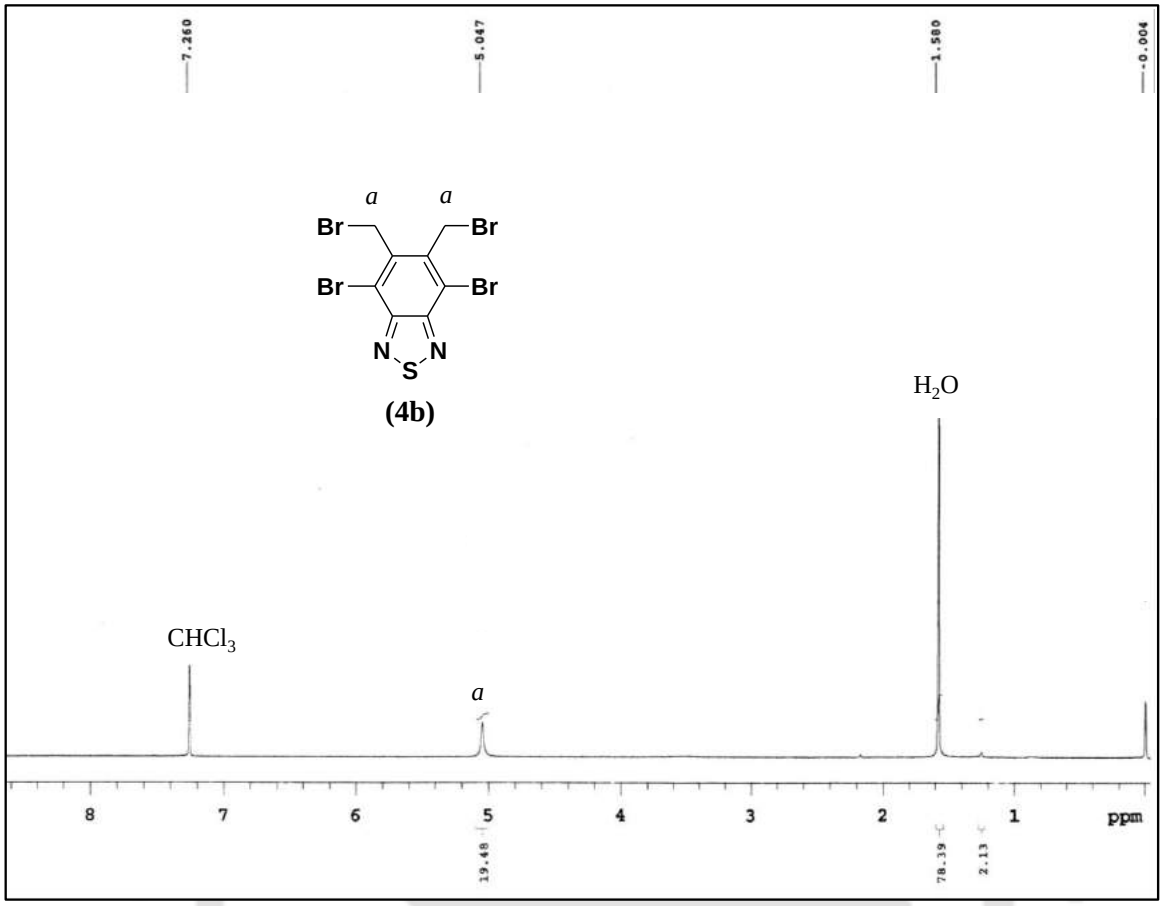

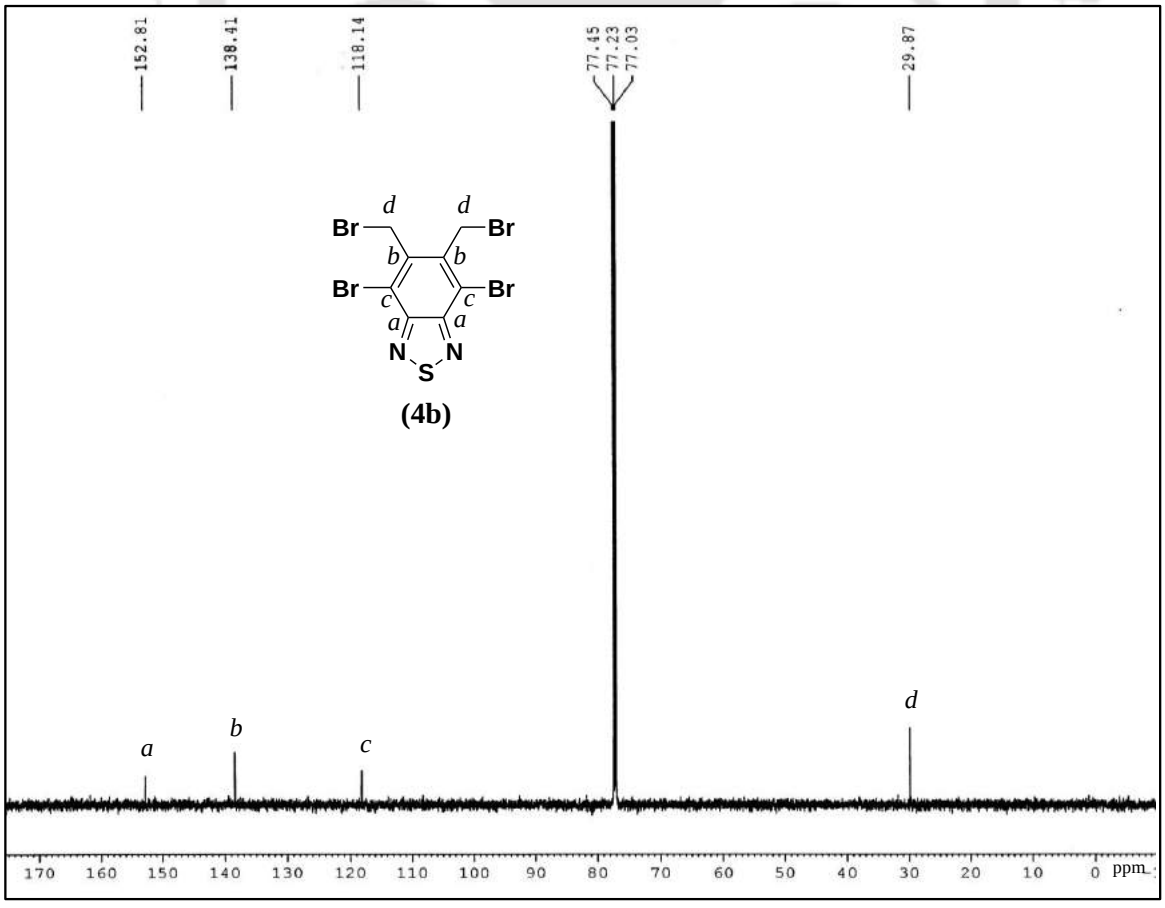

TH-1906_11615303

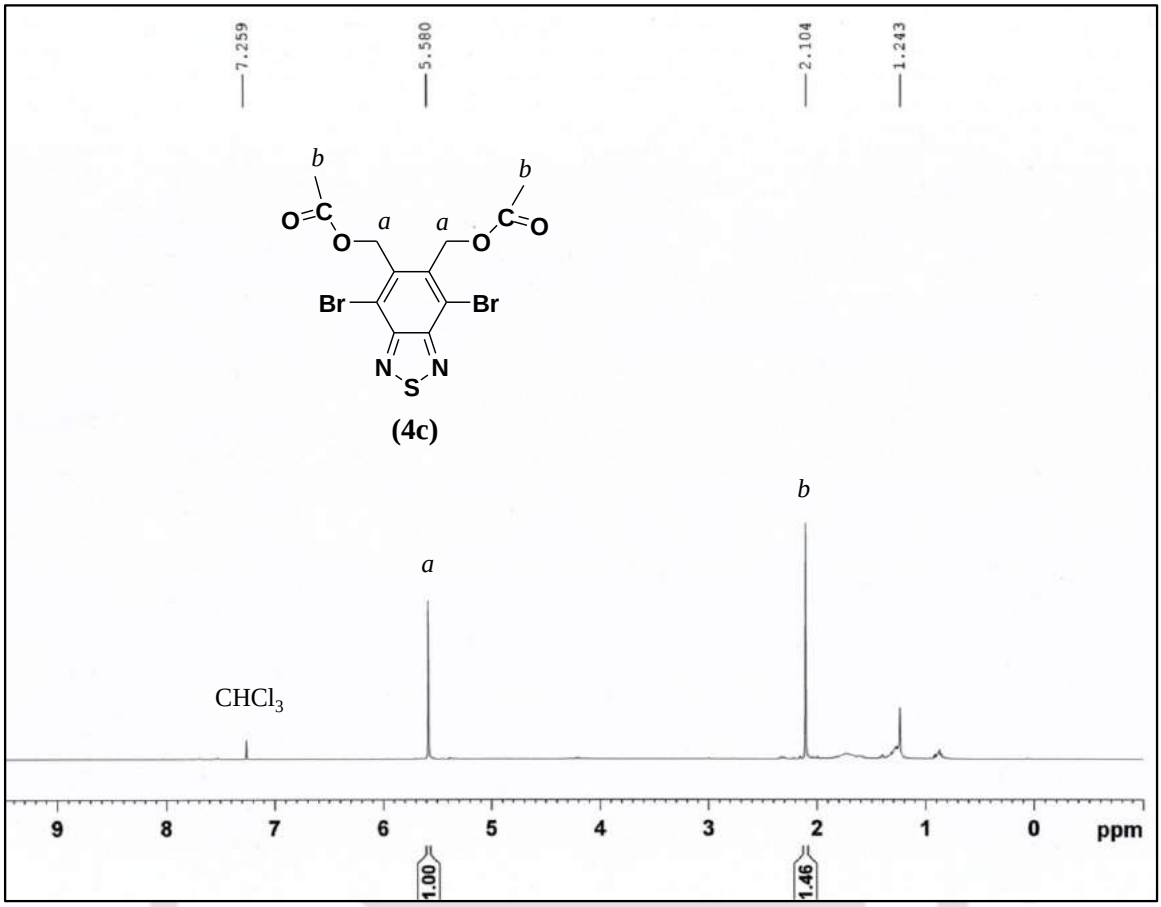

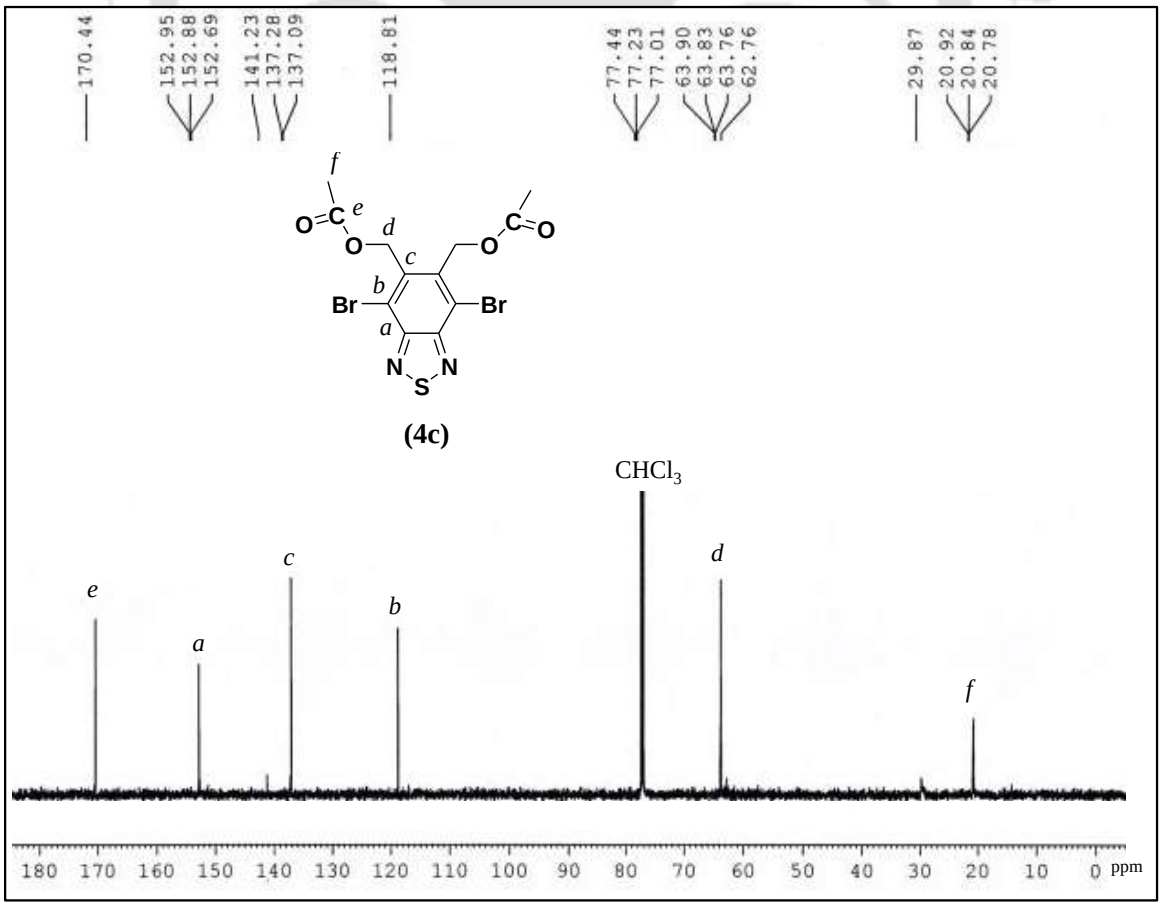

TH-1906_11615303

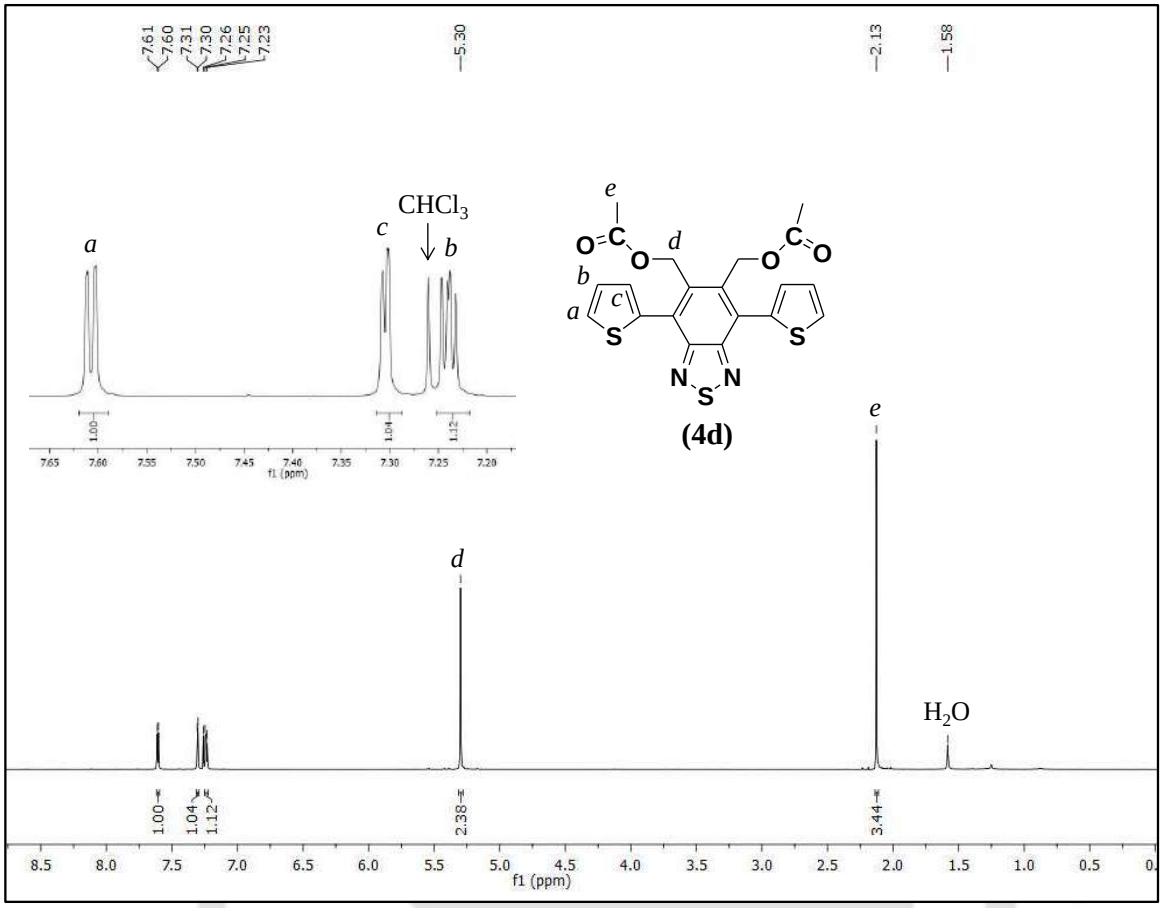

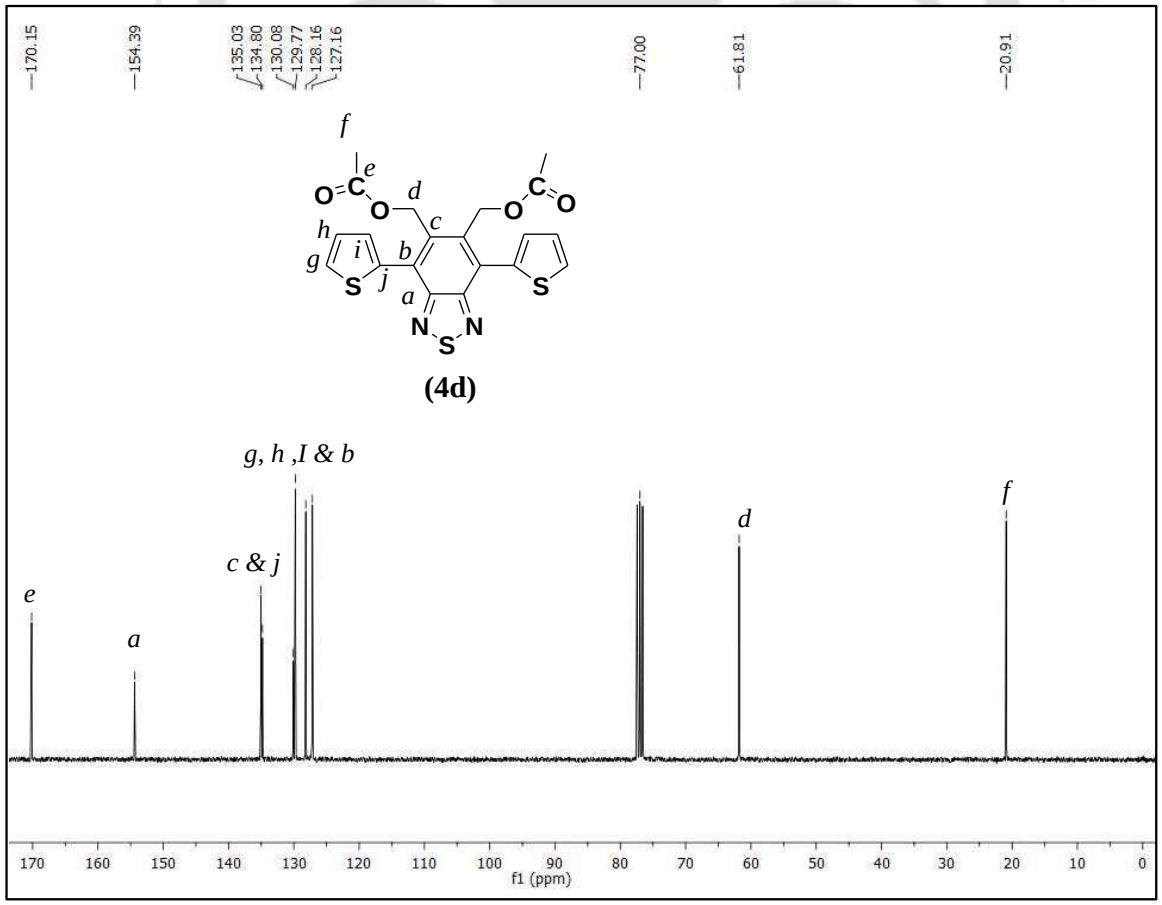

TH-1906_11615303

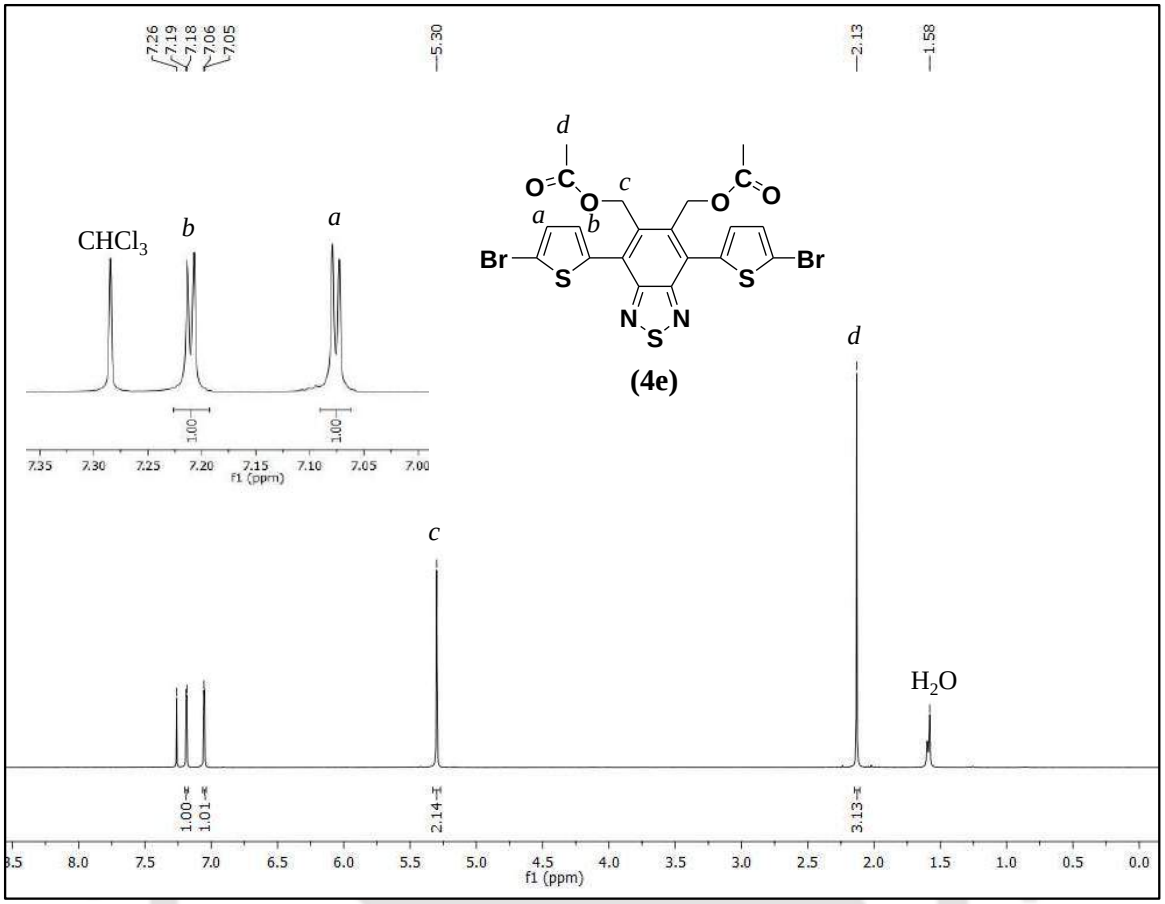

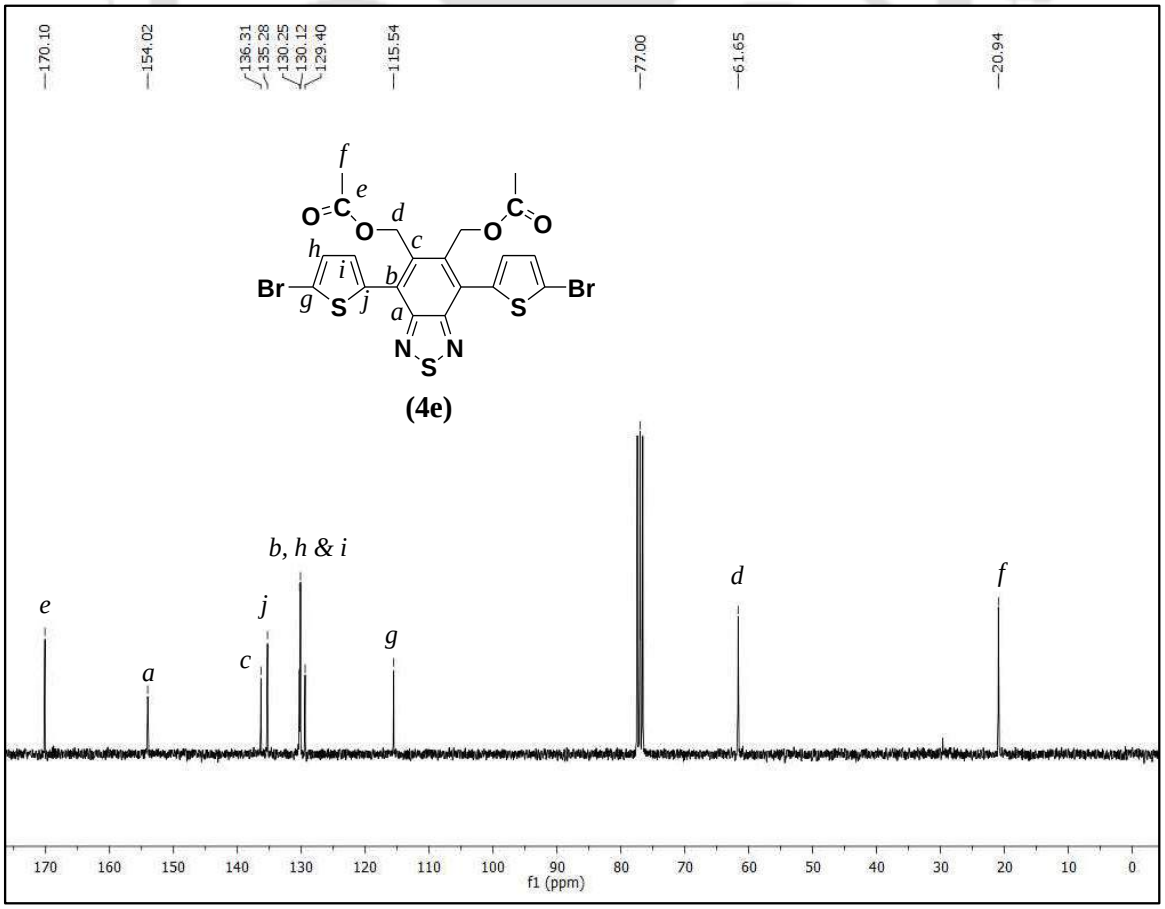

TH-1906_11615303

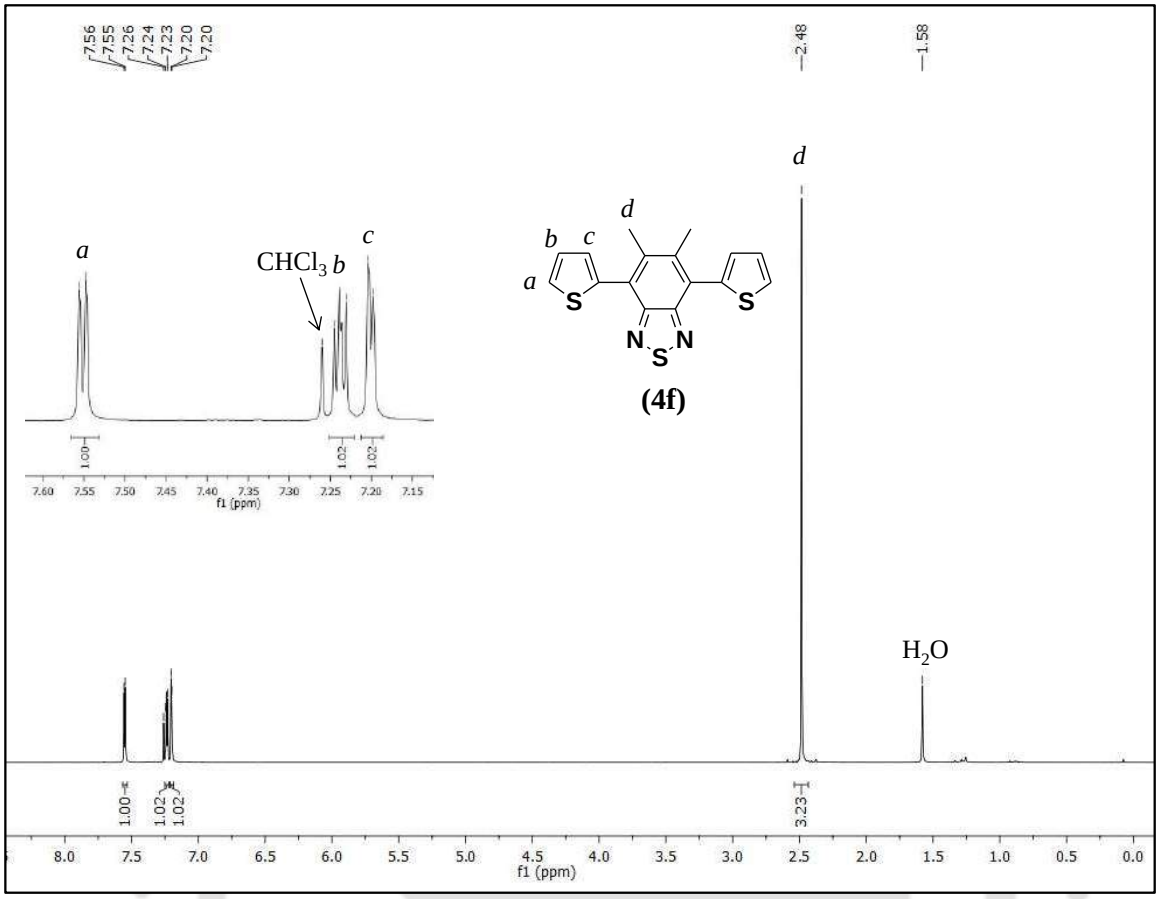

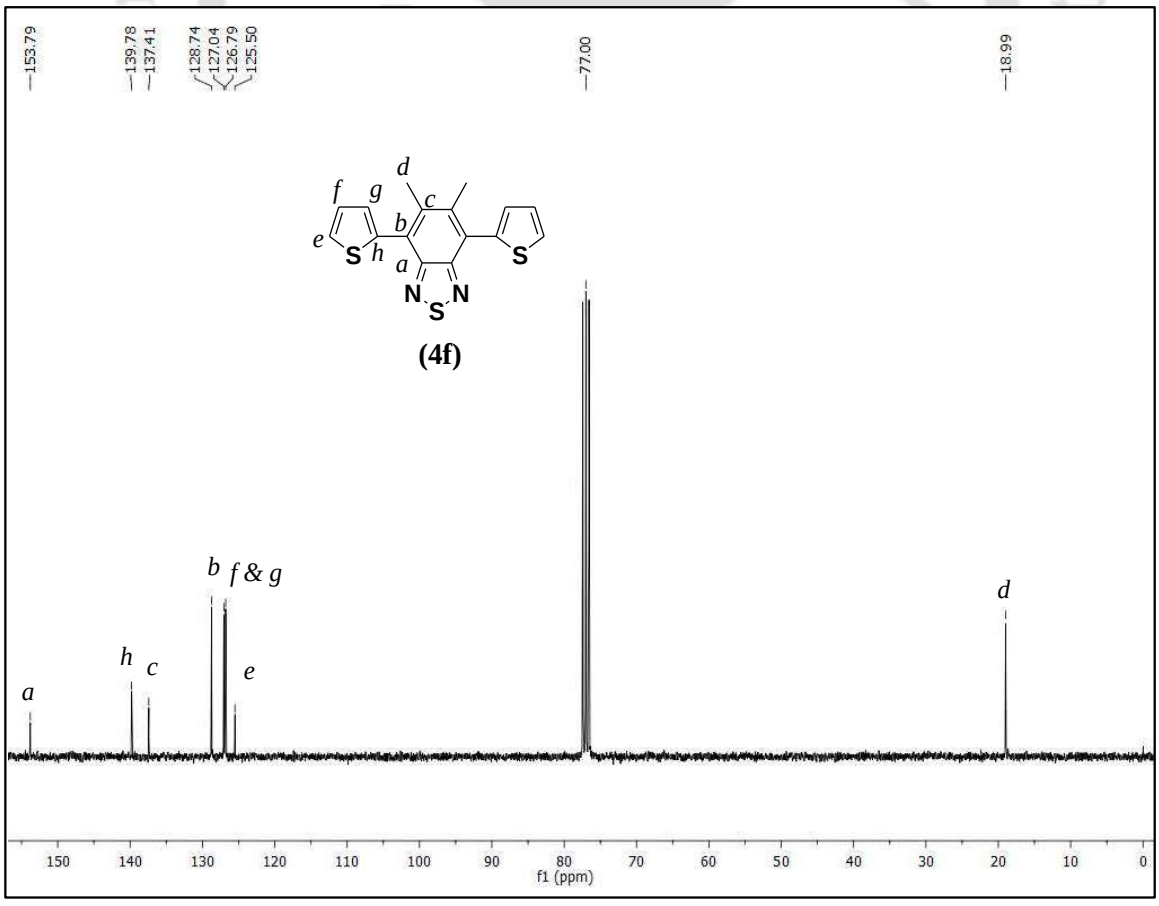

TH-1906_11615303

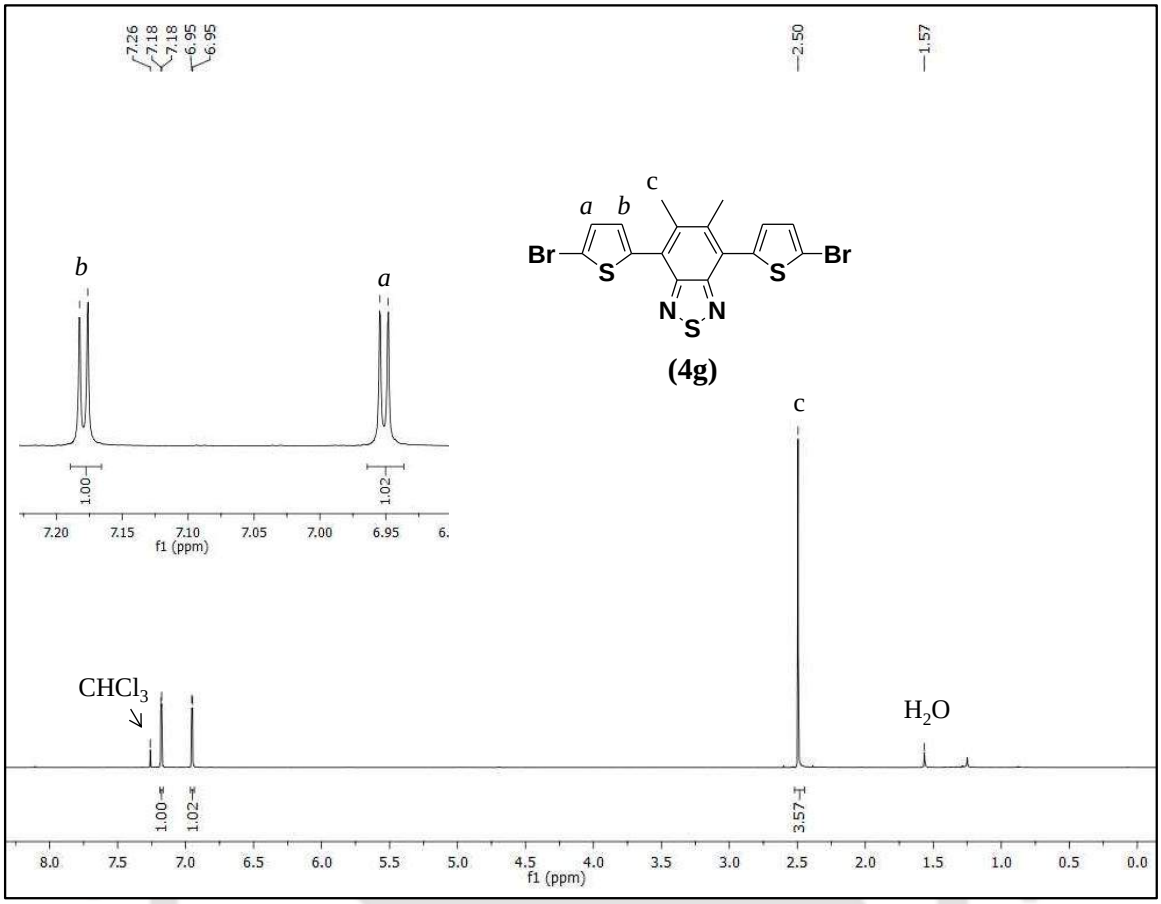

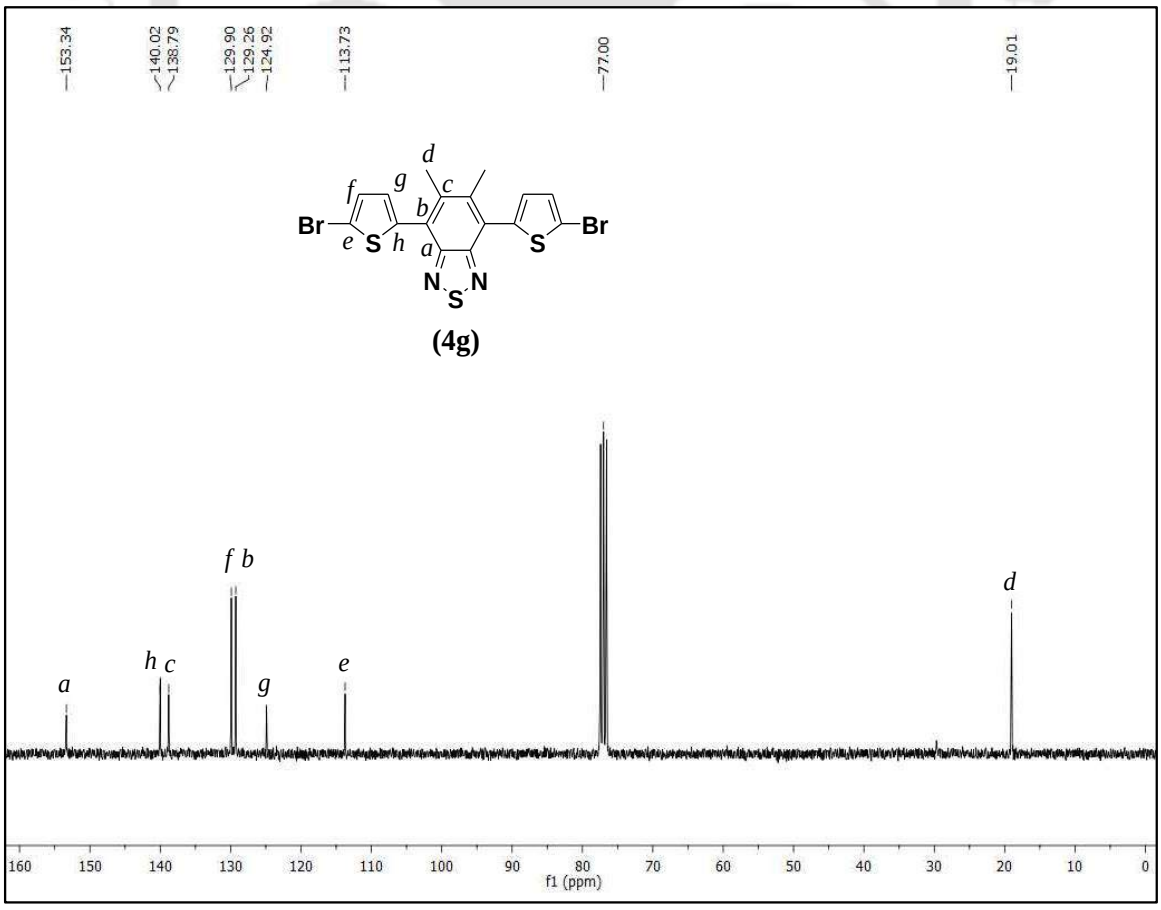

TH-1906_11615303

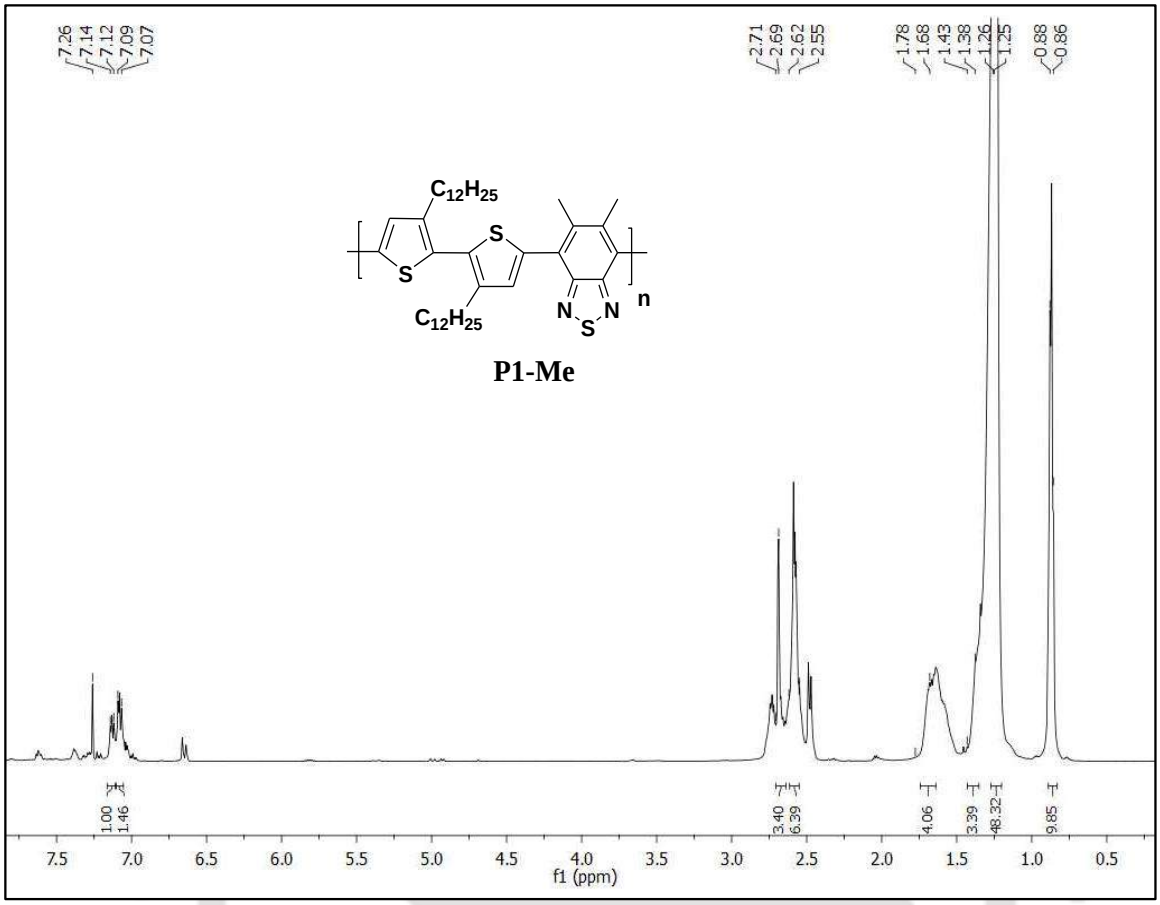

P1-Me

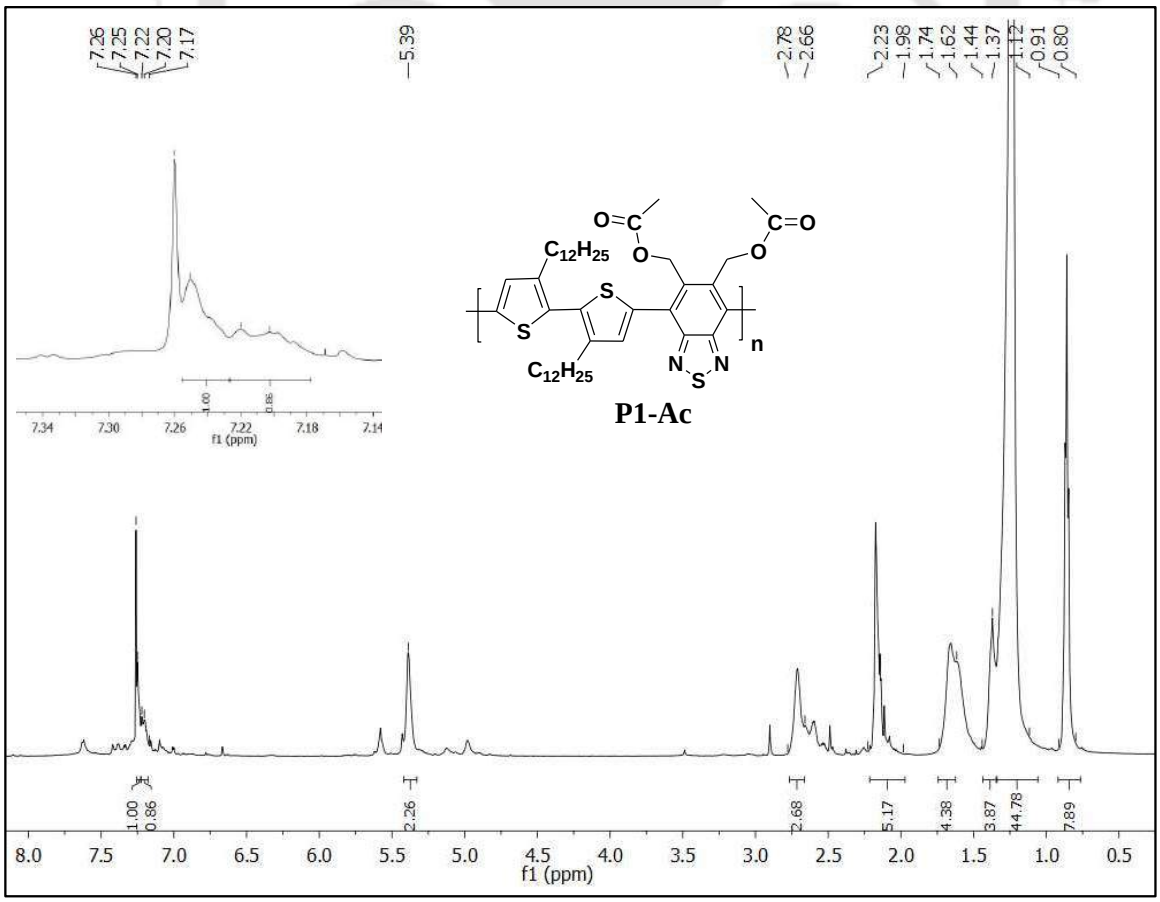

P1-Ac

TH-1906_11615303

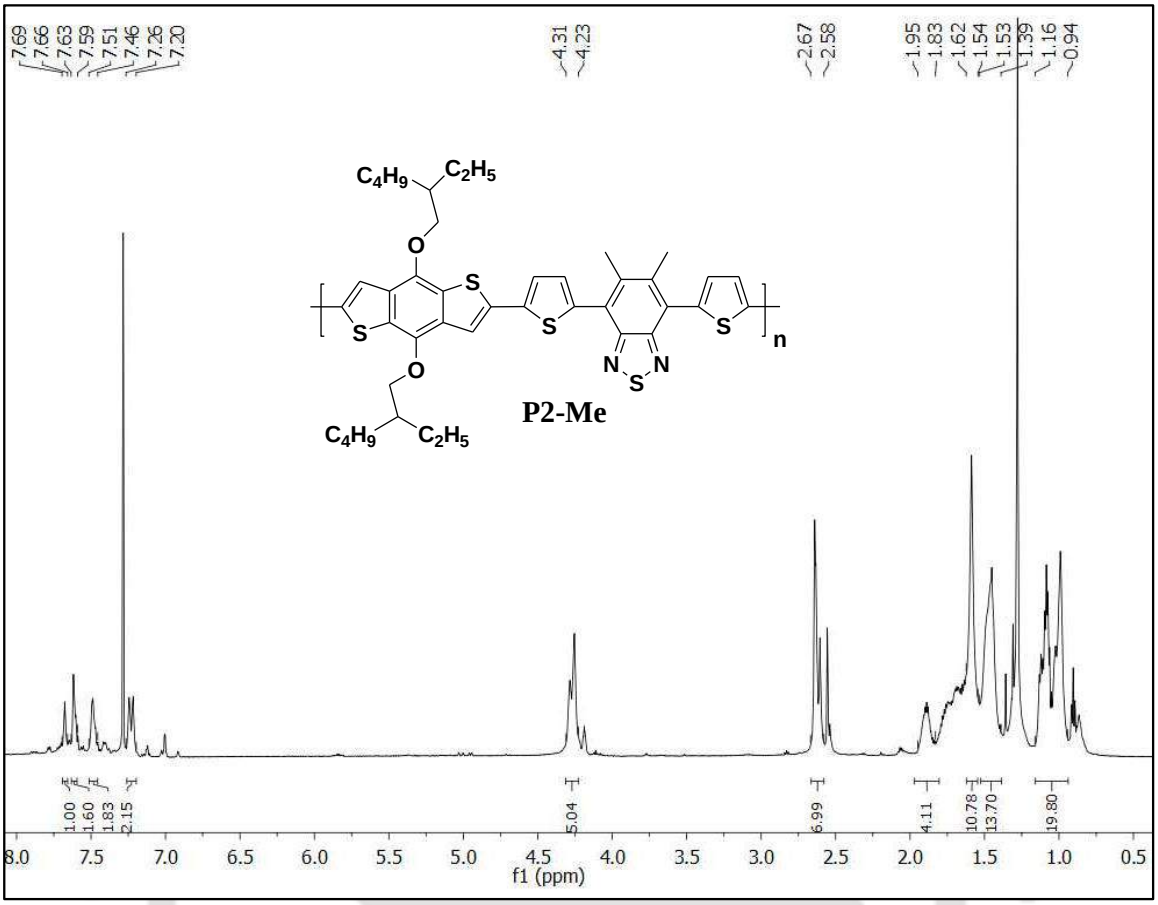

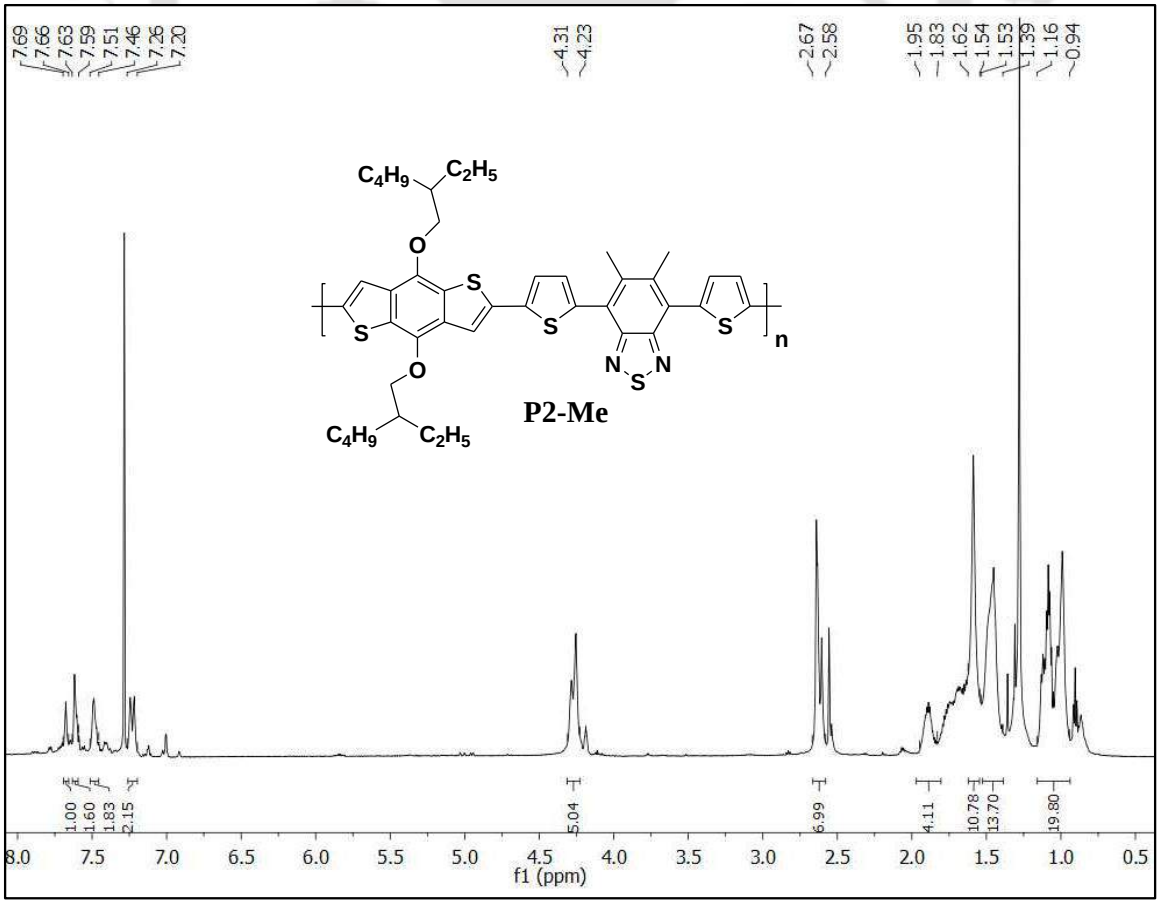

TH-1906_11615303

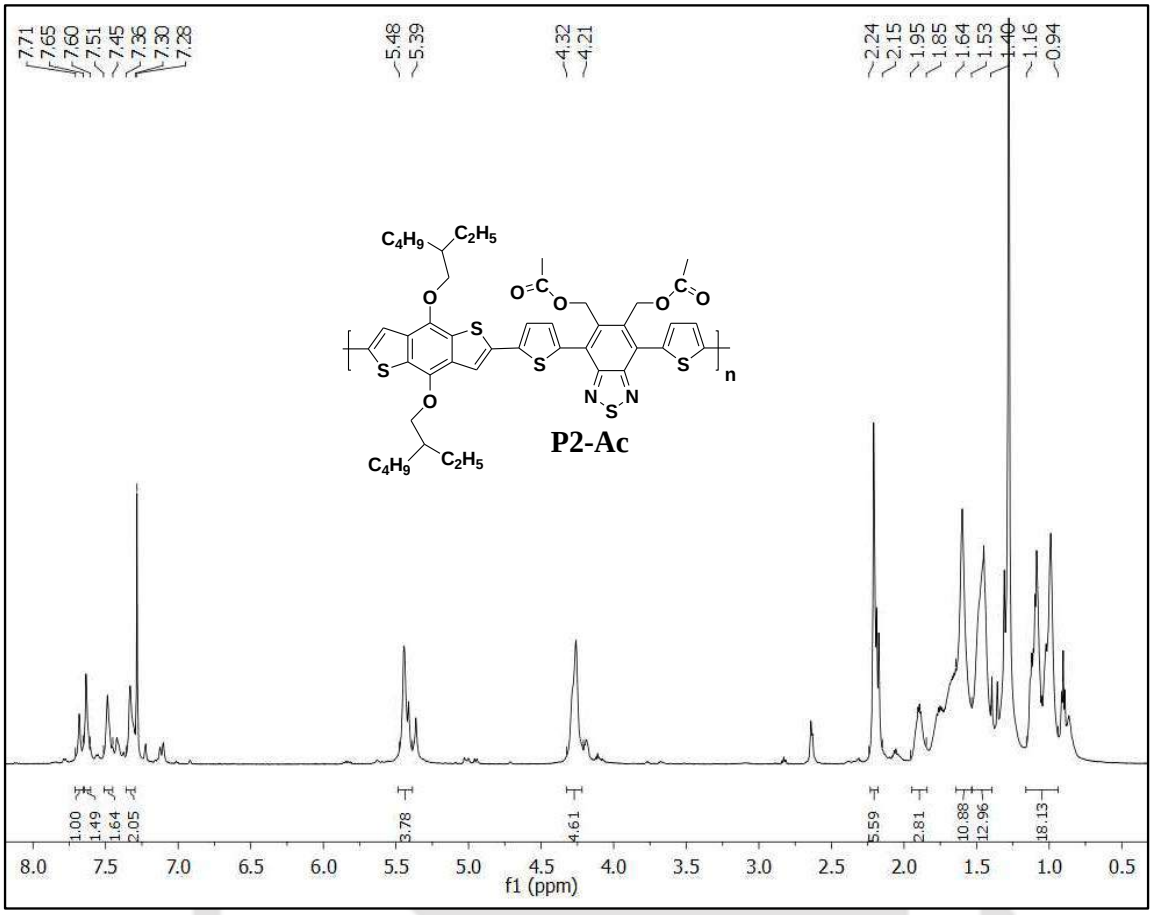

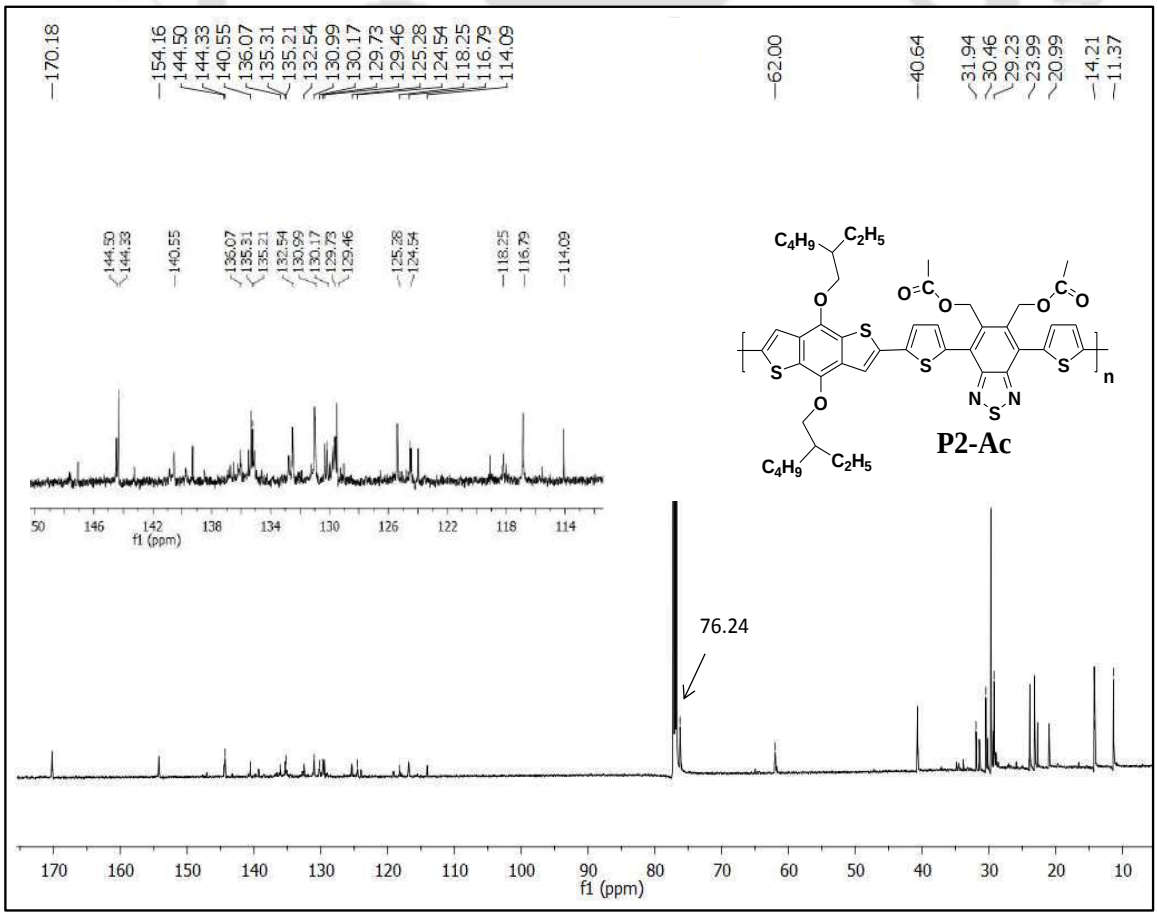

TH-1906_11615303

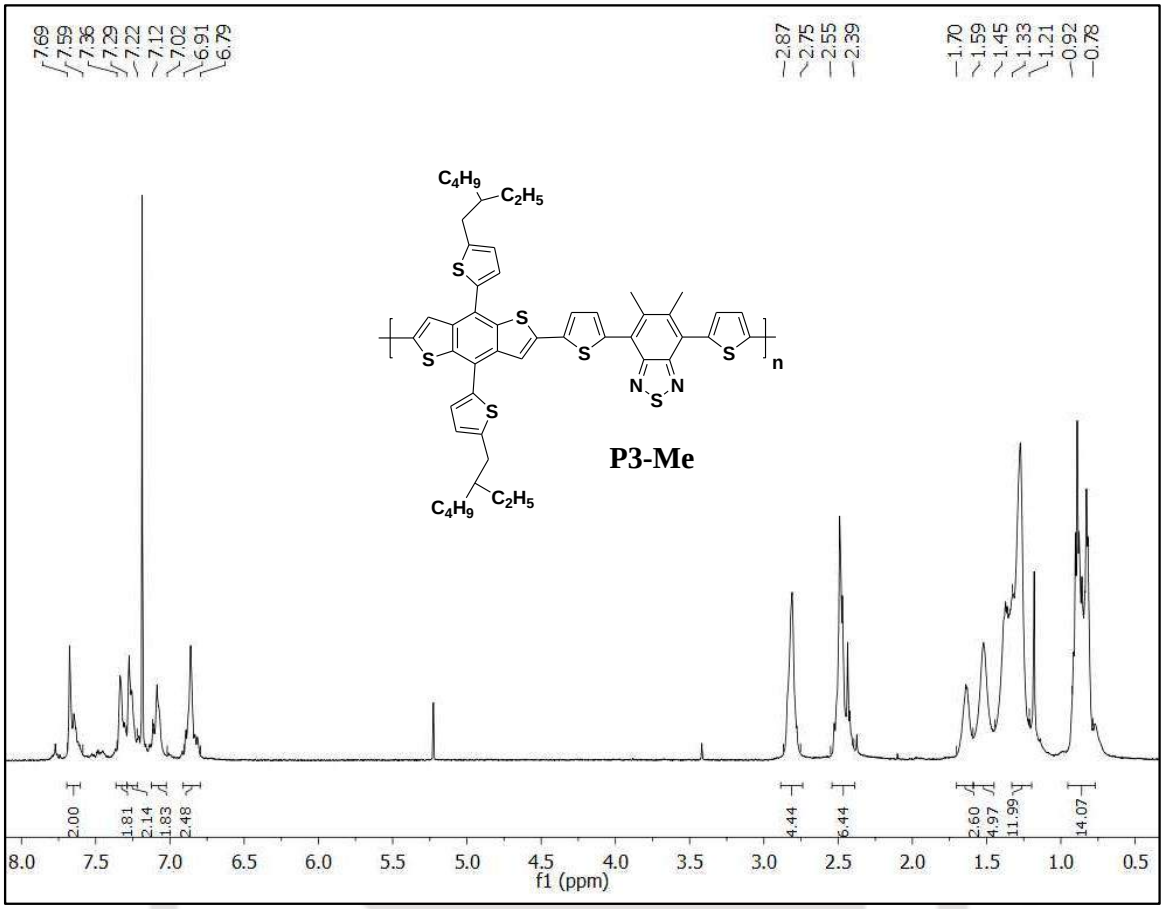

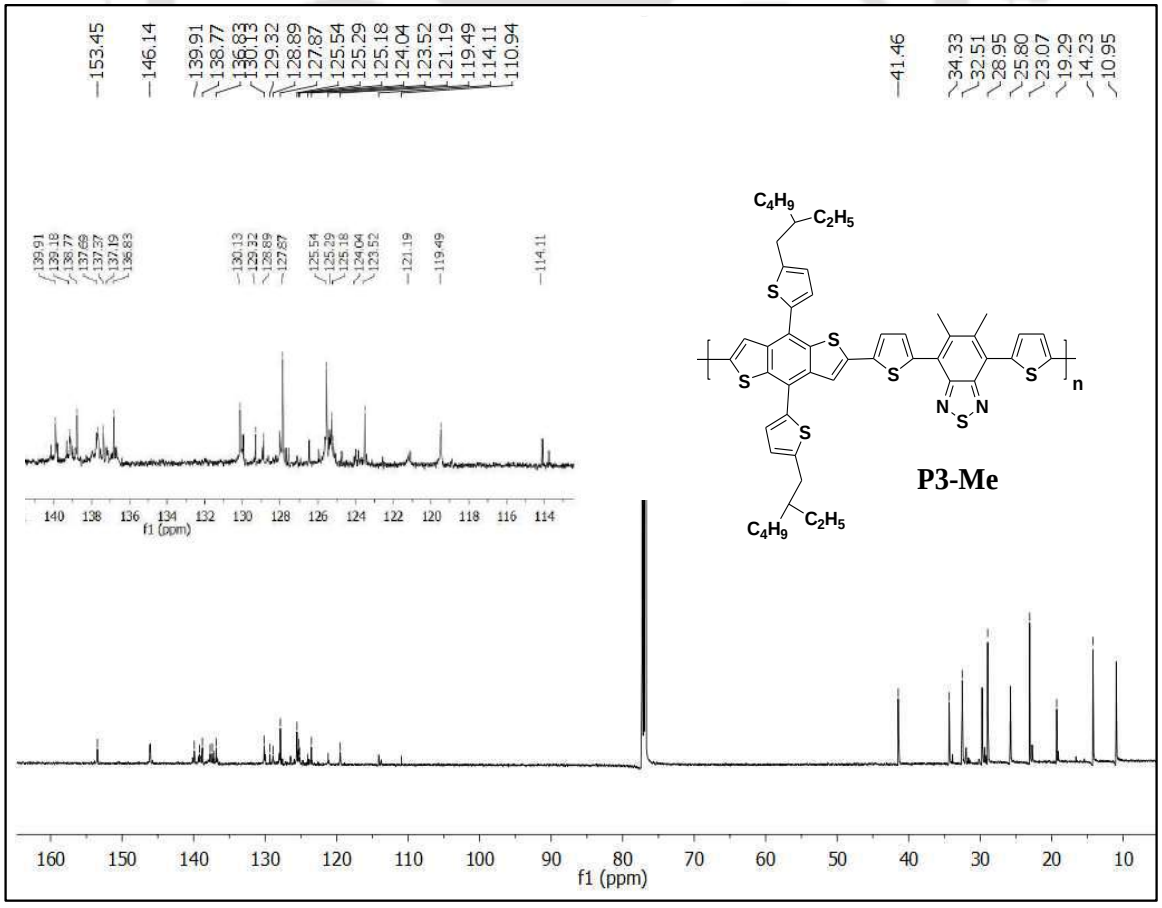

TH-1906_11615303

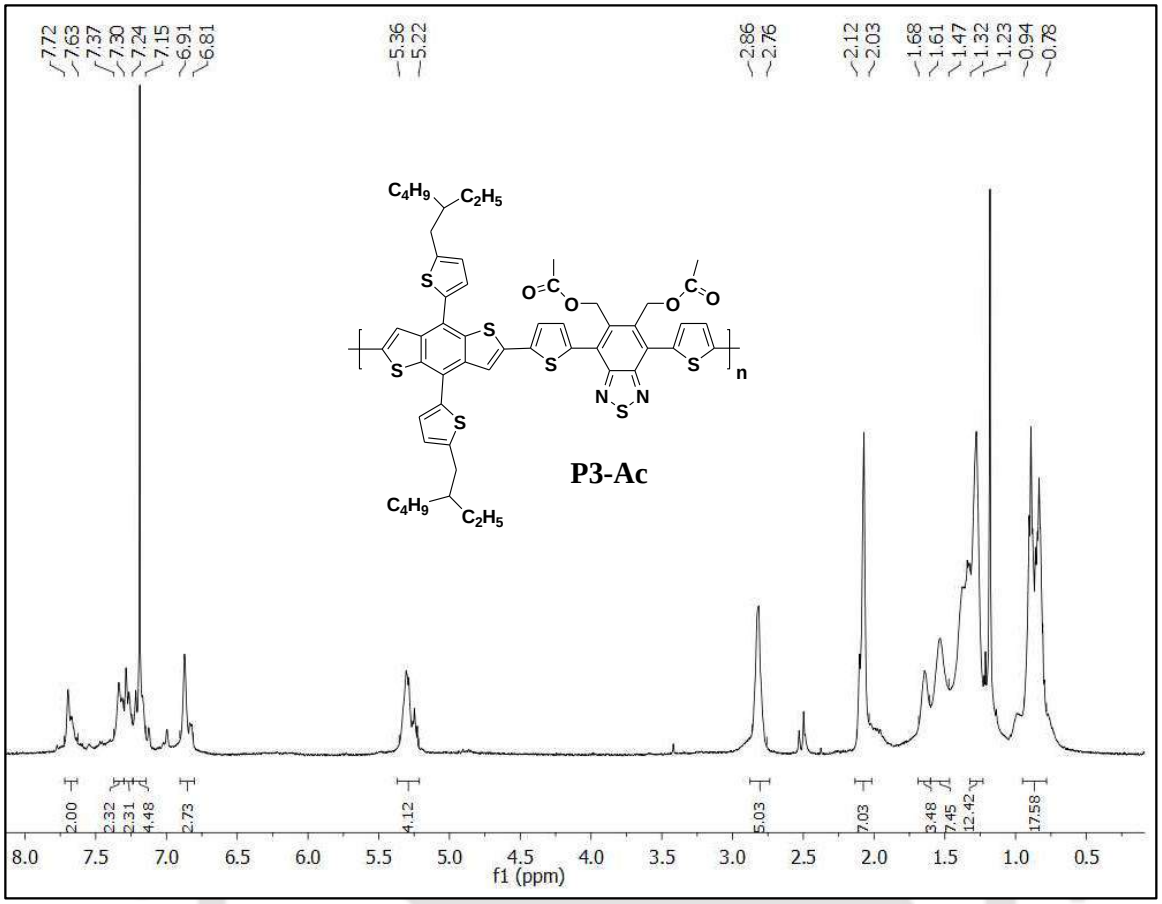

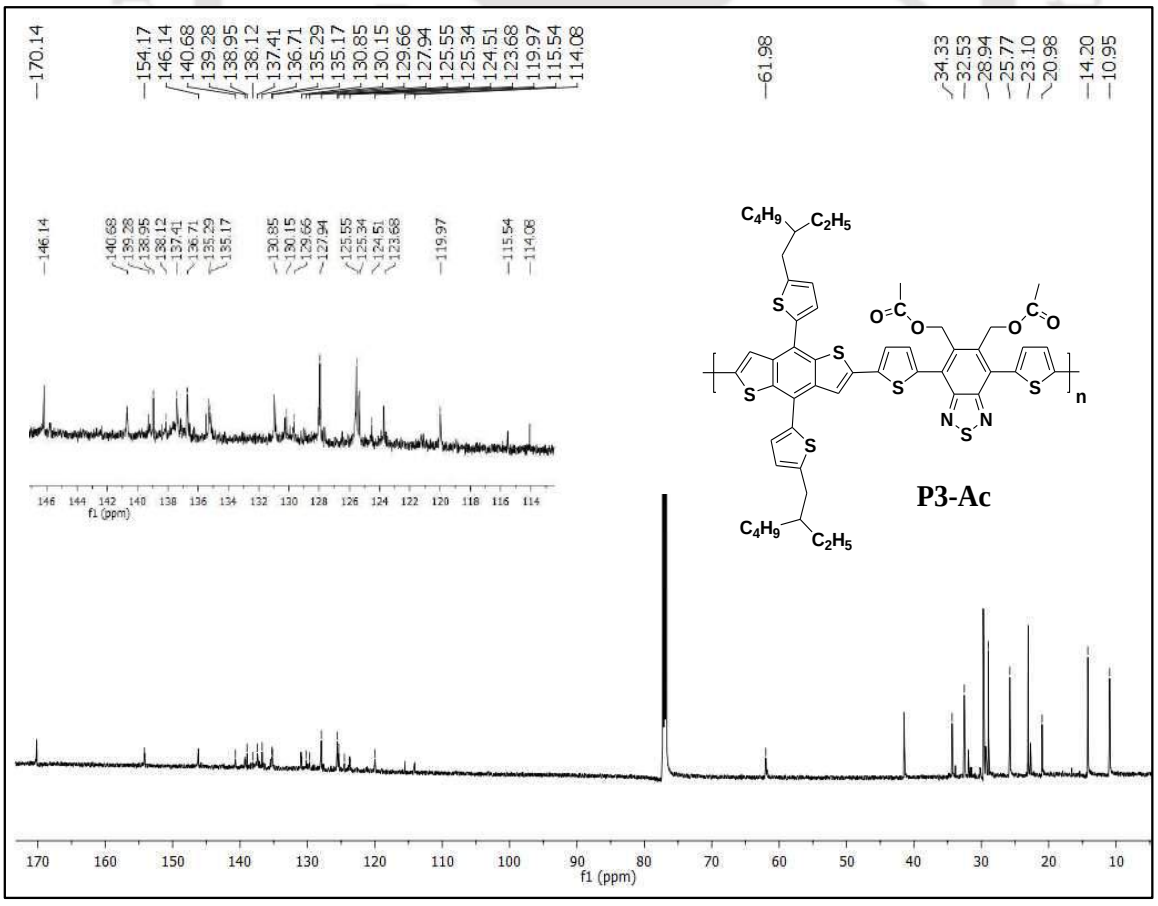

TH-1906_11615303

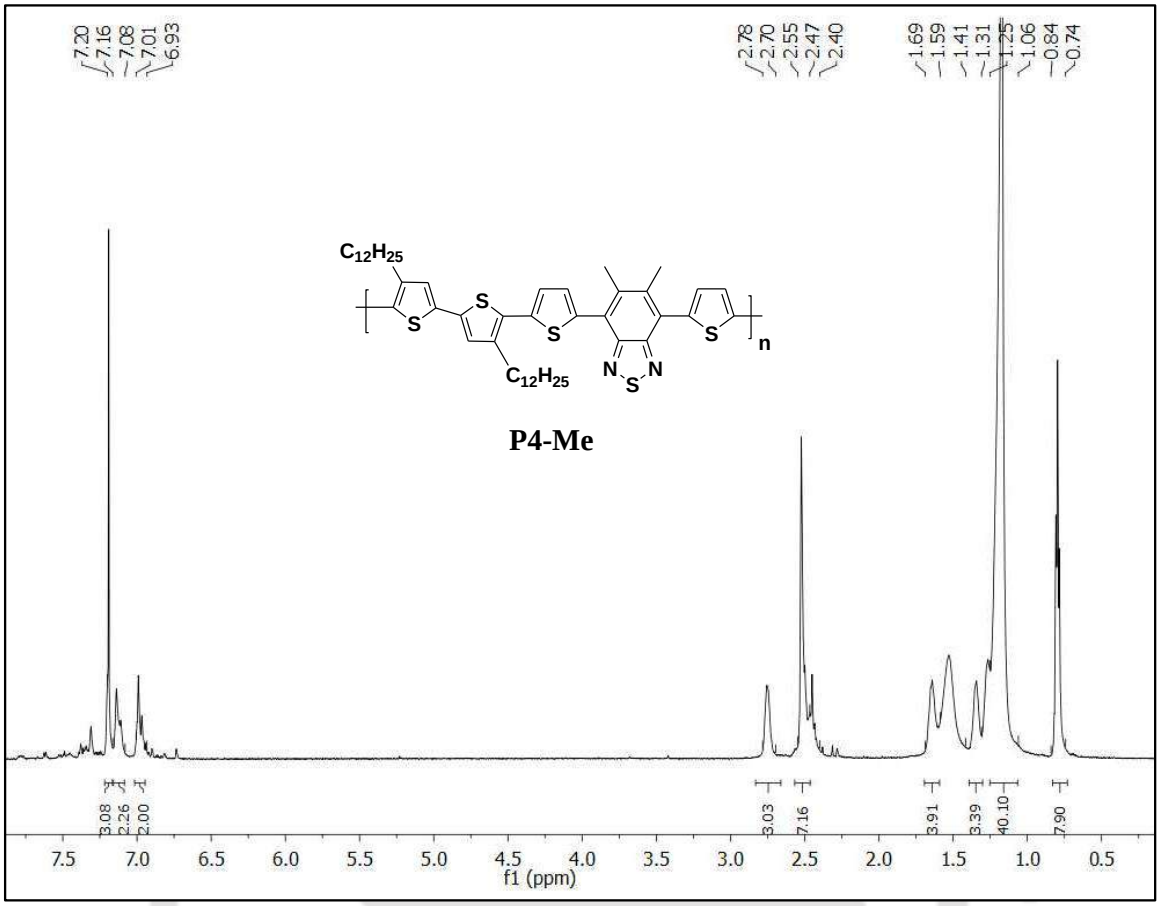

P4-Me

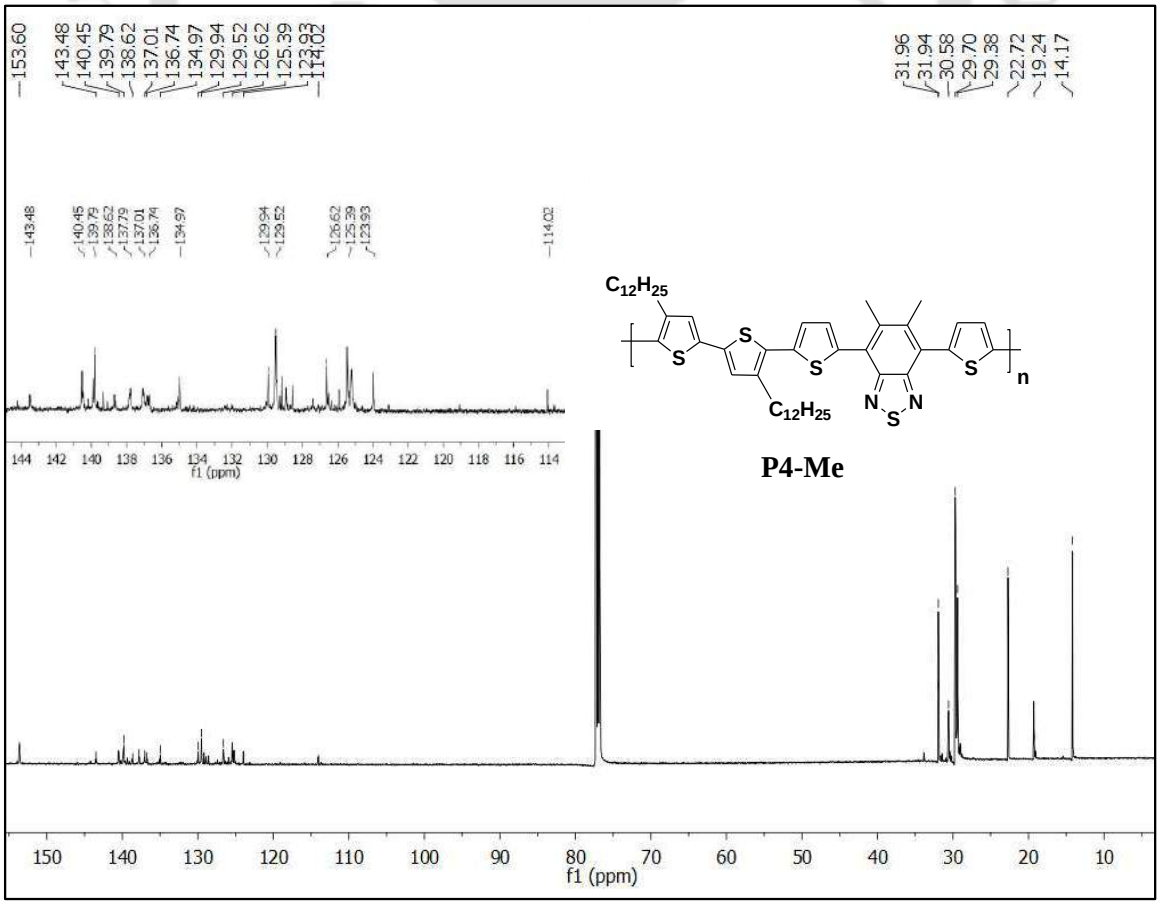

P4-Me

TH-1906_11615303

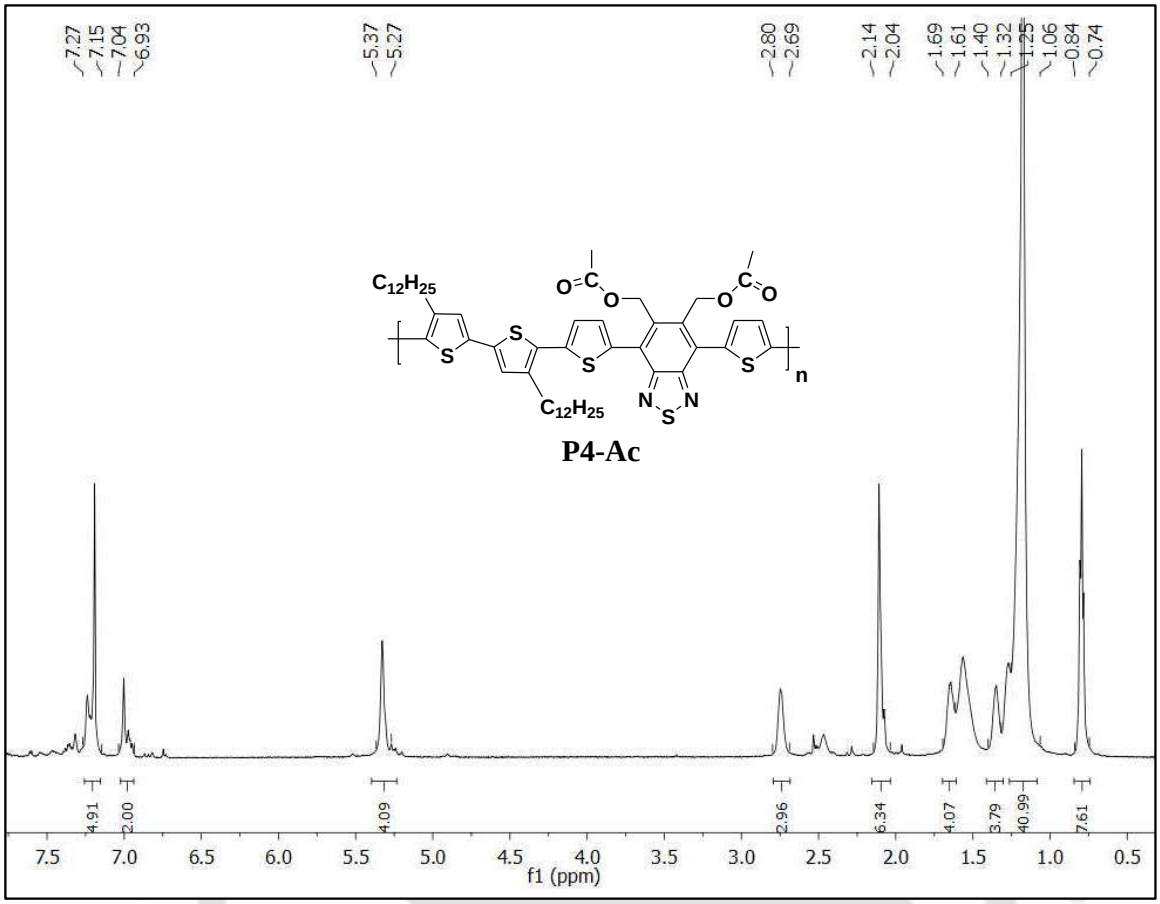

P4-Ac

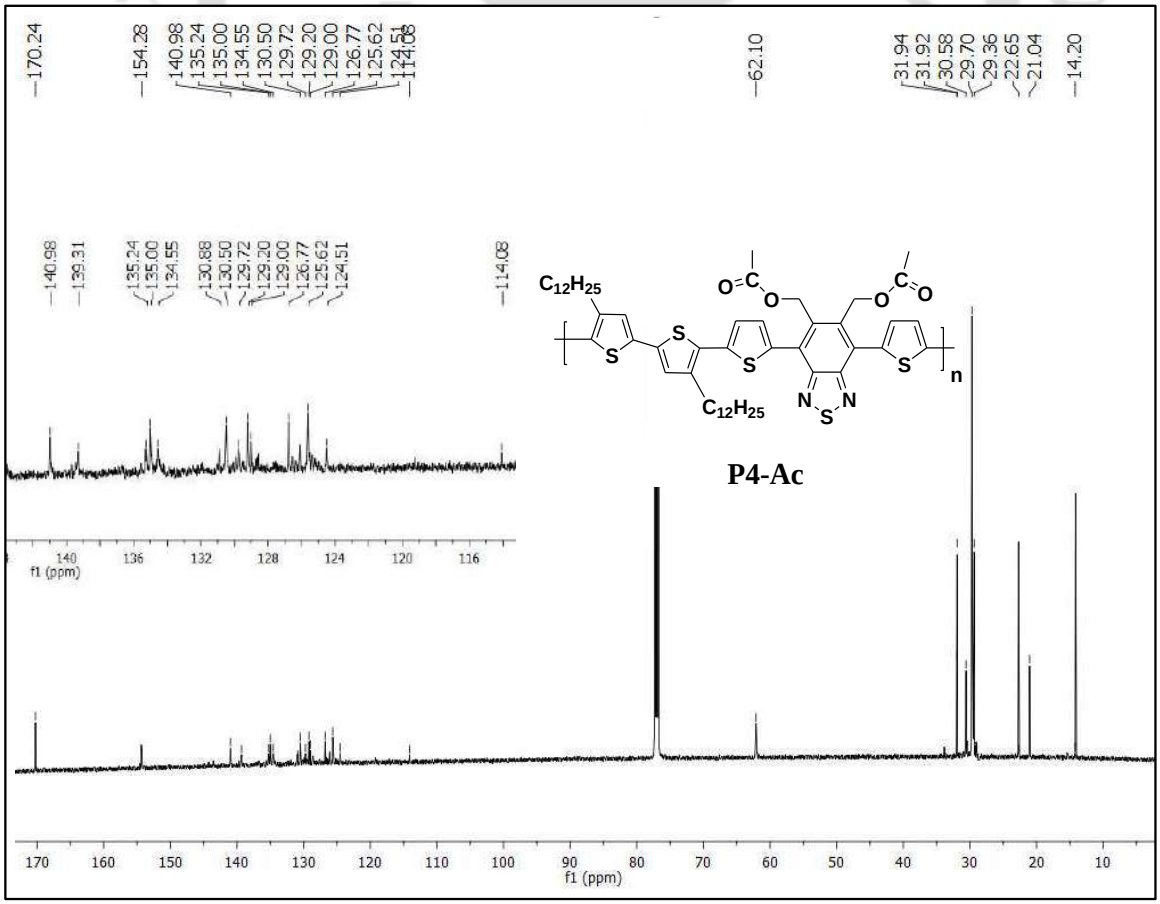

P4-Ac

TH-1906_11615303

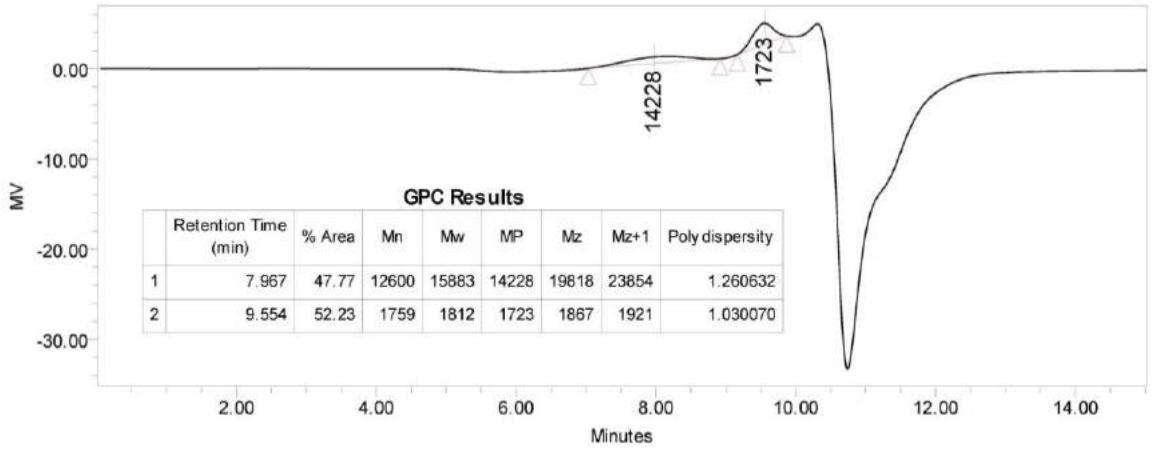

	Retention Time (min)	% Area	Mn	Mw	MP	Mz	Mz+1	Poly dispersity
1	7.967	47.77	12600	15883	14228	19818	23854	1.260632
2	9.554	52.23	1759	1812	1723	1867	1921	1.030070

Figure A4.1 Determination of molecular weight of P1-Me.

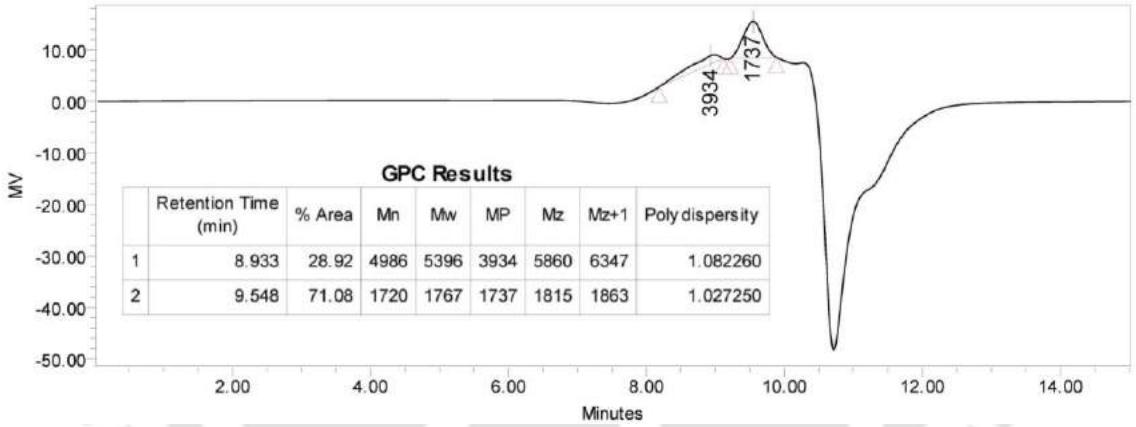

	Retention Time (min)	% Area	Mn	Mw	MP	Mz	Mz+1	Poly dispersity
1	8.933	28.92	4986	5396	3934	5860	6347	1.082260
2	9.548	71.08	1720	1767	1737	1815	1863	1.027250

Figure A4.2 Determination of molecular weight of P1-Ac.

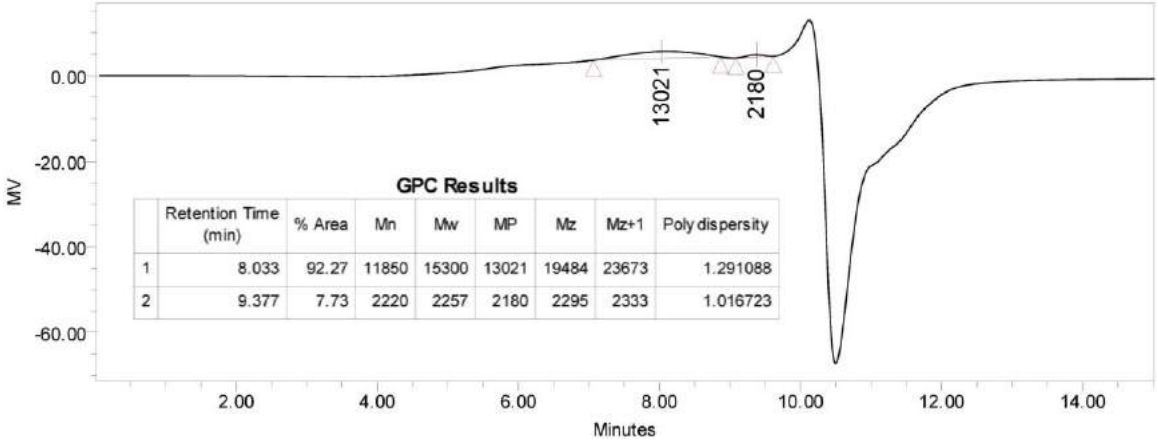

	Retention Time (min)	% Area	Mn	Mw	MP	Mz	Mz+1	Poly dispersity
1	8.033	92.27	11850	15300	13021	19484	23673	1.291088
2	9.377	7.73	2220	2257	2180	2295	2333	1.016723

Figure A4.3 Determination of molecular weight of P2-Me.

TH-1906_11615303

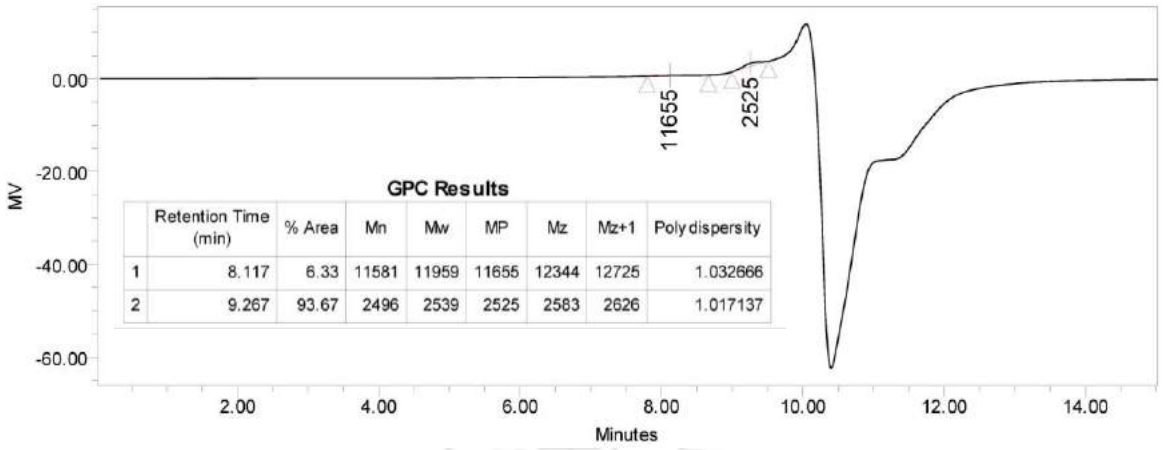

GPC Results

	Retention Time (min)	% Area	Mn	Mw	MP	Mz	Mz+1	Poly dispersity
1	8.117	6.33	11581	11959	11655	12344	12725	1.032666
2	9.267	93.67	2496	2539	2525	2583	2626	1.017137

Figure A4.4 Determination of molecular weight of P2-Ac.

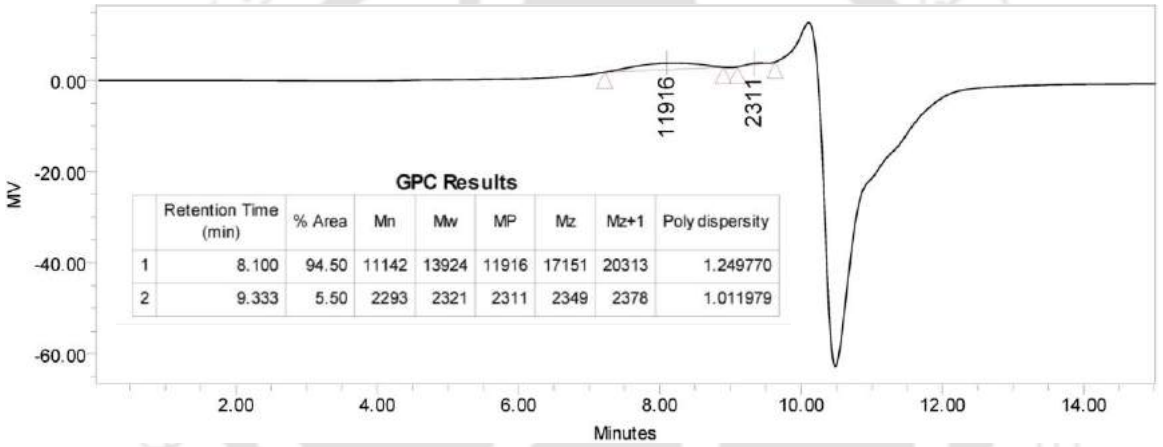

GPC Results

	Retention Time (min)	% Area	Mn	Mw	MP	Mz	Mz+1	Poly dispersity
1	8.100	94.50	11142	13924	11916	17151	20313	1.249770
2	9.333	5.50	2293	2321	2311	2349	2378	1.011979

Figure A4.5 Determination of molecular weight of P3-Me.

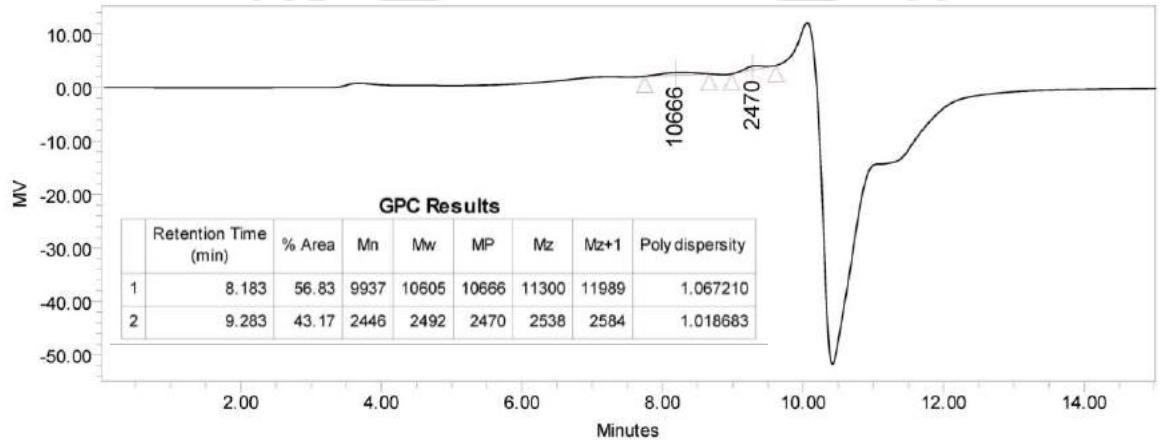

GPC Results

	Retention Time (min)	% Area	Mn	Mw	MP	Mz	Mz+1	Poly dispersity
1	8.183	56.83	9937	10605	10666	11300	11989	1.067210
2	9.283	43.17	2446	2492	2470	2538	2584	1.018683

Figure A4.6 Determination of molecular weight of P3-Ac.

TH-1906_11615303

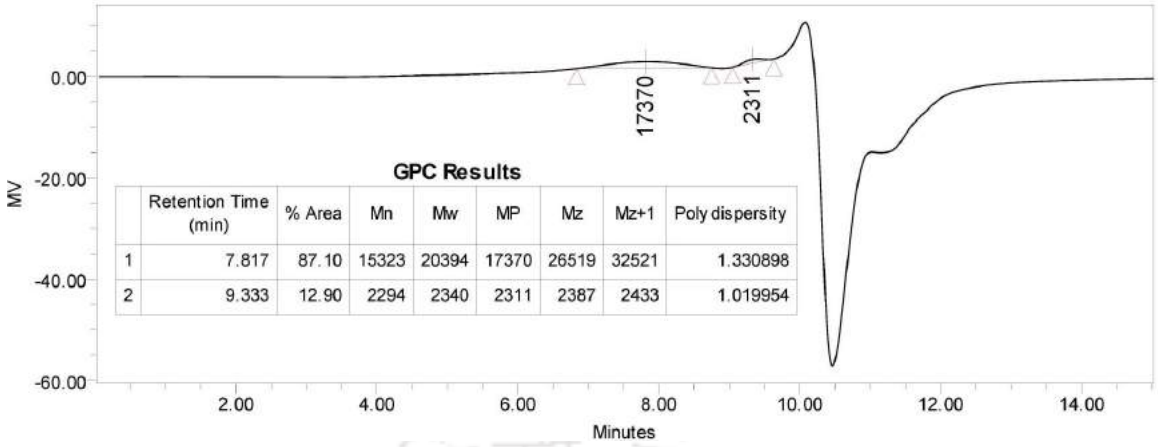

GPC Results

	Retention Time (min)	% Area	Mn	Mw	MP	Mz	Mz+1	Poly dispersity
1	7.817	87.10	15323	20394	17370	26519	32521	1.330898
2	9.333	12.90	2294	2340	2311	2387	2433	1.019954

Figure A4.7 Determination of molecular weight of P4-Me.

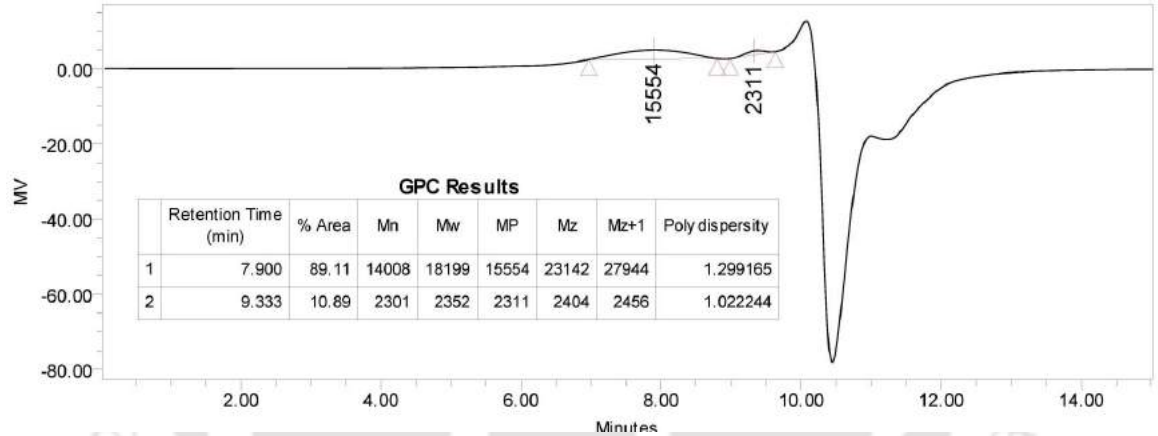

GPC Results

	Retention Time (min)	% Area	Mn	Mw	MP	Mz	Mz+1	Poly dispersity
1	7.900	89.11	14008	18199	15554	23142	27944	1.299165
2	9.333	10.89	2301	2352	2311	2404	2456	1.022244

Figure A4.8 Determination of molecular weight of P4-Ac.

TH-1906_11615303

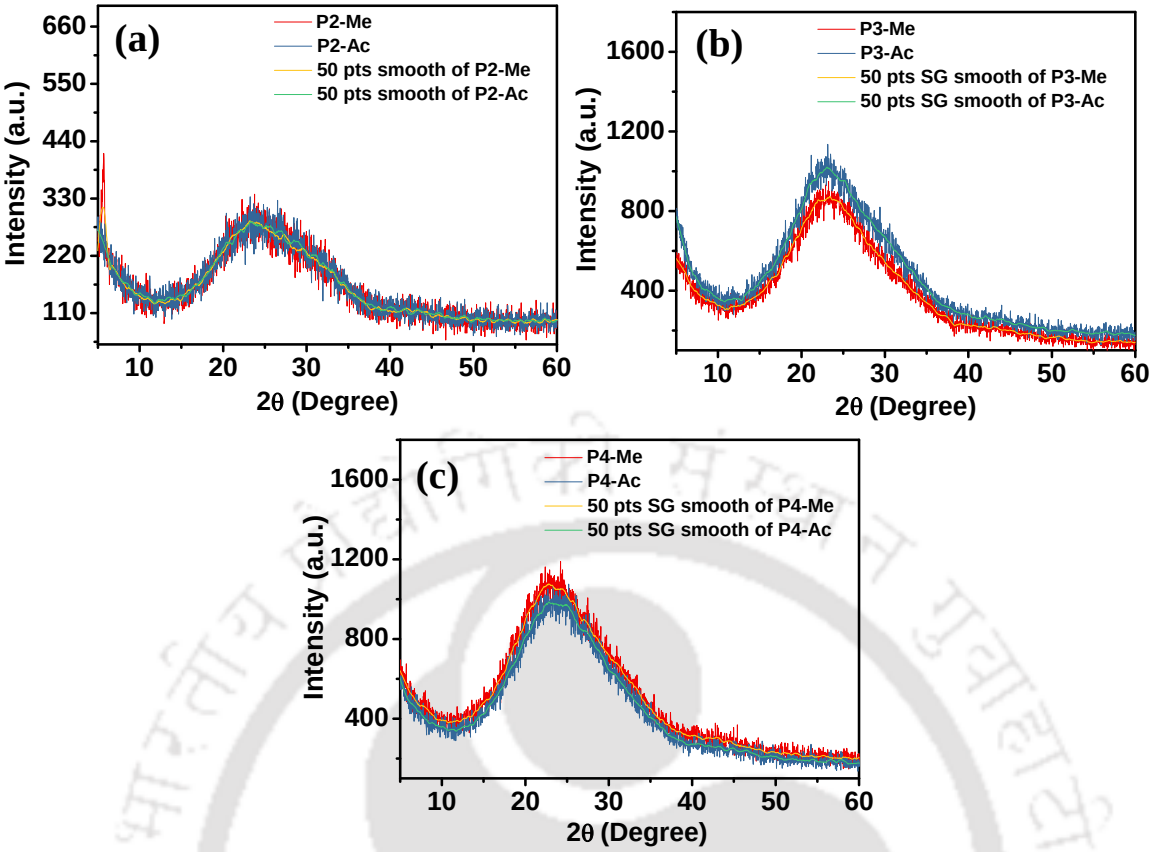

Figure A4.9 Thin film X-ray diffraction patterns with fit files confirming better π-π stacking in ester functionalized polymers with low dihedral angle along conjugation main chain (a) P2-Me and P2-Ac (b) P3-Me and P3-Ac (c) P4-Me and P4-Ac.

TH-1906_11615303

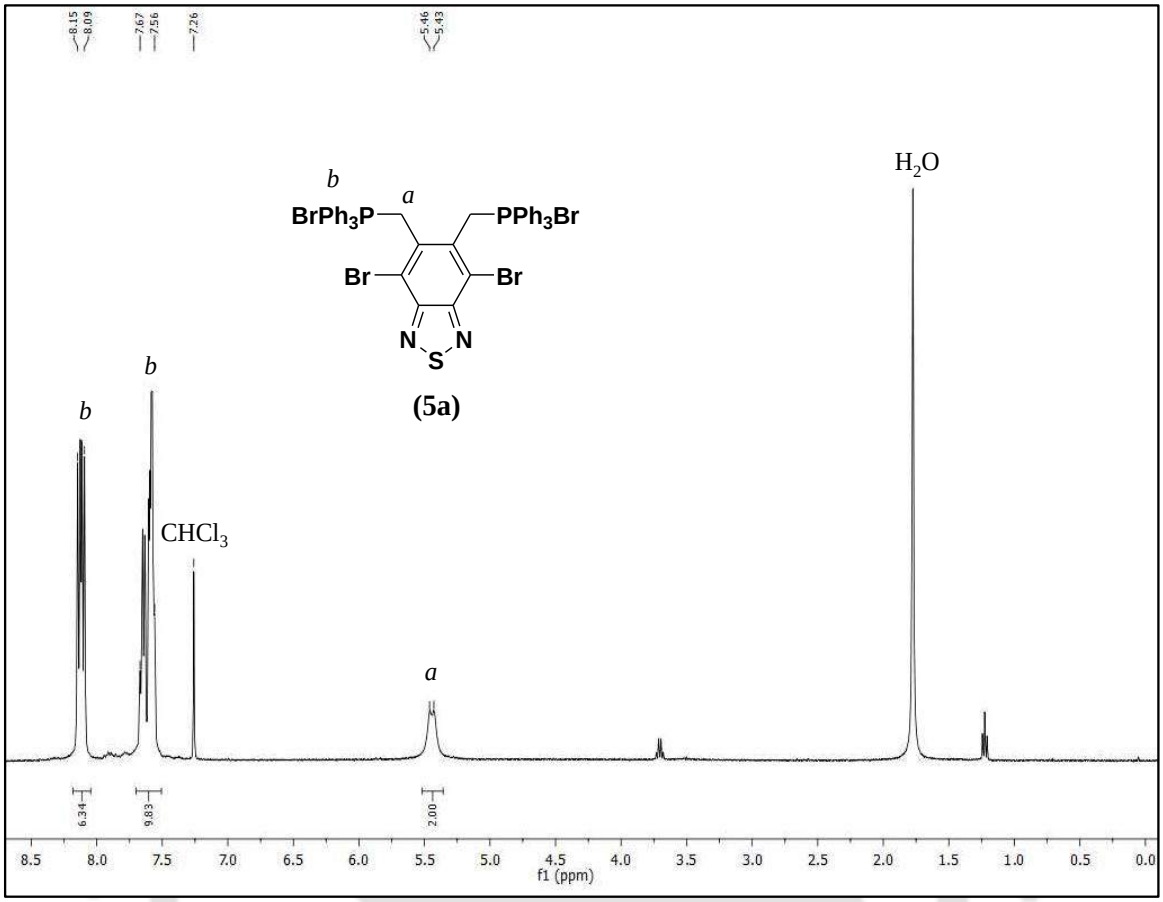

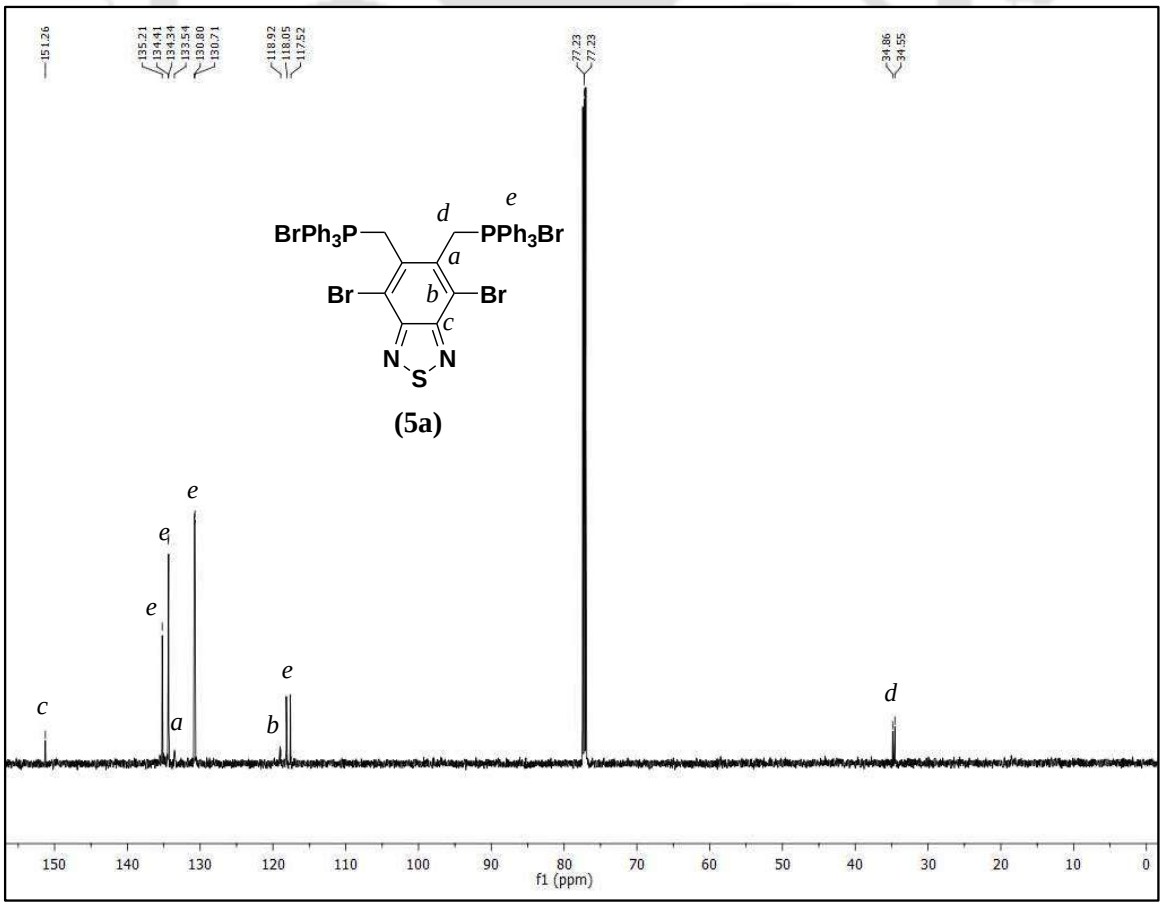

TH-1906_11615303

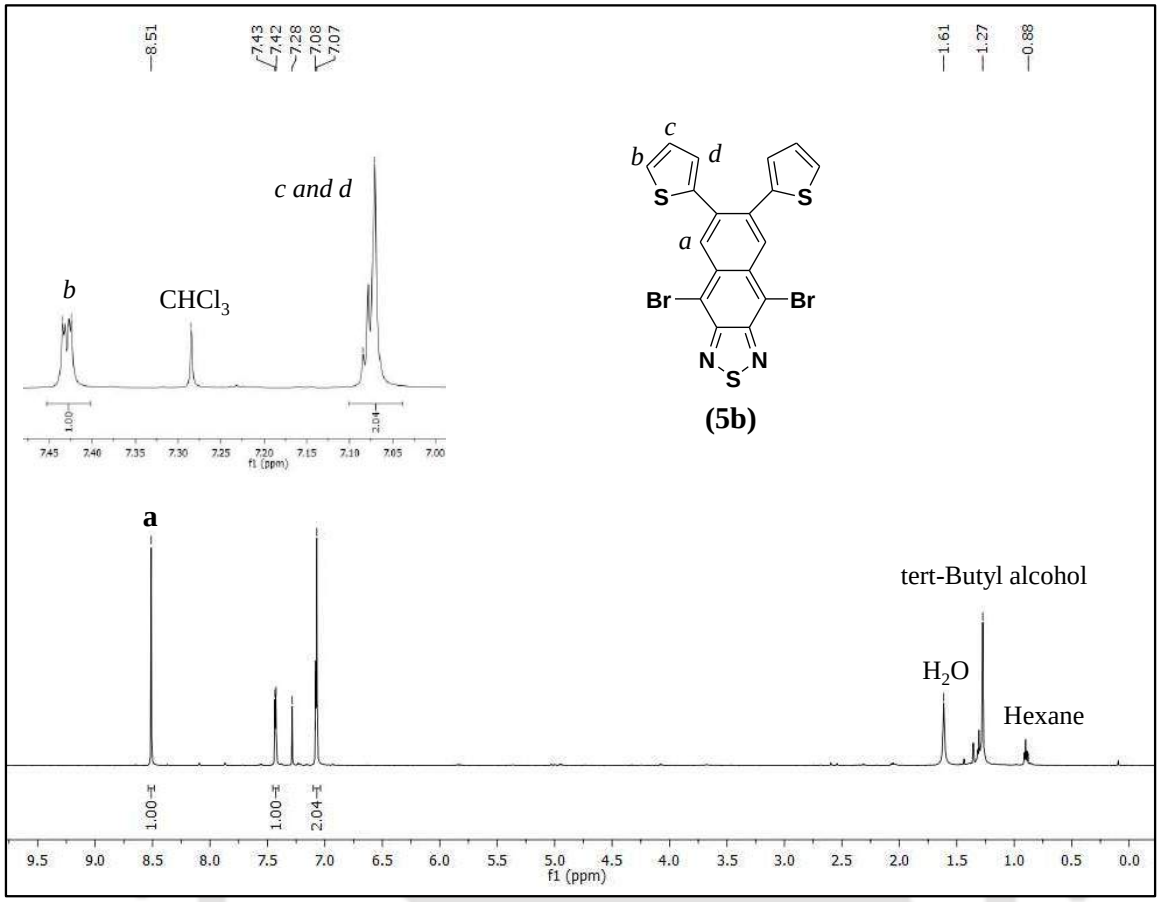

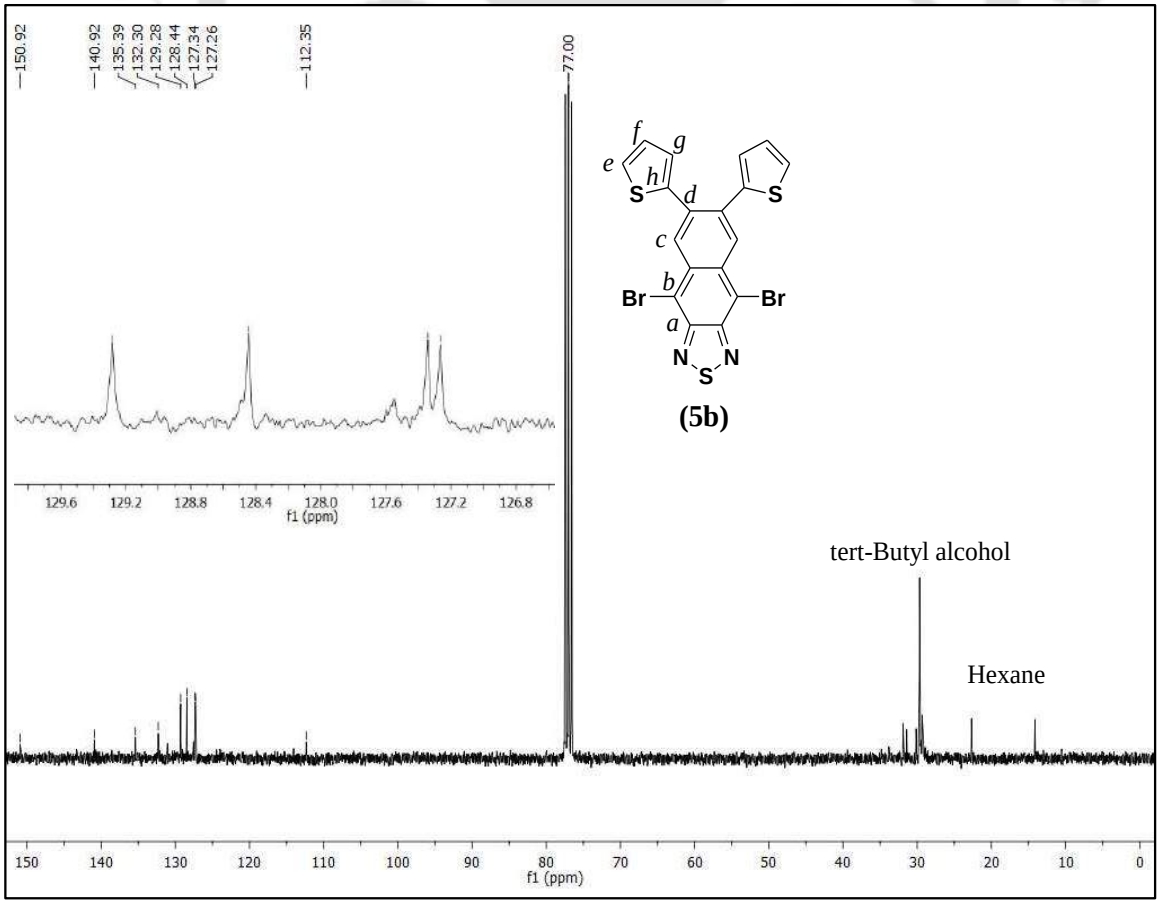

TH-1906_11615303

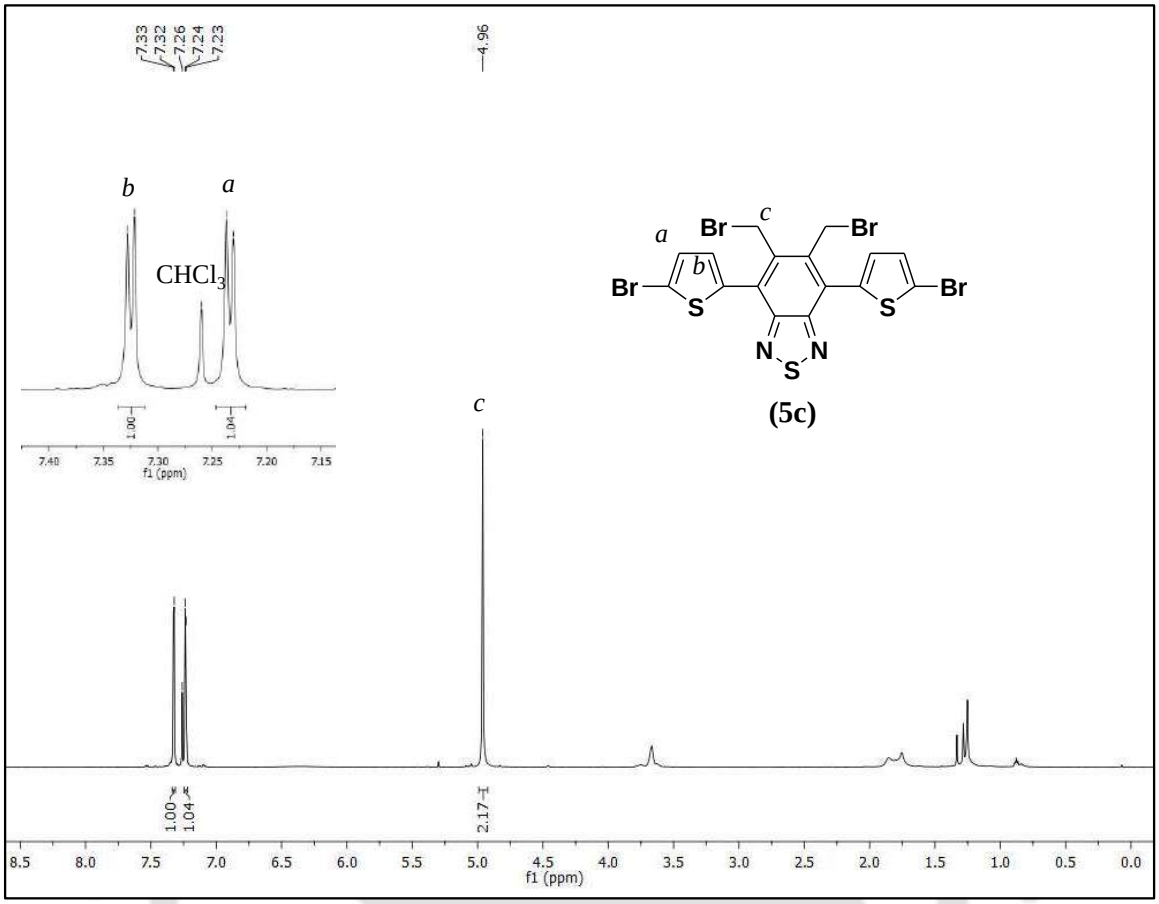

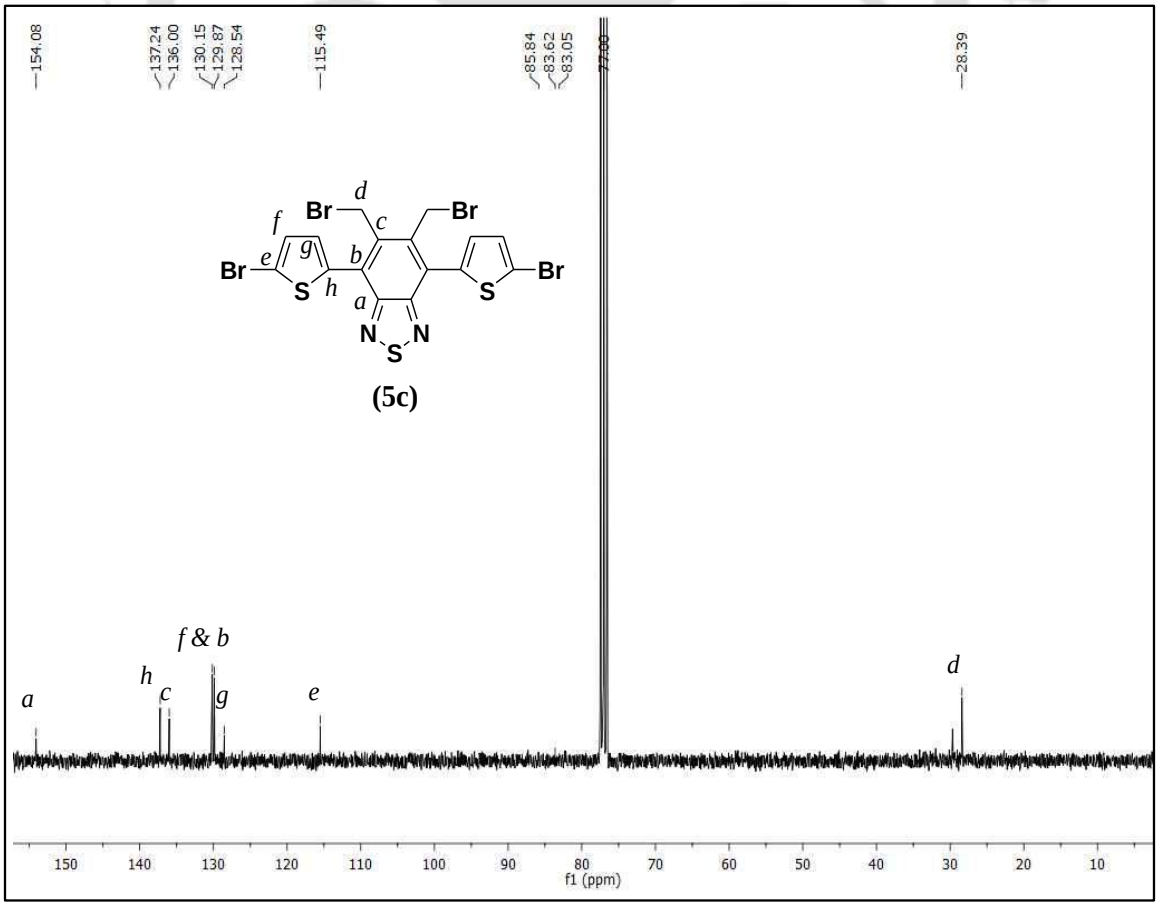

TH-1906_11615303

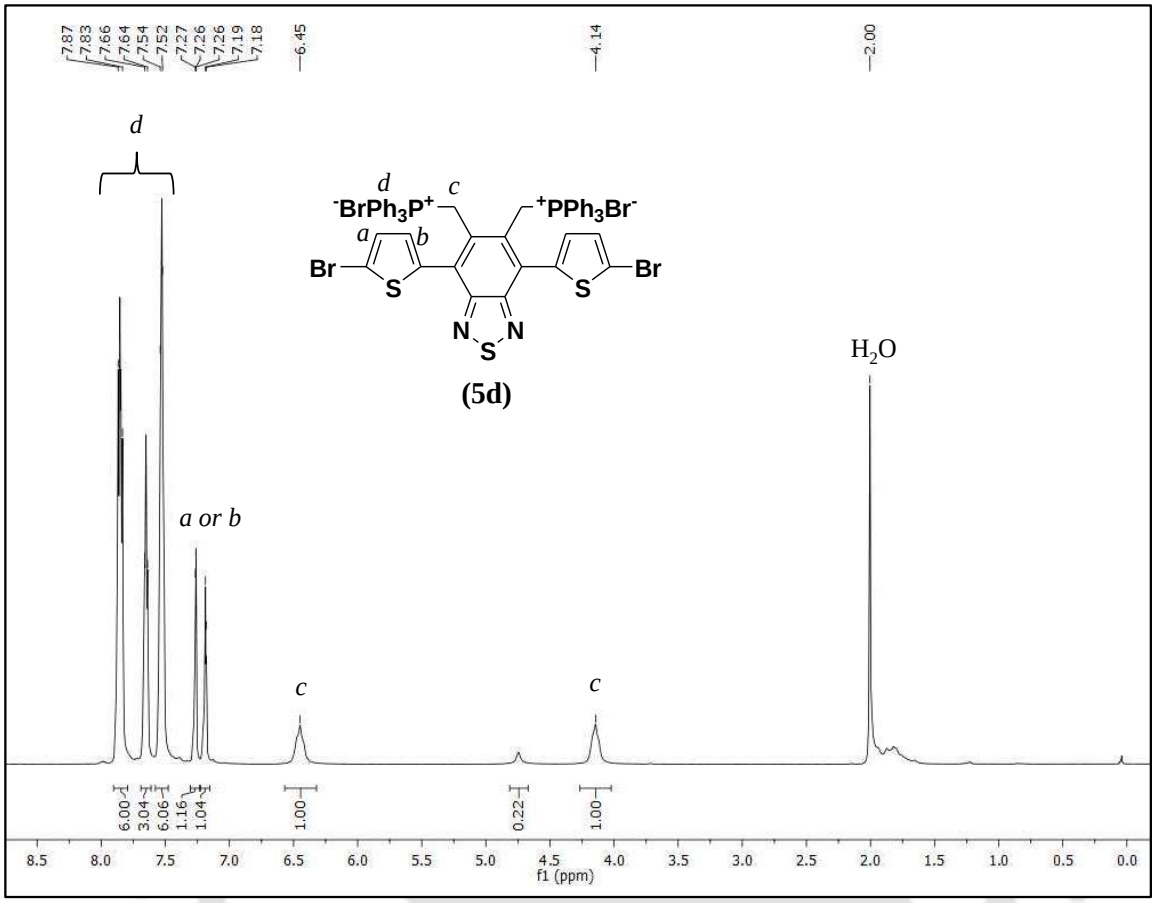

(5d)

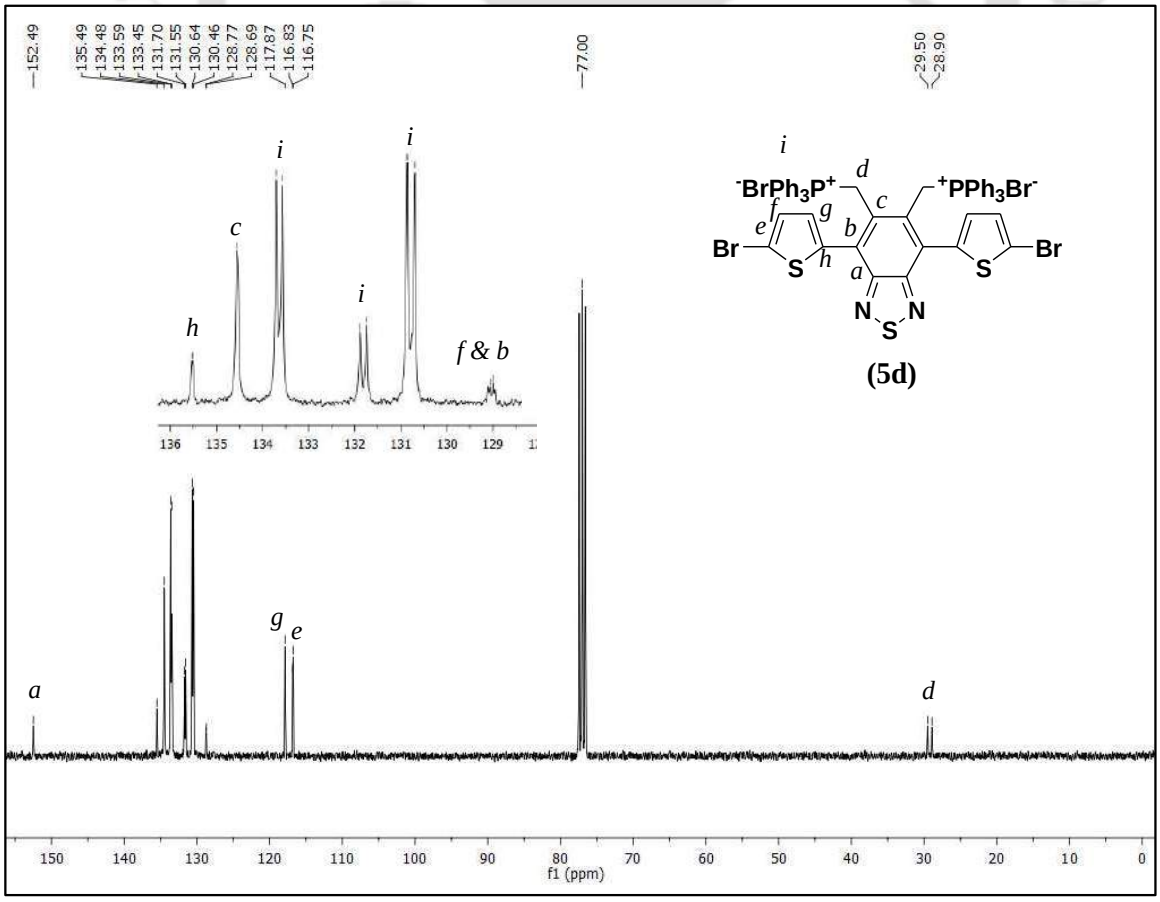

(5d)

TH-1906_11615303

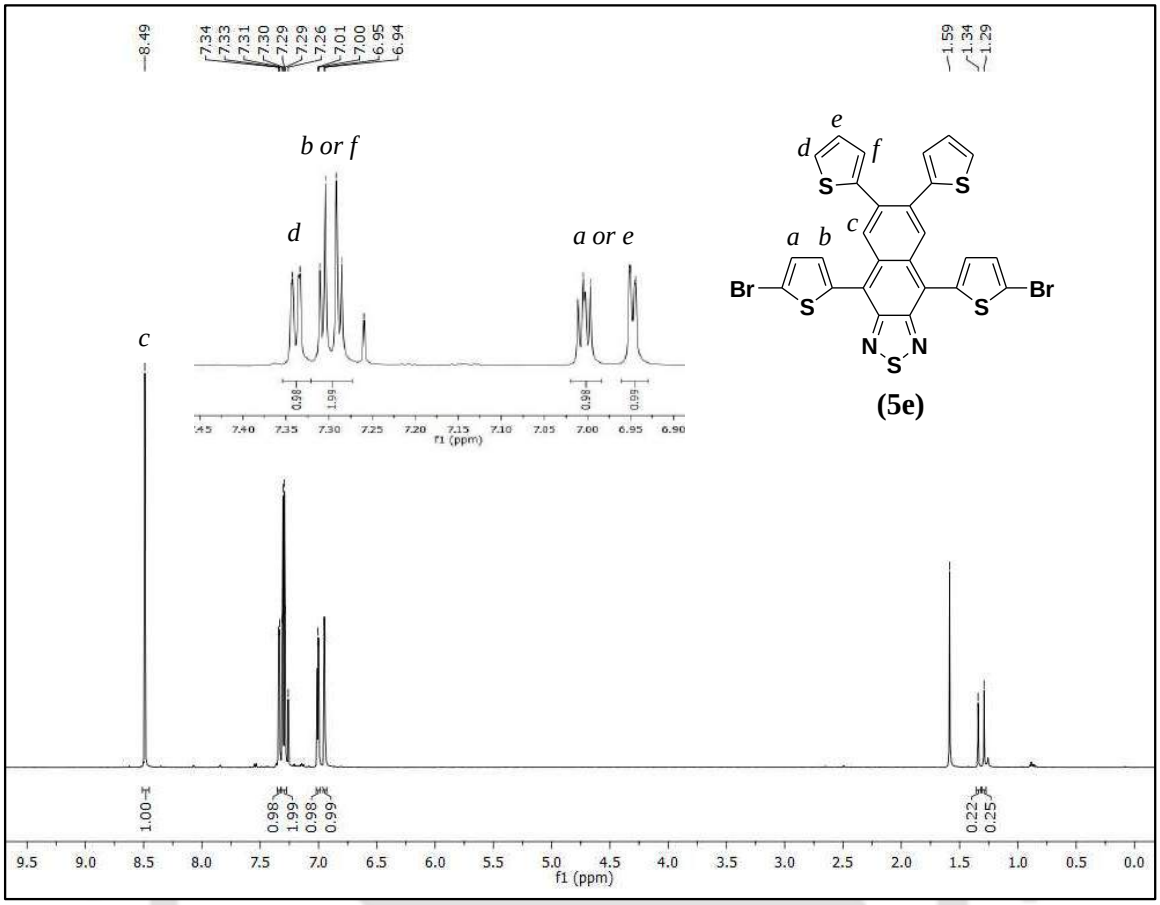

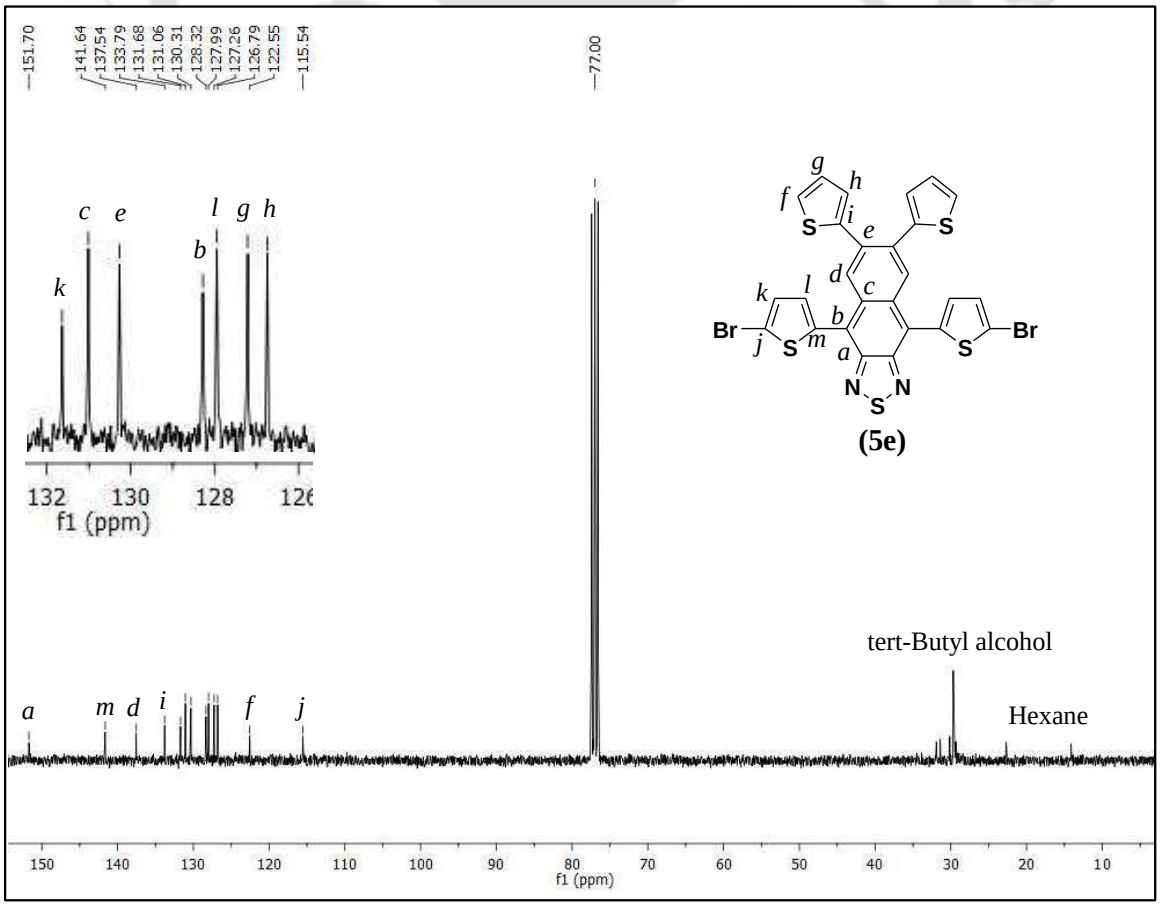

TH-1906_11615303

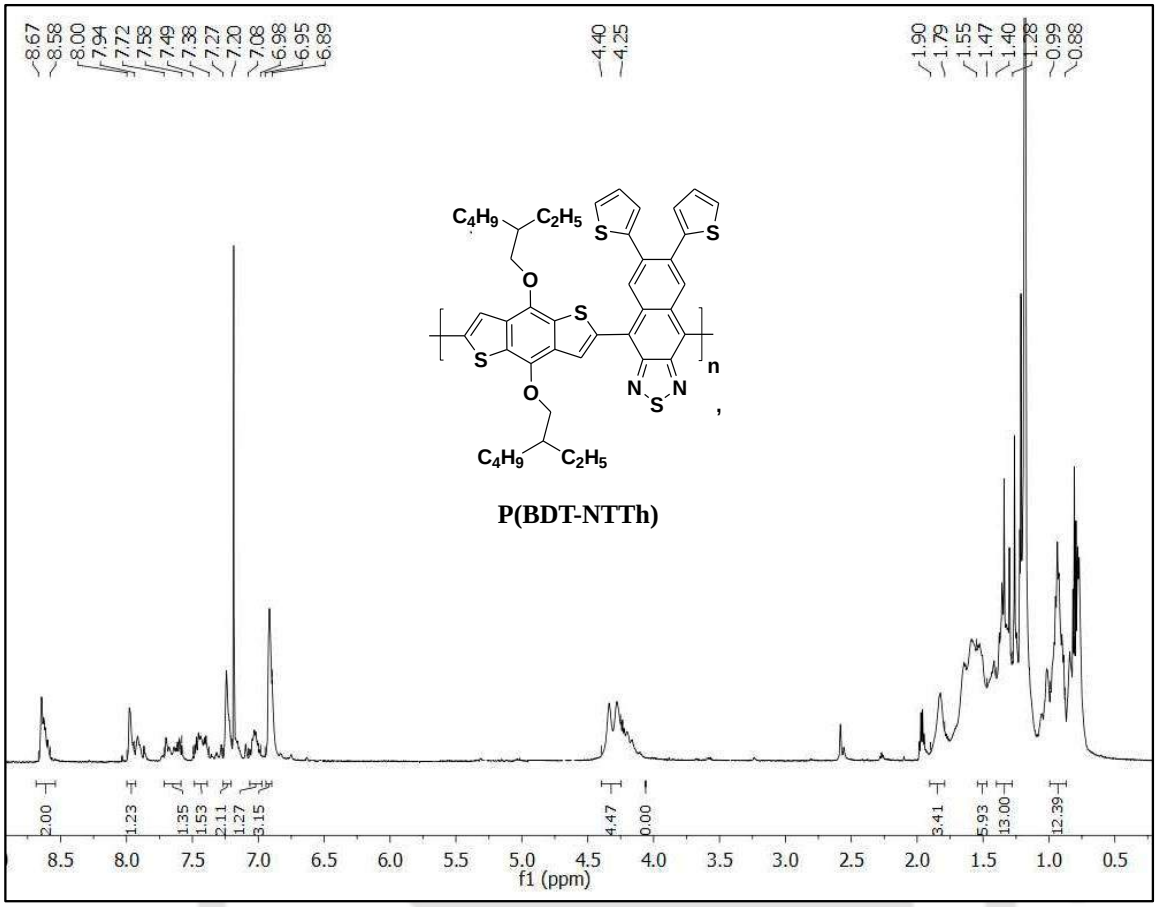

P(BDT-NTTh)

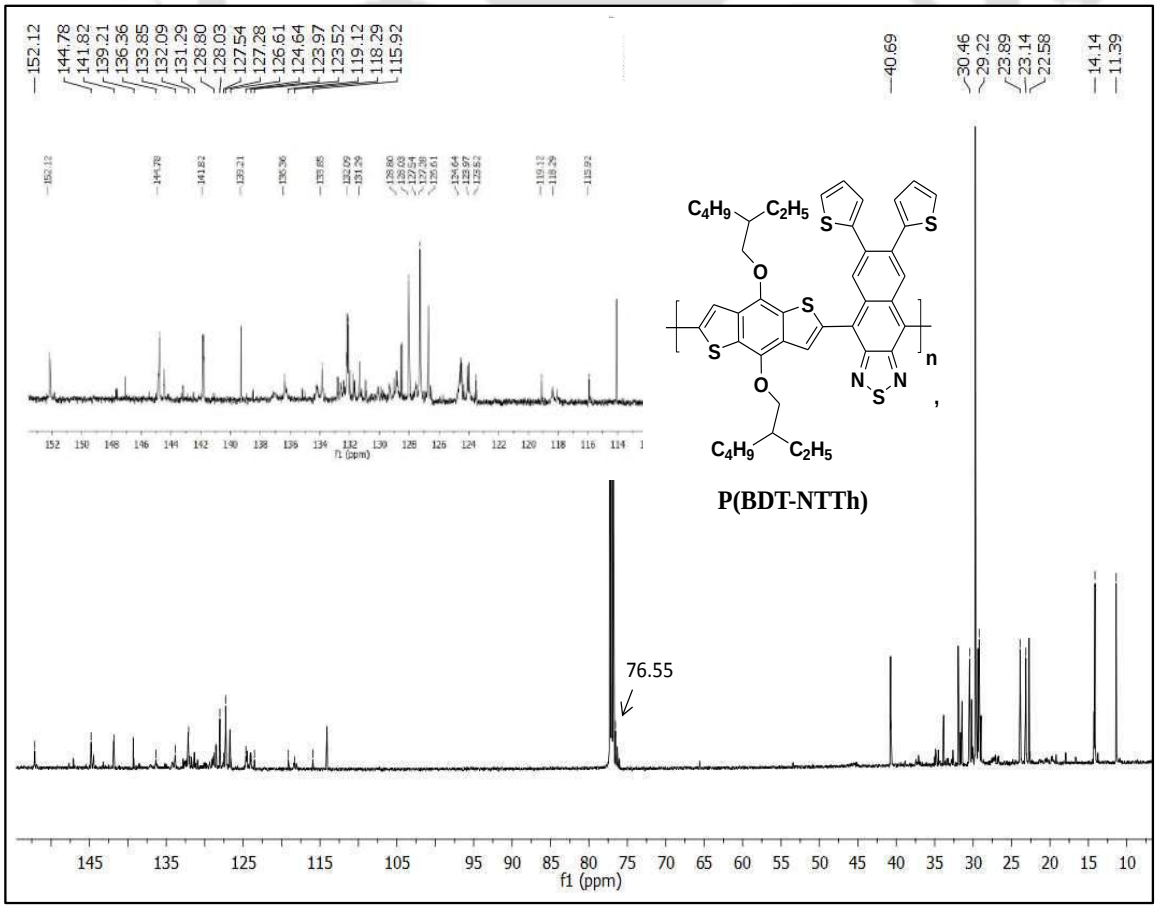

P(BDT-NTTh)

TH-1906_11615303

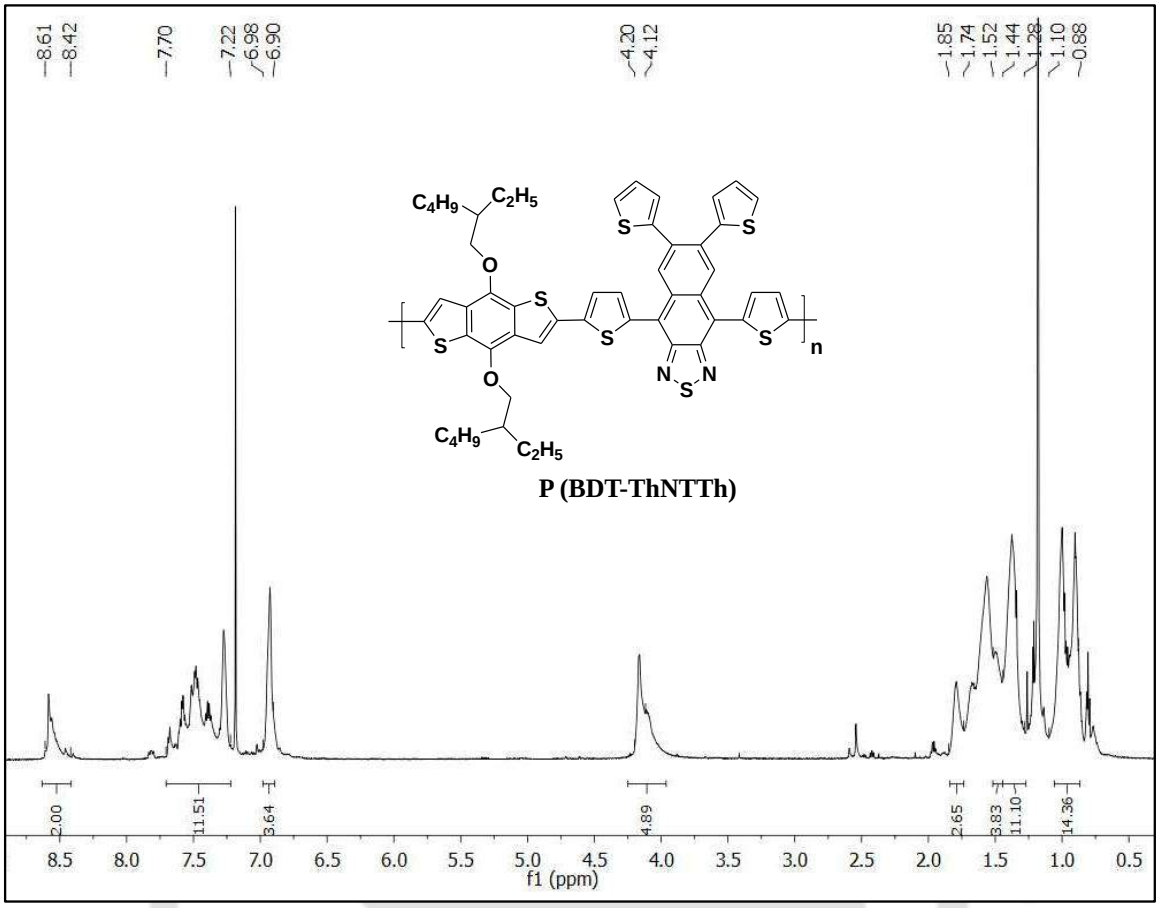

P (BDT-ThNTTh)

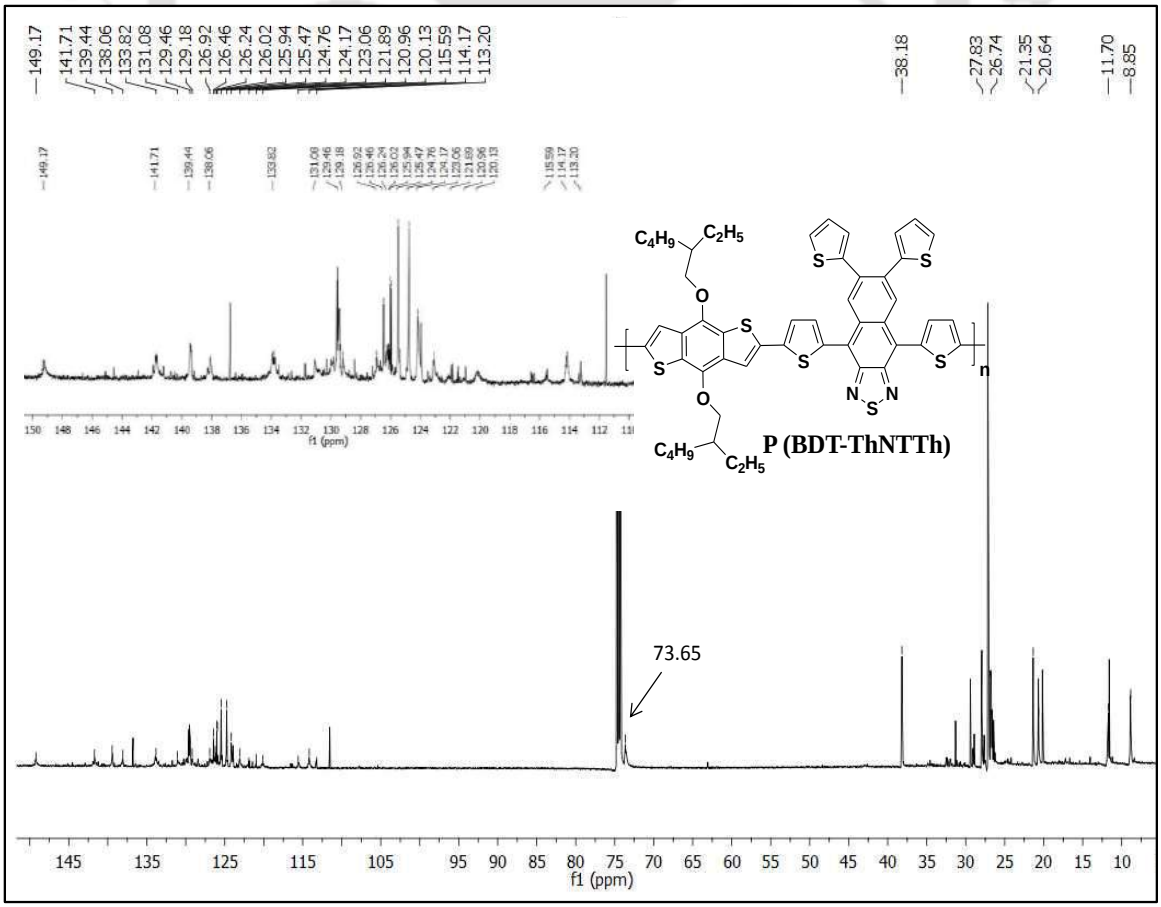

P (BDT-ThNTTh)

TH-1906_11615303

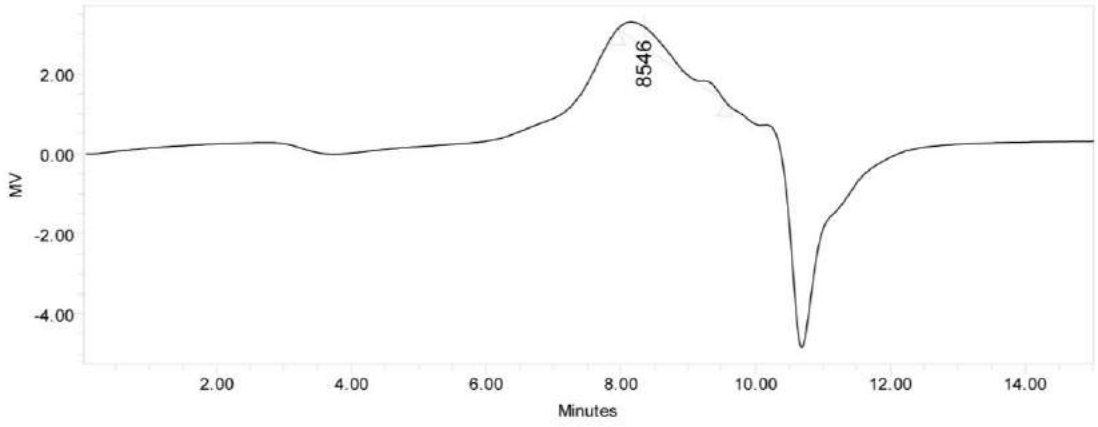

GPC Results

	Retention Time (min)	% Area	Mn	Mw	MP	Mz	Mz+1	Poly dispersity
1	8.350	100.00	5657	7393	8546	8666	9532	1.306900

Figure A5.1 Determination of molecular weight of P(BDT-NTTh).

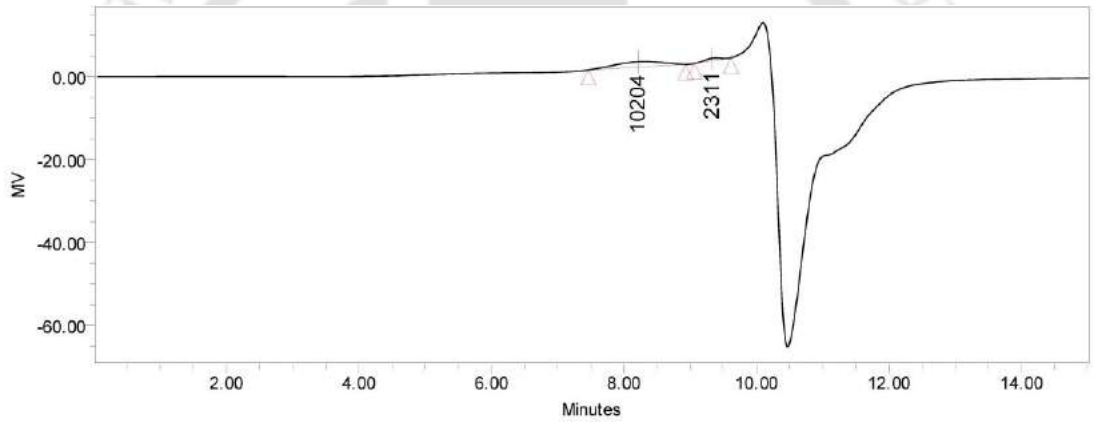

GPC Results

	Retention Time (min)	% Area	Mn	Mw	MP	Mz	Mz+1	Poly dispersity
1	8.217	86.47	9544	11116	10204	12873	14647	1.164697
2	9.333	13.53	2327	2365	2311	2404	2443	1.016433

Figure A5.2 Determination of molecular weight of P(BDT-ThNTTh).

TH-1906_11615303

Thesis Overview

A wide variety of CPs are being used for polymer solar cell (PSC) and other optoelectronic devices. In PSC polymers suffer from low PCE and photo degradation nature of them on exposure to UV light makes them less suitable and demands much extensive study on them in terms of structural changes and/or addition of other entity to solve it. In addition extensive study in past decade on structural tunability on polymer main chain/side chain, along with device engineering helps researcher to achieve a PCE of 13% for PSC. Here effort has been given to investigate further, on structural change leading to change in optoelectronic property by synthesizing newer acceptor units using with 5,6-position of BT. Synthesized acceptor units for donor (D)-acceptor (A)-based conjugated polymers used in photovoltaic devices are 4,9-dibromo-6,7-di(thiophen-2-yl)naphtho[2,3-c][1,2,5]thiadiazole(NT-Th), 4,9-bis(5-bromothiophen-2-yl)-6,7-di(thiophen-2-yl)naphtho[2,3-c][1,2,5]thiadiazole (Th-NT-Th) and (4,7-bis(5-bromothiophen-2-yl)benzo[c][1,2,5]thiadiazole-5,6-diyl)bis(methylene)diacetate. Further efforts have been given towards durability measures for blend of thiophene containing donor polymer and acceptor used for solar cell fabrication (such as PCBM), by preparing composites with MWCNT. Such systems can be used to bring high performance material with improved photo stability for future optoelectronic application.

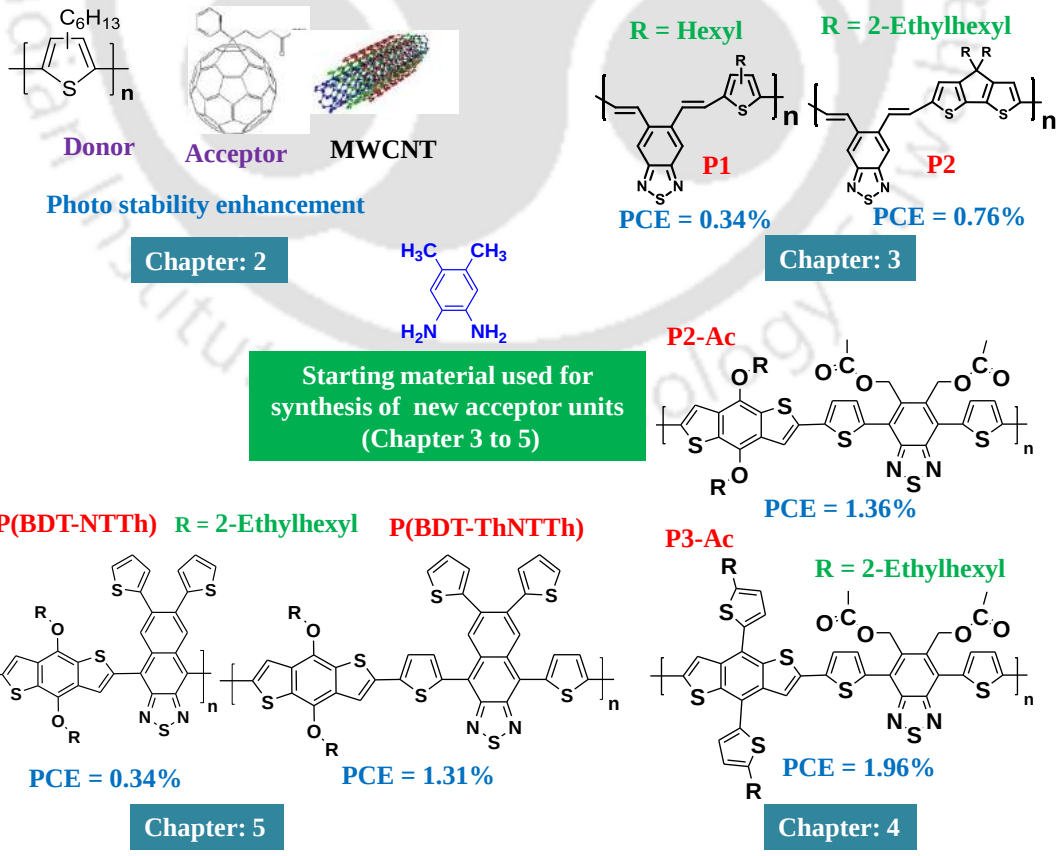

TH-1906_11615303

List of publications

1. **Ratha, R**.; Goutam, P. J.; Iyer, P. K. Photo stability enhancement of poly(3-hexylthiophene)-PCBM nano composites by addition of multi walled carbon nanotubes under ambient conditions, *Org. Electron.* **2014**, *15*, 1650-1656.
2. **Ratha, R**.; Singh, A.; Raju, T. B.; Iyer, P. K. Insight into the synthesis and fabrication of 5,6-*alt*-benzothiadiazole based D-π-A conjugated co-polymers for bulk-heterojunction solar cell, *Polym. Bull*. **2017**, DOI:10.1007/s00289-017-2193-x.
3. **Ratha, R**.; Afroz, M. A.; Gupta, R. K.; Iyer, P. K. Substituting non-conjugating ester group into side chain of benzothiadiazole improves optical, electrochemical properties, morphology of active layer and solar cell performance of D-A polymer for photovoltaics (to be communicated).
4. **Ratha, R**.; Singh, A.; Afroz, M. A.; Gupta, R. K.; Iyer, P. K. 6,7-Di(thiophen-2-yl)naphtho[2,3-c][1,2,5]thiadiazole and 4,6,7,9-tetra(thiophen-2-yl)naphtho[2,3-c][1,2,5]thiadiazole as new acceptor units for D-A type co-polymer towards fabrication of polymer solar cell (to be communicated).

List of conferences attended

1. **Ratha, R**.; Goutam, P. J.; Iyer, P. K. Enhancing the photo stability of poly-(3-hexylthiophene)-PCBM by preparing composites with multiwalled carbon nanotube (International Symposium on Advances in Chemical Sciences (30th January 2012, IIT Guwahati, India) (poster).
2. **Ratha, R**.; Goutam, P. J.; Singh, D. K.; Iyer, P. K. Enhancing the photostability of poly-(3-hexylthiophene)-PCBM by preparing composites with carbon nanotubes (^{11}th International Symposium on Functional π-Electron Systems (Fπ-11), 2-7 June, 2013, Palais des Congrès in Arcachon, France (poster).
3. **Ratha, R**.; Singh, A.; Raju, T. B.; Iyer, P. K. An insight into synthesis of 5, 6-*alt*-benzothiadiazole based D-π-A CPs and their potential as donor polymer for solar cells (4th International Conference on Advanced Nanomaterials and Nanotechnology 8-11 December 2015, IIT Guwahati, India) (poster).
4. **Ratha, R**.; Raju, T. B.; Yedla, S.; Iyer, P. K. Photodegradation pattern of P3HT, PCPDT, 3HT/CPDT based poly(o-aryl-vinyl) as donor material in solar cells and

TH-1906_11615303

their photostability enhancement using π-electron rich MWCNT and/or PCBM (MRSI North East Symposium on Advanced Materials for Sustainable Application 18-20 February 2016, CSIR Jorahat, India) (poster).

5. **Ratha, R**.; Singh, A.; Iyer, P. K. Synthesis of 6,7-di(thiophen-2-yl)naphtho[2,3-c][1,2,5]thiadiazole as a new acceptor for D-A polymer towards fabrication of bulk heterojunction solar cell (Frontiers in Chemical Science 08-10 Decemebr 2016, IIT Guwahati, India) (poster).
6. **Ratha, R**.; Afroz, M. A.; Gupta, R. K.; Iyer, P. K. Inserting non-conjugating ester group into side chain of benzothiadiazole improves optical, electrochemical, crystalline property and photo stability of D-A polymer used for solar cell (20th CRSI National Symposium in Chemistry 02-05 February 2017, Guwahati University, India) (poster).
7. **Ratha, R**.; Afroz, M. A.; Gupta, R. K.; Iyer, P. K. Implementing new strategy to improve durability of D-A and D-π-A type conjugated polymers used for solar cell application (Research Conclave-17, 16-19 March 2017, IIT Guwahati, India) (poster).
8. **Ratha, R**.; Afroz, M. A.; Gupta, R. K.; Iyer, P. K. Implementing new strategy to improve durability of D-A and D-π-A type conjugated polymers used for solar cell application (Reflux-2017, 24 to 26 March 2017, IIT Guwahati, India) (poster).

TH-1906_11615303

Shockley–Queisser (S-Q) limit

The Shockley–Queisser limit or Shockley Queisser Efficiency Limit (first calculated by William Shockley and Hans-Joachim Queisser at Shockley Semiconductor in 1961) refers to the maximum theoretical efficiency of a solar cell using a single p-n junction. It says that the maximum solar conversion efficiency is around 33.7% for a single p-n junction photovoltaic cell, assuming typical sunlight conditions (unconcentrated, AM 1.5 solar spectrum) and this maximum occurs at a band gap of 1.34 eV. Shockley–Queisser limit not applicable for tandem cells and the corresponding limit is 86.8% using concentrated sunlight). The most popular solar cell material, silicon, has a less favorable band gap of 1.1 eV, resulting in a maximum efficiency of about 32%. Modern commercial mono-crystalline solar cells produce about 24% conversion efficiency; the losses are mainly due to reflection off the front of the cell and light blockage from the thin wires on the cell surface.

Similarly the maximum open circuit voltage limit of a p-n junction solar cell can be less than 3 volt for a semiconductor with band gap of 3 eV and follow the pattern as show in figure.

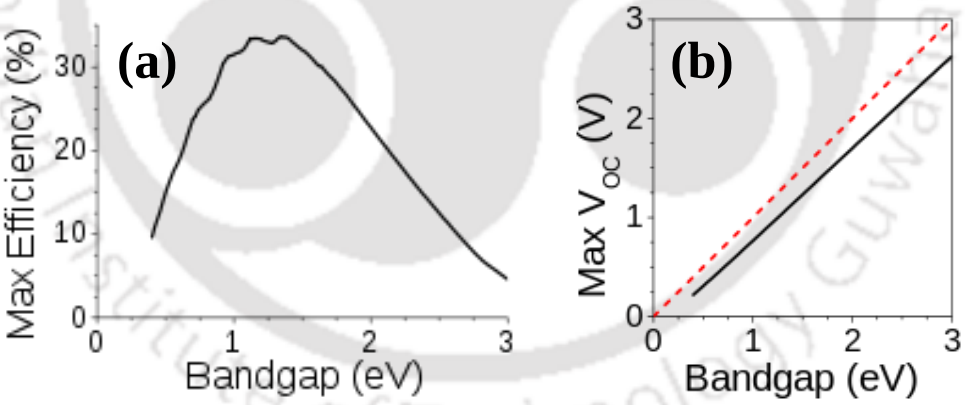

Figure 1. (a) Shockley-Queisser efficiency limit (b) the limit for open-circuit voltage in the Shockley-Queisser model. The red dotted line shows that this voltage is always below the band gap. This voltage is limited by recombination (Figure taken from e-source).

TH-1906_11615303

Future Prospective

Based on the presented thesis, it is very important to address the future prospective of the synthesized acceptor units and D-A polymers. Following listed research work can be carried forward in future to make the design strategy, synthesize acceptor units or conjugated polymer more viable so far as PSC or other optoelectronic applications are concerned.

F1. Ternary and tandem device using synthesized CPs

Synthesized polymers in this thesis though did not provide a high PCE with BHJ solar cell devices, but polymer such as P2-Ac and P3-Ac can be used to fabricate ternary active layer BHJ-PSC and tandem configuration solar cell devices. Because absorption range for above listed polymers are complimentary (~400 to 600 nm) to the UV-visible spectra of CP with which high PCE (~10 to 12%) have been achieved in last few years such as PTB7, PTB7-DT or PBDTT-S-TT-SF with absorption maximum ranging from 600 nm to 800 nm (as shown in Figure F1).

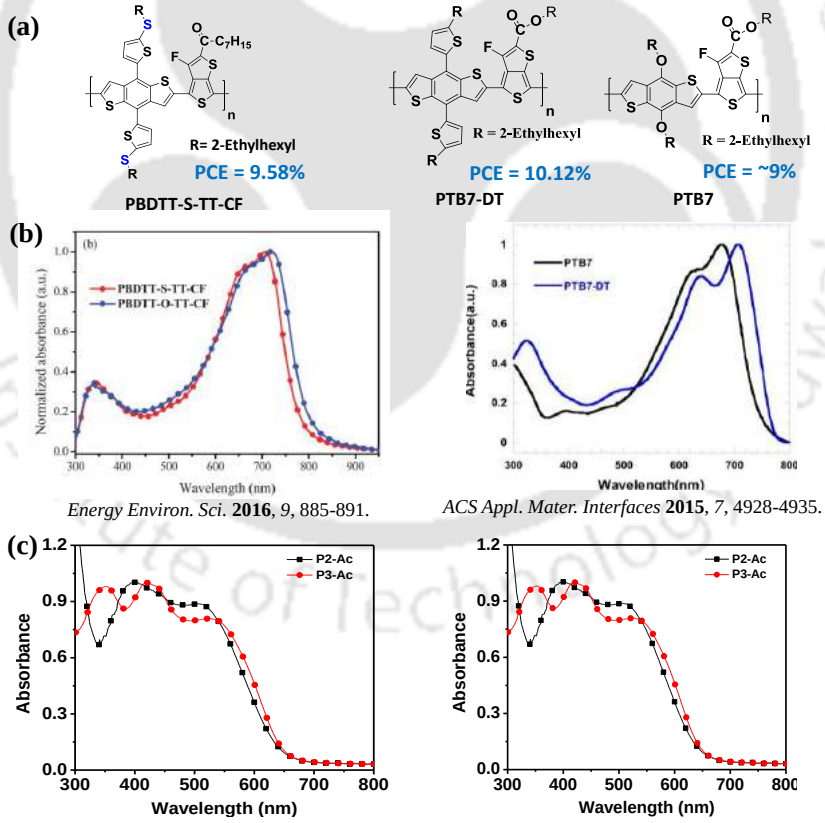

Energy Environ. Sci. **2016**, *9*, 885-891.

ACS Appl. Mater. Interfaces **2015**, *7*, 4928-4935.

Figure F1. (a) Structure of CPs with which high PCE are being achieved (b) their corresponding UV-visible spectra (c) absorption spectra for P2-Ac and P3-Ac showing complementary to absorbance of CPs PTB7, PTB7-DT and PBDTT-S-TT-SF. For Figure F1b copy right permission has been taken.

TH-1906_11615303

F2. Design and synthesis of new monomer units and CPs

F2.1. Largely, using the synthetic strategy developed in chapter 5: Wittig coupling at Ortho-position on aromatic unit will open newer approach to design new donor and acceptor units for solar cell and other organic electronic device.

F2.2. While looking into the chapter 4, it has been established that ester at side chain can improve both optical and solar cell performance. Hence side chain ester can be introduced into various aromatic core/unit to improve optical property as well as PCE for CPs. Some structures which can be synthesized immediately have been given bellow as well.

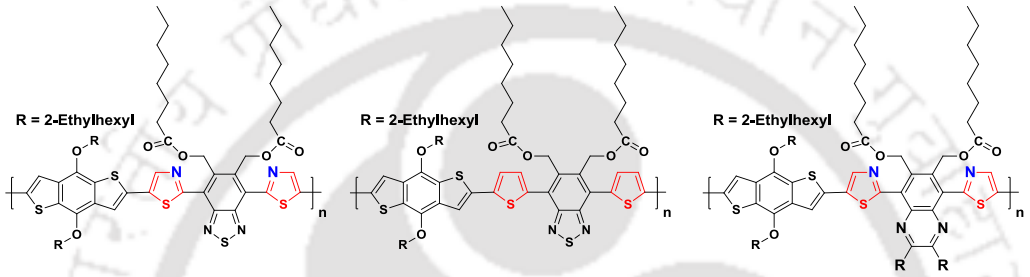

P(BDT-Tz-BT$_{5,6\text{-MO}}$-Tz) **P(BDT-Th-BT$_{5,6\text{-MO}}$-Th)** **P(BDT-Th-Q$_{5,6\text{-MO}}$-Th)**

Figure F2. New CPs that can be synthesized in future.

F2.3. POAV (Zig-Zag arranged aromatic units) as new design can be used to synthesize non-fullerene-based acceptor molecules, where non-planar geometry is highly essential to achieve phase separation within active layer for PSC.

F2.4. Using a vinyl group between donor and acceptor retards its ICT, as a result optical property, V_{oc}, J_{sc} were seen to reduce and hence the PCE gets lowered too. A further approach that has been implemented is to use a vinyl group within donor unit or within acceptor unit and polymerize the both. This design has been very promising in providing PCE as well as mobility in PPAV (poly Para Aryl Vinyl). [For example in literature reference (*Polym. Chem.* **2017**, *8*, 421-430) a PCE of 6.79% has been achieved with vinyl bridged donor and acceptor as D-A conjugated polymer (Figure F3)

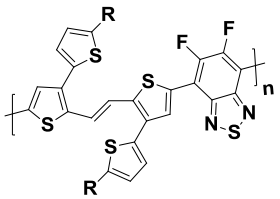

R = 2-Ethylhexyl

Polym. Chem. **2017**, *8*, 421-430.

TH-1906_11615303

Figure F3. Vinyl bridged CP with PCE 6.79%.

When one has a design as stated above, the final polymerization method need not be a Wittig polymerization. Most commonly Stille type condensation using palladium (0) catalyst can provide high molecular weight as well. Hence POAV structure can be used to design donor acceptor units as discussed (Figure F3) above in future as well.

F3. Stability study of PSC with the newly synthesized donor polymers

We have carried out stability studies for the methyl ester substituted and corresponding methyl counterpart. Photo stability improvement for methyl acetate substituted polymers has been observed compared to their methyl counterpart (Figure F4).

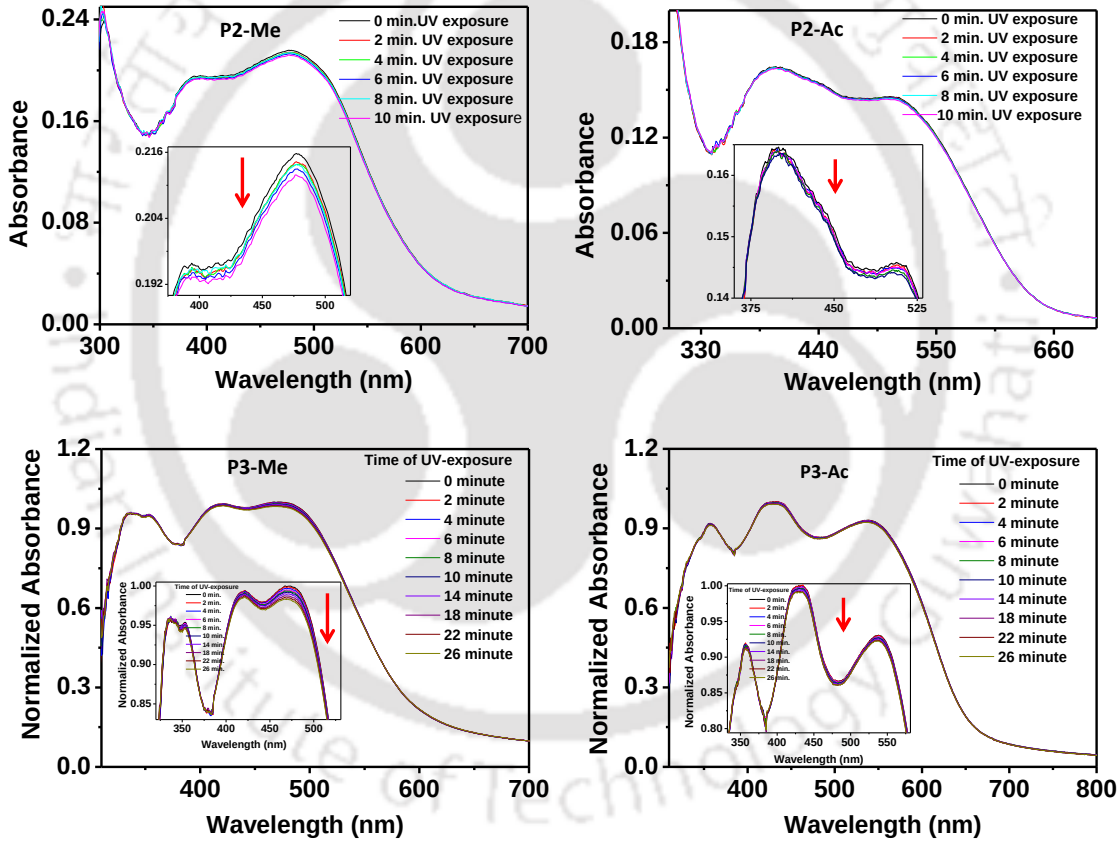

Figure F4. Photo-degradation study for P2-Me, P2-Ac, P3-Me, P3-Ac.

To produce a completely investigated result requires rigorous study (cannot be included briefly in the thesis or can be considered as future prospective). Here we are attaching photo stability studies of few set of polymer carried out (these results have been presented in conference proceedings as well). All the CPs investigated are stable to photo

TH-1906_11615303

degradation under UV-irradiation, with degreasing absorbance intensity in P2-Me and P3-Me polymer compared to corresponding P2-Ac and P3-Ac CPs respectively.

F4. Durability improvement using MWCNT in fabricated PSC

In this thesis, investigation of photo stability improvement by MWCNT has been carried out using optical study only and has not been investigated in a fabricated polymer solar cell. The study for increasing device stability by using MWCNT as ternary blend component has not been done by any group yet or not investigated here. But as they can improve the stability under UV-exposure (as confirmed by solution and thin film optical study), they are likely to improve the durability of fabricated solar cell, which can be considered as future prospective work as well.

TH-1906_11615303

Copyright Clearance Center RightsLink®

Home | Account Info | Help

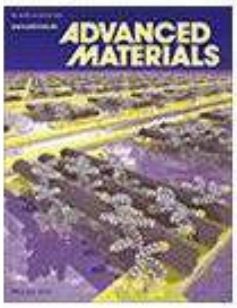

Title: An Easily Synthesized Blue Polymer for High-Performance Polymer Solar Cells

Author: Ergang Wang,Lintao Hou,Zhongqiang Wang,Stefan Hellström,Fengling Zhang,Olle Inganäs,Mats R. Andersson

Publication: Advanced Materials

Publisher: John Wiley and Sons

Date: Sep 8, 2010

Copyright © 2010 WILEY-VCH Verlag GmbH & Co. KGaA, Weinheim

Logged in as:
Radhakrishna Ratha
IIT Guwahati
Account #:
3001250293
LOGOUT

Order Completed

Thank you for your order.

This Agreement between IIT Guwahati -- Radhakrishna Ratha ("You") and John Wiley and Sons ("John Wiley and Sons") consists of your license details and the terms and conditions provided by John Wiley and Sons and Copyright Clearance Center.

Your confirmation email will contain your order number for future reference.

printable details

License Number	4291150286639
License date	Feb 17, 2018
Licensed Content Publisher	John Wiley and Sons
Licensed Content Publication	Advanced Materials
Licensed Content Title	An Easily Synthesized Blue Polymer for High-Performance Polymer Solar Cells
Licensed Content Author	Ergang Wang,Lintao Hou,Zhongqiang Wang,Stefan Hellström,Fengling Zhang,Olle Inganäs,Mats R. Andersson

Copyright Clearance Center RightsLink®

Home | Account Info | Help

Title:	Additives for morphology control in high-efficiency organic solar cells
Author:	Hsueh-Chung Liao,Chun-Chih Ho,Chun-Yu Chang,Meng-Huan Jao,Seth B. Darling,Wei-Fang Su
Publication:	Materials Today
Publisher:	Elsevier
Date:	September 2013

Copyright © 2013 Elsevier Ltd. Published by Elsevier Ltd.

Logged in as:
Radhakrishna Ratha
IIT Guwahati
Account #:
3001250293
LOGOUT

Order Completed

Thank you for your order.

This Agreement between IIT Guwahati -- Radhakrishna Ratha ("You") and Elsevier ("Elsevier") consists of your license details and the terms and conditions provided by Elsevier and Copyright Clearance Center.

Your confirmation email will contain your order number for future reference.

printable details

License Number	4291150677268
License date	Feb 17, 2018
Licensed Content Publisher	Elsevier
Licensed Content Publication	Materials Today
Licensed Content Title	Additives for morphology control in high-efficiency organic solar cells
Licensed Content Author	Hsueh-Chung Liao,Chun-Chih Ho,Chun-Yu Chang,Meng-Huan Jao,Seth B. Darling,Wei-Fang Su

Copyright Clearance Center RightsLink®

Home | Account Info | Help

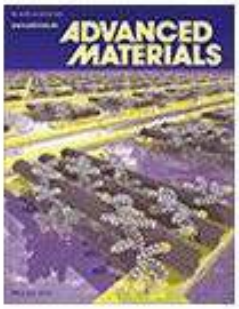

Title:	Photoluminescence Quenching in Carbon Nanotube-Polymer/Fullerene Films: Carbon Nanotubes as Exciton Dissociation Centres in Organic Photovoltaics
Author:	N. Aamina Nismy,K. D. G. Imalka Jayawardena,A. A. Damitha T. Adikaari,S. Ravi P. Silva
Publication:	Advanced Materials
Publisher:	John Wiley and Sons
Date:	Jul 18, 2011

Copyright © 2011 WILEY-VCH Verlag GmbH & Co. KGaA, Weinheim

Logged in as:
Radhakrishna Ratha
IIT Guwahati
Account #:
3001250293
LOGOUT

Order Completed

Thank you for your order.

This Agreement between IIT Guwahati -- Radhakrishna Ratha ("You") and John Wiley and Sons ("John Wiley and Sons") consists of your license details and the terms and conditions provided by John Wiley and Sons and Copyright Clearance Center.

Your confirmation email will contain your order number for future reference.

printable details

License Number	4291150921867
License date	Feb 17, 2018
Licensed Content Publisher	John Wiley and Sons
Licensed Content Publication	Advanced Materials

TH-1906_11615303

Copyright Clearance Center RightsLink®

Home | Account Info | Help

ACS Publications
Most Trusted. Most Cited. Most Read.

Title: Study on Photoluminescence Quenching and Photostability Enhancement of MEH-PPV by Reduced Graphene Oxide
Author: Chenxin Ran, Minqiang Wang, Weiyin Gao, et al
Publication: The Journal of Physical Chemistry C
Publisher: American Chemical Society
Date: Nov 1, 2012
Copyright © 2012, American Chemical Society

Logged in as:
Radhakrishna Ratha
IIT Guwahati
Account #:
3001250293
LOGOUT

PERMISSION/LICENSE IS GRANTED FOR YOUR ORDER AT NO CHARGE

This type of permission/license, instead of the standard Terms & Conditions, is sent to you because no fee is being charged for your order. Please note the following:

- Permission is granted for your request in both print and electronic formats, and translations.
- If figures and/or tables were requested, they may be adapted or used in part.
- Please print this page for your records and send a copy of it to your publisher/graduate school.
- Appropriate credit for the requested material should be given as follows: "Reprinted (adapted) with permission from (COMPLETE REFERENCE CITATION). Copyright (YEAR) American Chemical Society." Insert appropriate information in place of the capitalized words.
- One-time permission is granted only for the use specified in your request. No additional uses are granted (such as derivative works or other editions). For any other uses, please submit a new request.

Copyright Clearance Center RightsLink®

Home | Account Info | Help

ACS Publications Most Trusted. Most Cited. Most Read.

Title: Single-Junction Polymer Solar Cells with Over 10% Efficiency by a Novel Two-Dimensional Donor–Acceptor Conjugated Copolymer

Author: Chang Liu, Chao Yi, Kai Wang, et al

Publication: Applied Materials

Publisher: American Chemical Society

Date: Mar 1, 2015

Copyright © 2015, American Chemical Society

Logged in as:
Radhakrishna Ratha
IIT Guwahati
Account #:
3001250293

LOGOUT

PERMISSION/LICENSE IS GRANTED FOR YOUR ORDER AT NO CHARGE

This type of permission/license, instead of the standard Terms & Conditions, is sent to you because no fee is being charged for your order. Please note the following:

- Permission is granted for your request in both print and electronic formats, and translations.
- If figures and/or tables were requested, they may be adapted or used in part.
- Please print this page for your records and send a copy of it to your publisher/graduate school.
- Appropriate credit for the requested material should be given as follows: "Reprinted (adapted) with permission from (COMPLETE REFERENCE CITATION). Copyright (YEAR) American Chemical Society." Insert appropriate information in place of the capitalized words.
- One-time permission is granted only for the use specified in your request. No additional uses are granted (such as derivative works or other editions). For any other uses, please submit a new request.

TH-1906_11615303

Copyright Clearance Center RightsLink®

Home | Account Info | Help

Title: High-performance polymer solar cells based on a 2D-conjugated polymer with an alkylthio side-chain

Author: Chaohua Cui,Zhicai He,Yue Wu,Xiao Cheng,Hongbin Wu,Yongfang Li,Yong Cao,Wai-Yeung WongpublisherName=rsc

Publication: Energy & Environmental Science

Publisher: Royal Society of Chemistry

Date: Jan 14, 2016

Copyright © 2016, Royal Society of Chemistry

Logged in as:
Radhakrishna Ratha
IIT Guwahati
Account #:
3001250293
LOGOUT

Order Completed

Thank you for your order.

This Agreement between IIT Guwahati -- Radhakrishna Ratha ("You") and Royal Society of Chemistry ("Royal Society of Chemistry") consists of your license details and the terms and conditions provided by Royal Society of Chemistry and Copyright Clearance Center.

Your confirmation email will contain your order number for future reference.

printable details

License Number	4363741268211
License date	Jun 07, 2018
Licensed Content Publisher	Royal Society of Chemistry
Licensed Content Publication	Energy & Environmental Science
Licensed Content	High-performance polymer solar cells based on a 2D-conjugated polymer with an

TH-1906_11615303